Bone Formation and Skeletal Aging

- The effects of oxygen tension and DNA repair -

Claudia Nicolaije

evers + manders
subsidieadviseurs

Cover:

Origami Art by Dineke Boogaard
Pictures by Miriam Ten Haaf
Cover Design by Marco Bouwkamp

Bone Formation and Skeletal Aging

- The effects of oxygen tension and DNA repair -

Botvorming en veroudering

- de effecten van zuurstof en DNA schadeherstel –

Proefschrift

Ter verkrijging van de graad van doctor aan de Erasmus Universiteit Rotterdam

Op gezag van de rector magnificus Prof.dr. H.G. Schmidt

en volgens besluit van het College voor Promoties.

De openbare verdediging zal plaatsvinden op

vrijdag 7 december 2012 om 11.30 uur

door

Claudia Nicolaije

geboren te Heerlen

ERASMUS UNIVERSITEIT ROTTERDAM

Promotiecommissie

Promotoren:	Prof.dr. J.P.M.T. van Leeuwen
	Prof.dr. J.H.J. Hoeijmakers
Overige leden:	Prof.dr. G.T.J. van der Horst
	Prof.dr. H.B.J. Karperien
	Prof.dr.ir. H. Weinans

Een dag niet gedanst,

is een dag niet geleefd

Contents

CHAPTER 1

General Introduction

Aging is a process that affects everybody and importantly, affects all cells and therefore all the tissues in our body. In the worst cases, tissue aging leads to organ failure and death; in other cases, the effects of aging are more subtle and less dramatic. In our tissue of choice – bone and the skeletal system - aging manifests in the form of osteoporosis, low bone mineral density and a higher risk of fractures, all contributors to a higher morbidity [1].

There are several theories applicable to the process of aging, of which the free radical theory of aging is one of the oldest and well-studied. This theory, first proposed by Denham Harman in the 1950's, states that organisms age because cells accumulate free radical damage over time [2]. Free radicals are atoms or molecules that have a single unpaired electron in their outer shell. Many biologically relevant free radicals are highly reactive and can be produced by the cell's metabolic mechanisms. Free radicals can cause intracellular damage to DNA and proteins.

To limit damage caused by free radicals, which are often called reactive oxygen species (ROS), cells have antioxidant scavengers, which are reducing agents that limit oxidative damage to biological structures by scavenging free radicals (reviewed in [3]). ROS can function as regulators of cellular signalling and cellular processes but high levels of free radicals can cause oxidative damage when not regulated correctly (reviewed in [4]).

When damage occurs, the cell has a wide variety of repair mechanisms in place in order to prevent damage from derailing cell function and the induction of senescence or apoptosis [5,6]. DNA damage is counteracted in the cells by a range of DNA repair mechanisms that can repair a wide variety of DNA lesions (reviewed in [7]and [8]). One of these pathways is the nucleotide excision repair (NER) pathway, which removes helix-distorting and bulky lesions, caused by exposure to UV light, ROS or chemicals like tobacco smoke [7].

Oxygen is a very important regulator of cell differentiation and function. Interestingly, most cell culture experiments are performed at oxygen tension levels that are never reached *in vivo*. In many tissues, oxygen tension drops to hypoxic levels, inducing signalling pathways that alter the cell's proliferative and differentiation state [9,10,11]. More insight into cell signalling during low oxygen tension will be valuable in understanding *in vivo* cell functioning.

This thesis focuses on the influence of oxygen, defective DNA repair and oxidative damage on bone formation, remodelling and aging.

1. Bone

The skeleton forms the supporting structure of an organism and, in humans, is made up out of bone and cartilage. The human skeleton has 206 bones that protect soft tissues and vital organs, anchor muscles and, on a cellular level, function as calcium and phosphate storages, maintaining the body's serum calcium homeostasis [12]. More recently bone has also been described as an endocrine organ, producing regulatory factors like sclerostin (SOST) and fibroblast growth factor 23 (FGF23) that regulate vitamin D metabolism and phosphate homeostasis [13,14].

1.1 Bone structure

Long bones – which will be the main focus of this thesis – consist of several structural elements (depicted in detail in Figure 1).
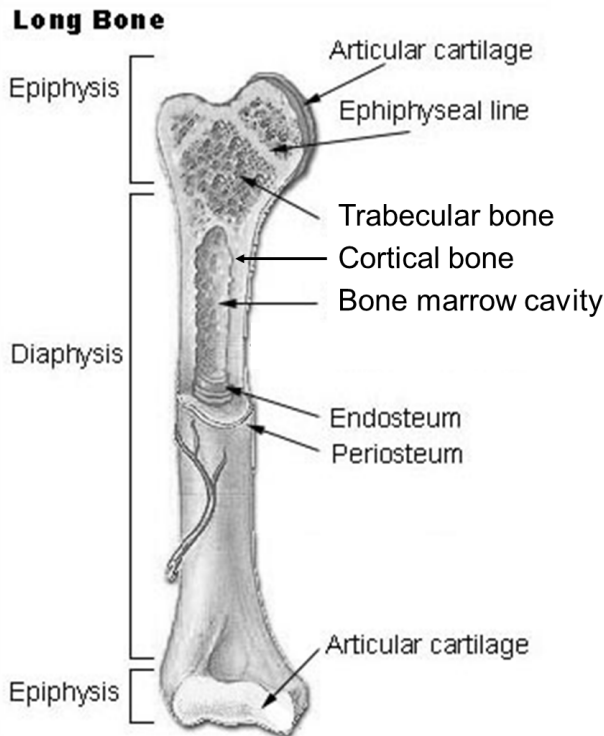
Figure 1: *Structural elements of long bones.* Adapted from http://training.seer.cancer.gov/ anatomy/skeletal/classification.html

The bone cortex, or cortical bone, forms the outer, compact layer of the bone. Cortical bone is very dense (70%- 95% bone) and accounts for about 80% of the total mass of the skeleton. Cortical bone is vascularised although the number of vessels is comparatively low compared to that of trabecular bone. Trabecular bone consists of a network of bony trabeculae with a high connectivity, localised within the cortical bone. The connecting trabeculae form a loose network with a lot of holes (90% free space) that create space for blood vessels and bone marrow cells.

The trabecular network looks like a sponge, and is often called spongy or cancellous bone. The overall trabecular structure is dependent on outside mechanistic stress and can be remodelled whenever necessary to adapt to changing outside forces on the bone. In contrast to cortical bone, trabecular bone is metabolically very active and plays an important role in calcium homeostasis.

There are several regions within a long bone, starting with the epiphysis, which mostly consist of trabecular bone surrounded by a layer of cortical bone. The part of the epiphysis adjacent to the epiphyseal lines is also called metaphysis and contains most of the trabecular bone. The middle part of the bone, called diaphysis, mainly consists of cortex and contains much less trabecular bone on the inside. Instead, it houses the bone marrow cavity in which mesenchymal stem cells (MSCs) and hematopoietic stem cells (HSCs) divide, differentiate and proliferate in order to form blood cells and mesenchymal progenitor cells that will enter the circulation to be transported to their target tissues. Epiphysis and diaphysis are separated from each other by the growth plates (physes) on either side of the long bone.

### 1.2 Bone development, modelling and remodelling

In humans we recognize two different ways of bone formation during early development. Most bones, including all long bones, are formed by a process called endochondral bone formation. Endochondral bone formation is characterised by the formation of a cartilage template, followed by ossification from several primary and secondary ossifications centres. Cartilage zones remain in the long bones and will later become the growth plates that will enable longitudinal growth of the bone. Intramembranous bone development on the other hand, which takes place in the flat bones of the skull, the mandible, maxilla and clavicles, does not make use of a cartilage template and only uses a single ossification centre (reviewed in [15]).

After bone development, all bones undergo modelling and remodelling (Figure 2). Bone modelling takes place during growth and prevents damage to the bone by adapting bone structure and strength, adapting the bone to new loading requirements. Modelling is regulated by physiologic influences and mechanical forces on the bone, leading to gradual adjustment of the skeleton to the forces that it encounters. During the modelling phase most of the bone formed during bone development is replaced by structurally stronger bone.
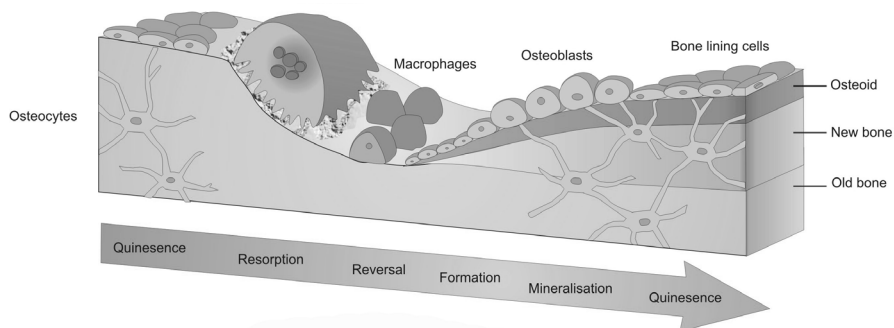
Figure 2: *Bone remodelling within the bone multicellular unit;* at the site of remodelling, osteoclasts resorb the old mineralised matrix after which osteoblasts produce a new bone matrix which mineralises. Most osteoblasts go into apoptosis, but some stay behind in the matrix and become osteocytes, whereas other transition into bone lining cells that will cover the bone surface. Adapted from http://www.york.ac.uk/res/bonefromblood/background/boneremodelling.html

Bone remodelling takes place throughout live and maintains the structural integrity and strength of the bone by removing old or damaged bone and replacing it by new, strong bone. Remodelling is a local process that can take place anywhere on the bone surface throughout the lifespan of a bone. Remodelling occurs in a temporary anatomic unit of osteoclasts and osteoblasts called a bone multicellular unit (BMU). The BMU is a sealed compartment in which bone resorption and subsequent formation are regulated. This coupled resorption and formation characterises and differentiates bone remodelling from bone modelling, in which bone resorption and formation do not have to occur at the same time and site. In extreme circumstances, like a fracture, the remodelling surface can be large and extremely active, but throughout life most of our bone surface gets renewed bit by bit due to remodelling [16].

1.3 The cells involved in bone formation and (re-)modelling

Independent of the kind of bone development, the type of cells involved in bone formation, modelling and remodelling is limited.

1.3.1. Mesenchymal stem cells and osteoblasts

Osteoblasts, also known as bone forming cells, originate from mesenchymal stem cells (MSCs) that can be found in the bone marrow. MSCs can differentiate into multiple cell types, including osteoblasts, chondrocytes and adipocytes [17]. After receiving the right differentiation cues, MSCs differentiate into osteoblast precursors, who then become mature, matrix producing osteoblasts (Figure 3).
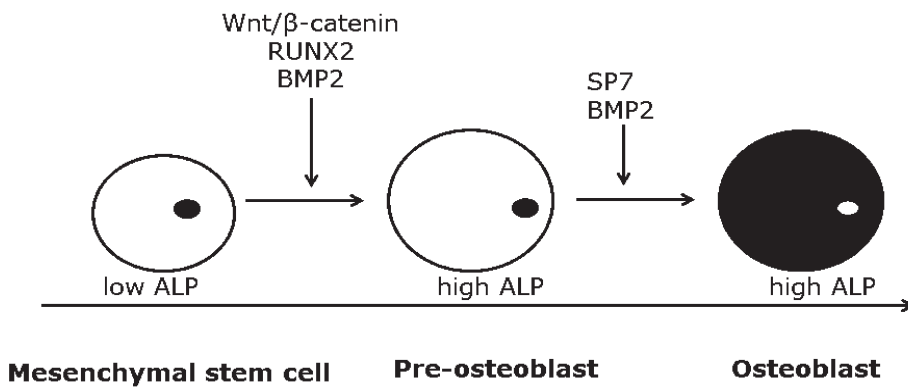
Figure 3: *Schematic depiction of osteoblast differentiation from MSC to mature osteoblast.* During the differentiation process several groups of transcription factors play an important role in driving the transition from MSC to mature osteoblast. In the early stages Wnt-signalling, BMP2 and RUNX2 are some of the key players, whereas later on BMP2 and SP7 regulate differentiation.

Osteoblast differentiation is regulated by a number of key players that drive the transition from pluripotent progenitor to pre-osteoblast and onwards to mature osteoblast. Important in early differentiation is bone matrix protein 2 (BMP2). Cell culture experiments showed that BMP2 plays a continuous role during the various transition stages, inducing the expression of osteoblast differentiation markers alkaline phosphatase (*ALP*) and

osteocalcin (*BGLAP*) [18,19]. More importantly, BMP2 can induce the expression of the essential osteoblast differentiation factor runt-related transcription factor 2 (*RUNX2*). In mice, a loss of *Runx2* results in a complete lack of skeletal ossification due to a lack of osteoblast differentiation [20,21]. RUNX2 regulates the expression of osterix (SP7), an osteoblast-specific transcription factor that drives the transition from pre-osteoblast to mature osteoblast [22]. *Sp7* null mice resemble *Runx2* null mice, displaying an inhibition of osteoblast differentiation and a lack of bone formation [23]. In addition, activation of Wnt-signalling is required for early osteoblastogenesis. Osteoblast differentiation is stimulated by the stabilisation and translocation of β-catenin to the nucleus, which leads to target gene expression (reviewed in [24]). Interestingly, during the later stages of osteoblast differentiation inhibitors of Wnt-signalling, like dickkopf homolog 1 (DKK1) and dickkopf homolog 2 (DKK2) play an important role in osteoblast maturation and matrix mineralisation by inhibiting Wnt-signalling in pre-osteoblasts [25]. To determine the differentiation stage of an osteoblast precursor, *ALP* expression and activity are commonly used as osteoblast differentiation markers. *ALP* expression is low in MSCs, but gradually rises during osteoblast differentiation [21,26].

Mature osteoblasts produce and secrete matrix molecules, for example collagens (collagen I is the most abundant protein in bone), which are the foundations of the bone matrix. These mature osteoblasts ultimately undergo one of three fates during matrix formation and mineralization. The largest percentage of the osteoblasts goes into apoptosis [27]. A number of mature osteoblasts become bone lining cells at the bone surface [28]. A number of osteoblasts, somewhere between 10-20%, become embedded in the matrix and transition into osteocytes. A number of genes may play a role in this transition and later on in osteocyte function, including metallo-matrix proteinase 2 (MMP2), dentin matrix protein 1 (DMP1) and matrix extracellular phosphoglycoprotein (MEPE) [29,30,31,32].

1.3.2. Osteocytes and bone lining cells

During matrix formation many osteoblasts undergo apoptosis, but some get buried inside of the matrix and transform into osteocytes [33]. Osteocytes are cells with long cytoplasmic extensions that extend throughout the matrix in little canals called canaliculi. Through these extensions the osteocytes stay in touch and communicate with each other. Osteocytes are thought to be involved in bone remodelling by measuring mechanic forces and pressure in the bones and regulating cellular signalling cascades that induce remodelling [34]. Micro damage occurs in our bones as a result of repetitive cyclic loading incidents. Small cracks accumulate in the mineralised matrix of bone in a load-dependent manner and reduce the strength of the bone [35,36,37,38]. Bone, however, is capable of removing accumulating micro damage by targeted bone remodelling [39,40,41]. Osteocyte apoptosis plays an important role in the initiation and localisation of the remodelling process [42]. Large-scale osteocyte apoptosis at the site of damage recruits osteoclasts by the secretion of unidentified signaling factors [43].

In addition, osteocytes are metabolically active cells under the control of external stimuli that produce a number of known signaling factors including SOST and FGF23. These relatively new findings have changed the way bone is viewed, since it suddenly seems to have an endocrine function instead of just being there to provide structural support. SOST is an inhibitor of bone formation and a lack of SOST activity leads to an overproduction of bone

and sclerosteosis [44]. Binding of parathyroid hormone (PTH) to receptors on the osteocyte surface leads to the inhibition of SOST production and secretion and a subsequent increase in bone formation [13]. FGF23 plays an important role in phosphate homeostasis and, in excess, leads to hypophosphatemia, aberrant vitamin D metabolism, impaired growth, and rickets [45,46,47]. Inversely, a loss of FGF23 results in hyperphosphatemia, excess $1,25(OH)_2D_3$, and soft tissue calcifications [14,48].

Bone lining cells are pre-osteoblasts that cover inactive bone surfaces. Throughout life, these bone lining cells can be activated and subsequently differentiated into osteoblasts involved in bone remodelling. Whether or not they become osteoblasts depends on the presence of the necessary signals, which are still largely undiscovered [28]. Recent evidence shows that intermittent PTH treatment leads to an increase in bone formation and the activation of bone lining cells, both in *in vivo* cultures and *in vitro* in rats [49,50].

1.3.3. Osteoclasts

Osteoclasts are bone resorbing cells. Unlike the cell types mentioned above, they do not originate from MSCs but from hematopoietic stem cells (HSCs) in the bone marrow. Osteoblasts/osteocytes secrete receptor activator of nuclear factor-kappa B ligand (RANKL), which binds to receptor activator of nuclear factor-kappa B (RANK), a receptor found on the osteoclast membrane [51].
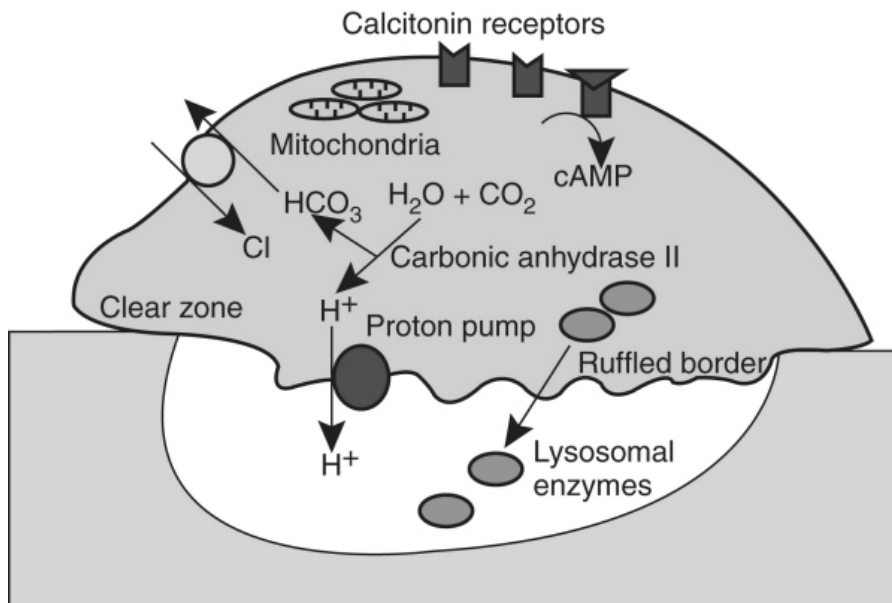
Figure 4: *Osteoclast resorption pit;* mature osteoclasts adhere to the bone, form a ruffled border and secrete hydrogen ions and lysosomal enzymes to resorb the matrix in order to form a resorption pit that can be filled with new bone matrix. Copyright © 2008 Elsevier Inc - www.mdconsult.com

Binding of RANKL to RANK drives osteoclast differentiation and subsequent bone resorption. Another regulating molecule secreted by osteoblasts is osteoprotegerin (OPG), which functions as a decoy receptor for RANKL [52]. The balance between OPG and RANKL determines eventually if and how much bone is resorbed [53]. Mature osteoclasts are multinucleated cells that produce and secrete molecules that will break down the mineralised bone matrix into its separate organic compounds.

Osteoclasts usually attach themselves to an area of bone that requires modelling or remodelling and resorb the covered area. One of the main characteristics of a resorbing osteoclast is the formation of a ruffled border at the side of the cell that covers the bone. The actively resorbing osteoclasts form a sealed resorption pit and secrete hydrogen ions, cathepsin K and metallo matrix proteinases (MMPs) into this space. The hydrogen ions demineralize the matrix, which is then degraded by cathepsin K, a lysosomal cysteine proteinase, and several MMPs, including collagenases (Figure 4)[54].

In order to maintain calcium homeostasis and bone mass, it is important that the amount of bone formation and resorption is extremely well balanced. This is why there is a natural coupling between osteoclast and osteoblast activity [55]. Whenever this coupling, and therefore the balance between resorption and formation is disturbed, bone homeostasis is severely affected, which in some cases leads to diminished bone strength and an increase in fracture risk.

1.4 Bone matrix

Bone matrix, is a specialized protein-rich extra cellular matrix (ECM) produced by osteoblasts and consists out of collagens, non-collagenous proteins (NCPs), mineral and water [56].

The main organic component of the bone matrix is collagen type I (COL1A1), although a wide variety of collagens can be found throughout the matrix. A variety of NCPs such as osteocalcin, osteonectin and bone sialoprotein (SPP1) - are present in the bone matrix. Previous studies have shown that most of these proteins are either involved in osteoblast differentiation and maturation or might play a role in matrix mineralization, functioning as nucleation factors for matrix mineralization [57]. The inorganic part of the matrix mainly consists of carbonated hydroxyapatite crystals deposited onto the matrix. Recent proteomic analysis of the bone matrix showed that there are still a great number of unknown proteins present in the matrix that could be involved in numerous regulatory processes [58].

There is an intricate interplay between the developing bone matrix and the osteoblasts responsible for that formation. The osteoblasts and the mineralising matrix mutually affect each other. Osteoblasts can secrete factors like metallo matrix proteinases (MMPs) that can remodel the matrix by cleaving matrix surface molecules. MMP mediated cleavage or processing of matrix molecules can also release important signalling factors from the matrix that influence osteoblast differentiation and matrix formation [59,60,61,62,63]. Mutations in MMPs affect bone formation and emphasise the importance of this bidirectional cell-matrix communication [64,65,66,67].

Structurally, two forms of bone matrix can be observed. In lamellar bone (matrix) collagen is deposited in a regular, parallel alignment of collagen sheets, which form a mechanically strong matrix. During the initial bone development, but also after a micro crack/fracture,

bone matrix is formed very rapidly. Due to the speed of this process, a woven bone matrix is formed, characterized by a more disorganised constellation of the collagen fibrils, which are not deposited in a regular, structured manner. Woven bone is weaker and easier to break and usually will be rapidly replaced by lamellar bone. This is why bones undergo a modelling phase early on in life and one of the main reasons for on-going bone remodelling [68,69].

1.5 Bone strength and periosteal apposition

Bone strength is highly dependent on the strictly regulated balance between bone formation and bone resorption. By regulating this balance, bone remodelling and bone repair take place in a structured and regulated fashion so that high quality bone matrix is formed and kept.

a more mathematical point of view, the size of a bone is of particular importance to bone strength. The resistance of bone to torsional forces or bending is exponentially related to its diameter [70]. A small addition to the bone diameter will therefore significantly increase its strength. Throughout life, new cortical bone is deposited at the outside (periosteal side) of the cortex. This process of radial bone growth is called periosteal apposition, and is of great importance to maintain bone strength later on in life when endosteal bone loss increases. Endosteal bone loss is most obvious in post-menopausal women but in general affects both men and women with aging.

The mechanisms that control periosteal apposition are still largely unknown, but sex steroids seem to play a role. Androgens have a positive effect on periosteal apposition. The effect of estrogens appears to be dose dependent, with low doses being beneficial, whereas higher doses inhibit periosteal apposition [71,72]. Recent studies performed in male estrogen receptor α (ERα) knockout mice, however, showed a reduction in radial bone growth, suggesting that in fact, estrogens might stimulate radial growth alongside androgens [73]. Mechanical loading is also involved in bone strength, with an increase in bending stress leading to the stimulation of periosteal apposition [74].

1.6 Endocrine regulation of bone formation and resorption

Bone formation and resorption (together remodelling) are highly regulated processes. A wide variety of endocrine factors play a role in this regulation, many of which interact with each other. Three important groups of hormones are:

1.6.1 Sex steroids

Sex steroids play an important role in bone formation and resorption. Estrogens inhibit bone resorption by inhibiting osteoclast function and stimulating osteoclast apoptosis [55,75]. They also have an anti-apoptotic effect on osteoblasts, effectively inhibiting bone resorption while stimulating bone formation [71]. Consequently, a loss of estrogens, for example during menopause, leads to an increase in bone loss. Estrogens are also responsible for a rise in pubertal longitudinal bone growth and subsequent closure of the growth plates in the long bones [76].

Testosterone affects bone in a variety of ways. It can be converted into estradiol by aromatase and thus can have indirect effects through estrogen on bone. On the other hand,

there are clear direct effects of testosterones, including stimulation of bone formation in both males and females as well as inhibition of bone resorption in males. The effects of testosterone are mainly obtained by positively regulating the lifespan of osteoblasts and actively stimulating of osteoclast apoptosis [77].

1.6.2 Calcium homeostasis regulators parathyroid hormone/ 1,25(OH)$_2$D$_3$ axis

The regulation of serum calcium homeostasis is of great importance to bone maintenance and tightly interconnected with bone remodelling. Parathyroid hormone (PTH), Vitamin D (*1,25(OH)$_2$D$_3$*) and calcitonin regulate calcium homeostasis through effects on kidney, intestine and bone [55,74,78]. Most importantly, PTH stimulates osteoclast differentiation by regulating the expression of two important osteoclast growth factors, RANKL and OPG in osteoblasts. This leads to an increase in resorption and higher serum calcium [52]. Most interestingly, intermittent PTH treatment, using daily injections, is bone anabolic and is currently used in the clinic [79].

Vitamin D, which is originally produced in the skin or taken up from the diet, is processed in the liver and kidney in order to produce the biologically active metabolite 1,25(OH)$_2$D$_3$, using 25-hydroxylase and 1α-hydroxylase, respectively. The latter enzyme is activated by PTH and hypocalcemia and inhibited by 1,25(OH)$_2$D$_3$ and hypercalcemia. 1,25(OH)$_2$D$_3$ stimulates intestinal and renal calcium (re-) absorption and as a consequence increases serum calcium levels. Interestingly, 1,25(OH)$_2$D$_3$ also stimulates matrix mineralization in humans [80,81]. In addition, osteoblasts express 1α-hydroxylase as well, enabling local 1,25(OH)$_2$D$_3$ production in human osteoblasts [82].

1.6.3 The GH/IGF axis

The GH/IGF axis plays an important role in the maintenance of bone mass and density and promotes skeletal development and growth. Growth hormone (GH) secretion in the pituitary is stimulated by growth hormone releasing hormone (GHRH) and inhibited by somatostatin from the hypothalamus. Estrogens and glucocorticoids modulate the effect of GHRH on GH secretion [83]. GH can act directly or indirectly on a number of tissues by stimulating insulin-like growth factor 1 (IGF1) production and secretion. IGF1 synthesis takes place predominantly in the liver and is regulated by insulin as well. Both GH and IGF1 target bone and muscle, where they induce development, growth, and tissue regeneration as well as lipid and carbohydrate metabolism [84].

In addition, bone is a major storage reservoir for IGF1 that as such could function as a coupling factor between bone resorption and formation during bone remodelling. IGF1 secretion in bone is stimulated by a number of factors, including PTH and 1,25(OH)$_2$D$_3$. The IGFs embedded in newly formed bone are released when bone is resorbed, enabling stimulation of new bone formation. IGFs strongly inhibit osteoblast apoptosis *in vitro* and IGF1 prevents forkhead box O1 (FOXO1) from inhibiting RUNX2 activity, thereby stimulating osteoblast differentiation [85,86]. It also plays an important role in stimulating matrix mineralization [87]. On the other hand, IGFs may increase osteoclastogenesis [88]. At old age a reduction of IGF1 levels may contribute to a decline in remodelling and the pathogenesis of osteoporosis [84,89].

1.6.4 Leptin

Leptin is an endocrine factor produced by adipocytes that mainly acts in the hypothalamus. There it regulates body weight and fat mass by affecting appetite and energy expenditure [90]. A lack of leptin, as seen in ob/ob mice, leads to obesity and high bone mass, even though sex steroid levels are low, which indicates that leptin has a negative effect on bone [91]. More specifically, leptin can act directly on osteoblasts and osteoclasts to increase cortical bone mass or indirectly via the GH-IGF axis [92,93]. In addition, leptin can act via neuro-endocrine circuits, on one hand inhibiting bone resorption via stimulation of hypothalamic cocaine- and amphetamine-regulated transcript (CART) expression and on the other hand stimulating bone resorption and inhibiting bone formation via central circuits that stimulate sympathetic nervous system (SNS) function [94,95]. Recently published data showed that the balance between these two neuro-endocrine mechanisms is age-dependent, with a shift towards SNS-mediated inhibition of bone formation in older mice [96]. Interestingly, long bones and vertebrae are affected differently, which might be due to the presence or absence of trabecular bone [97].

1.7 Age-related bone loss

Humans reach peak bone mass between 23 and 35 years of age. From that moment onwards, they gradually start to lose bone at a rate of approximately 0.4% a year. This is mostly due to the incomplete filling of resorption pits during the remodelling cycle.

Age-related bone loss correlates with an increase in fractures, a decrease in quality of life and ultimately in high morbidity. Since the average age of the world population keeps rising, age-related health issues become an increasing burden for society, both medically and financially, with age-related bone loss being a typical example.

When studying age-related bone loss, a distinction should be made between men and women. Men only experience one stage of bone loss, which is characterised by a slow, gradual decline in mass that leads to approximately 20-25% loss of bone. Both cortical and trabecular bone are affected [98]. Women on the other hand, experience two phases of bone loss. They share the slow, gradual loss of bone found in men, but also undergo a stage of accelerated bone loss that starts during menopause and affects trabecular bone much more severely than cortical bone. In this accelerated phase, 20%-30% of all trabecular bone is lost, whereas only about 5% of cortical bone will be resorbed, before bone loss rates return back to the same rates as measured in aging men [98].

At a cellular level, age-related bone loss is caused by an imbalance between bone formation and resorption. In women, the loss of sex steroids during menopause has a positive effect on osteoclast activity, disrupting this balance [75]. Osteoblast apoptosis also increases throughout life, resulting in a shorter osteoblast life span and activity, which leads to lower bone formation rates. In addition, an age-related imbalance in MSC lineage divergence leads to an increase in adipocyte proliferation in the bone marrow, which is accompanied by a decrease in osteoblast differentiation. This phenomenon is also known as fatty bone marrow, since the marrow cavity fills up with adipocytes. This imbalance in MSC lineage divergence results in a decrease in bone formation, while resorption is unaffected, thereby further disrupting the process of coupled bone formation.

2. Oxygen

2.1 Oxygen tension and hypoxia

A sufficient supply of oxygen and nutrients is necessary and essential for cell survival and metabolism. Alterations in tissue oxygen tension have been postulated to contribute to numerous pathologies, including rheumatoid arthritis and chronic kidney injury [99,100].

Prolonged oxygen deprivation leads to cell death and is a major cause of mortality. Oxygen is distributed to tissues by blood vessels. Oxygen tension fluctuates around 21% in normal air, but in the body physiologic oxygen pressure is much lower, ranging from a maximum 10%-13% in arteries, lungs and liver, to as low as 1% in cartilage and bone marrow [101,102,103,104,105,106]. Within a tissue, oxygen tension can fluctuate depending on the distance between the cells and the vessel.

Oxygen tension plays an important regulatory role in many cellular processes. In the bone marrow, oxygen tension determines the proliferation and differentiation state of hematopoietic stem cells [107]. Cells can sense and adapt to changes in oxygen tension through a complex signalling cascade in which hypoxia-inducible factor1 α (HIF1α) plays the role of master switch [108].

HIF1α is stabilised in cells that are exposed to very low oxygen tension, a situation called hypoxia. Stabilisation of HIF1α leads to an upregulation of genes that orchestrate cell metabolism and survival under low oxygen conditions, including anaerobic glycolysis and blood vessel formation (see Figure 5) [109,110]. Hypoxia is not necessarily a bad or dangerous state to be in for cells and can be used as a regulatory switch [109,110].

2.2 Oxidative stress and antioxidant defences

Oxidative stress is characterised by an increase in the level of reactive oxygen species (ROS). ROS encompass a wide variety of chemical species such as superoxide anions, hydroxyl radicals and hydrogen peroxide. Some of them are highly unstable (superoxide anions) while others are relatively stable and long-lived (hydrogen peroxide).

ROS are generated inside of the cell, mostly during metabolic processes. The main source of ROS production are mitochondria, which produce ROS during the oxidative phosphorylation of adenosine diphosphate (ADP) to produce adenosine triphosphate (ATP) [111]. *In vitro,* mitochondria convert 1%-2% of oxygen molecules into superoxide anions, while further studies under more physiological conditions (i.e. *in vivo* isolated mitochondria, the use of specialised substrates) have reduced this basal value to about 0,2% [112,113]. At these basal rates, ROS play an important role in cellular signalling, regulating numerous processes, including cell metabolism, endocytosis and adhesion [114,115,116].

External stimuli, including UV radiation, cytokines, growth factors and hyperthermia, can generate extremely high levels of ROS that will disturb the normal redox balance of the affected cells and shift them into a state of oxidative stress. High levels of ROS cause oxidative damage to intracellular proteins, lipids and DNA [117]. They can cause a broad spectrum of oxidative DNA lesions, including 8-oxo-2'-deoxyguanosine (8-oxodG), thymine glycols, cyclopurines and single and double strand breaks of different nature [118].
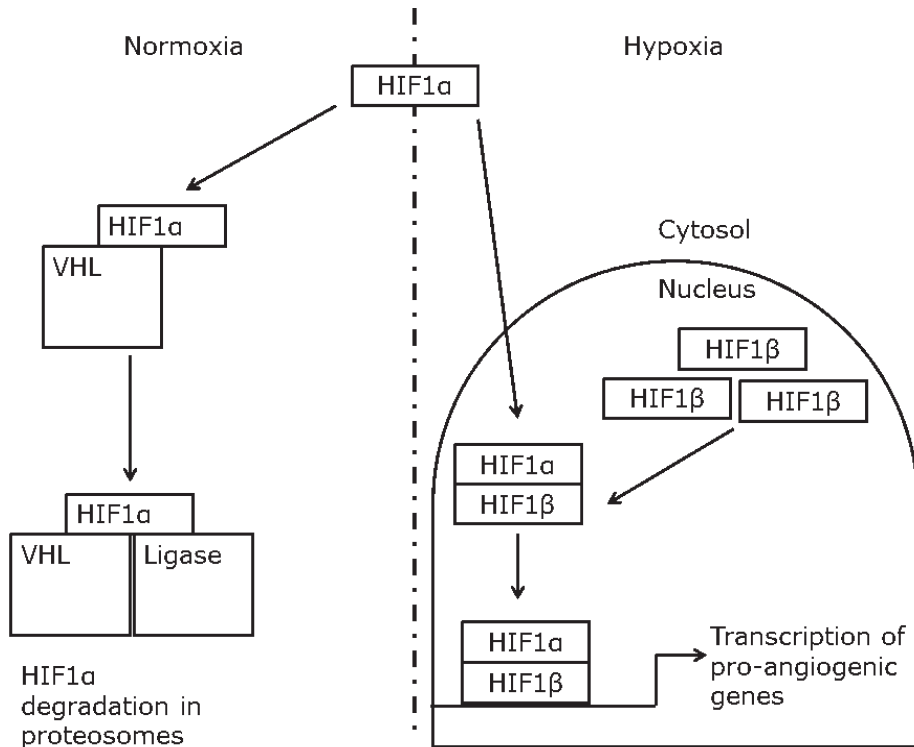
Figure 5: *Activation of HIF1α target genes during hypoxia;* under hypoxic conditions, HIF1α is stabilised and translocated to the nucleus where it dimerises and activates target gene expression. Several pro-angiogenic genes, including VEGF, are amongst HIF1α target genes.

Several studies have shown that aging cells accumulate ROS-induced damage and associated complications [119,120]. To protect themselves from ROS-induced oxidative damage, cells counteract ROS production by an intricate antioxidant defence system. This defence system consists of a large number of scavengers including antioxidant enzymes and FoxO proteins.

There are three classes of antioxidant enzymes (Figure 6). Superoxide dismutases (SODs) reduce superoxide radicals into H_2O_2. SOD1 is located in the cytoplasm and scavenges cytosolic ROS. SOD2 is located in mitochondria and scavenges at the source, preventing ROS diffusion into the cytoplasm. SOD3 on the other hand, is also called extra cellular SOD. It is secreted into the extra cellular space where it binds to the outside of the cell membrane where it can scavenge extracellular ROS [121,122]. Catalase (CAT) and glutathione peroxidases (GPXs) reduce H_2O_2 into H_2O [123]. In addition to this enzymatic scavenging system there are a number of small molecules, like ascorbate and pyruvate, that scavenges ROS as well [124,125].

FoxO proteins are a subgroup of a large family of forkhead proteins and represent another defence mechanism against oxidative stress. Oxidative stress promotes the translocation of FoxO proteins into the nucleus by a mechanism that involves c-Jun N-terminal kinase

(JNK) activation by ROS and the phosphorylation of FoxO proteins. This is followed by posttranslational modifications including ubiquitylation and acetylation [126]. These changes lead to the activation of FoxO proteins and induce FoxO-mediated oxidative stress responses. These include transcriptional regulation of antioxidant enzymes (*SOD2, CAT*) as well as genes involved in cell cycle and DNA repair [126,127]. In addition FoxO proteins can restrict angiogenesis by directly binding HIF1α, thereby preventing expression of HIF1α target genes [128,129].

$$O_2^{-}\cdot \xrightarrow{\text{SOD}} H_2O_2 \xrightarrow{\underset{\text{Lactoferrin}}{Fe^{2+}\ \ Fe^{3+}}} \cdot OH \xrightarrow{\text{Radical scavengers}} \text{Oxidative damage}$$

GSSG → GSH (GPx)

GPx → 2 H₂O

Catalase → H₂O + O₂
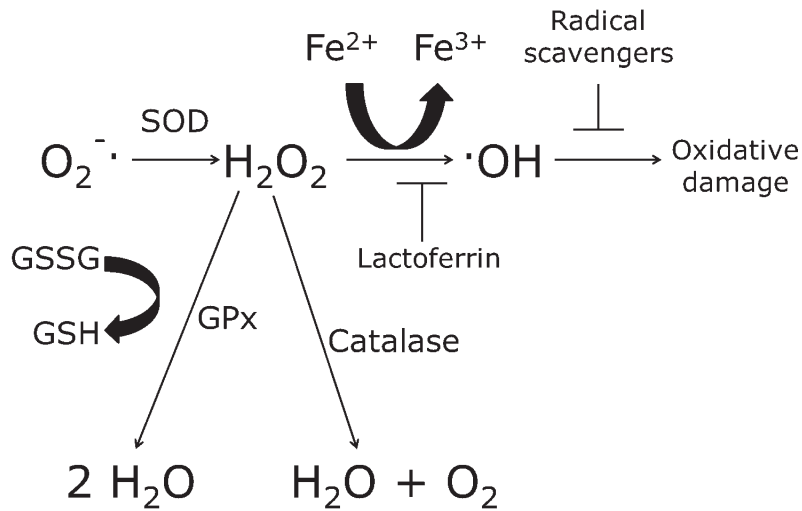
Figure 6: *Antioxidant enzymes protect the cell from ROS-induced oxidative damage;* three main groups of antioxidant enzymes reduce intracellular ROS into harmless substrates. Adapted from http://www.redlabs.be/red-labs/our-science/oxidative-stress.php

2.3 The role of oxygen tension in bone development, remodelling and fracture healing

During development, bone formation and angiogenesis are coupled. During endochondral bone formation, vessel formation and bone formation coincide within the cartilaginous template [130]. Interruption of the blood supply has been shown to decrease bone mineralization [131]. The vasculature supplies the bone with oxygen, nutrients and endocrine factors. During bone remodelling a BMU is created in which osteoblasts, osteoclasts and blood vessels interact in a self-contained environment to coordinate the remodelling process [132,133].

Hypoxia is believed to be a major stimulus for the initiation of the angiogenic cascade during bone development and following bone injury. Under hypoxic conditions chondrocytes produce vascular endothelial growth factor (VEGF), which leads to angiogenesis and vessel growth into the cartilage templates during endochondral bone formation. Inhibition

of VEGF production reduces bone formation and mineralization, while the addition of exogenous VEGF leads to enhanced bone formation in murine fracture healing models [134]. Many VEGF effects on bone formation are indirect, mediated through an increase in vascularisation. There is some evidence however, that also direct effects of VEGF on osteoblast differentiation and migration may occur [135,136].

As mentioned above, hypoxia-induced effects are often regulated by the stabilisation of HIF1α (Figure 5). *VEGF* is a HIF1α target gene. Osteoblast-specific overexpression of *HIF1α* showed a progressive increase in bone volume, whereas osteoblast-specific knock down of *HIF1α* leads to a decreased bone diameter in mice. In both cases the amount of bone was directly proportional to the amount of vasculature found, and the upregulation of *HIF1α* led to an increase in the expression of angiogenic factors, including *VEGF* [109,110].

2..4 Effects of hypoxia on MSC, osteoblast and osteoclast proliferation and differentiation

A lot of what we know concerning MSC and osteoblast differentiation is based on cell culture experiments performed under standard culture conditions, which includes 20% oxygen tension. This is considerably higher compared to the physiological oxygen tension to which osteoblasts are exposed, being usually around 1%-10% [104,105,106].

Culturing MSCs, primary osteoblasts or osteoblast cell lines under these lower, more physiological conditions, is usually regarded as a state of hypoxia. Experiments using low levels of oxygen (2%-5%) in general show decreased osteoblast differentiation and mineralization in a wide range of osteoblast cell lines and MSCs.

MSCs cultured under low oxygen tension retain their stemness and pluripotent characteristics, with increased proliferative ratios and an increase in colony forming potential but a decreased expression of osteoblast differentiation markers [137,138]. In addition, life span is prolonged for MSCs cultured on low oxygen [139]. MSCs circulate in the bloodstream, and in animals exposed to prolonged hypoxia, the amount of circulating MSCs drastically increases. This hypoxia-induced mobilisation is MSC-specific, with no concurrent increase in HSC mobilisation [140]. When comparing MSCs isolated from young and old rats cultured under low oxygen tension, MSCs from young rats are more responsive to oxygen changes and maintain their differentiation potential for a longer period of time, indicating that with age MSCs lose their oxygen responsiveness and differentiation potential [141].

Culture experiments with osteoblasts under low oxygen conditions display a decrease in osteoblast differentiation, characterised by a decrease in expression of numerous important osteoblast differentiation markers including *RUNX2*, *ALP* and *BGLAP* [142,143]. In addition, *VEGF* expression is upregulated and mitogen-activated kinase-like protein (MAPK) activated [144,145]. Hypoxia also stimulates the transformation of osteoblasts into osteocytes by increasing the expression of osteocyte markers, such as *DMP1*, *MEPE*, *FGF23* and connexion 43 (*CX43)* [146]. The effect of hypoxia on osteoblast proliferation rate is less conclusive, with some reporting an increase in proliferation rates, while others mention decreased proliferation rates [145,147]. Differences may be caused by variations in the differentiation state of the osteoblastic cells used for the various experiments.

Low oxygen tension affects osteoclast differentiation through osteoblasts. Hypoxia mediates the release of ATP by osteoblasts [148]. Increased extracellular ATP can have a positive effect on osteoclast differentiation and resorption [149]. Hypoxic bone marrow cultures displayed an increase in *IGF2* expression by non-osteoclastic cells that stimulated osteoclast differentiation [150]. Direct effects of hypoxia on osteoclasts include the stimulation of osteoclast differentiation and an increase in osteoclast size [151,152].

2.5 Effects of oxidative stress on osteoblast differentiation, bone formation and resorption

Over the last decade, more and more evidence has become available that links oxidative status (measured by determining plasma levels of i.e. thiobarbituric acid-reactive substances, erythrocyte glutathione, and glutathione peroxidase) of an individual to osteoporotic status. Decreased bone mineral density (BMD) is associated with a higher oxidative stress index value and total plasma oxidant status (i.e. the concentrations of different oxidants in the plasma) in osteoporotic patients [153]. A negative correlation between plasma lipid oxidation and BMD values was observed when comparing osteoporotic women to a healthy control group [154]. Murine *in vivo* experiments confirm these observations, with a decrease in bone formation rates during aging that was accompanied by an increase in ROS levels [155].

Oxidative stress depends on the balance between oxidant production and anti-oxidant activity. Interestingly, in osteoporotic, menopausal women, GPX and CAT activity is decreased [156,157]. Estrogen deficiency leads to a decrease in thiol antioxidant defences, leading to a TNFα-mediated acceleration of bone loss with aging [158]. Last but not least, SOD plasma levels and activity are negatively associated with lumbar spine BMD in humans [159,160].

At the cellular level, ROS affect both osteoblasts and osteoclasts. ROS stimulate the formation and activation of osteoclasts and therefore promote bone resorption [161,162,163]. In fact, RANKL-induced osteoclastogenesis requires ROS production and overexpression of the antioxidant enzyme *GPX1* – the main antioxidant scavenger in osteoclasts – prevents osteoclastogenesis [164,165]. In osteoblasts, increased levels of ROS lead to an increase in *RANKL* expression, indirectly stimulating osteoclastogenesis [161].

Oxidative stress inhibits osteoblast differentiation and matrix mineralization by decreasing the expression of *ALP*, *RUNX2*, *SPP1* and *COL1A1*, reducing the colony forming potential and inhibiting the phosphorylation of RUNX2 [166,167]. Besides differentiation and mineralization, ROS also affect osteoblast lifespan. Overexpression of glutaredoxin 5 (*GLRX5)* – which prevents ROS production – protects osteoblasts from ROS-induced apoptosis, through a SOD2 mediated mechanism [168]. Interestingly, osteoblasts appear to be less well protected against ROS than adipocytes, which can resist higher levels of ROS without dying [169]. ROS also affect matrix formation and mineralization. Deficient SOD function leads to an increase in collagenase expression and a decrease in collagen deposition [170]. ROS-mediated collagen degradation is reduced by SOD3 binding to collagen fibrils, although the production of hydrogen peroxide (H_2O_2) by SOD3 still leads to a certain amount of matrix degradation [122].

Induction of FoxO transcription factors by ROS antagonises Wnt-signalling in osteoblasts,

thereby inhibiting one of the essential stimuli for osteoblastogenesis. Activated FoxOs associate with β-catenin at the expense of Wnt-signalling, to induce FoxO target gene expression [171]. Conditional deletion or overexpression of FoxO genes leads to significant differences in bone mass. Loss of FoxO expression leads to an increase in oxidative stress and osteoblast apoptosis, leading to an osteoporotic phenotype. On the other hand, overexpression of *FOXO3* decreases oxidative stress, increased osteoblast numbers and higher bone formation rates [172].

From the above it is clear that the cellular defence mechanisms are of great importance to maintain normal bone formation and any deficiencies will lead to a disruption of the bone formation - resorption balance.

3. DNA damage and repair

3.1 DNA damage
As mentioned above, oxidative stress is one of many factors that can induce DNA damage which eventually will lead to apoptosis. Other factors are the intrinsic instability of our DNA, environmental and endogenous agents. UV light for example, gives rise to helix distorting cyclobutane pyrimidine dimers (CPDs) and pyrimidine –(6,4)- pyrimidone photoproducts (6-4PPs) (see Figure 7).
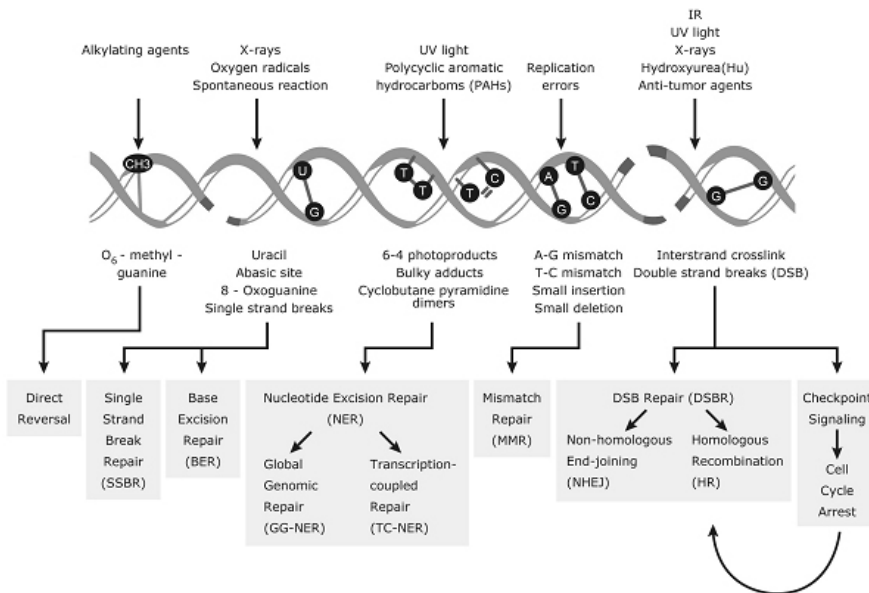
Figure 7: *Several DNA repair pathways protect the cell from the consequences of DNA damage;* different repair pathways are in place to repair a wide variety of DNA lesions that could induce cell cycle arrest, apoptosis or cancer when left untreated. Adapted from www.genetex.com.

Environmental agents, found in polluted air or tobacco smoke induce DNA lesions like cross links and mono-adducts. And sometimes DNA lesions occur spontaneously, without the intervention of a damaging agent, leaving altered, miscoded nucleotides [173]. In conclusion, a wide variety of damaging factors can cause a large variety of DNA lesions.

DNA damage directly affects cell function and can have serious long term consequences. DNA lesions can interfere with DNA transcription and gene expression as well as DNA replication [174,175]. Depending on the extent of the DNA damage, this will lead to dysfunctional cells, which in most cases will lead to cell cycle arrest and induced controlled cell death, better known as apoptosis [5]. Another mechanism that deals with cellular dysfunction after DNA damage is the induction of cellular senescence that leads to a growth arrest, stopping potentially malignant cells from dividing and expanding [6]. Both mechanisms contribute to the process of aging [176]. If DNA lesions are not repaired and the dysfunctional cells are not removed, this can lead to the introduction of mutations which can lead to malignancies like cancer [177].

3.2 DNA repair pathways

DNA damage is counteracted by the cells by a range of DNA repair mechanisms that can repair the wide variety of DNA lesions which are depicted in Figure 7 (reviewed in [7]and [8]). Base excision repair (BER) removes base adducts from ROS, methylation, deamination and hydroxylation and is regarded as the main repair pathway used to repair DNA lesions caused by the cellular metabolism. In BER a number of glycolases recognise and remove non helix-distorting nucleotide modifications from the DNA [178]. In mismatch repair, single base-base mismatches and small insertion/deletion loops are repaired, preventing the formation of mutations.

These mistakes often occur due to slipping of DNA polymerases during replication or recombination [179]. Cross-link repair removes toxic inter-strand cross-links, but its repair mechanism is not yet completely understood. Cross-link repair seems to borrow from several other repair processes, combining a number of their mechanisms for its own purpose [180]. There are at least two double strand break repair mechanisms present in our cells, non-homologous end joining and homologous recombination. They repair double strand breaks that are formed during the replication of single strand breaks or after exposure to ionizing radiation, free radicals or chemicals. Non homologous end joining is not error free due to the fact that it simply joins two DNA ends together, sometimes using small homology. Homologous recombination on the other hand uses the homologous sequence of the sister chromatid to promote accurate repair with little chance of error [181].

Nucleotide excision repair (NER) removes helix-distorting and bulky lesions, caused by exposure to UV light, ROS or chemicals like tobacco smoke [7]. NER has two sub-pathways that differ in the way they recognise the lesions (depicted in Figure 8). On one side there is global genome NER, which employs the RAD23 homolog A or B/xeroderma pigmentosum complementation group C (hHR23B/XPC) complex for lesion recognition, while on the other hand there is transcription-coupled repair which is initiated by the blockage of the elongating RNA polymerase II [183]. Global genome NER repairs lesions throughout the genome, while transcription coupled repair removes lesions during transcription. Independent of the sub-pathway, recognition of the lesion is followed by the recruitment

Chapter 1
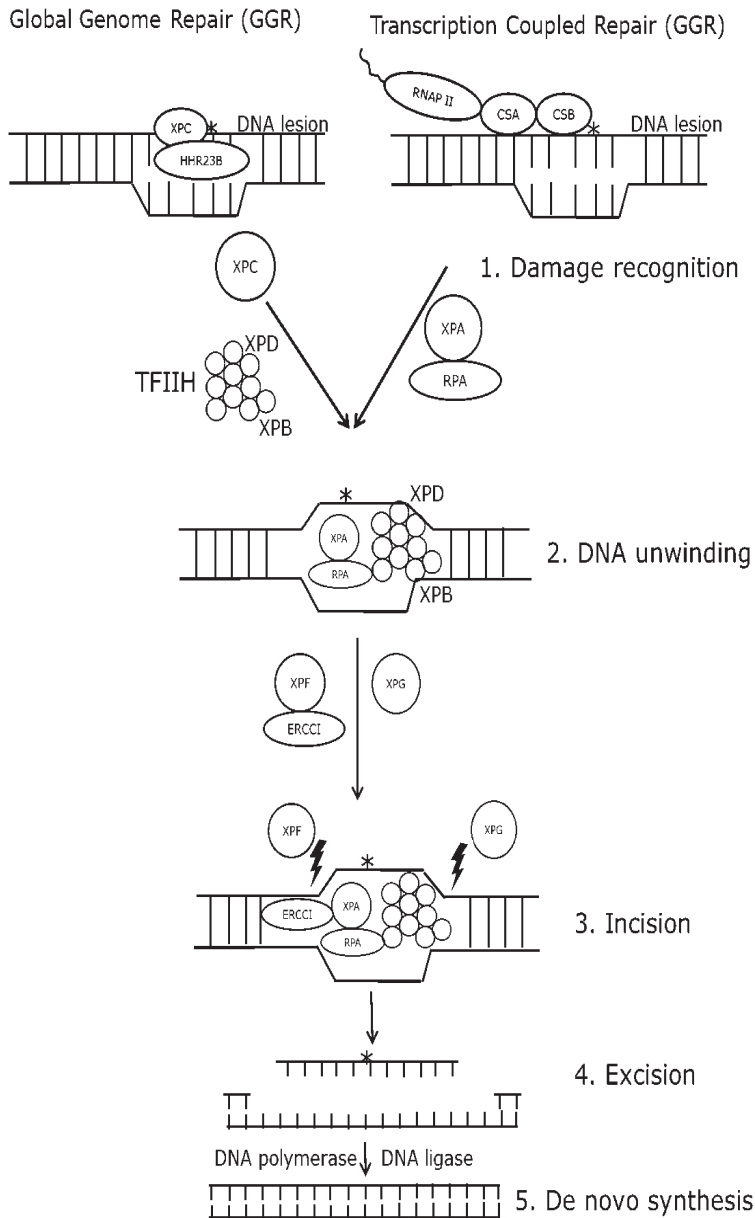
Figure 8: *The nucleotide excision repair (NER) pathway;* the NER pathway has two branches, global genome repair (GGR) and transcription-coupled repair (TCR). Each branch utilises a unique mechanism to recognise DNA damage after which they converge and both use the TFIIH complex to recruit the necessary proteins to locally unwind the DNA helix and excise the damaged piece of DNA followed by filling in of the gap and ligation to the pre-existing strand. Adapted from [182].

of transcription factor IIH (TFIIH), which is build up out of ten subunits and contains xeroderma pigmentosum complementation group B (XPB) and xeroderma pigmentosum complementation group D (XPD) helicases that can unwind the DNA helix at the side of the lesion [184]. Xeroderma pigmentosum complementation group A (XPA) then delimits the area surrounding the lesion, after which the affected region is cleaved 3' and 5' using respectively xeroderma pigmentosum complementation group G (XPG) and excision repair cross-complementing rodent repair deficiency complementation group 1 (ERCC1)/ XPF endonucleases. The gap is filled using ordinary replication machinery and the final nick is sealed using ligase I or III [185].

3.3. Trichothiodystrophy
There are numerous disorders caused by mutations in DNA repair genes, including mutations in NER components. One of these diseases is trichothiodystrophy (TTD), which is caused by phenotype specific mutations in *XPB, XPD, TTDA* and TTD non-photosensitive 1 protein *(TTDN1)*, with a majority having a mutation in *XPD* [186,187,188]. TTD involves a broad spectrum of symptoms and encompasses a number of syndromes. Some of the most common characteristics of TTD are photosensitivity, impaired intelligence, decreased fertility, short stature, scaly skin and brittle hair [189].

Since XPD is a subunit of the TFIIH complex, it plays a dual role. TFIIH is involved in NER, as described above, but also during the initiation of basal transcription. When comparing both processes, the function of XPD is quite different however.

In DNA repair, XPD is an essential component, necessary to unwind the DNA helix at the site of a lesion. In basal transcription, XPD has mostly a structural function, providing complex stability. Due to this functional difference, many *XPD* mutations lead to severe repair defects while they hardly affect transcription and consequently viability [174]. Still, XPD's dual role should always be taken into consideration when studying complex syndromes like TTD. Since more than one component of the TFIIH complex can be involved in TTD, the link between defective basal transcription and the onset of TTD has been firmly established [190]. A number of skeletal abnormalities have been reported in TTD patients, including axial osteosclerosis, peripheral osteopenia, thoracic kyphosis and peripheral osteoporosis [191,192,193].

3.4. The TTD mouse model
Mice carrying a specific point mutation in their XPD gene (Arg722 Trp (R722W)), which is found in several patients, display partial defects in repair and transcription and adequately reflect the human disorder (TTD)[194,195]. Interestingly, these TTD mice develop features of premature aging [196]. After crossing the TTD mice into a pure C57Bl/6 background the overall phenotype of the mice was documented. TTD-specific characteristics were observed, including typical TTD skin lesions like hyperkeratosis, a general decline in condition, cachexia and subsequent anorectal prolapse, a frequent cause of death in TTD mice. A number of phenotypical characteristics pointed towards accelerated aging including kidney and liver abnormalities, osteoporosis, kyphosis, progressive neurological degeneration and a loss of hypodermal fat. Interestingly a third group of characteristics was identified, which pointed towards dietary restriction. This last group of characteristics was however not caused by a difference in food uptake between TTD and control mice [197].

Chapter 1

In TTD mice, bone development seemed to be normal, with no visible skeletal abnormalities in 3 month old mice. At 14 months however, prominent kyphosis and a reduction in the radio density of large parts of the skeleton were observed. Interestingly, the skull of these 14 month old mice displayed a higher radio density, an aging phenomenon called osteosclerosis [198]. The observed kyphosis is likely caused by osteoporosis, but further analysis will be required to validate this hypothesis.

4. Scope of this thesis

In order to gain more insight into the mechanisms and processes involved in effects of oxygen tension and oxidative stress on bone formation, remodelling and aging, we set out to study the effects of low oxygen tension and deficient DNA repair on bone formation, using cellular as well as mouse models.

First, in **chapter 2** we studied the effect of low oxygen tension on osteoblast differentiation and matrix mineralization and determined the effects of hypoxia on ROS production and anti-oxidant protection. The expression of a number of target genes was investigated to determine if hypoxia has a positive or negative effect on several important cellular processes.

Next, in **chapter 3**, we studied the effect of low oxygen tension on osteoblast gene expression during the different stages of osteoblast differentiation, determining the most oxygen responsive phase of differentiation. After dividing the osteoblast differentiation process into three phases, we studied the effect of a variety of low oxygen regimes on gene expression to gain insight into which genes, signalling pathways and biological processes are regulated by a switch in oxygen tension. We also studied the difference between continuous and intermittent low oxygen treatments and their effect on the final differentiation and mineralisation status of the cultures.

Then, to get more insight into the *in vivo* effects of increased oxidative stress on bone formation and aging, we extensively studied the bone phenotype observed in DNA repair deficient TTD mice, comparing the long bones of wild type and TTD mice throughout life. As described above, the processes that regulate bone formation and skeletal aging are often sex-specific. In order to obtain clear results and define sex specific effects of defective DNA repair, we separately analysed female and male mice. In **chapter 4**, we describe the observed effects of defective DNA repair on skeletal aging in female mice, which are then compared to those observed in male mice in **chapter 5.**

5. References

1. Levine JP (2011) Identification, diagnosis, and prevention of osteoporosis. Am J Manag Care 17 Suppl 6: S170-176.
2. Harman D (1956) Aging: a theory based on free radical and radiation chemistry. J Gerontol 11: 298-300.
3. Balaban RS, Nemoto S, Finkel T (2005) Mitochondria, oxidants, and aging. Cell 120: 483-495.
4. Janssen-Heininger YM, Mossman BT, Heintz NH, Forman HJ, Kalyanaraman B, et al. (2008) Redox-based regulation of signal transduction: principles, pitfalls, and promises. Free Radic Biol Med 45: 1-17.
5. Bernstein C, Bernstein H, Payne CM, Garewal H (2002) DNA repair/pro-apoptotic dual-role proteins in five major DNA repair pathways: fail-safe protection against carcinogenesis. Mutat Res 511: 145-178.
6. Campisi J, Kim SH, Lim CS, Rubio M (2001) Cellular senescence, cancer and aging: the telomere connection. Exp Gerontol 36: 1619-1637.
7. Hoeijmakers JH (2001) Genome maintenance mechanisms for preventing cancer. Nature 411: 366-374.
8. Friedberg EC (2003) DNA damage and repair. Nature 421: 436-440.
9. Chen HL, Pistollato F, Hoeppner DJ, Ni HT, McKay RD, et al. (2007) Oxygen tension regulates survival and fate of mouse central nervous system precursors at multiple levels. Stem Cells 25: 2291-2301.
10. Mancino A, Schioppa T, Larghi P, Pasqualini F, Nebuloni M, et al. (2008) Divergent effects of hypoxia on dendritic cell functions. Blood 112: 3723-3734.
11. Sheehy EJ, Buckley CT, Kelly DJ (2012) Oxygen tension regulates the osteogenic, chondrogenic and endochondral phenotype of bone marrow derived mesenchymal stem cells. Biochem Biophys Res Commun 417: 305-310.
12. Bouillon R, Bischoff-Ferrari H, Willett W (2008) Vitamin D and health: perspectives from mice and man. J Bone Miner Res 23: 974-979.
13. Rhee Y, Bivi N, Farrow E, Lezcano V, Plotkin LI, et al. (2011) Parathyroid hormone receptor signaling in osteocytes increases the expression of fibroblast growth factor-23 in vitro and in vivo. Bone 49: 636-643.
14. Shimada T, Hasegawa H, Yamazaki Y, Muto T, Hino R, et al. (2004) FGF-23 is a potent regulator of vitamin D metabolism and phosphate homeostasis. J Bone Miner Res 19: 429-435.
15. Yang Y (2009) Skeletal morphogenesis during embryonic development. Crit Rev Eukaryot Gene Expr 19: 197-218.
16. Martin TJ, Seeman E (2008) Bone remodelling: its local regulation and the emergence of bone fragility. Best Pract Res Clin Endocrinol Metab 22: 701-722.
17. Pittenger MF, Mackay AM, Beck SC, Jaiswal RK, Douglas R, et al. (1999) Multilineage potential of adult human mesenchymal stem cells. Science 284: 143-147.
18. Katagiri T, Yamaguchi A, Ikeda T, Yoshiki S, Wozney JM, et al. (1990) The non-osteogenic mouse pluripotent cell line, C3H10T1/2, is induced to differentiate into osteoblastic cells by recombinant human bone morphogenetic protein-2. Biochem Biophys Res Commun 172: 295-299.
19. Yamaguchi A, Katagiri T, Ikeda T, Wozney JM, Rosen V, et al. (1991) Recombinant human bone morphogenetic protein-2 stimulates osteoblastic maturation and inhibits myogenic differentiation in vitro. J Cell Biol 113: 681-687.
20. Ducy P, Zhang R, Geoffroy V, Ridall AL, Karsenty G (1997) Osf2/Cbfa1: a transcriptional activator of osteoblast differentiation. Cell 89: 747-754.
21. Komori T, Yagi H, Nomura S, Yamaguchi A, Sasaki K, et al. (1997) Targeted disruption of Cbfa1 results in a complete lack of bone formation owing to maturational arrest of osteoblasts. Cell 89: 755-764.
22. Nishio Y, Dong Y, Paris M, O'Keefe RJ, Schwarz EM, et al. (2006) Runx2-mediated regulation of the zinc finger Osterix/Sp7 gene. Gene 372: 62-70.
23. Nakashima K, Zhou X, Kunkel G, Zhang Z, Deng JM, et al. (2002) The novel zinc finger-containing transcription factor osterix is required for osteoblast differentiation and bone formation. Cell 108: 17-29.
24. Westendorf JJ, Kahler RA, Schroeder TM (2004) Wnt signaling in osteoblasts and bone diseases. Gene 341: 19-39.
25. van der Horst G, van der Werf SM, Farih-Sips H, van Bezooijen RL, Lowik CW, et al. (2005) Downregulation of Wnt signaling by increased expression of Dickkopf-1 and -2 is a prerequisite for late-stage osteoblast differentiation of KS483 cells. J Bone Miner Res 20: 1867-1877.
26. Rawadi G, Vayssiere B, Dunn F, Baron R, Roman-Roman S (2003) BMP-2 controls alkaline phosphatase

expression and osteoblast mineralization by a Wnt autocrine loop. J Bone Miner Res 18: 1842-1853.

27. Jilka RL, Weinstein RS, Parfitt AM, Manolagas SC (2007) Quantifying osteoblast and osteocyte apoptosis: challenges and rewards. J Bone Miner Res 22: 1492-1501.
28. Miller SC, Jee WS (1987) The bone lining cell: a distinct phenotype? Calcif Tissue Int 41: 1-5.
29. Aubin JE LF (1996) The osteoblast lineage. In: Bilezikian JP R, LG, Rodan GA, editor. The principles of bone biology. Toronto: Academic Press.
30. Inoue K, Mikuni-Takagaki Y, Oikawa K, Itoh T, Inada M, et al. (2006) A crucial role for matrix metalloproteinase 2 in osteocytic canalicular formation and bone metabolism. J Biol Chem 281: 33814-33824.
31. Petersen DN, Tkalcevic GT, Mansolf AL, Rivera-Gonzalez R, Brown TA (2000) Identification of osteoblast/osteocyte factor 45 (OF45), a bone-specific cDNA encoding an RGD-containing protein that is highly expressed in osteoblasts and osteocytes. J Biol Chem 275: 36172-36180.
32. Toyosawa S, Shintani S, Fujiwara T, Ooshima T, Sato A, et al. (2001) Dentin matrix protein 1 is predominantly expressed in chicken and rat osteocytes but not in osteoblasts. J Bone Miner Res 16: 2017-2026.
33. Franz-Odendaal TA, Hall BK, Witten PE (2006) Buried alive: how osteoblasts become osteocytes. Dev Dyn 235: 176-190.
34. Lanyon LE (1993) Osteocytes, strain detection, bone modeling and remodeling. Calcif Tissue Int 53 Suppl 1: S102-106; discussion S106-107.
35. Carter DR, Hayes WC (1977) Compact bone fatigue damage--I. Residual strength and stiffness. J Biomech 10: 325-337.
36. Frost HM (1960) Presence of microscopic cracks in vivo in bone. Henry Ford Hosp Bull 8: 27-35.
37. Reilly GC, Currey JD (2000) The effects of damage and microcracking on the impact strength of bone. J Biomech 33: 337-343.
38. Schaffler MB, Radin EL, Burr DB (1989) Mechanical and morphological effects of strain rate on fatigue of compact bone. Bone 10: 207-214.
39. Burr DB, Martin RB, Schaffler MB, Radin EL (1985) Bone remodeling in response to in vivo fatigue microdamage. J Biomech 18: 189-200.
40. Burr DB MR (1993) Calculating the probability that microcracks initiate resorption spaces. J Biomech Apr-May;26(4-5):: 613-616.
41. Parfitt AM (2001) The bone remodeling compartment: a circulatory function for bone lining cells. J Bone Miner Res 16: 1583-1585.
42. Noble B (2005) Microdamage and apoptosis. Eur J Morphol 42: 91-98.
43. Al-Dujaili SA, Lau E, Al-Dujaili H, Tsang K, Guenther A, et al. (2011) Apoptotic osteocytes regulate osteoclast precursor recruitment and differentiation in vitro. J Cell Biochem 112: 2412-2423.
44. Balemans W, Ebeling M, Patel N, Van Hul E, Olson P, et al. (2001) Increased bone density in sclerosteosis is due to the deficiency of a novel secreted protein (SOST). Hum Mol Genet 10: 537-543.
45. Bai X, Miao D, Li J, Goltzman D, Karaplis AC (2004) Transgenic mice overexpressing human fibroblast growth factor 23 (R176Q) delineate a putative role for parathyroid hormone in renal phosphate wasting disorders. Endocrinology 145: 5269-5279.
46. White KE, Larsson TE, Econs MJ (2006) The roles of specific genes implicated as circulating factors involved in normal and disordered phosphate homeostasis: frizzled related protein-4, matrix extracellular phosphoglycoprotein, and fibroblast growth factor 23. Endocr Rev 27: 221-241.
47. Yamazaki Y, Okazaki R, Shibata M, Hasegawa Y, Satoh K, et al. (2002) Increased circulatory level of biologically active full-length FGF-23 in patients with hypophosphatemic rickets/osteomalacia. J Clin Endocrinol Metab 87: 4957-4960.
48. Liu S, Tang W, Zhou J, Stubbs JR, Luo Q, et al. (2006) Fibroblast growth factor 23 is a counter-regulatory phosphaturic hormone for vitamin D. J Am Soc Nephrol 17: 1305-1315.
49. Dobnig H, Turner RT (1995) Evidence that intermittent treatment with parathyroid hormone increases bone formation in adult rats by activation of bone lining cells. Endocrinology 136: 3632-3638.
50. Kim SW, Pajevic PD, Selig M, Barry KJ, Yang JY, et al. (2012) Intermittent PTH administration converts quiescent lining cells to active osteoblasts. J Bone Miner Res.
51. Nakashima T, Hayashi M, Fukunaga T, Kurata K, Oh-Hora M, et al. (2011) Evidence for osteocyte regulation of bone homeostasis through RANKL expression. Nat Med 17: 1231-1234.
52. Boyle WJ, Simonet WS, Lacey DL (2003) Osteoclast differentiation and activation. Nature 423: 337-342.

53. Cao J, Venton L, Sakata T, Halloran BP (2003) Expression of RANKL and OPG correlates with age-related bone loss in male C57BL/6 mice. J Bone Miner Res 18: 270-277.
54. Hill PA (1998) Bone remodelling. Br J Orthod 25: 101-107.
55. Harada S, Rodan GA (2003) Control of osteoblast function and regulation of bone mass. Nature 423: 349-355.
56. Clarke B (2008) Normal bone anatomy and physiology. Clin J Am Soc Nephrol 3 Suppl 3: S131-139.
57. Qin C, Baba O, Butler WT (2004) Post-translational modifications of sibling proteins and their roles in osteogenesis and dentinogenesis. Crit Rev Oral Biol Med 15: 126-136.
58. Alves RD, Demmers JA, Bezstarosti K, van der Eerden BC, Verhaar JA, et al. (2011) Unraveling the human bone microenvironment beyond the classical extracellular matrix proteins: a human bone protein library. J Proteome Res 10: 4725-4733.
59. Giannelli G, Falk-Marzillier J, Schiraldi O, Stetler-Stevenson WG, Quaranta V (1997) Induction of cell migration by matrix metalloprotease-2 cleavage of laminin-5. Science 277: 225-228.
60. Levi E, Fridman R, Miao HQ, Ma YS, Yayon A, et al. (1996) Matrix metalloproteinase 2 releases active soluble ectodomain of fibroblast growth factor receptor 1. Proc Natl Acad Sci U S A 93: 7069-7074.
61. Lochter A, Galosy S, Muschler J, Freedman N, Werb Z, et al. (1997) Matrix metalloproteinase stromelysin-1 triggers a cascade of molecular alterations that leads to stable epithelial-to-mesenchymal conversion and a premalignant phenotype in mammary epithelial cells. J Cell Biol 139: 1861-1872.
62. Powell WC, Fingleton B, Wilson CL, Boothby M, Matrisian LM (1999) The metalloproteinase matrilysin proteolytically generates active soluble Fas ligand and potentiates epithelial cell apoptosis. Curr Biol 9: 1441-1447.
63. Suzuki M, Raab G, Moses MA, Fernandez CA, Klagsbrun M (1997) Matrix metalloproteinase-3 releases active heparin-binding EGF-like growth factor by cleavage at a specific juxtamembrane site. J Biol Chem 272: 31730-31737.
64. Holmbeck K, Bianco P, Caterina J, Yamada S, Kromer M, et al. (1999) MT1-MMP-deficient mice develop dwarfism, osteopenia, arthritis, and connective tissue disease due to inadequate collagen turnover. Cell 99: 81-92.
65. Mosig RA, Dowling O, DiFeo A, Ramirez MC, Parker IC, et al. (2007) Loss of MMP-2 disrupts skeletal and craniofacial development and results in decreased bone mineralization, joint erosion and defects in osteoblast and osteoclast growth. Hum Mol Genet 16: 1113-1123.
66. Stickens D, Behonick DJ, Ortega N, Heyer B, Hartenstein B, et al. (2004) Altered endochondral bone development in matrix metalloproteinase 13-deficient mice. Development 131: 5883-5895.
67. Zhou Z, Apte SS, Soininen R, Cao R, Baaklini GY, et al. (2000) Impaired endochondral ossification and angiogenesis in mice deficient in membrane-type matrix metalloproteinase I. Proc Natl Acad Sci U S A 97: 4052-4057.
68. Gorski JP (1998) Is all bone the same? Distinctive distributions and properties of non-collagenous matrix proteins in lamellar vs. woven bone imply the existence of different underlying osteogenic mechanisms. Crit Rev Oral Biol Med 9: 201-223.
69. Smith JW (1960) Collagen fibre patterns in mammalian bone. J Anat 94: 329-344.
70. Orwoll ES (2003) Toward an expanded understanding of the role of the periosteum in skeletal health. J Bone Miner Res 18: 949-954.
71. Riggs BL, Khosla S, Melton LJ, 3rd (2002) Sex steroids and the construction and conservation of the adult skeleton. Endocr Rev 23: 279-302.
72. Turner RT (1999) Mice, estrogen, and postmenopausal osteoporosis. J Bone Miner Res 14: 187-191.
73. Vidal O, Lindberg MK, Hollberg K, Baylink DJ, Andersson G, et al. (2000) Estrogen receptor specificity in the regulation of skeletal growth and maturation in male mice. Proc Natl Acad Sci U S A 97: 5474-5479.
74. Lee KC, Jessop H, Suswillo R, Zaman G, Lanyon LE (2004) The adaptive response of bone to mechanical loading in female transgenic mice is deficient in the absence of oestrogen receptor-alpha and -beta. J Endocrinol 182: 193-201.
75. Chan GK, Duque G (2002) Age-related bone loss: old bone, new facts. Gerontology 48: 62-71.
76. Perry RJ, Farquharson C, Ahmed SF (2008) The role of sex steroids in controlling pubertal growth. Clin Endocrinol (Oxf) 68: 4-15.
77. Manolagas SC (2000) Birth and death of bone cells: basic regulatory mechanisms and implications for the pathogenesis and treatment of osteoporosis. Endocr Rev 21: 115-137.

78. Hoff AO, Catala-Lehnen P, Thomas PM, Priemel M, Rueger JM, et al. (2002) Increased bone mass is an unexpected phenotype associated with deletion of the calcitonin gene. J Clin Invest 110: 1849-1857.

79. Drake MT, Srinivasan B, Modder UI, Ng AC, Undale AH, et al. (2011) Effects of intermittent parathyroid hormone treatment on osteoprogenitor cells in postmenopausal women. Bone 49: 349-355.

80. Goltzman D, Miao D, Panda DK, Hendy GN (2004) Effects of calcium and of the Vitamin D system on skeletal and calcium homeostasis: lessons from genetic models. J Steroid Biochem Mol Biol 89-90: 485-489.

81. Suda T, Ueno Y, Fujii K, Shinki T (2003) Vitamin D and bone. J Cell Biochem 88: 259-266.

82. van Driel M, Koedam M, Buurman CJ, Roelse M, Weyts F, et al. (2006) Evidence that both 1alpha,25-dihydroxyvitamin D3 and 24-hydroxylated D3 enhance human osteoblast differentiation and mineralization. J Cell Biochem 99: 922-935.

83. Toogood AA (2003) Growth hormone (GH) status and body composition in normal ageing and in elderly adults with GH deficiency. Horm Res 60: 105-111.

84. Zofkova I (2003) Pathophysiological and clinical importance of insulin-like growth factor-I with respect to bone metabolism. Physiol Res 52: 657-679.

85. Hill PA, Tumber A, Meikle MC (1997) Multiple extracellular signals promote osteoblast survival and apoptosis. Endocrinology 138: 3849-3858.

86. Yang S, Xu H, Yu S, Cao H, Fan J, et al. (2011) Foxo1 mediates insulin-like growth factor 1 (IGF1)/insulin regulation of osteocalcin expression by antagonizing Runx2 in osteoblasts. J Biol Chem 286: 19149-19158.

87. Zhang M, Xuan S, Bouxsein ML, von Stechow D, Akeno N, et al. (2002) Osteoblast-specific knockout of the insulin-like growth factor (IGF) receptor gene reveals an essential role of IGF signaling in bone matrix mineralization. J Biol Chem 277: 44005-44012.

88. Hill PA, Reynolds JJ, Meikle MC (1995) Osteoblasts mediate insulin-like growth factor-I and -II stimulation of osteoclast formation and function. Endocrinology 136: 124-131.

89. Geusens PP, Boonen S (2002) Osteoporosis and the growth hormone-insulin-like growth factor axis. Horm Res 58 Suppl 3: 49-55.

90. Leininger GM (2009) Location, location, location: the CNS sites of leptin action dictate its regulation of homeostatic and hedonic pathways. Int J Obes (Lond) 33 Suppl 2: S14-17.

91. Steppan CM, Crawford DT, Chidsey-Frink KL, Ke H, Swick AG (2000) Leptin is a potent stimulator of bone growth in ob/ob mice. Regul Pept 92: 73-78.

92. Hamrick MW, Ferrari SL (2008) Leptin and the sympathetic connection of fat to bone. Osteoporos Int 19: 905-912.

93. Welt CK, Chan JL, Bullen J, Murphy R, Smith P, et al. (2004) Recombinant human leptin in women with hypothalamic amenorrhea. N Engl J Med 351: 987-997.

94. Elefteriou F, Ahn JD, Takeda S, Starbuck M, Yang X, et al. (2005) Leptin regulation of bone resorption by the sympathetic nervous system and CART. Nature 434: 514-520.

95. Takeda S, Elefteriou F, Levasseur R, Liu X, Zhao L, et al. (2002) Leptin regulates bone formation via the sympathetic nervous system. Cell 111: 305-317.

96. van der Velde M, van der Eerden BC, Sun Y, Almering JM, van der Lely AJ, et al. (2012) An Age-Dependent Interaction with Leptin Unmasks Ghrelin's Bone-Protective Effects. Endocrinology 153: 3593-3602.

97. Hamrick MW, Pennington C, Newton D, Xie D, Isales C (2004) Leptin deficiency produces contrasting phenotypes in bones of the limb and spine. Bone 34: 376-383.

98. Riggs BL (2002) Endocrine causes of age-related bone loss and osteoporosis. Novartis Found Symp 242: 247-259; discussion 260-244.

99. Heyman SN, Khamaisi M, Rosen S, Rosenberger C (2008) Renal parenchymal hypoxia, hypoxia response and the progression of chronic kidney disease. Am J Nephrol 28: 998-1006.

100. Muz B, Khan MN, Kiriakidis S, Paleolog EM (2009) Hypoxia. The role of hypoxia and HIF-dependent signalling events in rheumatoid arthritis. Arthritis Res Ther 11: 201.

101. Cipolleschi MG, Dello Sbarba P, Olivotto M (1993) The role of hypoxia in the maintenance of hematopoietic stem cells. Blood 82: 2031-2037.

102. Grant JL, Smith B (1963) Bone marrow gas tensions, bone marrow blood flow, and erythropoiesis in man. Ann Intern Med 58: 801-809.

103. Kofoed H, Sjontoft E, Siemssen SO, Olesen HP (1985) Bone marrow circulation after osteotomy. Blood

flow, pO2, pCO2, and pressure studied in dogs. Acta Orthop Scand 56: 400-403.

104. Chow DC, Wenning LA, Miller WM, Papoutsakis ET (2001) Modeling pO(2) distributions in the bone marrow hematopoietic compartment. II. Modified Kroghian models. Biophys J 81: 685-696.

105. Chow DC, Wenning LA, Miller WM, Papoutsakis ET (2001) Modeling pO(2) distributions in the bone marrow hematopoietic compartment. I. Krogh's model. Biophys J 81: 675-684.

106. Harrison JS, Rameshwar P, Chang V, Bandari P (2002) Oxygen saturation in the bone marrow of healthy volunteers. Blood 99: 394.

107. Parmar K, Mauch P, Vergilio JA, Sackstein R, Down JD (2007) Distribution of hematopoietic stem cells in the bone marrow according to regional hypoxia. Proc Natl Acad Sci U S A 104: 5431-5436.

108. Semenza GL (1998) Hypoxia-inducible factor 1: master regulator of O2 homeostasis. Curr Opin Genet Dev 8: 588-594.

109. Wang Y, Wan C, Deng L, Liu X, Cao X, et al. (2007) The hypoxia-inducible factor alpha pathway couples angiogenesis to osteogenesis during skeletal development. J Clin Invest 117: 1616-1626.

110. Wang Y, Wan C, Gilbert SR, Clemens TL (2007) Oxygen sensing and osteogenesis. Ann N Y Acad Sci 1117: 1-11.

111. Turrens JF (1997) Superoxide production by the mitochondrial respiratory chain. Biosci Rep 17: 3-8.

112. Boveris A, Chance B (1973) The mitochondrial generation of hydrogen peroxide. General properties and effect of hyperbaric oxygen. Biochem J 134: 707-716.

113. St-Pierre J, Buckingham JA, Roebuck SJ, Brand MD (2002) Topology of superoxide production from different sites in the mitochondrial electron transport chain. J Biol Chem 277: 44784-44790.

114. Dada LA, Chandel NS, Ridge KM, Pedemonte C, Bertorello AM, et al. (2003) Hypoxia-induced endocytosis of Na,K-ATPase in alveolar epithelial cells is mediated by mitochondrial reactive oxygen species and PKC-zeta. J Clin Invest 111: 1057-1064.

115. Nemoto S, Takeda K, Yu ZX, Ferrans VJ, Finkel T (2000) Role for mitochondrial oxidants as regulators of cellular metabolism. Mol Cell Biol 20: 7311-7318.

116. Werner E, Werb Z (2002) Integrins engage mitochondrial function for signal transduction by a mechanism dependent on Rho GTPases. J Cell Biol 158: 357-368.

117. Stadtman ER (1992) Protein oxidation and aging. Science 257: 1220-1224.

118. Cadet J, Douki T, Gasparutto D, Ravanat JL (2003) Oxidative damage to DNA: formation, measurement and biochemical features. Mutat Res 531: 5-23.

119. Beckman KB, Ames BN (1998) The free radical theory of aging matures. Physiol Rev 78: 547-581.

120. Valko M, Leibfritz D, Moncol J, Cronin MT, Mazur M, et al. (2007) Free radicals and antioxidants in normal physiological functions and human disease. Int J Biochem Cell Biol 39: 44-84.

121. Fukai T, Ushio-Fukai M (2011) Superoxide dismutases: role in redox signaling, vascular function, and diseases. Antioxid Redox Signal 15: 1583-1606.

122. Petersen SV, Oury TD, Ostergaard L, Valnickova Z, Wegrzyn J, et al. (2004) Extracellular superoxide dismutase (EC-SOD) binds to type i collagen and protects against oxidative fragmentation. J Biol Chem 279: 13705-13710.

123. Mates JM, Sanchez-Jimenez F (1999) Antioxidant enzymes and their implications in pathophysiologic processes. Front Biosci 4: D339-345.

124. Frei B, England L, Ames BN (1989) Ascorbate is an outstanding antioxidant in human blood plasma. Proc Natl Acad Sci U S A 86: 6377-6381.

125. Miwa H, Fujii J, Kanno H, Taniguchi N, Aozasa K (2000) Pyruvate secreted by human lymphoid cell lines protects cells from hydrogen peroxide mediated cell death. Free Radic Res 33: 45-56.

126. van der Horst A, Burgering BM (2007) Stressing the role of FoxO proteins in lifespan and disease. Nat Rev Mol Cell Biol 8: 440-450.

127. Salih DA, Brunet A (2008) FoxO transcription factors in the maintenance of cellular homeostasis during aging. Curr Opin Cell Biol 20: 126-136.

128. Emerling BM, Weinberg F, Liu JL, Mak TW, Chandel NS (2008) PTEN regulates p300-dependent hypoxia-inducible factor 1 transcriptional activity through Forkhead transcription factor 3a (FOXO3a). Proc Natl Acad Sci U S A 105: 2622-2627.

129. Paik JH, Kollipara R, Chu G, Ji H, Xiao Y, et al. (2007) FoxOs are lineage-restricted redundant tumor suppressors and regulate endothelial cell homeostasis. Cell 128: 309-323.

130. Gerber HP, Vu TH, Ryan AM, Kowalski J, Werb Z, et al. (1999) VEGF couples hypertrophic cartilage remodeling, ossification and angiogenesis during endochondral bone formation. Nat Med 5: 623-628.

131. Trueta J, Trias A (1961) The vascular contribution to osteogenesis. IV. The effect of pressure upon the epiphysial cartilage of the rabbit. J Bone Joint Surg Br 43-B: 800-813.
132. Eriksen EF, Eghbali-Fatourechi GZ, Khosla S (2007) Remodeling and vascular spaces in bone. J Bone Miner Res 22: 1-6.
133. Hauge EM, Qvesel D, Eriksen EF, Mosekilde L, Melsen F (2001) Cancellous bone remodeling occurs in specialized compartments lined by cells expressing osteoblastic markers. J Bone Miner Res 16: 1575-1582.
134. Street J, Bao M, deGuzman L, Bunting S, Peale FV, Jr., et al. (2002) Vascular endothelial growth factor stimulates bone repair by promoting angiogenesis and bone turnover. Proc Natl Acad Sci U S A 99: 9656-9661.
135. Mayr-Wohlfart U, Waltenberger J, Hausser H, Kessler S, Gunther KP, et al. (2002) Vascular endothelial growth factor stimulates chemotactic migration of primary human osteoblasts. Bone 30: 472-477.
136. Midy V, Plouet J (1994) Vasculotropin/vascular endothelial growth factor induces differentiation in cultured osteoblasts. Biochem Biophys Res Commun 199: 380-386.
137. D'Ippolito G, Diabira S, Howard GA, Roos BA, Schiller PC (2006) Low oxygen tension inhibits osteogenic differentiation and enhances stemness of human MIAMI cells. Bone 39: 513-522.
138. Krinner A, Zscharnack M, Bader A, Drasdo D, Galle J (2009) Impact of oxygen environment on mesenchymal stem cell expansion and chondrogenic differentiation. Cell Prolif 42: 471-484.
139. Fehrer C, Brunauer R, Laschober G, Unterluggauer H, Reitinger S, et al. (2007) Reduced oxygen tension attenuates differentiation capacity of human mesenchymal stem cells and prolongs their lifespan. Aging Cell 6: 745-757.
140. Rochefort GY, Delorme B, Lopez A, Herault O, Bonnet P, et al. (2006) Multipotential mesenchymal stem cells are mobilized into peripheral blood by hypoxia. Stem Cells 24: 2202-2208.
141. Jiang S, Kh Haider H, Ahmed RP, Idris NM, Salim A, et al. (2008) Transcriptional profiling of young and old mesenchymal stem cells in response to oxygen deprivation and reparability of the infarcted myocardium. J Mol Cell Cardiol 44: 582-596.
142. Gruber R, Kandler B, Agis H, Fischer MB, Watzek G (2008) Bone cell responsiveness to growth and differentiation factors under hypoxia in vitro. Int J Oral Maxillofac Implants 23: 417-426.
143. Salim A, Nacamuli RP, Morgan EF, Giaccia AJ, Longaker MT (2004) Transient changes in oxygen tension inhibit osteogenic differentiation and Runx2 expression in osteoblasts. J Biol Chem 279: 40007-40016.
144. Matsuda N, Morita N, Matsuda K, Watanabe M (1998) Proliferation and differentiation of human osteoblastic cells associated with differential activation of MAP kinases in response to epidermal growth factor, hypoxia, and mechanical stress in vitro. Biochem Biophys Res Commun 249: 350-354.
145. Steinbrech DS, Mehrara BJ, Saadeh PB, Chin G, Dudziak ME, et al. (1999) Hypoxia regulates VEGF expression and cellular proliferation by osteoblasts in vitro. Plast Reconstr Surg 104: 738-747.
146. Hirao M, Hashimoto J, Yamasaki N, Ando W, Tsuboi H, et al. (2007) Oxygen tension is an important mediator of the transformation of osteoblasts to osteocytes. J Bone Miner Metab 25: 266-276.
147. Utting JC, Robins SP, Brandao-Burch A, Orriss IR, Behar J, et al. (2006) Hypoxia inhibits the growth, differentiation and bone-forming capacity of rat osteoblasts. Exp Cell Res 312: 1693-1702.
148. Orriss IR, Knight GE, Ranasinghe S, Burnstock G, Arnett TR (2006) Osteoblast responses to nucleotides increase during differentiation. Bone 39: 300-309.
149. Morrison MS, Turin L, King BF, Burnstock G, Arnett TR (1998) ATP is a potent stimulator of the activation and formation of rodent osteoclasts. J Physiol 511 (Pt 2): 495-500.
150. Fukuoka H, Aoyama M, Miyazawa K, Asai K, Goto S (2005) Hypoxic stress enhances osteoclast differentiation via increasing IGF2 production by non-osteoclastic cells. Biochem Biophys Res Commun 328: 885-894.
151. Arnett TR, Gibbons DC, Utting JC, Orriss IR, Hoebertz A, et al. (2003) Hypoxia is a major stimulator of osteoclast formation and bone resorption. J Cell Physiol 196: 2-8.
152. Bozec A, Bakiri L, Hoebertz A, Eferl R, Schilling AF, et al. (2008) Osteoclast size is controlled by Fra-2 through LIF/LIF-receptor signalling and hypoxia. Nature 454: 221-225.
153. Altindag O, Erel O, Soran N, Celik H, Selek S (2008) Total oxidative/anti-oxidative status and relation to bone mineral density in osteoporosis. Rheumatol Int 28: 317-321.
154. Sendur OF, Turan Y, Tastaban E, Serter M (2009) Antioxidant status in patients with osteoporosis: a

controlled study. Joint Bone Spine 76: 514-518.

155. Almeida M, Han L, Martin-Millan M, Plotkin LI, Stewart SA, et al. (2007) Skeletal involution by age-associated oxidative stress and its acceleration by loss of sex steroids. J Biol Chem 282: 27285-27297.

156. Ozgocmen S, Kaya H, Fadillioglu E, Aydogan R, Yilmaz Z (2007) Role of antioxidant systems, lipid peroxidation, and nitric oxide in postmenopausal osteoporosis. Mol Cell Biochem 295: 45-52.

157. Ozgocmen S, Kaya H, Fadillioglu E, Yilmaz Z (2007) Effects of calcitonin, risedronate, and raloxifene on erythrocyte antioxidant enzyme activity, lipid peroxidation, and nitric oxide in postmenopausal osteoporosis. Arch Med Res 38: 196-205.

158. Jagger CJ, Lean JM, Davies JT, Chambers TJ (2005) Tumor necrosis factor-alpha mediates osteopenia caused by depletion of antioxidants. Endocrinology 146: 113-118.

159. Sanchez-Rodriguez MA, Ruiz-Ramos M, Correa-Munoz E, Mendoza-Nunez VM (2007) Oxidative stress as a risk factor for osteoporosis in elderly Mexicans as characterized by antioxidant enzymes. BMC Musculoskelet Disord 8: 124.

160. Yalin S, Bagis S, Polat G, Dogruer N, Cenk Aksit S, et al. (2005) Is there a role of free oxygen radicals in primary male osteoporosis? Clin Exp Rheumatol 23: 689-692.

161. Bai XC, Lu D, Liu AL, Zhang ZM, Li XM, et al. (2005) Reactive oxygen species stimulates receptor activator of NF-kappaB ligand expression in osteoblast. J Biol Chem 280: 17497-17506.

162. Garrett IR, Boyce BF, Oreffo RO, Bonewald L, Poser J, et al. (1990) Oxygen-derived free radicals stimulate osteoclastic bone resorption in rodent bone in vitro and in vivo. J Clin Invest 85: 632-639.

163. Ha H, Kwak HB, Lee SW, Jin HM, Kim HM, et al. (2004) Reactive oxygen species mediate RANK signaling in osteoclasts. Exp Cell Res 301: 119-127.

164. Lean JM, Jagger CJ, Kirstein B, Fuller K, Chambers TJ (2005) Hydrogen peroxide is essential for estrogen-deficiency bone loss and osteoclast formation. Endocrinology 146: 728-735.

165. Lee NK, Choi YG, Baik JY, Han SY, Jeong DW, et al. (2005) A crucial role for reactive oxygen species in RANKL-induced osteoclast differentiation. Blood 106: 852-859.

166. Arai M, Shibata Y, Pugdee K, Abiko Y, Ogata Y (2007) Effects of reactive oxygen species (ROS) on antioxidant system and osteoblastic differentiation in MC3T3-E1 cells. IUBMB Life 59: 27-33.

167. Liu AL, Zhang ZM, Zhu BF, Liao ZH, Liu Z (2004) Metallothionein protects bone marrow stromal cells against hydrogen peroxide-induced inhibition of osteoblastic differentiation. Cell Biol Int 28: 905-911.

168. Linares GR, Xing W, Govoni KE, Chen ST, Mohan S (2009) Glutaredoxin 5 regulates osteoblast apoptosis by protecting against oxidative stress. Bone 44: 795-804.

169. Bruedigam C, Eijken M, Koedam M, van de Peppel J, Drabek K, et al. (2010) A new concept underlying stem cell lineage skewing that explains the detrimental effects of thiazolidinediones on bone. Stem Cells 28: 916-927.

170. Dasgupta J, Kar S, Van Remmen H, Melendez JA (2009) Age-dependent increases in interstitial collagenase and MAP Kinase levels are exacerbated by superoxide dismutase deficiencies. Exp Gerontol 44: 503-510.

171. Almeida M, Han L, Martin-Millan M, O'Brien CA, Manolagas SC (2007) Oxidative stress antagonizes Wnt signaling in osteoblast precursors by diverting beta-catenin from T cell factor- to forkhead box O-mediated transcription. J Biol Chem 282: 27298-27305.

172. Ambrogini E, Almeida M, Martin-Millan M, Paik JH, Depinho RA, et al. (2010) FoxO-mediated defense against oxidative stress in osteoblasts is indispensable for skeletal homeostasis in mice. Cell Metab 11: 136-146.

173. Lindahl T (1993) Instability and decay of the primary structure of DNA. Nature 362: 709-715.

174. Lehmann AR (1979) The relationship between pyrimidine dimers and replicating DNA in UV-irradiated human fibroblasts. Nucleic Acids Res 7: 1901-1912.

175. Mayne LV, Lehmann AR, Waters R (1982) Excision repair in Cockayne syndrome. Mutat Res 106: 179-189.

176. Hasty P, Campisi J, Hoeijmakers J, van Steeg H, Vijg J (2003) Aging and genome maintenance: lessons from the mouse? Science 299: 1355-1359.

177. Mitchell JR, Hoeijmakers JH, Niedernhofer LJ (2003) Divide and conquer: nucleotide excision repair battles cancer and ageing. Curr Opin Cell Biol 15: 232-240.

178. Krokan HE, Nilsen H, Skorpen F, Otterlei M, Slupphaug G (2000) Base excision repair of DNA in mammalian cells. FEBS Lett 476: 73-77.

179. Marti TM, Kunz C, Fleck O (2002) DNA mismatch repair and mutation avoidance pathways. J Cell Physiol 191: 28-41.

180. Niedernhofer LJ, Lalai AS, Hoeijmakers JH (2005) Fanconi anemia (cross)linked to DNA repair. Cell 123: 1191-1198.

181. Valerie K, Povirk LF (2003) Regulation and mechanisms of mammalian double-strand break repair. Oncogene 22: 5792-5812.

182. van Steeg H (2001) The role of nucleotide excision repair and loss of p53 in mutagenesis and carcinogenesis. Toxicol Lett 120: 209-219.

183. Bohr VA, Smith CA, Okumoto DS, Hanawalt PC (1985) DNA repair in an active gene: removal of pyrimidine dimers from the DHFR gene of CHO cells is much more efficient than in the genome overall. Cell 40: 359-369.

184. Coin F, Oksenych V, Egly JM (2007) Distinct roles for the XPB/p52 and XPD/p44 subcomplexes of TFIIH in damaged DNA opening during nucleotide excision repair. Mol Cell 26: 245-256.

185. Moser J, Kool H, Giakzidis I, Caldecott K, Mullenders LH, et al. (2007) Sealing of chromosomal DNA nicks during nucleotide excision repair requires XRCC1 and DNA ligase III alpha in a cell-cycle-specific manner. Mol Cell 27: 311-323.

186. Nakabayashi K, Amann D, Ren Y, Saarialho-Kere U, Avidan N, et al. (2005) Identification of C7orf11 (TTDN1) gene mutations and genetic heterogeneity in nonphotosensitive trichothiodystrophy. Am J Hum Genet 76: 510-516.

187. Stefanini M, Lagomarsini P, Arlett CF, Marinoni S, Borrone C, et al. (1986) Xeroderma pigmentosum (complementation group D) mutation is present in patients affected by trichothiodystrophy with photosensitivity. Hum Genet 74: 107-112.

188. Weeda G, Eveno E, Donker I, Vermeulen W, Chevallier-Lagente O, et al. (1997) A mutation in the XPB/ERCC3 DNA repair transcription gene, associated with trichothiodystrophy. Am J Hum Genet 60: 320-329.

189. Itin PH, Sarasin A, Pittelkow MR (2001) Trichothiodystrophy: update on the sulfur-deficient brittle hair syndromes. J Am Acad Dermatol 44: 891-920; quiz 921-894.

190. Bergmann E, Egly JM (2001) Trichothiodystrophy, a transcription syndrome. Trends Genet 17: 279-286.

191. Civitelli R, McAlister WH, Teitelbaum SL, Whyte MP (1989) Central osteosclerosis with ectodermal dysplasia: clinical, laboratory, radiologic, and histopathological characterization with review of the literature. J Bone Miner Res 4: 863-875.

192. Leupold D (1979) [Ichthyosis congenita, cataract, mental retardation, ataxia, osteosclerosis and immunologic deficiency--a particular syndrome?]. Monatsschr Kinderheilkd 127: 307-308.

193. Wakeling EL, Cruwys M, Suri M, Brady AF, Aylett SE, et al. (2004) Central osteosclerosis with trichothiodystrophy. Pediatr Radiol 34: 541-546.

194. de Boer J, de Wit J, van Steeg H, Berg RJ, Morreau H, et al. (1998) A mouse model for the basal transcription/DNA repair syndrome trichothiodystrophy. Mol Cell 1: 981-990.

195. de Boer J, van Steeg H, Berg RJ, Garssen J, de Wit J, et al. (1999) Mouse model for the DNA repair/basal transcription disorder trichothiodystrophy reveals cancer predisposition. Cancer Res 59: 3489-3494.

196. de Boer J, Hoeijmakers JH (2000) Nucleotide excision repair and human syndromes. Carcinogenesis 21: 453-460.

197. Wijnhoven SW, Beems RB, Roodbergen M, van den Berg J, Lohman PH, et al. (2005) Accelerated aging pathology in ad libitum fed Xpd(TTD) mice is accompanied by features suggestive of caloric restriction. DNA Repair (Amst) 4: 1314-1324.

198. de Boer J, Andressoo JO, de Wit J, Huijmans J, Beems RB, et al. (2002) Premature aging in mice deficient in DNA repair and transcription. Science 296: 1276-1279.

CHAPTER 2

Decreased oxygen tension lowers reactive oxygen species and apoptosis and inhibits osteoblast matrix mineralization through changes in early osteoblast differentiation

C. Nicolaije[1], M. Koedam[1], J.P.T.M. van Leeuwen[1]

[1] Department of Internal Medicine, Erasmus Medical Center, Rotterdam, The Netherlands

Chapter 2

Abstract

Accumulating data show that oxygen tension can have an important effect on cell function and fate. We used the human pre-osteoblastic cell line SV- HFO, which forms a mineralizing extracellular matrix, to study the effect of low oxygen tension (2%) on osteoblast differentiation and mineralization. Mineralization was significantly reduced by 60-70% under 2% oxygen, which was paralleled by lower intracellular levels of reactive oxygen species (ROS) and apoptosis. Following this reduction in ROS the cells switched to a lower level of protection by down-regulating their antioxidant enzyme expression. The downside of this is that it left the cells more vulnerable to a subsequent oxidative challenge. Total collagen content was reduced in the 2% oxygen cultures and expression of matrix genes and matrix-metabolizing enzymes was significantly affected. Alkaline phosphatase activity and RNA expression as well as RUNX2 expression were significantly reduced under 2% oxygen. Time phase studies showed that high oxygen in the first phase of osteoblast differentiation and prior to mineralization is crucial for optimal differentiation and mineralization. Switching to 2% or 20% oxygen only during mineralization phase didn't change the eventual level of mineralization. In conclusion, this study shows the significance of oxygen tension for proper osteoblast differentiation, ECM formation and eventual mineralization. We demonstrated that the major impact of oxygen tension is in the early phase of osteoblast differentiation. Low oxygen in this phase leaves the cells in a premature differentiation state that can't provide the correct signals for matrix maturation and mineralization.

Introduction

Bone strength is heavily dependent on the quality of bone matrix formation and its subsequent mineralization. This specialized extra cellular matrix (ECM) is produced by differentiating osteoblasts and consists out of collagens, non-collagenous proteins (NCPs), mineral and water [1].

Osteoblast differentiation can be divided in three stages. First there is a rapid proliferative phase, followed by a matrix deposition phase and finally the matrix mineralization phase. Osteoblast differentiation and subsequent matrix mineralization can be influenced by the already deposited ECM through cell-ECM interaction and the secretion or activation of cell signaling molecules [2]. Collagens play an important part in this process. Without the deposition of a correctly structured collagen matrix, osteoblast differentiation is impaired [3,4,5,6]. NCPs, like osteocalcin (OC), osteopontin (OP), bone sialoprotein (BSP) and MEPE might also influence osteoblast differentiation [7] but seem to have an additional and more predominant effect on matrix mineralization. Many NCPs function as nucleation factors and regulate hydroxyapaptite crystal formation and size [8,9,10,11].

Most of what we know about the process of matrix maturation and mineralization has been investigated in cells cultured under regular (20% oxygen) culture conditions. Oxygen levels in the bone marrow and the surrounding bone tissue however, have been measured and modeled to be somewhere between 1-10% [12,13]. Oxygen tension can influence gene expression and modulate cell-cell interactions [14,15]. In addition low oxygen levels might influence cell metabolism and induce stress, modulating the levels of reactive oxygen species (ROS) and the scavenging mechanisms cells employ. High levels of ROS can cause DNA and protein damage, usually followed by the activation of regulated apoptosis [16]. Lower levels of ROS however play a role in intra-cellular signaling cascades [17]. In order to regulate ROS levels in the cell, several ROS scavenging mechanisms are in place amongst which a number of antioxidant enzymes. These antioxidant enzymes can be divided into three groups; Superoxide dismutases (SODs), Catalase (CAT) and Glutathione Peroxidases (GPXs). SODs reduce superoxide radicals into H_2O_2, which can be further reduced into H_2O by either CAT or any of the GPXs [18].

Previous studies using MSCs or murine osteoblast cell lines show a decrease in ALP expression and a severe inhibition of mineralization in cells cultured under low oxygen conditions [19,20,21,22]. Little is known about what happens to the interplay between osteoblasts and the matrix, cell metabolism or the induction of apoptosis during low oxygen conditions as well as the antioxidant enzyme expression and protection against ROS.

We investigated the effects of low oxygen tension on osteoblast metabolism, ROS production, and ROS protection as well as on matrix formation and mineralization, focusing on a number of known regulatory mechanisms that might affect these processes in order to determine whether low oxygen levels affect ECM-osteoblast interactions that regulate osteoblast differentiation and matrix formation.

Chapter 2

Material and Methods

Cell culture:

Human SV-HFO cells are pre-osteoblasts [23,24] and were seeded in a density of 5×10^3 vital cells/cm^2 and pre-cultured for 1 week in α-MEM (GIBCO, Paisley, UK) supplemented with 20 mM HEPES, pH 7.5 (Sigma, St. Louis, MO, USA), streptomycin/penicillin, 1.8 mM CaCl$_2$ (Sigma) and 10% heat-inactivated FCS (GIBCO) under standard conditions at 37°C and 5% CO$_2$ in a humidified atmosphere. During pre-culture cells remained in an undifferentiated stage. At this point cells were seeded in a density of 1×10^4 vital cells/cm^2 in the presence of 2% charcoal-treated FCS. For induction of osteoblast differentiation and mineralization the basal medium was freshly supplemented with 10 mM β-glycerophosphate (Sigma) and 100 nM dexamethasone (Sigma). The medium was replaced every 2-3 days. Cells were cultured at 37°C under standard conditions or in hypoxia chambers (Billups Rothenberg Inc.) gassed with a mixture of 2% oxygen, 5% CO$_2$ and 93% nitrogen at days of medium refreshment.

DNA, mineralization, protein and proliferation assays:

DNA and calcium measurements were performed as described previously [24]. Briefly, for DNA measurements cell lysates were incubated with heparin (8 IU/ml in PBS) and Ribonuclease A (50mg/ml in PBS) for 30 min at 378C. DNA was stained by adding ethidium bromide (25mg/ml in PBS). Analyses were performed by using a Victor2 plate reader (PerkinElmer Life and Analytical Science) with an extinction filter of 340 nm and an emission filter of 590 nm. For calcium measurements, cell lysates were incubated overnight with 0.24M HCl at 48C. Calcium content was determined colorimetrically with a calcium assay kit (Sigma) according to the manufacturer's description. Results were adjusted for DNA content of the cell lysates. For Alizarin Red S staining cell cultures were fixed for 60 min with 70% ethanol on ice. After fixation, cells were washed twice with PBS and stained for 10 min with Alizarin Red S solution (saturated Alizarin Red S in demineralized water adjusted to pH 4.2 using 0.5% ammonium hydroxide). For protein measurement 200ml of working reagent (50 volumes BCATM reagent A, 1 volume BCATM reagent B; PierceQ5) was added to 10ml of sonicated cell lysate. The mixture was incubated for 30 min at 378C, cooled down to room temperature and absorbance was measured, using a Victor2 plate reader at 595 nm. Proliferation was measured using a BrdU labeling kit (Roche) to load, incorporate, wash and release BrdU which was measured using a plate reader (Victor^2 1420 multilabel counter, Wallac) according to the manufacturer's protocol.

Collagen staining and quantification:

Cells were fixed for 1 hour using 10% formaldehyde. After fixation cells are washed with PBS and stained with Sirius Red Staining Solution (Direct Red, Sigma) for 1hour, followed by three wash steps with 0.01% HCl to get rid of excess dye. The dye was extracted and quantification took place using a Victor2 plate reader at 550nm.

Apoptosis assay:

Apoptosis was measured through the binding of annexin V and the uptake of propidium iodide (IQ products) by flow cytometry. For analysis 10.000 cells were counted (FACS Canto II, BD Biosciences) and the percentage of apoptotic cells was determined by counting vital (unstained), early apoptotic (annexin V stained), necrotic (PI stained) and late apoptotic cells (double stained).

qPCR analysis:

Total RNA was isolated using TRIzol reagent (Invitrogen) according to the manufacturer's protocol. RNA was isolated as previously described [24]. Total RNA amount was determined using a spectrophotometer (ND1000, Nanodrop). For cDNA synthesis 1 μg of total RNA was reverse transcribed using a cDNA synthesis kit according to the manufacturer's protocol (MBI Fermentas). qPCR analysis was performed using a ABI 7500 Fats Real-Time PCR detection system (Applied Biosystems). Reactions were performed in 25 μl volumes using a qPCR core kit (for assays using a probe) or a qPCR kit for SYBR green I (for assays using SYBR Green) (Eurogentec). Primer and probe sets were designed using Primer Express software (version 2.0, Applied Biosystems).

Stress induction and ROS measurement:

Cells were incubated with 1mM H_2O_2 (30%, Merck) in order to induce oxidative stress at various time points to induce oxidative stress. In order to visualize and measure superoxide radical production, cells were incubated with MitoSox Red (Invitrogen) after which pictures were taken on a fluorescent microscope (Axiovert 200 MOT, Zeiss) for quantification using Cell Profiler cell image analysis software (http://www.cellprofiler.org, Broad Institute). Total ROS production was measured after incubating the cells with DCF-DA (Sigma), after which fluorescence was measured on a plate reader (Victor[2] 1420 multilabel counter, Wallac).

Statistics:

All experiments have been performed three times with biological triplicates for each condition in each experiment. Differences between experimental and control conditions have been statistically analysed by using two-tailed t-tests.

Results

Osteoblast mineralization

Human pre-osteoblast SV-HFO cells were cultured for three weeks under normal (20% O_2) or low (2% O_2) oxygen conditions. SV-HFO cells undergo a three week differentiation and mineralization process in which the first week consists mostly out of proliferation and matrix production, followed by a second week of matrix maturation which is followed by a third week of matrix mineralization. Alizarin red staining of mineralized matrix on day 19 of culture, showed strong reduction of matrix mineralization by 2% O_2 (Figure 1A). Staining quantification showed that mineralization still occurred but to a significantly reduced extent (Figure 1B).

ROS production

We assessed the ROS production of cells cultured under high or low O_2. Total ROS production was significantly lower in cells cultured under 2% O_2 (Figure 2A). Next we determined the amount of superoxide radicals produced in both cell systems using the specific fluorescent stain mitosox red (Figure 2B). Quantification showed a significant decrease of superoxide radicals in cells cultured under 2% O_2, indicating reduced mitochondrial activity and a down-scaled cellular metabolism (Figure 2C).
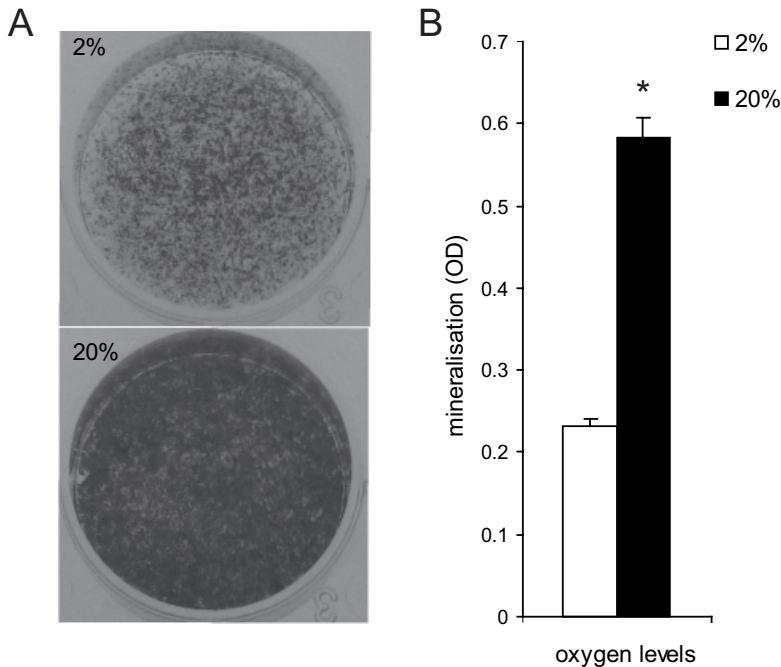
Figure 1: *Inhibition of osteoblast matrix mineralization by 2% oxyge*n. Cell cultures grown under 2% O_2 mineralize to a lesser extend compared to cells cultured under 20% O_2. (A) Alizarin Red staining (ARS) of SV-HFO cultures on day 19, cultured under 2% (upper panel) or 20% O_2 (lower panel) (B) Quantification of ARS on day 19 cells cultured under 2% (white) or 20% O_2 (black). * p<0.05 20% versus 2%

Since ROS production was strongly decreased, we examined the state of the cell's protection mechanism against oxidative stress. We determined the expression levels of several antioxidant enzymes in cells cultured under high or low O_2 levels at day 12, around the onset of mineralization (Figures 2D and 2E). Both cytoplasmic (SOD1) and mitochondrial (SOD2) SOD expression was significantly down-regulated in cells cultured under 2% O_2, suggesting a down-scaled protection mechanism. This was supported by the significantly down-regulated expression of the H_2O_2 radical scavenger catalase under low oxygen conditions (Figure 2D). Surprisingly, SOD3, which is localized extracellular to scavenge ROS in the ECM [25,26], was significantly up-regulated. Expression of the various GPX genes was not significantly altered by O2 (Figure 2E).

Proliferation and apoptosis
Next, we examined the effects of oxygen tension on proliferation and apoptosis. For both conditions, proliferation significantly decreased between day 3 and day 10. At day 3 of culture the proliferation rate of cells cultured under 2% O_2 was significantly lower compared to cells cultured under 20% O_2. However, at day 10 of culture the situation was reversed, with higher proliferation rates in cells cultured under low oxygen tension. This shows that cells cultured under low oxygen condition retained a higher proliferative capacity while
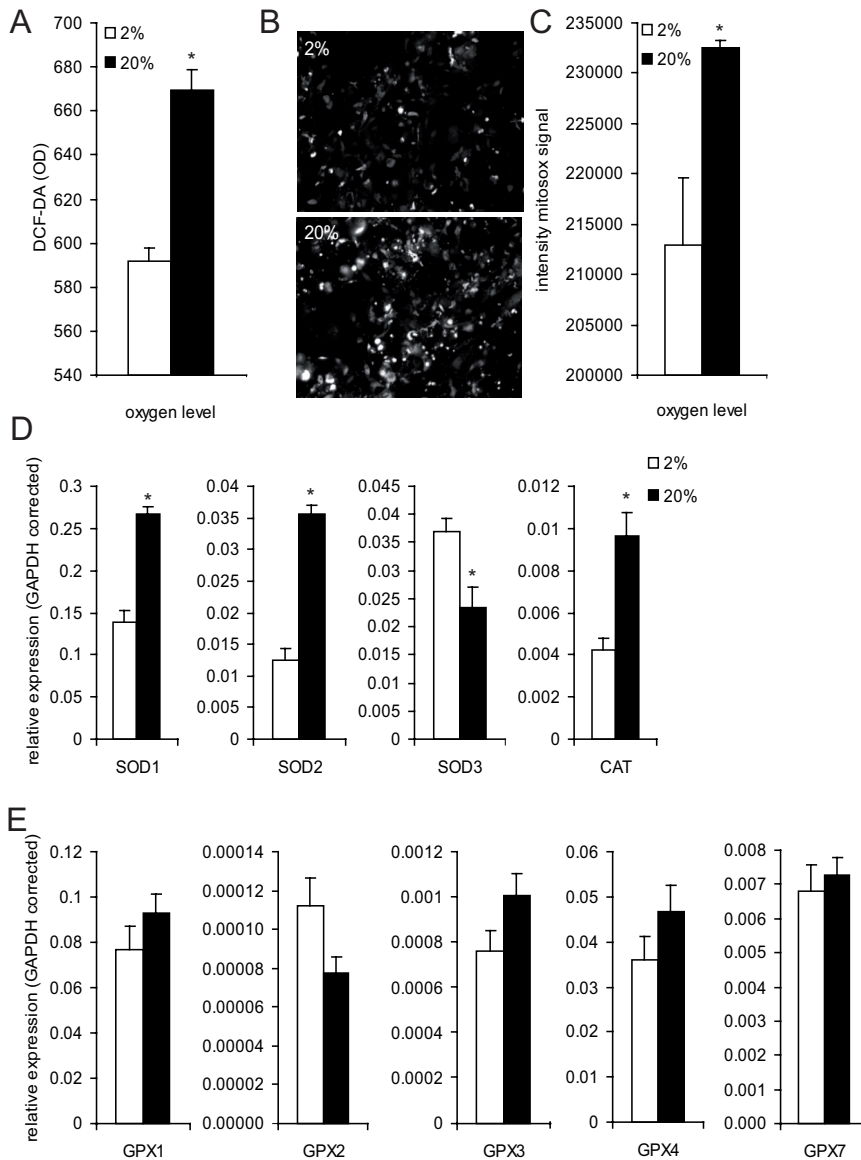
Figure 2: *Effect of 2% and 20% oxygen on ROS production and gene expression of antioxidants.* (A) Total radical production on day 12 of culture in cells cultured on high (black) or low (white) oxygen. (B) Pictures of mitosox red super oxide radical staining in day 12 cells cultured on high (lower panel) or low (upper panel) oxygen. (C) Quantification of mitosox red super oxide staining on day 12 in cells cultured on high (black) or low (white) oxygen. (D-E) Relative gene expression levels of anti oxidant scavengers, corrected for GAPDH. * $p < 0.05$ 20% versus 2%.

under high oxygen tension their proliferative capacity decreased with about 50% (Figure 3A).Up to the onset of mineralization at day 12 of culture there was no significant difference in apoptosis between 2% and 20% O_2 cultured osteoblasts. A strong and significant increase in apoptotic cells and a concomitant decrease in living cells was observed after culture for 19 days under 20% but not under 2% O_2 (Figure 3B). This difference in apoptosis was also reflected in the difference in expression of apoptosis-related genes. Both the caspases 3 and 6 as well as cytochrome C were significantly lower in the 2% O_2 condition while BAX expression stayed the same (Figure 3C).

Induced oxidative stress

Next, we investigated the effect of induced oxidative stress on the osteoblasts cultured under either 2% or 20% O_2, and having different levels of radical protection. To this end we induced oxidative stress by treatment with 1mM H_2O_2 for 24 hours followed by analyses of apoptosis. In line with the reduced expression of antioxidant enzymes, cells cultured under 2% O_2 had an increased susceptibility to oxidative stress as demonstrated by the significant decrease in living and increase in apoptotic cells (Figure 4B). This was supported by gene expression levels showing a significant increase in cytochrome C and caspase 3 expression in cells cultured under 2% O_2 (Figure 4C,D). Cells cultured under 20% O_2 displayed a smaller but significant increase in caspase 3 levels as well, but lacked a response in cytochrome C levels (Figure4C, D). ROS formation and increased apoptosis have been linked to increased matrix mineralization and may explain the increased mineralization seen for 20% oxygen (Figure 1) [27] [28,29,30]. Therefore, we questioned whether the reduced antioxidant enzymes expression (Figures 2D and 2E) and increased apoptosis (Figure 4B) after H_2O_2 treatment in the 2% O_2 condition would lead to enhanced mineralization. In order to test this, we induced oxidative stress using 1mM H_2O_2 at the onset of mineralization (day 12) in osteoblasts cultured on either 2% (Figure 4E) or 20% O_2 (Figure 4F). Although we measured increased levels of apoptosis in 2% O_2 cultured cells (Figure 4B), this had no effect on mineralization as measured on day 19 (Figure 4E). Most interestingly, induction of oxidative stress by H_2O_2 significantly enhanced mineralization in 20% O_2 osteoblast cultures (Figure 4F). This implicates that there must be additional differences in the 2% and 20 % O_2 cultures in osteoblast differentiation which are important to explain the differences in matrix mineralization. Strong induction of oxidative stress by continuous treatment with H_2O_2 from the start of osteoblast differentiation was detrimental for mineralization, irrespective of O_2 regimen (Figures 4E and 4F).

Matrix production and turnover

To study effects on the collagenous ECM we performed Sirius Red Collagen staining on day 19 after culture under 2% O_2 or 20% O_2. Osteoblasts cultured under 2% O_2 showed less collagen staining (Figure 5A) which was confirmed by extraction and quantification demonstrating a significant decrease in the total amount of collagen (Figure 5B). In contrast, expression of various collagen genes, including COL1A1, was significantly increased on day 5 and day 19 in the 2% oxygen condition (Figure 5C). Next we examined the expression of matrix-metalloproteinases (MMPs) and their inhibitors, tissue-inhibitor-of-metallo-proteinases (TIMPs), which both are involved in breakdown of ECM and can regulate cell differentiation and apoptosis [31,32]. MMP1 and MMP23B were expressed by the human osteoblasts and were reduced in the low oxygen condition at day 19, but not at day 5 (Figure 5D). The expression levels of TIMP3 were significantly lower in the 2% O_2

cultured osteoblasts at day 19. TIMP1 expression was slightly but not significantly lower as well (Figure 5D). These data demonstrate that oxygen tension is of significance for the formation and turnover of the ECM.
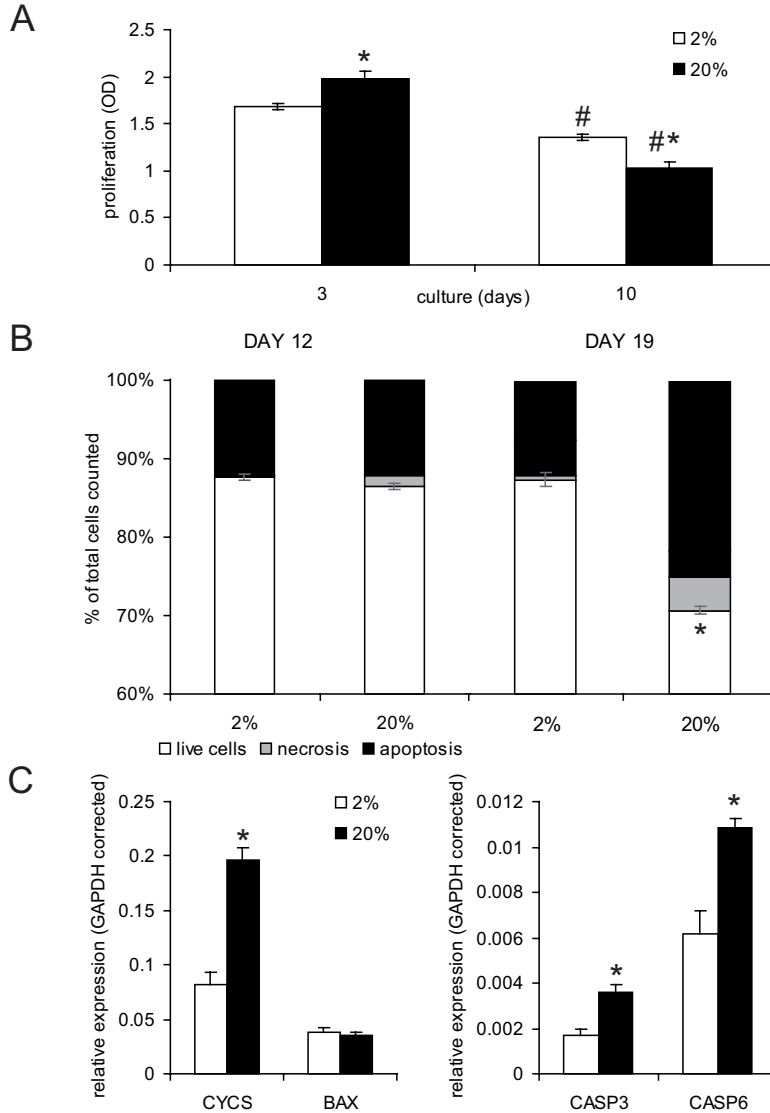
Figure 3: *Effects of 2% and 20% oxygen on osteoblast cell proliferation and apoptosis.* (A) Cell proliferation on day 3 and day 10 of culture, measured by BrdU incorporation in cells cultured on high (black) or low (white) oxygen. (B) FACS analysis of cells cultured on high or low oxygen tension on day 12 (left) or day 19 (right). Cells are sorted in living cells (white), apoptotic cells (black) and necrotic cells (grey). (C) Relative gene expression levels corrected for GAPDH of apoptosis related genes measured in cells cultured on high (black) or low (white) oxygen tension. * p<0.05 20% versus 2% ; # p<0.05 day 3 versus day 10.

Osteoblast differentiation

Changes in ECM composition, could lead to a delay in differentiation, leaving the cells in an immature stage at the onset of mineralization. We investigated cell differentiation throughout the entire culture period by measuring alkaline phosphatase (ALP) activity in the cells. In the 20% O_2 condition, ALP activity peaked at the onset of mineralization after which it declined. In the osteoblasts cultured under 2% oxygen, we saw a similar pattern, with a peak at day 12 albeit that at all stages of differentiation the ALP levels were significantly reduced in 2% O_2 osteoblasts (Figure 6A). This was supported by the significant reduction in ALP gene expression levels (Figure 6B). Inhibition of osteoblast differentiation was further demonstrated by reduced RUNX2 expression (Figure 6C). These data show that differences in O_2 may cause differences in osteoblast differentiation already at an early stage.

To further test this we cultured osteoblasts for various periods during differentiation on either 2 % or 20% oxygen and then switched the percentage oxygen (see Figure 6D left panel for schematic representation). These analyses demonstrated that 20% O_2 in the first week of osteoblast differentiation is crucial to observe the increased mineralization after 3 weeks compared to 2% O_2 (Figure 6D). Longer incubation with 20% O_2 didn't result in any further increase in mineralization. These data corroborate the observations on early changes in ALP activity and expression and RUNX2 expression (Figures 6A-C) and that the effect of oxygen on eventual mineralization originates in the early phase of osteoblast differentiation.

Discussion

The current study demonstrates the significance of oxygen tension for osteoblast proliferation, differentiation, apoptosis and mineralization as well as the level of ROS production and the expression of antioxidant enzymes. Low oxygen tension inhibits osteoblast-mediated mineralization due to an inhibition of osteoblast differentiation. Time phase studies demonstrated that this inhibition is time dependent and caused by effects in the early phase of osteoblast differentiation. We propose that oxygen tension affects osteoblast differentiation via effects on genes like RUNX2 and ALP and alters osteoblast differentiation via changes in the ECM composition. We observed changes in ECM and genes involved in ECM production and turnover in cells cultured under low oxygen. These would lead to alterations in matrix formation and may eventually inhibit osteoblast differentiation and matrix mineralization. It has been shown that osteoblast differentiation and subsequent matrix mineralization can be influenced by the already deposited ECM through cell-ECM interaction and the secretion or activation of cell signaling molecules [2]. Collagens play an important part in this process. Without the deposition of a correctly structured collagen matrix, osteoblast differentiation is impaired [3,4,5,6]. In parallel with the decrease in differentiation, under low oxygen tension the osteoblasts retain a more proliferative phenotype while high oxygen tension decreased the proliferation rate by 50 % in the first 10 days of culture. This is in line with the general observation that low levels of ROS are associated with cells in a proliferative state [33].

Our current observations on low oxygen and osteoblast differentiation are in line with previous studies on osteoblast cell lines and human MSCs [19,21,22,34]. We extent these
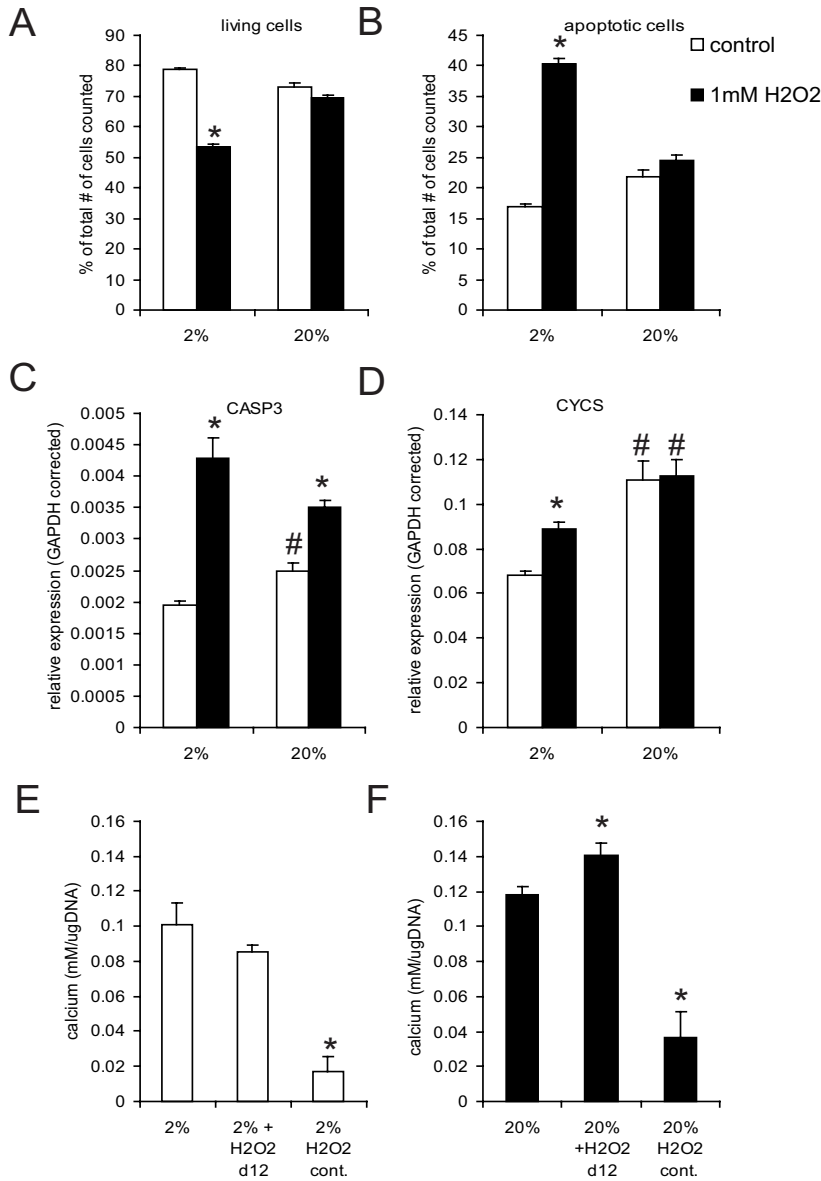
Figure 4: *Effect of oxygen radical challenge on cells cultured under 2% and 20% oxygen.* (A,B): FACS analysis of (A) living (left panel) and (B) apoptotic (right panel) cells, 24h after stress induction (1mM H_2O_2) cultured on high or low oxygen. (C,D): Relative gene expression levels corrected for GAPDH measured 24h after stress induction (1mM H_2O_2) of apoptosis related genes measured in cells cultured under 2 or 20% oxygen. In parts A-D the open bars indicate vehicle and the solid bars 1mM H_2O_2 treatment. E,F: The effect of continuous (days 0 -19) or timed (days 12 – 19 = mineralization phase) induction of apoptosis (1mM H_2O_2) on matrix mineralization measured on day 19 in cells cultured under 2% (E) or 20% (F) oxygen. # $p<0.05$ 20% versus 2% , * $p<0.05$ control versus H_2O_2.

observations by demonstrating that the oxygen sensitivity for regulating differentiation and ECM mineralization is limited to the early phase of osteoblast differentiation. Also we provide for the first time data about the impact of oxygen tension on the metabolic state with respect to ROS production. We focused on ROS production and scavenging mechanisms and were interested in their production and expression in relation to osteoblast differentiation and ECM mineralization. ROS are produced by mitochondria and play a role in numerous cellular signaling pathways like the Pi_3K pathway, FOXO signaling and TNFα mediated cell death [35]. ROS levels in the cell can determine its fate, from proliferation to immediate cell death [36]. The cellular response to hypoxia requires the mitochondrial generation of ROS to propagate signaling events that regulate transcription, calcium stores, and energy stores at the cellular level [36,37]. We observed a decrease in total ROS production as well as a reduction in super oxide radicals under 2% O_2. This indicates that the osteoblasts do not necessarily recognize this 2% level of oxygen tension as a severe state of hypoxia.

The reduced ROS production in cells cultured under 2% O_2 is followed by a decrease in gene expression of the protective antioxidant enzymes SOD1 and SOD2 and CAT. This indicates a decrease in ROS and H_2O_2 radical scavenging in cells cultured on low oxygen tension. This would be an expected adjustment in line with the cell's decreased oxygen consumption and metabolic state. In other words the osteoblasts switch from using energy for a high protection state to a low protection state. At the same time safeguarding a minimum level of ROS needed for cell survival and proliferation. Although there might be a trend towards lower levels, the GPX subfamily of scavengers was never significantly different between 2 and 20% oxygen. A drawback of this switch to lower ROS protection under low oxygen condition is that this leaves the cells vulnerable to oxidative stress and ROS challenges, leading to increased apoptosis as shown by the H2O2 studies. An interesting observation from an ECM and bone formation perspective is the fact that, in contrast to SOD1 and 2, SOD3 expression is significantly up-regulated in osteoblasts cultured under low oxygen tension. A major difference with SOD1 and 2 is that these SODs are located intracellular, while SOD3 is excreted and can be found in extracellular fluids [38]. After secretion it can bind heparin sulphate proteoglycans found on cell surfaces or in the ECM from where it can scavenge radicals in the extracellular environment [39]. Little is known about its role in bone formation, but there is a direct link between SOD3 levels and the occurrence of osteoarthritis [40], which suggests that SOD3 in the extracellular space is involved in skeletal processes. It is interesting to link this difference in SOD3 expression under 2% O_2 to the changes in ECM and ECM metabolizing enzymes and thereby osteoblast differentiation as discussed above. The concept that ECM, ECM turnover and SOD3 play a role in the control of osteoblast differentiation is subject to ongoing studies.

ROS levels also affect cell survival. High levels can activate signaling pathways that lead to the induction of apoptosis [16]. Here we show that a decrease in ROS levels is accompanied by a decrease in apoptotic cells and a down regulation of the expression of apoptotic genes. *In vivo*, osteoblast apoptosis occurs frequently and plays a role in controlling bone metabolism [41]. Apoptosis has also been shown to be actively involved in mineralization [42]. We also recently provided evidence that an increase in apoptosis leads to enhanced matrix mineralization [27]. Here we show that the osteoblast cultures with the highest level of apoptosis (20%) produce more mineralized matrix than cultures with less apoptotic cells

(2%). To test the relationship between 2% and 20% oxygen, apoptosis and mineralization we increased ROS and induced apoptosis by adding H_2O_2. In this experiment, an increase in apoptosis was, however, not sufficient to overrule the inhibition of matrix mineralization in cells cultured under 2% O_2 (Figure 4E). An explanation for this might be that in the 2% O_2 condition the cells are not properly differentiated and ECM maturation is inappropriate to lead to full mineralization.

Chapter 2
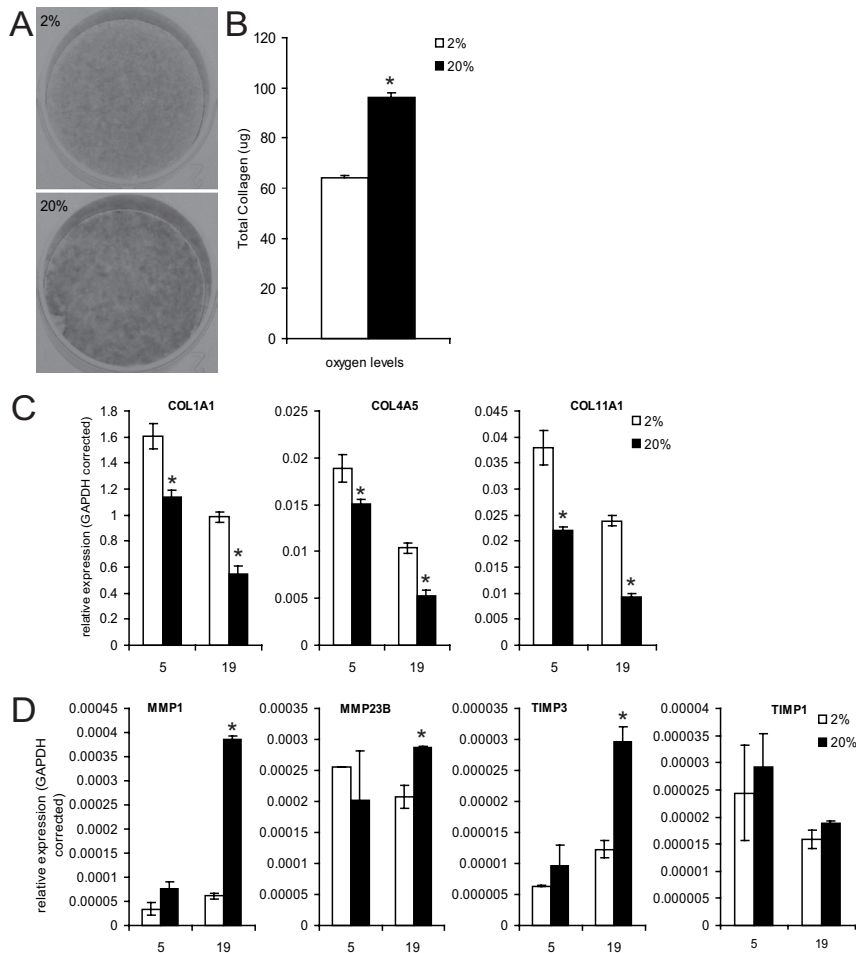
Figure 5: *Impact of oxygen on collagen production and ECM-related genes.* (A) Amount of collagen in the ECM is lower in 2% (upper panel) compared to 20% (lower panel) oxygen cultured osteoblasts as assess by Sirius red staining at day 19 cells (B) Quantification of the Sirius red staining of cells cultured on 20% (black) or 2% (white) oxygen. (C) Relative expression levels of several collagen genes corrected for GAPDH on day 5 and day 19 of culture for cells cultured on high (solid squares) or low (open squares) oxygen. (D) Relative gene expression levels on day 5 and day 19 corrected for GAPDH for a number of MMPs and TIMPs produced by the cells when cultured on high (black) or low (white) oxygen. * $p<0.05$ 20% versus 2%.

Following this we focused on matrix formation. Overall collagen protein analyses in the ECM demonstrated a significant decrease in the 2% oxygen condition. However, 2% oxygen led to a significant increase in the expression of various collagen genes, an observation that fits with data found in rat calvarial osteoblasts after Northern analysis [43]. A discrepancy between protein and gene expression is not unique and has been described before. These observations on collagen may be related to a negative auto-feedback system. In other words the level of collagen protein may regulate the expression of the collagen gene [44]. Alternatively, it has been reported that intracellular collagen fragments suppress collagen gene expression [44,45] but yet a definitive explanation for the protein – mRNA discrepancy remains elusive.

We hypothesized that an explanation for the differences in ECM between 2 and 20% oxygen may lie in differences in collagen metabolism. MMPs are the major enzymes involved in matrix remodeling and collagen break down and influence a great number of signaling processes. While degrading matrix, MMPs may release bioactive breakdown products, such as stored pools of growth factors, and disrupt matrix adherence. [46,47,48,49] In addition, they also can act directly on cell surfaces by releasing bioactive cell surface molecules [50,51] or cleaving surface signaling molecules [52,53]. MMP expression was significantly reduced by 2% O_2 indicating that it is highly unlikely that the difference in ECM mineralization can be explained by increased ECM turnover in the 2% O_2 condition.

Alternatively, it is tempting to speculate that MMP activity limited ECM turnover, is important for maturation of ECM and thereby mineralization. Thereby a reduction in MMP expression might partially contribute to the inhibition of bone formation and mineralization. This is supported by data from several MMP knock out models [54,55,56,57]. Also mutations in the human MMP2 gene have been linked to multicentric osteolysis with arthritis (MOA), an osteolytic bone disease [58]. All these data indicate that a decrease in MMP expression can have a negative influence on matrix formation and mineralization as observed in the 2% oxygen condition. Activity of MMPs is regulated by TIMPs. These proteins have been reported to inhibit MMPS by binding their catalytic domain [59], but also to activate MMPs [60,61] and having growth promoting activity [62]. Interestingly, TIMP-3 may contribute to the increased apoptosis in the 20% oxygen condition as its expression is significantly higher in this condition and TIMP-3 has been shown to induce apoptosis of osteoblasts [63].

The studies shown in Figure 6D are important for understanding the overall effect of oxygen on bone formation and mineralization. These data demonstrate that the oxygen concentration in the first week of osteoblast differentiation is crucial for a proper differentiation and eventual mineralization after 3 weeks. In other words, at low (2%) oxygen tension osteoblast differentiation is delayed compared to high (20%) oxygen tension leading to diminished mineralization after 3 weeks. This is supported by the observations on RUNX2 and alkaline phosphatase activity. Under 2% O_2 cells have not reached a certain state of differentiation, produced the correct proteins, and created the proper environment to jump start mineralization at the correct point in time. It appears that cultures that have been switched back from 2% in the first week of culture to 20% O_2 thereafter try to catch up but they don't reach the full mineralization as seen when they were exposed to 20% in the first week.
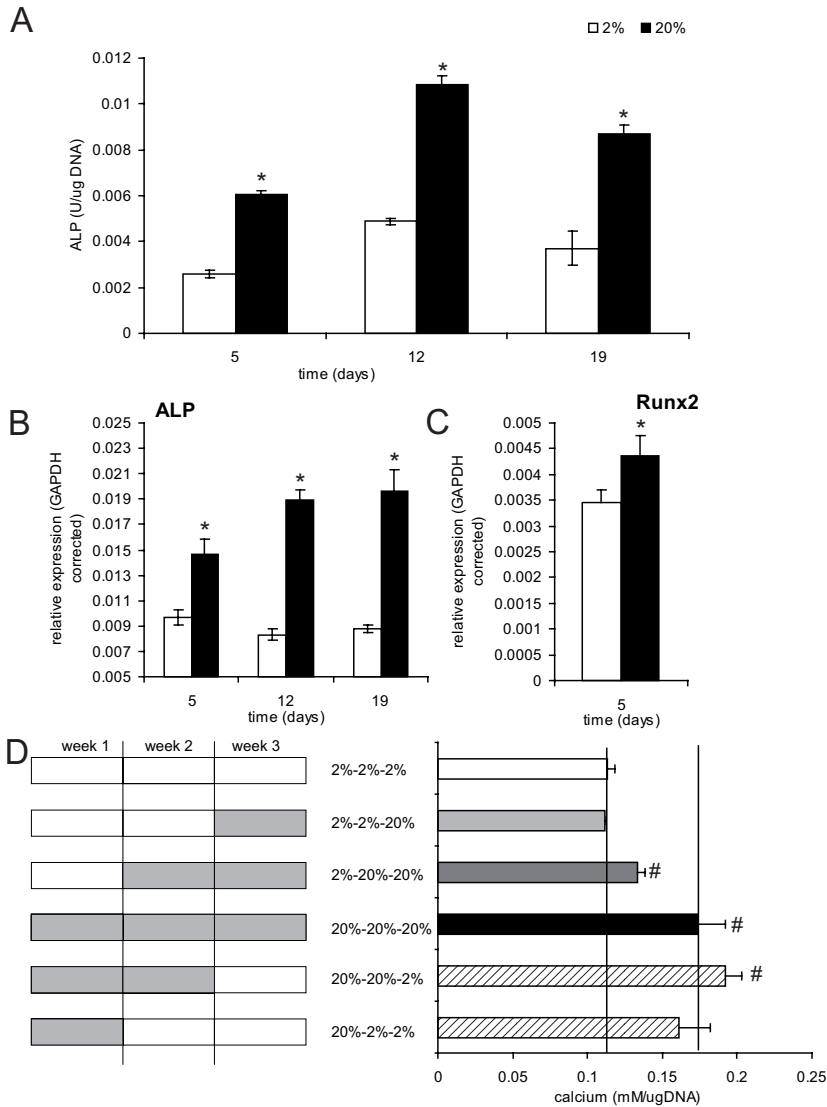
Figure 6: *Effect of oxygen on ALP, RUNX2 and timing of effects on mineralization.* Low oxygen tension inhibits osteoblast differentiation. A: ALP activity corrected for DNA amount measured on day 5, 12 and 19 of culture grown on high (black) or low (white) oxygen tension. B,C: Relative gene expression levels corrected for GAPDH of ALP throughout the culture and Runx2 on day 5 in cells cultured on high (black) or low (white) oxygen. D: Schematic representation of oxygen tension (left part) during culture and matrix mineralization measured as the amount of calcium corrected by DNA (corresponding right part). Cells were cultured on low (white squares in the schematic) or high (grey squares in the schematic) oxygen for varying amounts of time during the three week culture period each depicted by another color. Striped bars depict matrix mineralization in cells cultured on 20% oxygen for varying amounts of time. * p<0.05 20% versus 2%, # p<0.05 versus the 2%-2%-2% condition.

Chapter 2

In conclusion, this study shows the significance of oxygen tension for proper osteoblast differentiation, ECM formation and eventual mineralization. Low oxygen tension affects the interplay between osteoblast differentiation and matrix formation at multiple levels, changing key players in the process. It affects apoptosis as well as matrix production, but also directly influences osteoblast differentiation and gene expression. We have demonstrated that the major impact of oxygen tension is in the early phase of osteoblast differentiation.

Finally, induction of oxidative stress at non toxic levels leads to a much higher increase in apoptosis in cells cultured under 2% O_2 and having reduced antioxidant enzymes protection compared to those cultured on 20% O_2 (Figure 4B). These observations hold implications for human tissue regeneration, where cells are often moved from the body (low O_2) into a laboratory culture environment (high O_2) and back into the body (low O_2). This might affect not only their chances of survival but also their capacity to differentiate and form qualitative bone matrix.

References

1. Clarke B (2008) Normal bone anatomy and physiology. Clin J Am Soc Nephrol 3 Suppl 3: S131-139.

2. Franceschi RT, Iyer BS (1992) Relationship between collagen synthesis and expression of the osteoblast phenotype in MC3T3-E1 cells. J Bone Miner Res 7: 235-246.

3. Franceschi RT, Iyer BS, Cui Y (1994) Effects of ascorbic acid on collagen matrix formation and osteoblast differentiation in murine MC3T3-E1 cells. J Bone Miner Res 9: 843-854.

4. Quarles LD, Yohay DA, Lever LW, Caton R, Wenstrup RJ (1992) Distinct proliferative and differentiated stages of murine MC3T3-E1 cells in culture: an in vitro model of osteoblast development. J Bone Miner Res 7: 683-692.

5. Vetter U, Fisher LW, Mintz KP, Kopp JB, Tuross N, et al. (1991) Osteogenesis imperfecta: changes in noncollagenous proteins in bone. J Bone Miner Res 6: 501-505.

6. Wenstrup RJ, Witte DP, Florer JB (1996) Abnormal differentiation in MC3T3-E1 preosteoblasts expressing a dominant-negative type I collagen mutation. Connect Tissue Res 35: 249-257.

7. Ducy P, Desbois C, Boyce B, Pinero G, Story B, et al. (1996) Increased bone formation in osteocalcin-deficient mice. Nature 382: 448-452.

8. Boskey AL, Maresca M, Ullrich W, Doty SB, Butler WT, et al. (1993) Osteopontin-hydroxyapatite interactions in vitro: inhibition of hydroxyapatite formation and growth in a gelatin-gel. Bone Miner 22: 147-159.

9. Hunter GK, Goldberg HA (1994) Modulation of crystal formation by bone phosphoproteins: role of glutamic acid-rich sequences in the nucleation of hydroxyapatite by bone sialoprotein. Biochem J 302 (Pt 1): 175-179.

10. Rowe PS, Garrett IR, Schwarz PM, Carnes DL, Lafer EM, et al. (2005) Surface plasmon resonance (SPR) confirms that MEPE binds to PHEX via the MEPE-ASARM motif: a model for impaired mineralization in X-linked rickets (HYP). Bone 36: 33-46.

11. Qin C, D'Souza R, Feng JQ (2007) Dentin matrix protein 1 (DMP1): new and important roles for biomineralization and phosphate homeostasis. J Dent Res 86: 1134-1141.

12. Chow DC, Wenning LA, Miller WM, Papoutsakis ET (2001) Modeling pO(2) distributions in the bone marrow hematopoietic compartment. II. Modified Kroghian models. Biophys J 81: 685-696.

13. Harrison JS, Rameshwar P, Chang V, Bandari P (2002) Oxygen saturation in the bone marrow of healthy volunteers. Blood 99: 394.

14. Haase VH (2009) Oxygen regulates epithelial-to-mesenchymal transition: insights into molecular mechanisms and relevance to disease. Kidney Int 76: 492-499.

15. Park JH, Park BH, Kim HK, Park TS, Baek HS (2002) Hypoxia decreases Runx2/Cbfa1 expression in human osteoblast-like cells. Mol Cell Endocrinol 192: 197-203.

16. Giorgio M, Migliaccio E, Orsini F, Paolucci D, Moroni M, et al. (2005) Electron transfer between cytochrome c and p66Shc generates reactive oxygen species that trigger mitochondrial apoptosis. Cell 122: 221-233.

17. Janssen-Heininger YM, Mossman BT, Heintz NH, Forman HJ, Kalyanaraman B, et al. (2008) Redox-based regulation of signal transduction: principles, pitfalls, and promises. Free Radic Biol Med 45: 1-17.

18. Mates JM, Sanchez-Jimenez F (1999) Antioxidant enzymes and their implications in pathophysiologic processes. Front Biosci 4: D339-345.

19. Grayson WL, Zhao F, Izadpanah R, Bunnell B, Ma T (2006) Effects of hypoxia on human mesenchymal stem cell expansion and plasticity in 3D constructs. J Cell Physiol 207: 331-339.

20. Tuncay OC, Ho D, Barker MK (1994) Oxygen tension regulates osteoblast function. Am J Orthod Dentofacial Orthop 105: 457-463.

21. Utting JC, Robins SP, Brandao-Burch A, Orriss IR, Behar J, et al. (2006) Hypoxia inhibits the growth, differentiation and bone-forming capacity of rat osteoblasts. Exp Cell Res 312: 1693-1702.

22. D'Ippolito G, Diabira S, Howard GA, Roos BA, Schiller PC (2006) Low oxygen tension inhibits osteogenic differentiation and enhances stemness of human MIAMI cells. Bone 39: 513-522.

23. Chiba H, Sawada N, Ono T, Ishii S, Mori M (1993) Establishment and characterization of a simian virus 40-immortalized osteoblastic cell line from normal human bone. Jpn J Cancer Res 84: 290-297.

24. Eijken M, Koedam M, van Driel M, Buurman CJ, Pols HA, et al. (2006) The essential role of glucocorticoids for proper human osteoblast differentiation and matrix mineralization. Mol Cell Endocrinol 248: 87-93.

Chapter 2

25. Carlsson LM, Jonsson J, Edlund T, Marklund SL (1995) Mice lacking extracellular superoxide dismutase are more sensitive to hyperoxia. Proc Natl Acad Sci U S A 92: 6264-6268.

26. Marklund SL (1984) Extracellular superoxide dismutase and other superoxide dismutase isoenzymes in tissues from nine mammalian species. Biochem J 222: 649-655.

27. Bruedigam C, Eijken M, Koedam M, van de Peppel J, Drabek K, et al. (2010) A new concept underlying stem cell lineage skewing that explains the detrimental effects of thiazolidinediones on bone. Stem Cells 28: 916-927.

28. Clarke MC, Figg N, Maguire JJ, Davenport AP, Goddard M, et al. (2006) Apoptosis of vascular smooth muscle cells induces features of plaque vulnerability in atherosclerosis. Nat Med 12: 1075-1080.

29. Liberman M, Bassi E, Martinatti MK, Lario FC, Wosniak J, Jr., et al. (2008) Oxidant generation predominates around calcifying foci and enhances progression of aortic valve calcification. Arterioscler Thromb Vasc Biol 28: 463-470.

30. Proudfoot D, Skepper JN, Hegyi L, Bennett MR, Shanahan CM, et al. (2000) Apoptosis regulates human vascular calcification in vitro: evidence for initiation of vascular calcification by apoptotic bodies. Circ Res 87: 1055-1062.

31. Bond M, Murphy G, Bennett MR, Newby AC, Baker AH (2002) Tissue inhibitor of metalloproteinase-3 induces a Fas-associated death domain-dependent type II apoptotic pathway. J Biol Chem 277: 13787-13795.

32. Buxton PG, Bitar M, Gellynck K, Parkar M, Brown RA, et al. (2008) Dense collagen matrix accelerates osteogenic differentiation and rescues the apoptotic response to MMP inhibition. Bone 43: 377-385.

33. Bell EL, Klimova TA, Eisenbart J, Schumacker PT, Chandel NS (2007) Mitochondrial reactive oxygen species trigger hypoxia-inducible factor-dependent extension of the replicative life span during hypoxia. Mol Cell Biol 27: 5737-5745.

34. Salim A, Nacamuli RP, Morgan EF, Giaccia AJ, Longaker MT (2004) Transient changes in oxygen tension inhibit osteogenic differentiation and Runx2 expression in osteoblasts. J Biol Chem 279: 40007-40016.

35. Manolagas SC (2010) From estrogen-centric to aging and oxidative stress: a revised perspective of the pathogenesis of osteoporosis. Endocr Rev 31: 266-300.

36. Hamanaka RB, Chandel NS (2010) Mitochondrial reactive oxygen species regulate cellular signaling and dictate biological outcomes. Trends Biochem Sci 35: 505-513.

37. Chandel NS, Maltepe E, Goldwasser E, Mathieu CE, Simon MC, et al. (1998) Mitochondrial reactive oxygen species trigger hypoxia-induced transcription. Proc Natl Acad Sci U S A 95: 11715-11720.

38. Marklund SL, Holme E, Hellner L (1982) Superoxide dismutase in extracellular fluids. Clin Chim Acta 126: 41-51.

39. Sandstrom J, Carlsson L, Marklund SL, Edlund T (1992) The heparin-binding domain of extracellular superoxide dismutase C and formation of variants with reduced heparin affinity. J Biol Chem 267: 18205-18209.

40. Regan E, Flannelly J, Bowler R, Tran K, Nicks M, et al. (2005) Extracellular superoxide dismutase and oxidant damage in osteoarthritis. Arthritis Rheum 52: 3479-3491.

41. Weinstein RS, Jilka RL, Parfitt AM, Manolagas SC (1998) Inhibition of osteoblastogenesis and promotion of apoptosis of osteoblasts and osteocytes by glucocorticoids. Potential mechanisms of their deleterious effects on bone. J Clin Invest 102: 274-282.

42. Lynch MP, Capparelli C, Stein JL, Stein GS, Lian JB (1998) Apoptosis during bone-like tissue development in vitro. J Cell Biochem 68: 31-49.

43. Warren SM, Steinbrech DS, Mehrara BJ, Saadeh PB, Greenwald JA, et al. (2001) Hypoxia regulates osteoblast gene expression. J Surg Res 99: 147-155.

44. Fouser L, Sage EH, Clark J, Bornstein P (1991) Feedback regulation of collagen gene expression: a Trojan horse approach. Proc Natl Acad Sci U S A 88: 10158-10162.

45. Ingber DE (2006) Cellular mechanotransduction: putting all the pieces together again. FASEB J 20: 811-827.

46. Giannelli G, Falk-Marzillier J, Schiraldi O, Stetler-Stevenson WG, Quaranta V (1997) Induction of cell migration by matrix metalloprotease-2 cleavage of laminin-5. Science 277: 225-228.

47. Petitclerc E, Stromblad S, von Schalscha TL, Mitjans F, Piulats J, et al. (1999) Integrin alpha(v)beta3 promotes M21 melanoma growth in human skin by regulating tumor cell survival. Cancer Res 59: 2724-2730.

48. Alexander CM, Selvarajan S, Mudgett J, Werb Z (2001) Stromelysin-1 regulates adipogenesis during mammary gland involution. J Cell Biol 152: 693-703.
49. Lochter A, Galosy S, Muschler J, Freedman N, Werb Z, et al. (1997) Matrix metalloproteinase stromelysin-1 triggers a cascade of molecular alterations that leads to stable epithelial-to-mesenchymal conversion and a premalignant phenotype in mammary epithelial cells. J Cell Biol 139: 1861-1872.
50. Powell WC, Fingleton B, Wilson CL, Boothby M, Matrisian LM (1999) The metalloproteinase matrilysin proteolytically generates active soluble Fas ligand and potentiates epithelial cell apoptosis. Curr Biol 9: 1441-1447.
51. Suzuki M, Raab G, Moses MA, Fernandez CA, Klagsbrun M (1997) Matrix metalloproteinase-3 releases active heparin-binding EGF-like growth factor by cleavage at a specific juxtamembrane site. J Biol Chem 272: 31730-31737.
52. Levi E, Fridman R, Miao HQ, Ma YS, Yayon A, et al. (1996) Matrix metalloproteinase 2 releases active soluble ectodomain of fibroblast growth factor receptor 1. Proc Natl Acad Sci U S A 93: 7069-7074.
53. Sheu BC, Hsu SM, Ho HN, Lien HC, Huang SC, et al. (2001) A novel role of metalloproteinase in cancer-mediated immunosuppression. Cancer Res 61: 237-242.
54. Holmbeck K, Bianco P, Caterina J, Yamada S, Kromer M, et al. (1999) MT1-MMP-deficient mice develop dwarfism, osteopenia, arthritis, and connective tissue disease due to inadequate collagen turnover. Cell 99: 81-92.
55. Mosig RA, Dowling O, DiFeo A, Ramirez MC, Parker IC, et al. (2007) Loss of MMP-2 disrupts skeletal and craniofacial development and results in decreased bone mineralization, joint erosion and defects in osteoblast and osteoclast growth. Hum Mol Genet 16: 1113-1123.
56. Stickens D, Behonick DJ, Ortega N, Heyer B, Hartenstein B, et al. (2004) Altered endochondral bone development in matrix metalloproteinase 13-deficient mice. Development 131: 5883-5895.
57. Zhou Z, Apte SS, Soininen R, Cao R, Baaklini GY, et al. (2000) Impaired endochondral ossification and angiogenesis in mice deficient in membrane-type matrix metalloproteinase I. Proc Natl Acad Sci U S A 97: 4052-4057.
58. Martignetti JA, Aqeel AA, Sewairi WA, Boumah CE, Kambouris M, et al. (2001) Mutation of the matrix metalloproteinase 2 gene (MMP2) causes a multicentric osteolysis and arthritis syndrome. Nat Genet 28: 261-265.
59. Willenbrock F, Murphy G (1994) Structure-function relationships in the tissue inhibitors of metalloproteinases. Am J Respir Crit Care Med 150: S165-170.
60. Butler GS, Butler MJ, Atkinson SJ, Will H, Tamura T, et al. (1998) The TIMP2 membrane type 1 metalloproteinase "receptor" regulates the concentration and efficient activation of progelatinase A. A kinetic study. J Biol Chem 273: 871-880.
61. Strongin AY, Collier I, Bannikov G, Marmer BL, Grant GA, et al. (1995) Mechanism of cell surface activation of 72-kDa type IV collagenase. Isolation of the activated form of the membrane metalloprotease. J Biol Chem 270: 5331-5338.
62. Gomez DE, Alonso DF, Yoshiji H, Thorgeirsson UP (1997) Tissue inhibitors of metalloproteinases: structure, regulation and biological functions. Eur J Cell Biol 74: 111-122.
63. Yuan LQ, Liu YS, Luo XH, Guo LJ, Xie H, et al. (2008) Recombinant tissue metalloproteinase inhibitor-3 protein induces apoptosis of murine osteoblast MC3T3-E1. Amino Acids 35: 123-127.

Chapter 2

CHAPTER 3

Oxygen-induced transcriptional dynamics in human osteoblasts are most prominent at the onset of mineralization

Claudia Nicolaije[1], Jeroen van de Peppel[1],

Johannes P.T.M. van Leeuwen[1*]

[1] Department of Internal Medicine, Erasmus Medical Center, Rotterdam, The Netherlands

Submitted

Chapter 3

Abstract

Oxygen tension plays an important role in the regulation of cellular processes. During hematopoietic stem cell (HSC) differentiation, HSCs migrate from one stem cell niche to the next, each with a different oxygen tension that determines which signalling pathways are on and off, determining the differentiation stage of the cell. Oxygen tension influences osteoblast differentiation and mineralization. Low oxygen levels inhibit matrix formation and mineralization. We were interested in the regulatory mechanisms that underlie this inhibition and wondered whether a switch in oxygen tension could have varying effects depending on the differentiation phase of the osteoblasts. We performed an oxygen tension switch phase study in which we switched osteoblasts from high to low oxygen tension during their three week differentiation and mineralization process. We performed microarray expression profiling on samples collected during this three week period and analyzed biochemical and histo-chemical endpoint parameters to determine the effect of a switch in oxygen levels on mineralization. We found that low oxygen tension has the most profound impact on mineralization when administered during the period of matrix maturation. Additionally, a large set of genes was regulated by oxygen, independent of the differentiation phase. These genes were involved in cell metabolisms and matrix formation. Our study demonstrates that variation in oxygen tension strongly affects gene expression in differentiating osteoblasts. The magnitude of this change for either expression levels or the number of regulated probes, depends on the osteoblast differentiation stage, with the phase prior to the onset of mineralization being most sensitive.

Introduction

Oxygen is an important regulatory factor in numerous cellular processes, from stem cell differentiation to pancreatic development and cardiomyogenesis [1,2,3]. In the bone marrow environment, oxygen tension plays an important role regulating hematopoietic (HSC) and mesenchymal stem cell (MSC) differentiation [4,5].

The oxygen level in the bone marrow and its surrounding bone tissue ranges somewhere between 1% and 10% under normal *in vivo* conditions and can be as low as 0.1% at fracture sites [6,7]. MSC and osteoblast differentiation has been extensively studied in cell culture experiments performed under traditional culture conditions, using 20% O_2. More recently performed studies show that hypoxic culture conditions cause a delay in osteoblast differentiation and mineralization, leaving the cells in a more stem-like state [8,9,10,11]. In addition, hypoxic conditions are often found at the side of fractures and inside the callus during repair [12,13]. Here they play an important role in repair, since a hypoxic state leads to the activation of VEGF expression, initiating essential vessel formation in the affected region [14], which in the end leads to re-oxygenation. Prolonged hypoxia at fracture sites leads to a decrease in fracture healing rates [15]. More recently it has also been shown that hypoxia responsive MSCs have a greater differentiation potential than unresponsive MSCs [16]. This indicates that hypoxia can be used to improve fracture repair rates and bone healing. More detailed knowledge about the regulatory processes underlying these hypoxic conditions, which potentially mimic *in vivo* conditions more closely, will provide novel insights into the processes that regulate MSC and osteoblast differentiation and the role of oxygen in those processes. This knowledge will be of invaluable use in the field of fracture healing and tissue engineering, but also provides us with new insights and possibilities when studying bone marrow stem cells niches and MSC-HSC interaction. In a previous study, we used our human pre-osteoblast SV-HFO model to study osteoblast differentiation under low oxygen tension and concluded that low oxygen tension decreases matrix mineralization by inhibiting osteoblast differentiation at an early stage [17]. SV-HFO cells undergo a three week differentiation and mineralization process that can be divided into three phases; a differentiation phase (day 0-5; Phase 1), the matrix maturation phase in which matrix is produced (day 5-12; Phase 2) and the mineralization phase that results in a mineralized matrix (day 12-19; Phase 3).

We hypothesized that the impact of oxygen tension on osteoblast differentiation is dependent on the stage of osteoblast differentiation. Following this hypothesis, the aim of the current study was to investigate the impact of oxygen tension on gene expression against the backdrop of osteoblast differentiation. In order to study this, we performed oxygen switch experiments during the 3 phases of osteoblast differentiation. We collected data from cells that were continuously cultured under 20% (high) or 2% (low) oxygen to determine long term effects, as well as data from cells that were switched to low oxygen during their last phase of culture. We analyzed these data in parallel for phenotypic differentiation and mineralization endpoints, and used gene expression profiling to identify the genes, molecular functions and processes that are under oxygen control.

Chapter 3

Materials & Methods

Cell culture:

Human SV-HFO cells are pre-osteoblasts [18,19] and were seeded in a density of $5x10^3$ vital cells/cm^2 and pre-cultured for 1 week in α-MEM (GIBCO, Paisley, UK) supplemented with 20 mM HEPES, pH 7.5 (Sigma, St. Louis, MO, USA), streptomycin/penicillin, 1.8 mM $CaCl_2$ (Sigma) and 10% heat-inactivated FCS (GIBCO) under standard conditions at 37C, 20% O_2 and 5% CO_2 in a humidified atmosphere. During pre-culture cells remained in an undifferentiated stage. At this point cells were seeded in a density of 1×10^4 vital cells/cm^2 in the presence of 2% charcoal-treated FCS. For induction of osteoblast differentiation and mineralization the basal medium was freshly supplemented with 10 mM β-glycerophosphate (Sigma) and 100 nM dexamethasone (Sigma). The medium was replaced every 2-3 days. Cells were cultured at 37°C under standard conditions (20% oxygen) or in hypoxia chambers (Billups Rothenberg Inc., Delmar, CA, USA) gassed with a mixture of 2% oxygen, 5% CO_2 and 93% nitrogen at days of medium refreshment.

DNA, protein, alkaline phosphatase activity and mineralization assays:

DNA, protein, alkaline phosphatase (ALP) activity and calcium measurements were performed as previously described [20].

Collagen staining and quantification:

Cells were fixed for 1 hour using 10% formaldehyde. After fixation cells were washed with PBS and stained with Sirius Red Staining Solution (Direct Red, Sigma) for 1 hour, followed by three wash steps with 0.01% HCl to remove excess dye. The dye was extracted and quantification took place using a Victor2 (Wallac, Waltham, MA, USA) plate reader at 550nm and a collagen (Sigma) standard calibration curve.

Illumina gene chip-based gene expression profiling:

Illumina HumanHT-12 v3 BeadChip (Illumina, Inc.) human whole-genome expression arrays were used. RNA integrity of isolated RNA was assessed by RNA 6000 Nano assay on a 2100 Bioanalyzer (Agilent Technologies). The RNA of three biological replicates for each condition was analyzed. RNA amplification of each sample was carried out using Illumina TotalPrep RNA Amplification Kit (Ambion) according to manufacturer's instructions. In short, T7 oligo(dT) primer was used to generate single stranded cDNA followed by a second strand synthesis to generate double-stranded cDNA. *In vitro* transcription using T7 RNA polymerase was done to synthesize biotin-labeled cRNA. The cRNA was column purified and checked for quality by RNA 6000 Nano assay. A total of 750 ng of cRNA was hybridized on each array using standard Illumina protocol. Hybridized transcripts were detected with streptavidin-Cy3 (GE healthcare) and microarrays were scanned on an iScan and analyzed using GenomeStudio (both from Illumina, Inc.).

Microarray analysis:

Raw data was background subtracted using GenomeStudio (V2010.1, Illumina)), and processed using the Bioconductor R2.10.1 lumi-package [21]. Data was variance stabilization transformed and quantile normalized. Probes that were at least 3 times present in the experiments (detection p-value <0.01), were considered to be expressed and further analyzed. Differential expressed probes were identified using Bioconductor

package 'limma', with a q-value (FDR) < 0.01[22]. Selected Illumina IDs (logFC >2 and a q-value < 0.01) were analyzed through the use of gene ontology analyses using DAVID (http://david.abcc.ncifcrf.gov/) [23,24].

Statistics:

At least three separate experiments were performed to obtain the histochemical and biochemical cell culture data shown. For statistical analysis we performed students t-tests (p<0.05).

Results

We divided the osteoblast differentiation and mineralization period into three phases as previously described [20]; the differentiation phase in which the pre-osteoblasts proliferate and start to differentiate (day 0-5; Phase 1), the matrix maturation phase in which extracellular matrix is produced and deposited (day 5-12; Phase 2) and the mineralization phase in which the extracellular matrix is mineralized (day 12-19; Phase 3).

A

B

Condition	Oxygen regime			
1	20% - 20% - 20%	▨	▨	▨
2	20% - 20% - 2%	▨	▨	
3	2% - 2% - 2%			
4	20% - 20%	▨	▨	
5	20% - 2%	▨		
6	2% - 2%			
7	20%	▨		
8	2%			
	Phase	1	2	3
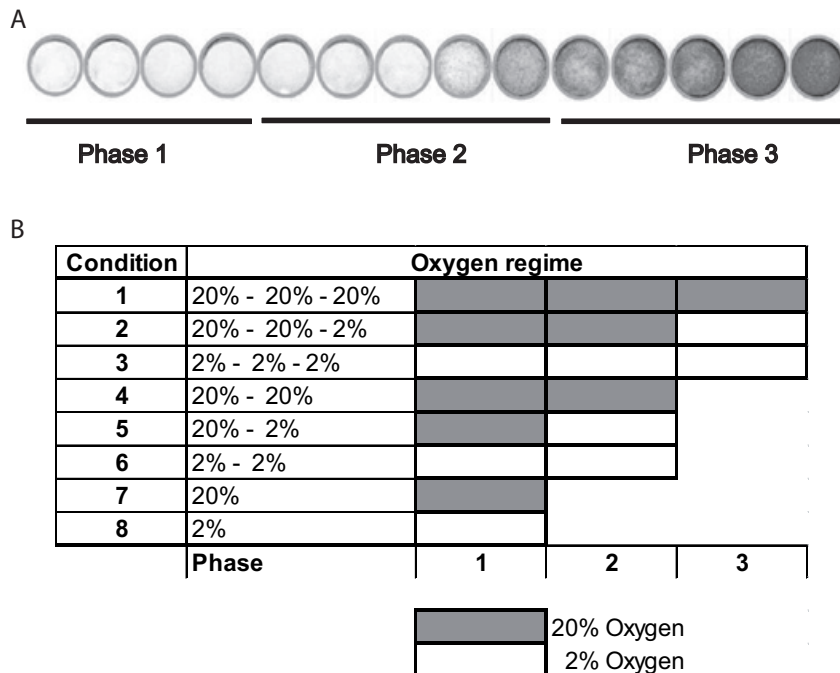
▨ 20% Oxygen
☐ 2% Oxygen

Figure 1: *Experimental set up of the oxygen phase switch experiment.* (A) Alizarin Red stained SV-HFO cells throughout the 19 day long culture period. Depicted are the three phases of osteoblast differentiation and mineralization in cells cultured under 20% oxygen. Phase 1 is the differentiation stage, phase 2 is the matrix formation and maturation stage and phase 3 is the mineralization stage (respectively days 5, 12 and 19 of culture). (B) Cells were cultured for a three week period of time, divided in three phases of 1 week. Cells were cultured under low (2% -white boxes) or high (20% -grey boxes) oxygen tension in several combinations. Cultures were stopped after phase 1 (day 5), phase 2 (day 12) and phase 3 (day 19).

These 3 phases are illustrated in Figure 1A which shows the osteoblast differentiation as reflected by mineralization. Figure 1B displays the experimental layout showing the different combinations of 2% and 20% oxygen according to the osteoblast differentiation phase mentioned. There are three conditions (conditions 1-3) that have been cultured for the entire three phases on different combinations of oxygen concentrations. In addition, cultures were included that were analyzed after the second phase (conditions 4-6) and after the first phase (conditions 7 and 8).

First, we phenotypically analyzed the cultures to assess the impact of the various oxygen regimes on total DNA, total protein, ALP activity, collagen content and mineralization at the end of each respective culture period (i.e. conditions 1-8; Figure 2).
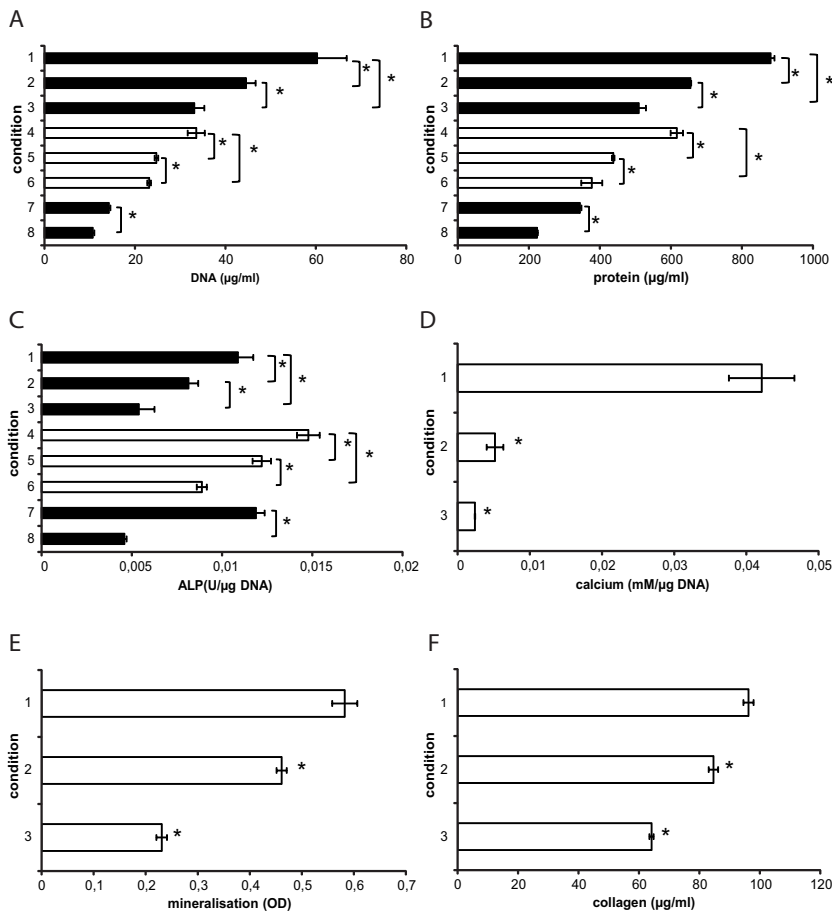
Figure 2: *Biochemical and histochemical analysis on endpoint parameters.* We performed histochemical and biochemical analysis on cell culture samples collected on day 5, 12 or 19 of culture at the end of each phase. (A) DNA content, (B) protein content, (C) ALP activity, (D) calcium content, (E) ARS quantification of mineral content, (F) Sirius red quantification of collagen content. * t-test $p < 0,05$ – compared to condition 1 (20%-20%-20%), 4 (20%-20%) or 7 (20%).

Chapter 3

DNA (Figure 2A): When comparing the 20%-20%-20% oxygen regime to the 20%-20%-2% and the 2%-2%-2% oxygen regimes, we observed a significant decrease in the DNA content as soon as cells were cultured on 2% oxygen, which increased with the duration of the 2% culture period (comparing conditions 1-3). The same was observed at the end of phase 2 (conditions 4-6); cells cultured on a 20%-2% oxygen regimen had significantly lower DNA content than cells cultured on a 20%-20% oxygen regimen. An additional and significant decrease in DNA content was observed in cells cultured on a 2%-2% oxygen regimen (comparing conditions 4-6). A significant difference in DNA content was also observed when cells were cultured for one week on 20% or 2% oxygen (comparing conditions 7 and 8).

Protein (Figure 2B): For total protein content, we observed the same differences as for DNA content. The conditions that received low oxygen tension have the lowest total protein content independent of the differentiation phase.

ALP activity (Figure 2C): In standard 20% oxygen cultures, ALP activity peaks around day 12 and then decreases [17]. This peak can still be observed in 20% cultures when comparing conditions 7, 4 and 1. In cells cultured exclusively on 2% oxygen (conditions 8, 6 and 3) phase 2 peak activity was also observed, but overall ALP activity as well as peak activity was significantly lower than in 20% cultures. In general, a significant decrease in ALP activity was observed during all three phases when a period of 2% oxygen was included.

Mineralization (Figure 2D and 2E): We determined mineralization of the cultures using biochemical analyses and Alizarin Red staining in day 19 (end of phase 3) samples. Mineralization was significantly reduced in cells continuously cultured under 2% oxygen (condition 3) compared to those continuously cultured under 20% oxygen (condition 1) (Figure 2D). Alizarin Red Staining, and quantitative analyses (Figure 2E) supported the biochemically analyses that mineralization is significantly reduced under 2% oxygen. Interestingly, also a single phase of low oxygen during mineralization (the 20%-20%-2% regimen (condition 2) resulted in a significant decrease in mineralization, suggestive for a direct role of oxygen tension in the mineralization process (Figures 2D and E).

Collagen (Figure 2F): Collagen production was significantly decreased in osteoblasts cultured under 2% oxygen (compare conditions 1 and 3 in Figure 2F). Collagen production was also significantly affected by 2% oxygen only during the mineralization period; the 20%-20%-2% regimen (condition 2).

In conclusion, low oxygen tension had an inhibitory effect on osteoblast differentiation and mineralization. Analyses of the two- and three-weeks culture regimens demonstrated that a single week of low oxygen already reduced differentiation and mineralization but that longer exposure to low oxygen had a stronger effect.

Gene expression profiling
In order to identify the molecular processes underlying the observed differences in oxygen regulation, we performed unbiased, gene expression profiling analysis. First we documented the impact of oxygen tension on the expression of several known osteoblast/bone genes (Figure 3A). Alkaline phosphatase (*ALPL*) was expressed significantly lower in

cells cultured under continuous 2% oxygen conditions after phase 1 and 3 and reduced expression was observed in phase 2, albeit not significant. On the other hand, Collagen (*COL1A1*) was significantly higher expressed during phase 2 and 3 in cultures cultured under 2% oxygen. *RUNX2* expression was not affected, with similar levels in cultures cultured under 20% or 2% oxygen. To determine whether cells cultured under 2% oxygen do initiate a hypoxic response, we documented the expression pattern of three well known HIF1α target genes (Figure 3B). We observed a higher expression during all three phases for target genes *VEGF*, *SLC2A1*, and *BNIP3* in cells cultured under 2% oxygen.
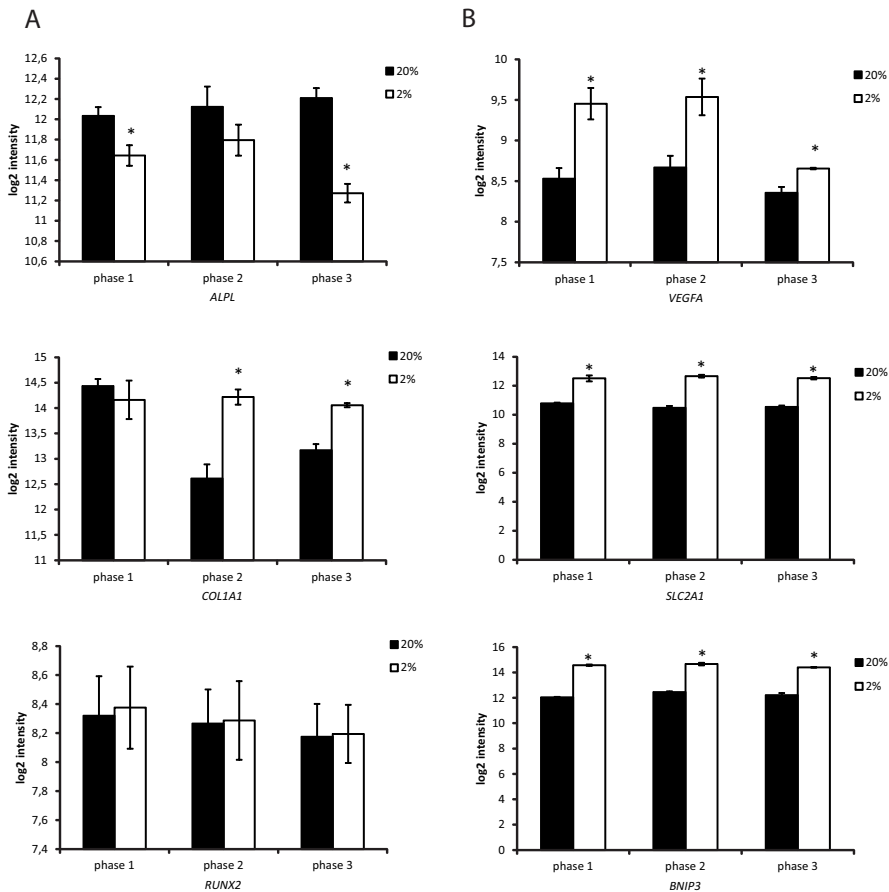
Figure 3: *Expression pattern of osteoblast markers and HIF1α target genes.* Expression patterns of selected genes in cells continuously cultured under 20% (black) or 2% (white). (A) Osteoblast differentiation and marker genes; Alpl, Col1A1 and Runx2. (B) HIF1α target genes; Vegfa, Slc2A1, Bnip3. * t-test p<0,05.

Next in an unbiased approach, we assessed the number of probes differentially expressed when comparing osteoblasts continuously (i.e. without oxygen switch) cultured under 2% or 20% oxygen (Figure 4A). The highest number of differentially regulated probes was found in phase 2, the matrix maturation phase. In phase 1 (comparing condition 8 with 7),

a total of 111 probes were differentially expressed, compared to 263 in phase 2 (comparing condition 6 with 4), and 132 probes when the switch was made in phase 3 (comparing condition 3 with 1). In all three phases more probes were significantly higher expressed than lower expressed in 2% compared to 20% oxygen (Figure 4A).
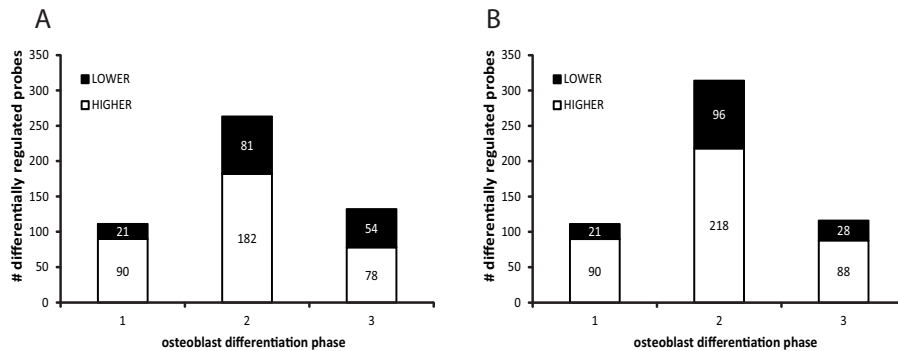
Figure 4: *Differentially expressed probes regulated by a switch in oxygen tension.* Cells were cultured on low oxygen continuously (A) or only during the last phase of culture (B). Depicted is the total number of probes regulated during each phase, as well as the direction of the regulation (fold/qvalue) e.g. higher (white) or lower (black) in 2% oxygen compared to 20 % oxygen.

Next we constructed a heatmap based on the comparison of expression within each phase, i.e. comparison of condition 8 with 7, condition 6 with 4, and condition 3 with 1 (lanes 1, 2, and 3 in Supplemental Figure 1, respectively). Included in the heatmap were all probes that were significantly different expressed in at least one of the three comparisons (2-fold regulated, q< 0.01).

We first analyzed the probes that were expressed higher in cells cultured under 2% oxygen compared to cells cultured under 20% oxygen. Heatmap representation of the differentially expressed genes identified a number of interesting subsets of probes (Supplemental Figure 2). The first subset we analyzed (Figure 5A), consisted of probes that were differentially expressed in both phase 2 and 3 but not in phase 1. The top 5 overrepresented GO terms are depicted in the table in Figure 5B. Both in Molecular Function and Cellular Processes, GO-terms related to collagen and the regulation of extracellular matrix formation, are highly significantly overrepresented. Genes underlying these processes included a range of collagen genes such as *COL1A1, COL1A2, COL4A1, COL4A2, COL5A1 and COL8A1*. In addition we observed an important role for the regulation of vascularisation (*COL1A1, COL1A2, COL5A1, EDN1, LEPR, and THBS1*) and growth factor binding (*COL1A1, COL1A2, COL4A1, COL5A1, THSB1*).

The next subset we analyzed consisted of probes that were expressed higher in all three phases when comparing 2% cultures to 20% cultures (Supplemental Figure 2, subset 2). These probes were mainly involved in the regulation of the cell's glucose metabolism, including glycolysis, hexose- and monosaccharide metabolism (*ENO2, ALDOA, ALDOC, GPI, IRS2 and LDHA*) (Figure 5C). The third subset contained probes that were expressed higher in phase 1 and 2 of 2% oxygen cultures compared to 20% oxygen cultures, but not or to a lesser extend in phase 3 (Supplemental Figure 2, subset 3).

A

phase 1 | phase 2 | phase 3

```
DKFZP451A211
EDN1
NPIP
CORIN
FSCN1
ACTG2
OXTR
ADAM19
ITGA5
MYADM
GOLGA8B
COL8A1
ING2
RPESP
C13ORF15
LOC387882
THBS1
COL4A1
KIAA0363
COL1A1
COL4A2
LEPR
PXDN
C1ORF198
COL5A1
AHNAK
TUBB2B
ACTA1
SF3A2
COL1A2
PPP1R14A
FSTL1
HNRPDL
COL1A2
TGFB1I1
CYB5R3
GADD45B
PTPRF
RAB11FIP5
TGFB1I1
```

B

Category	Process	# genes	p-value
BP	Blood circulation	6	0.042
	Circulatory system proces	6	0.042
	Regulation of blood pressure	5	0.050
CC	Collagen	6	2.55E-10
	Extracellular matrix part	6	0.001
	Sheet-forming collagen	3	0.016
	Extracellular matrix	7	0.019
	Extracellular region part	10	0.038
MF	Platelet derived growth factor binding	4	1.65E-12
	Extracellular matrix structural constituent	5	0.003
	Growth factor binding	5	0.007
	Structural molecule activity	8	0.023

C

Category	Process	# genes	p-value
BP	hexose metabolic process	12	2.07E-07
	monosaccharide metabolic process	12	1.01E-08
	glycolysis	8	2.87E-07
	glucose catabolic process	8	1.34E-08
	glucose metabolic process	10	1.89E-09
MF	L-ascorbic acid binding	4	0.005

D

Category	Process	# genes	p-value
BP	glucose metabolic process	7	0.001
	hexose metabolic process	7	0.005
	generation of precursor metabolites	8	0.006
	monosaccharide metabolic process	7	0.012
MF	monosaccharide binding	4	0.007

E

Category	Process	# genes	p-value
MF	ATP binding	9	0.036
	adenyl ribonucleotide binding	9	0.039
	adenyl nucleotide binding	9	0.050

Figure 5: *Functional analysis of differentially expressed probes in continuous cultures.* Functional GO analysis was performed on subsets of probes extracted from the heatmap (312 probes). (A) Example of a subset, extracted from the heatmap. Depicted are differentially expressed probes of the following comparisons; phase 1 = 2%/20% (conditions 7 and 8), phase 2 = 2%-2%/20%-20% (comparisons 4 and 6) and phase 3 = 2%-2%-2%/20%-20%-20% (conditions 1 and 3). Phase 1 data are obtained by comparing cells cultured under 20% and 2% oxygen during phase 1, which could be seen as a switch at the start of culture. (B-E) Depicted are the top 5 significantly (p<0.05) overrepresented GO terms for biological processes (BP), cellular compartments (CC) and molecular functions (MF) regulated for each analyzed subset, the number of genes represented by those probes in each process and the p-value for each process. P-values are Bonferroni corrected. (B) Subset 1, 35 probes – probes regulated in phase 2 and 3 but not in phase 1, (C) Subset 2, 58 probes – genes regulated in all three phases, (C) Subset 3, 61 probes – genes regulated in phase 1 and 2, but not or less in phase 3, (E) Subset 4, 23 probes – genes regulated in phase 1 and 2 but not in phase 3.

This set of probes turned out to be involved in the regulation of cell metabolism, including glucose metabolic process and monosaccharide binding (*GYS1, HK2, PFKP, PFKL*) (Figure 5D). The number of probes that were expressed lower in 2% cultures compared to 20% cultures was relatively small, thereby limiting the power to identify overrepresented GO-terms in subsets of expressed probes similar to that performed for the probes that were expressed higher. The only subset of probes identifying significantly overrepresented GO-terms was that representing lower expressed probes in phase 1 and 2 but not or to a lesser extend in phase 3 (Supplemental Figure 2, subset 4). This subset of probes was significantly linked to ribonucleotide binding, more specifically ATP binding (*ASNS, WARS, MARS, OAS1 and OAS2*). Although the induction of an interferon response did not show up in the analyses, we noticed a number of interferon related genes in this subset, including *IFIT1, IFIT2, IFIT3 and IRF1* (Figure 5E and supplemental figure 2, subset 4).

Phase 2 was most sensitive to low oxygen in terms of number of genes changed in expression when comparing cells continuously cultured under 2% oxygen to cells cultured under 20% oxygen (Figure 4A). Previously we have shown that low oxygen in phase 1 is crucial for inhibition of osteoblast differentiation. We asked the question whether 2% oxygen in the first phase is essential for the gene expression changes observed in the second week. In order to address this we designed an experiment in which the cells were cultured under 20% oxygen in the first phase and switched to 2% in the second phase (Figure 1B, condition 5) and compared them to cells cultured under 2% oxygen in both phases (Figure 1B, condition 4). In addition, we performed a similar experiment with an oxygen switch in phase 3 (Figure 1B, conditions 1 and 2). In line with the analyses of cells cultured continuously under either 2% or 20% oxygen, the matrix maturation phase (phase 2) was the most sensitive to lowering oxygen tension as assessed by the number of probes changed in expression. Switching in phase 2 from 20% to 2% oxygen (comparing conditions 5 and 4) led to significant change in expression of 314 probes. An oxygen switch in the third phase (comparing conditions 2 and 1) led to change in expression of only 116 probes (Figure 4B and Supplemental Table 1). Similar to the initial analyses comparing cultures continuously cultured on high or low oxygen (Figure 4A) more probes were higher expressed than lower expressed in the 2% oxygen condition. We compared the probes regulated in phase 2 after continuous culture under 2% oxygen (2%-2%, 263 probes) with those found in phase 2 after culturing under 2% oxygen during phase 2 only (20%-2%, 314 probes). Figures 6A and B depict the outcomes of a GO analysis on both sets of genes. There was a wide overlap between the significant GO terms found.

In order to get more insight into the differences between the two sets, we determined the overlap in probes between the two sets. 214 probes were overlapping between the two sets, with 100 specific probes for the 20%-2% probe set and 49 specific probes for the 2%-2% probe set (Figure 6C). GO analysis on the two sets of specific genes didn't reveal any significantly overrepresented GO terms. Figure 6D depicts the top 5 process (all not significantly overrepresented) for each GO category for each set of specific probes. Cells that received 20% oxygen in phase 1 before being switched to 2% oxygen in phase 2 expressed specifically regulated probes that were involved in ligase activity (*GCLM, PSMD1, PSMB9*) as well as the regulation of apoptosis (*EGFR, FOXO3, GCLM, IFI16, VEGFA, VEGFB, and ZBTB16*).

A

2%-2%	Process	# genes	p-value
BP	response to organic substance	36	1,94E-08
	response to endogenous stimulus	26	9,89E-08
	hexose metabolic process	18	3,07E-10
	glucose metabolic process	16	6,97E-09
	monosaccharide metabolic process	18	2,80E-11
CC	collagen	9	4,29E-09
	extracellular matrix part	11	9,14E-10
	extracellular region part	32	9,83E-10
	extracellular region	47	0.017

B

20%-2%	Process	# genes	p-value
BP	response to organic substance	34	1,40E-12
	hexose metabolic process	17	1,90E-12
	glucose metabolic process	15	3,81E-11
	response to endogenous stimulus	24	4,08E-10
	response to virus	13	4,14E-12
CC	collagen	8	2,82E-11
	extracellular matrix part	12	5,33E-10
	extracellular region part	34	0.003
	basement membrane	9	0.007
	extracellular region	52	0.023

C

D

	2%-2%	20%-2%
BP	regulation of fat cell differentiation	response to virus
	response to organic substance	positive regulation of ligase activity
	apoptosis	regulation of ligase activity
	programmed cell death	negative regulation of molecular function
	response to abiotic stimulus	regulation of apoptosis
CC	intracellular organelle lumen	vesicle
	organelle lumen	cytosol
	membrane-enclosed lumen	proteasome complex
		proteasome core complex
		cytoplasmic vesicle
MF	nuclear hormone receptor binding	threonine-type peptidase activity
	hormone receptor binding	threonine-type endopeptidase activity
	platelet-derived growth factor binding	protein dimerization activity
	chaperone binding	vascular endothelial growth factor receptor binding
	transcription factor binding	protein heterodimerization activity

Figure 6: *Regulation of expression in phase 2 is partially dependent on the situation in phase 1.* Phase 2 probe sets from cells cultured continuously on 2% (2%-2%) and cells cultured on 20% in phase 1 and 2% in phase 2 (20%-2%) were compared to determine the influence of phase 1 on the regulation of expression in phase 2. (A) Functional GO analysis of the phase 2 probe set of cells continuously cultured under 2% (2%-2%). (B) Functional GO analysis of the phase 2 probe set of cells cultured under 2% during phase 2 but not phase 1 (20%-2%). (C) Venn diagram depicting the overlap between the two probe sets. (D) GO analysis for both condition specific probe sets (2%-2% specific and 20%-2% specific).

Cellular compartments in which these probes can be found were vesicles and the proteasome complex. In addition probes were involved in threonine-type peptidase and protein dimerization activities (*PSMA3, PSMA4, PSMB9, CENPF, EGFR, HSP90AA2, THRA*). Cells continuously cultured under 2% on the other hand expressed a specific set of probes involved in adipocyte differentiation (*PPARγ, SOD2, TGFβ1I1*), hormone receptor binding (*OASL, TGFβ1I1, PPARγ)* and transcription factor binding (*PIR, TRIB3, OASL)*, processes located inside of membrane enclosed lumens. In addition, they also were involved in the regulation of apoptosis (*GREM1, HSPE1, NGF*) and autophagy (*SQSTM1* and *VCP*).

Finally, using the data depicted in Figure 4B, we constructed a Venn diagram to determine the overlap in regulated probes between the three phases as well as phase specific regulation of gene expression (Figure 7A and Supplemental Table 1). Of the 111, 314 and 116 probes that were differentially regulated after a switch to low oxygen in phase 1, phase 2 or phase 3, respectively, 64 probes were regulated in the same direction in all three the phases upon the switch from 20% to 2% oxygen. GO analysis of these 64 probes showed their involvement in cell metabolism related processes as glycolysis and glucose metabolism, which were significantly overrepresented Biological Processes (*ALDOA, ALDOC, ENO2, HK2, IRS2*) (Figure 7B). Many of these probes were also found in our gene expression profiling studies of cells continuously cultured on high or low oxygen (Figure 4). There were 12, 18 and 195 probes specifically regulated in phase 1, 2 and 3, respectively. The phase specific probes didn't reveal any significant GO-terms (data not shown).

Discussion

The current study describes for the first time the impact of oxygen on the gene expression dynamics against the backdrop of human osteoblast differentiation. Changes in oxygen tension can have profound effects on a wide variety of cellular processes by influencing their underlying gene regulation. Although several studies have looked at the effect of low oxygen tension on specific osteoblast marker genes and signalling cascades, little is known about the effects of changing oxygen tension on the different osteoblast differentiation stages [11,25,26,27]. We demonstrate that the impact of changes in oxygen tension depends on the osteoblast differentiation stage. The matrix maturation phase, including the onset of mineralization (phase 2), is most sensitive to differences in oxygen tension in terms of the number of probes changed in expression but also the overall magnitude of that change in expression. This is seen when osteoblast are cultured permanently from the start under different oxygen tensions as well as when oxygen was switched to 2% in the specific phases.

In line with previous observations by us and others the current study demonstrates a decrease in osteoblast differentiation and mineralization whenever cells are cultured under low oxygen tension [10,11,17]. The current study shows that a single phase of 2% oxygen during differentiation (condition 2) is sufficient to reduce mineralization, demonstrating a direct impact of oxygen on the mineralization process. However, in a previous study we have demonstrated that low oxygen tension in the first phase of osteoblast differentiation, preceding the matrix formation, also leads to decreased mineralization [17]. It should therefore be concluded that oxygen affects eventual mineralization by effects at various stages of osteoblast differentiation positioning oxygen as an important regulator of
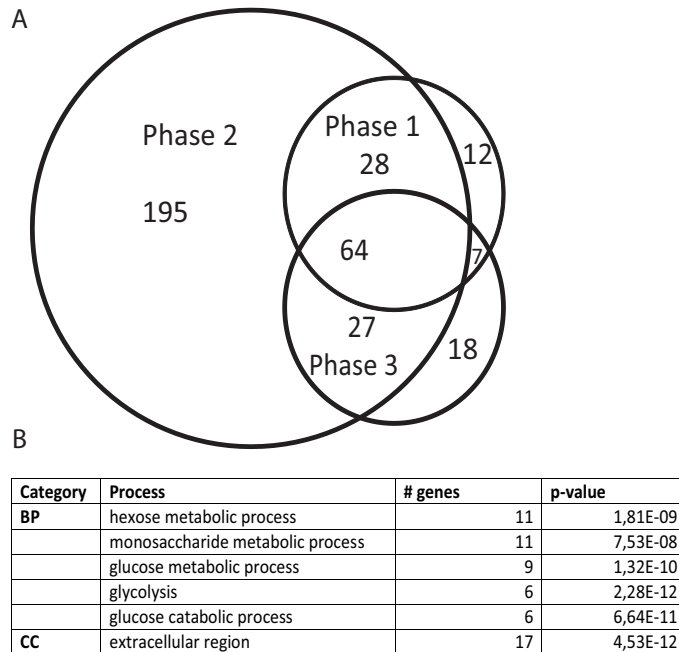
Chapter 3

osteoblast function and bone formation.

Our current gene expression profiling analyses were designed to gain insight into the genes and processes affected by oxygen during the various stages of osteoblast differentiation. These profiling studies show a clear impact of oxygen tension on gene expression, and that one single phase of low oxygen already leads to clear differences in gene expression. Focussing on three known HIF1α target genes showed increased expression of these genes by 2% oxygen in all phases of osteoblast differentiation. This is in line with previous studies showing that activation of HIF1α target genes during periods of low oxygen tension is involved in osteogenesis, indicating that these are indeed direct effects of the drop in oxygen tension [28].

The unbiased heatmap analyses (Supplemental figure 1) identified several specific probe subsets based on regulation during osteoblast differentiation. GO-annotation analyses of the probes that were regulated in all phases of differentiation (subset 2; figure 5C) or predominantly in the first 2 phases (subset 3; Figure 5D) revealed that 2% oxygen significantly impacted on the cell's energy metabolism, in particular carbohydrate metabolism. Most interestingly in this respect is that osteoblast differentiation consists of several high energy demanding processes including matrix production, maturation, and mineralization, which is coordinated by a switch from glycolysis to respiration that involves increased mitochondrial biogenesis [29,30]. We've previously shown that low oxygen tension impacts on mitochondrial activity and downscales cell metabolism, whereas high oxygen tension leads to a higher metabolism, accompanied by differentiation and mineralization [17]. Further support for an important role of energy metabolism and control of energy metabolism in osteoblast differentiation is one of our previous studies which demonstrated a role for peroxisome proliferator-activated receptor-γ in osteoblast differentiation and mineralization [31]. In general more probes were higher expressed in 2% than in 20% oxygen but one set of probes (subset 4) contained probes that were lower expressed under 2% oxygen in phase 1 and 2, but not in phase 3.

These probes were annotated to the molecular function of ribonucleotide binding and more specifically in ATP binding. Obviously, the regulation of ATP binding loops back into the regulation of the cell's metabolism, but interestingly, ATP has also been shown to be directly involved in matrix mineralization [32] as well as in osteoblast differentiation [33]. This suggests that changes in ATP binding, caused by low oxygen tension, can directly affect osteoblast differentiation and mineralization and contribute to the observed decrease in differentiation and mineralization. Overall, current gene expression profiling analyses demonstrates that low oxygen directly impacts on energy metabolism and thereby controls osteoblast differentiation and the energy-demanding processes of matrix formation and mineralization. These findings substantiate the important role of energy metabolism and optimal energy control in bone formation.A specific subset of probes consisted of those increased in expression only during phases 2 and 3 (subset 1). GO-annotation analyses of these genes revealed different biological processes, cellular components and molecular functions than those directly related to energy metabolism. Interestingly, and supportive for a role in osteoblast differentiation and bone formation, were the terms collagen, extracellular matrix and growth factor binding. Numerous collagen genes are expressed to a higher extend in cells cultured continuously on 2%, including *COL1A1*, the main

component of bone matrix. This is in contrast with findings in chondrocytes, which showed a down regulation of collagen type I expression [34] and could indicate osteoblast specific regulation of collagen expression during low oxygen tension. In addition, important hydroxylases including *PLOD1, PLOD2* and *P4HA2,* essential for collagen fibril formation, are higher expressed as well. This corresponds with previous findings in vascular smooth muscle cells and is most likely a direct response to HIF1α induction, caused by the drop in oxygen tension [35].

Category	Process	# genes	p-value
BP	hexose metabolic process	11	1,81E-09
	monosaccharide metabolic process	11	7,53E-08
	glucose metabolic process	9	1,32E-10
	glycolysis	6	2,28E-12
	glucose catabolic process	6	6,64E-11
CC	extracellular region	17	4,53E-12

Figure 7: *Functional analysis of differentially expressed probes after a phase specific switch.* Cells were cultured on low oxygen during the last phase of culture, after which data were collected and analyzed. Differentially regulated probes for all three phases were compared for overlapping probes by means of a Venn diagram. The following comparisons were used for analysis; phase 1 = 2%/20% (conditions 7 and 8), phase 2 = 20%-2%/20%-20% (comparisons 4 and 5) and phase 3 = 20%-20%-2%/20%-20%-20% (conditions 1 and 2). Phase 1 data are obtained by comparing cells cultured under 20% and 2% oxygen during phase 1, which could be seen as a switch at the start of culture. (A) Venn diagram depicting the overlap between differentially expressed probes of all three phases. 64 probes were differentially regulated in all three phases. (B) Depicted are the top 5 significantly (p<0.05) overrepresented biological processes (BP), cellular compartments (CC) and molecular functions (MF) regulated for the 64 probes that were differentially regulated in all three phases. Depicted are the processes, the number of genes represented by the probes in each process and the p-value for each process. P-values are Bonferroni corrected.

These current findings on collagen gene expression are in apparent contradiction with the observed reduced collagen staining in the extracellular matrix. However, this discrepancy is in line with an earlier observation [17] and indicates that extracellular matrix components

are still expressed, even though biochemical analysis showed that matrix mineralization is inhibited and the total collagen content of the matrix is reduced in cells cultured under low oxygen tension. Further studies will be necessary to explain these initially counterintuitive findings, but it is likely that there are changes in translation and fibril formation caused by the reduced oxygen levels. Together these analyses demonstrate that oxygen can also regulate bone formation via changes in extracellular matrix gene expression and probably also at the level of extracellular matrix assembly. In addition to extracellular matrix-related GO-terms this set of oxygen-regulated probes is also linked to the biological process terms circulatory system and blood circulation. This is intuitively logical in view of the link between oxygen tension and angiogenesis [28,36] and is supportive of an involvement of angiogenesis in bone formation and fracture repair [37].

Focussing on a specific phase of osteoblast differentiation it is clear that the matrix maturation phase (phase 2) is most responsive. In cells cultured under 20% oxygen tension cell proliferation decreases, ALP expression peaks and the production and secretion of matrix components becomes important during this phase and mineralization is initiated [20]. It's interesting to see that in this intermediate stage of differentiation, while the cells gear up for matrix maturation and mineralization, the switch in oxygen tension has the most profound effect on gene regulation in terms of numbers and dynamics. We detected 195 probes that were specifically regulated in phase 2 after a switch to 2% oxygen at the end of phase 1, while only 18 probes were changed in expression specifically in phase 3 after a switch to 2 % oxygen. These 195 probes are linked to energy metabolism-related GO terms substantiating the link between oxygen and cellular energy control. Furthermore it is strongly suggestive that this osteoblast differentiation stage of matrix formation and the start of mineralization is the most energy demanding stage. Since we have previously shown the impact of low oxygen in the first phase of osteoblast differentiation [17], we assessed the impact of either 2 % or 20% of oxygen in the first phase followed by 2% in the second phase (conditions 5 and 6). This comparative analysis shows that the number of probes regulated in phase 2 was higher for cells that had previously received 20% oxygen in phase 1 (compare bars of phase 2 in Figure 4A and 4B, 263 and 314 probes, respectively). Additional processes have to be regulated compared to cells continuously cultured on 2% oxygen. However, 81 % of the 263 regulated probes in the 2%-2% condition (condition 6) overlapped with those regulated in the 20%-2% condition (condition 5) and were linked to largely the same biological processes and cellular components including cell metabolism-related biological processes and extracellular matrix-related cellular components. Functional annotation of the 100 specific probes of the 20%-2% condition as well as the 49 specific probes of 2%-2% condition didn't identify any significant biological process or cellular components. Amongst the 100 specific probes for the 20%-2% condition, where both VEGFA and VEGFB, strengthening the link we've observed between hypoxia and angiogenesis which is at least in part regulated by osteoblasts expressing these important regulators of angiogenesis. The list of 49 probes specifically regulated in the 2%-2% condition contained several important genes related to bone metabolism. Among these were collagens and collagen-related proteins as well as PPAR which we have recently shown to regulate osteoblast differentiation [31]. Most interestingly it contained the authophagy-related genes sequestosome 1 (SQSTM1) and vasolin containing peptide (VCP). Interestingly, both these genes are linked to Paget's disease of bone [38,39]. These data are also in line with and support the role of autophagy in bone metabolism [40].

Thereby these data further demonstrate an effect of oxygen on genes/processes related to bone metabolism and suggests a role for other genes on this list in bone metabolism. Moreover these bone-related genes in the group of 2%-2% specific regulated genes stresses that 2% oxygen in the first phase is essential to observe these effects and holds interesting clues for the early stage effects of low oxygen on osteoblast differentiation and bone formation [17].

In conclusion, the current study demonstrates that variation in oxygen tension strongly affects gene expression in differentiating osteoblasts. The magnitude of the change in both expression level and number of regulated probes depends on the osteoblast differentiation stage, with the phase just prior to the onset of mineralization being the most sensitive. The unbiased gene expression profiling analyses pinpoints the inhibition of osteoblast differentiation and mineralization by lowering oxygen to two main processes. First, changes in energy metabolism in genes and processes such as glycolysis and hexose metabolic processes, thereby further substantiating the significance of these processes for the energy demanding process of osteoblast differentiation and bone formation. Secondly, it affects expression of extracellular matrix proteins. These analyses thereby identify processes and genes to target and control for optimal osteoblast differentiation and bone formation in situations of changing oxygen tension such as fracture repair and regenerative medicine.

Chapter 3

References

1. Fraker CA, Ricordi C, Inverardi L, Dominguez-Bendala J (2009) Oxygen: a master regulator of pancreatic development? Biol Cell 101: 431-440.
2. Mazumdar J, O'Brien WT, Johnson RS, LaManna JC, Chavez JC, et al. (2010) O2 regulates stem cells through Wnt/beta-catenin signalling. Nat Cell Biol 12: 1007-1013.
3. van Oorschot AA, Smits AM, Pardali E, Doevendans PA, Goumans MJ (2011) Low oxygen tension positively influences cardiomyocyte progenitor cell function. J Cell Mol Med.
4. Eliasson P, Jonsson JI (2010) The hematopoietic stem cell niche: low in oxygen but a nice place to be. J Cell Physiol 222: 17-22.
5. Raheja LF, Genetos DC, Yellowley CE (2010) The effect of oxygen tension on the long-term osteogenic differentiation and MMP/TIMP expression of human mesenchymal stem cells. Cells Tissues Organs 191: 175-184.
6. Chow DC, Wenning LA, Miller WM, Papoutsakis ET (2001) Modeling pO(2) distributions in the bone marrow hematopoietic compartment. II. Modified Kroghian models. Biophys J 81: 685-696.
7. Harrison JS, Rameshwar P, Chang V, Bandari P (2002) Oxygen saturation in the bone marrow of healthy volunteers. Blood 99: 394.
8. D'Ippolito G, Diabira S, Howard GA, Roos BA, Schiller PC (2006) Low oxygen tension inhibits osteogenic differentiation and enhances stemness of human MIAMI cells. Bone 39: 513-522.
9. Fehrer C, Brunauer R, Laschober G, Unterluggauer H, Reitinger S, et al. (2007) Reduced oxygen tension attenuates differentiation capacity of human mesenchymal stem cells and prolongs their lifespan. Aging Cell 6: 745-757.
10. Utting JC, Robins SP, Brandao-Burch A, Orriss IR, Behar J, et al. (2006) Hypoxia inhibits the growth, differentiation and bone-forming capacity of rat osteoblasts. Exp Cell Res 312: 1693-1702.
11. Salim A, Nacamuli RP, Morgan EF, Giaccia AJ, Longaker MT (2004) Transient changes in oxygen tension inhibit osteogenic differentiation and Runx2 expression in osteoblasts. J Biol Chem 279: 40007-40016.
12. Epari DR, Lienau J, Schell H, Witt F, Duda GN (2008) Pressure, oxygen tension and temperature in the periosteal callus during bone healing--an in vivo study in sheep. Bone 43: 734-739.
13. Lu C, Rollins M, Hou H, Swartz HM, Hopf H, et al. (2008) Tibial fracture decreases oxygen levels at the site of injury. Iowa Orthop J 28: 14-21.
14. Steinbrech DS, Mehrara BJ, Saadeh PB, Chin G, Dudziak ME, et al. (1999) Hypoxia regulates VEGF expression and cellular proliferation by osteoblasts in vitro. Plast Reconstr Surg 104: 738-747.
15. Heppenstall RB, Goodwin CW, Brighton CT (1976) Fracture healing in the presence of chronic hypoxia. J Bone Joint Surg Am 58: 1153-1156.
16. Nagano M, Kimura K, Yamashita T, Ohneda K, Nozawa D, et al. (2010) Hypoxia responsive mesenchymal stem cells derived from human umbilical cord blood are effective for bone repair. Stem Cells Dev 19: 1195-1210.
17. Nicolaije C, Koedam M, van Leeuwen JP (2011) Decreased oxygen tension lowers reactive oxygen species and apoptosis and inhibits osteoblast matrix mineralization through changes in early osteoblast differentiation. J Cell Physiol.
18. Chiba H, Sawada N, Ono T, Ishii S, Mori M (1993) Establishment and characterization of a simian virus 40-immortalized osteoblastic cell line from normal human bone. Jpn J Cancer Res 84: 290-297.
19. Eijken M, Meijer IM, Westbroek I, Koedam M, Chiba H, et al. (2008) Wnt signaling acts and is regulated in a human osteoblast differentiation dependent manner. J Cell Biochem 104: 568-579.
20. Eijken M, Hewison M, Cooper MS, de Jong FH, Chiba H, et al. (2005) 11beta-Hydroxysteroid dehydrogenase expression and glucocorticoid synthesis are directed by a molecular switch during osteoblast differentiation. Mol Endocrinol 19: 621-631.
21. Du P, Kibbe WA, Lin SM (2008) lumi: a pipeline for processing Illumina microarray. Bioinformatics 24: 1547-1548.
22. Smyth GK (2004) Linear models and empirical bayes methods for assessing differential expression in microarray experiments. Stat Appl Genet Mol Biol 3: Article3.
23. Huang da W, Sherman BT, Lempicki RA (2009) Systematic and integrative analysis of large gene lists using DAVID bioinformatics resources. Nat Protoc 4: 44-57.
24. Huang da W, Sherman BT, Lempicki RA (2009) Bioinformatics enrichment tools: paths toward the comprehensive functional analysis of large gene lists. Nucleic Acids Res 37: 1-13.

25. Grayson WL, Zhao F, Bunnell B, Ma T (2007) Hypoxia enhances proliferation and tissue formation of human mesenchymal stem cells. Biochem Biophys Res Commun 358: 948-953.

26. Park JH, Park BH, Kim HK, Park TS, Baek HS (2002) Hypoxia decreases Runx2/Cbfa1 expression in human osteoblast-like cells. Mol Cell Endocrinol 192: 197-203.

27. Warren SM, Steinbrech DS, Mehrara BJ, Saadeh PB, Greenwald JA, et al. (2001) Hypoxia regulates osteoblast gene expression. J Surg Res 99: 147-155.

28. Wang Y, Wan C, Gilbert SR, Clemens TL (2007) Oxygen sensing and osteogenesis. Ann N Y Acad Sci 1117: 1-11.

29. Chen CT, Shih YR, Kuo TK, Lee OK, Wei YH (2008) Coordinated changes of mitochondrial biogenesis and antioxidant enzymes during osteogenic differentiation of human mesenchymal stem cells. Stem Cells 26: 960-968.

30. Komarova SV, Ataullakhanov FI, Globus RK (2000) Bioenergetics and mitochondrial transmembrane potential during differentiation of cultured osteoblasts. Am J Physiol Cell Physiol 279: C1220-1229.

31. Bruedigam C, Eijken M, Koedam M, van de Peppel J, Drabek K, et al. (2010) A new concept underlying stem cell lineage skewing that explains the detrimental effects of thiazolidinediones on bone. Stem Cells 28: 916-927.

32. Nakano Y, Addison WN, Kaartinen MT (2007) ATP-mediated mineralization of MC3T3-E1 osteoblast cultures. Bone 41: 549-561.

33. Costessi A, Pines A, D'Andrea P, Romanello M, Damante G, et al. (2005) Extracellular nucleotides activate Runx2 in the osteoblast-like HOBIT cell line: a possible molecular link between mechanical stress and osteoblasts' response. Bone 36: 418-432.

34. Wernike E, Li Z, Alini M, Grad S (2008) Effect of reduced oxygen tension and long-term mechanical stimulation on chondrocyte-polymer constructs. Cell Tissue Res 331: 473-483.

35. Hofbauer KH, Gess B, Lohaus C, Meyer HE, Katschinski D, et al. (2003) Oxygen tension regulates the expression of a group of procollagen hydroxylases. Eur J Biochem 270: 4515-4522.

36. Genetos DC, Toupadakis CA, Raheja LF, Wong A, Papanicolaou SE, et al. (2010) Hypoxia decreases sclerostin expression and increases Wnt signaling in osteoblasts. J Cell Biochem 110: 457-467.

37. Portal-Nunez S, Lozano D, Esbrit P (2012) Role of angiogenesis on bone formation. Histol Histopathol 27: 559-566.

38. Hocking LJ, Lucas GJ, Daroszewska A, Mangion J, Olavesen M, et al. (2002) Domain-specific mutations in sequestosome 1 (SQSTM1) cause familial and sporadic Paget's disease. Hum Mol Genet 11: 2735-2739.

39. Watts GD, Wymer J, Kovach MJ, Mehta SG, Mumm S, et al. (2004) Inclusion body myopathy associated with Paget disease of bone and frontotemporal dementia is caused by mutant valosin-containing protein. Nat Genet 36: 377-381.

40. Hocking LJ, Whitehouse C, Helfrich MH (2012) Autophagy: A new player in skeletal maintenance? J Bone Miner Res 27: 1439-1447.

Chapter 3

CHAPTER 4

Bone fragility and decline in stem cells in prematurely aging DNA repair deficient trichothiodystrophy mice

Karin E.M. Diderich[1,†], Claudia Nicolaije[2,†], Matthias Priemel[3,†], Jan H. Waarsing[4], Judd S. Day[4], Renata M.C. Brandt[1], Arndt F. Schilling[3,5], Sander M. Botter[1,2], Harrie Weinans[4], Gijsbertus T.J. van der Horst[1], Jan H.J. Hoeijmakers[1], and Johannes P.T.M. van Leeuwen[2]

[1]MGC Dept. of Cell Biology & Genetics, Center for Biomedical Genetics, Erasmus MC, [2]Dept. of Internal Medicine, Erasmus MC, [3]Center of Biomechanics and Skeletal Biology, Dept. Trauma Surgery, University Medical Center Hamburg Eppendorf, 20246 Hamburg, Germany, [4]Dept. of Orthopaedics, Erasmus MC, 3000 DR Rotterdam, The Netherlands, [5]Biomechanics Section, Hamburg University of Technology, 21073 Hamburg, Germany

[†] Authors contributed equally to the manuscript.

Chapter 4

Abstract

Trichothiodystrophy (TTD) is a rare, autosomal recessive Nucleotide Excision Repair (NER) disorder caused by mutations in components of the dual functional NER/basal transcription factor TFIIH. TTD mice, carrying a patient-based point mutation in the *Xpd* gene, strikingly resemble many features of the human syndrome and exhibit signs of premature aging. To examine to which extent TTD mice resemble the normal process of aging, we thoroughly investigated the bone phenotype. Here we show that female TTD mice exhibit accelerated bone aging from 39 weeks onwards as well as lack of periosteal apposition leading to reduced bone strength. Prior to 39 weeks long bones of wild type and TTD mice are identical excluding a developmental defect. Albeit that bone formation is decreased, osteoblasts in TTD mice retain bone-forming capacity as *in vivo* PTH treatment leads to increased cortical thickness. *In vitro* bone marrow cell cultures showed that TTD osteoprogenitors retain the capacity to differentiate into osteoblasts. However, after 13 weeks of age TTD females show decreased bone nodule formation. No increase in bone resorption or the number of osteoclasts was detected. In conclusion, TTD mice show premature bone aging, which is preceded by a decrease in mesenchymal stem cells/osteoprogenitors and a change in systemic factors, identifying DNA damage and repair as key determinants for bone fragility by influencing osteogenesis and bone metabolism.

Introduction

TTD is a rare, autosomal recessive DNA repair disorder in which patients present an array of symptoms, including *P*hotosensitivity, *I*chthyosis, *B*rittle hair and nails (hallmark feature), *I*mpaired intelligence, *D*ecreased fertility, *s*hort stature (hence the acronym PIBIDS) and a severely reduced life span [9]. In addition, skeletal abnormalities, i.e. osteopenia in long bones and osteosclerosis in vertebrae, have been described [1,2,3,4,5,6,7,8,9]. A significant proportion of TTD patients exhibit marked photosensitivity, due to impaired repair of UV-induced DNA lesions. Complementation analysis of UV-sensitive TTD patients revealed the involvement of three repair genes (*XPB*, *XPD* and *TTDA*), encoding subunits of the dual functional DNA repair/basal transcription factor TFIIH [10]. This 10-subunit protein complex is involved in the Nucleotide Excision Repair (NER) pathway, as well as in the initiation of transcription by RNA polymerases I and II. [11,12,13,14,15,16]. NER consists of a complex 'cut-and-patch' type reaction involving ~30 proteins and is comprised of 2 sub-pathways, differing in the initial steps of DNA damage recognition [17]. Global genome NER removes a wide class of helix-distorting DNA damage (e.g. UV-induced photoproducts) from the overall genome [18]. This pathway is primarily important for preventing DNA damage-induced mutations and thereby for preventing cancer. The second sub-pathway called transcription-coupled NER focuses on the preferential excision of lesions in the transcribed strand of active genes that actually block transcription elongation, to allow rapid resumption of arrested gene expression and thereby promoting cell survival after genotoxic stress [19,20,21]. This sub-pathway is thought to counteract the cytotoxic consequences of DNA damage. TFIIH is as DNA helix opener implicated in both NER sub-pathways as well as in transcription initiation by promoter opening to allow the RNA polymerase to get hold of the transcribed strand for transcription elongation.

We have generated a mouse model in which we precisely mimicked a causative point mutation in the essential *XPD* gene of a TTD patient (TTD1BEL, mutation at the protein level R^{722}W) [22]. TTD mice have a phenotype that strikingly resembles the symptoms of TTD patients and they were found to exhibit several premature aging-like features. Although TTD was not recognized as a segmental premature aging syndrome, some of the features observed in the mouse model were also incidentally reported in patients: deterioration of renal, liver and heart tissues, lymphoid depletion, reduced hypodermal fat, aortic sarcopenia, skeletal abnormalities and an (in patients strongly, in mice moderately) reduced life span [1,2,3,4,5,6,7,8,23,24,25]. Concerning skeletal aging, Price and co-workers reported a patient who at the age of 7 years showed decreased bone density in the distal bones on roentgenographic examination [7]. Chapman reported a 5-year old child who exhibited decreased bone density in the distal limbs and osteopenia in the most distal parts [6].

Recent studies suggest that aging and the associated increase in reactive oxygen species (ROS) may account for the increased bone resorption associated with the acute loss of estrogens or androgens rather than estrogen deficiency *per se* ([26] and references therein). Loss of these hormones decreases defence against oxidative stress in bone while ROS greatly influence the generation and survival of osteoclasts, osteoblasts, and osteocytes ([26] and references therein). Forkhead box O (FoxO) transcription factors defend against oxidative stress by activating genes involved in free radical scavenging and apoptosis. Recently, it

was shown that loss of FoxO transcription factors leads to an increase in oxidative stress and consequently osteoblast apoptosis with an osteoporotic phenotype characterized by decreased bone mass at both cancellous and cortical sites as a result [27] and specifically deletion of FoxO1 in osteoblasts decreased osteoblast numbers, bone formation rate, and bone volume [28].

Thus the TTD mouse could be a model for bone fragility, which is observed in both aging women and men. Whereas postmenopausal women show an accelerated loss of predominantly trabecular bone, due to increased number and activity of osteoclasts, in bone fragility both women and men show a slow continuous phase of decrease in bone mass in which the density of trabecular bone reduces and cortical bone thins [29,30,31,32,33]. This is partly counteracted by increased periosteal apposition [34], i.e. bone formation on the outside of the bone (periosteum), a critical process that continues throughout life [31,32,35]. Periosteal apposition is thought to be a response to the loss of trabecular bone as well as endosteal resorption and aims to maintain bone strength by increasing the bone perimeter [36]. The mechanisms underlying these age-related changes are poorly understood.

To assess the contribution of deficiencies in DNA repair/basal transcription in skeletal aging and to determine to which extent the progeroid features in the mouse and human disorder truly reflect *bona fide* aging we decided to thoroughly examine the skeletal aging as this process has been amply characterized in normal aging. The TTD mouse model may provide a unique tool to study aging and bone metabolism and to assess the impact of DNA repair on skeletal aging.

Materials & Methods

Mice and bones
The cohort of wild type and TTD mice included 8 female animals per age group per genotype. Mice were sacrificed at 13-week intervals up to an age of 104 and 78 weeks for wild type and TTD mice respectively. All mice were on a C57BL/6J background, maintained on a 12:12 h light-dark cycle and fed *ad libitum* with 'rat and mouse breeder and grower diet' from Special Diet's Services (minimal 0.5% Ca and 0.3% Pi). The animals were injected intra-peritoneal with calcein (10 µg /g body weight) 10 and 3 days before sacrifice in order to study the bone formation occurring in one week. After anaesthetization with isoflurane, blood was collected by an orbital puncture; subsequently the mice were killed by cervical dislocation. Femurs and tibiae were isolated and were either used immediately for bone marrow isolation, snap frozen in liquid nitrogen and stored at -80ºC or fixed in Burkhardt, which was replaced by 70% ethanol after 3 days. There was no significant difference in bone length between wild type and TTD mice (data not shown). As required by Dutch law, formal permission to generate and use genetically modified animals was obtained from the responsible local and national authorities. All animal studies were approved by an independent Animal Ethical Committee (Dutch equivalent of the IACUC).

Micro-computed tomography
Fixed tibiae from wild type and TTD mice of different ages (n = 4-6 per group) were scanned by micro-computed tomography (µCT) from proximal end to mid-diaphysis

using the SkyScan 1072 microtomograph (SkyScan, Antwerp, Belgium) with a voxel size of 8.82 μm. The reconstructed data sets were segmented using an automated algorithm based on local thresholds [57]. Three-dimensional (3D) morphometric analysis of the bone was performed using subsequent software packages, including Nrecon, CT-analyze and Dataviewer (http://www.skyscan.be/products/downloads.htm) and freely available software of the 3D-Calculator project (http://www.erasmusmc.nl/orthopaedie/research/labor/downloads). For all mice a standardized metaphyseal – diaphyseal area (3.7-6.9 mm from the proximal end; mainly consisting of cortical bone) and a metaphyseal area (100 sections starting 30 sections below our offset landmark within the epiphyseal growth plate; including more trabecular bone) were selected for analysis. It was previously shown that murine femur length does not increase after 26 weeks of age [58]. We determined the following parameters: cortical bone volume, 3D thickness distribution [59], cortical thickness, periosteal perimeter, endocortical volume, trabecular bone volume fraction (BV/TV), trabecular number and trabecular thickness. Polar moment of inertia (measure of the geometrical distribution and a proxy for mechanical stiffness and strength per transverse cross-section) was determined to analyse the consequence of differences in geometry. The 3D thickness distribution graph is similar to a usual frequency distribution, only with infinitely small bins. It is a continuous equivalent, similar to a probability density distribution in statistics. While with discrete bins the y-axis would show volume (fraction), this continuous case narrows it down to volume density (volume/um).

Histomorphometric analysis

To assess dynamic histomorphometric indices, mice received intraperitoneal injections with calcein 10 days and 3 days prior to sacrifice. One tibia of each mouse was dehydrated in ascending alcohol concentrations and embedded in poly-methylmetacrylate (PMMA) as described previously [60]. Sections of 5 μm were cut in the sagittal plane defined by the frontal aspect of the tibia and the fibula on a Microtec rotation microtome (Techno-Med GmbH, Munich, Germany). Consecutive serial sections are cut in this plane and the section with the widest diameter is used for analysis, thereby minimizing potential artifacts. Subsequently the sections were stained by toluidine blue, van Gieson/von Kossa and Giemsa procedures as described [60].

Parameters of static and dynamic histomorphometry were quantified on these undecalcified proximal tibia sections. For each animal, the bone formation rate was determined by fluorochrome (calcein) measurements using two non-consecutive 12μm-sections per animal.

Analysis of osteocyte number per bone area (per mm^2), osteoblast number per bone perimeter (per mm), osteoclast number per bone perimeter (per mm), osteoid volume per bone volume (percentage), osteoid surface per bone surface (percentage) was carried out according to standardized protocols [61] using the OsteoMeasure histomorphometry system (Osteometrics Inc., Atlanta, Georgia, USA).

Mechanical testing

Defrosted femurs from 13, 26, 52 and 78-week old wild type and TTD females as well as from 104-week-old wild type females (5-8 mice/group) were excised from the soft tissues. Femurs were tested in a three-point bending assay using a Lloyd LRX mechanical test frame, constructed with 3mm hemi-cylindrical supports with a 9 mm total span. The

Chapter 4

femurs were aligned such that the neutral axis was parallel to the sagittal plane (i.e. the femoral head was in the horizontal plane and the posterior aspect of the condyles were facing down). The lesser trochanter was used as a reference point and aligned with one of the two supports. All samples were preconditioned for 5 cycles to 2N at a rate of 0.01 mm/s before testing to failure at a rate of 0.02mm/s.

Backscatter Scanning Electron Microscopy

Processing and analyses were done as described previously [62]. In short, from each group (i.e. 26, 52 and 78-week-old wild type and TTD mice) the distal halves of the femurs used for mechanical testing were embedded in blocks of MMA, such that each block contained one distal femur from each genotype and age group. Within a block, all femurs were placed within a plane, such that the longitudinal lateral-medial plane of the femurs coincided with the plane of embedding. Embedding several samples in one block enabled us to image these samples within one scanning electron microscopy (SEM) session, thus decreasing the variance in the measurements. After embedding, the blocks were cut in two on an electric band saw (Exakt, Norderstedt, Germany), resulting in a slab of plastic with two parallel surfaces, parallel to the plane of embedding of the femurs. Starting from the posterior side of the bones, material was removed using an automatic grinding system (Buehler Phoenix 4000) with p400 grid paper until an interior surface, halfway between the ventral and dorsal external surfaces, was exposed. To reduce the roughness of the surface the blocks were ground with p1200 paper followed by polishing using 3 μm diamond paste with polishing paper (Buehler Texmet 1000). The resulting surface had a roughness (R_a) smaller than 0.05 μm. The blocks were cleaned, sonicated and sputter coated with a thin layer of carbon (Bio-Rad Temcarb Carbon Coater, Bio-Rad Microscience Division) to enable conduction of the electron beam to the sample surface.

Backscatter SEM images were taken of trabecular bone of the metaphyseal and epiphyseal regions of each bone sample, and of the cortex using methods described in detail previously [62]. The images were taken at an accelerating voltage of 25 kV, a working distance of 17 mm and 50x magnification. Before and after imaging calibration images were taken of an aluminum standard embedded in each block and of the MMA material. The equivalent Z-value (atomic number) of the MMA was obtained by calibration with aluminum (Z=13) and carbon (Z=6) standards (Micro Analysis Consultants).From each image the histogram of equivalent Z-values was calculated of which the mean value represented the mean mineralization of the bone tissue [63].

Tartrate-resistant acid phosphatase assay

Bone resorption was determined by measuring serum tartrate resistant acid phosphatase (TRAP) levels using the TRAP assay purchased from SBA Sciences (Turku, Finland).

Bone marrow isolation, cell culture and cell culture staining

Bone marrow was collected by spinning down the bone marrow into an eppendorf tube at 5000rpm for 2 min immediately after obtaining the bones from the mice. Erythrocytes were lysed using erylysis buffer (1.55M NH_4Cl, 0.1M $KHCO_3$, 1mM EDTA (10x)) and cells were washed and seeded at 1.000.000 cells/well (12 wells) for osteoblasts, 100.000 cells/well (96 wells) for osteoclasts and 750.000 cells/well, for adipocytes (24 wells). For osteoblast cultures the cells were cultured in phenol-red free α-minimal essential medium (GIBCO/BRL), supplemented with 100 units/ml penicillin, 100 μg/ml streptomycin (Life Technologies,

Breda, The Netherlands), 250 ng/ml amphotericin B (Sigma), 20 mM Hepes, 1.8 mM CaCl2, and 15% (vol/vol) heat-inactivated FCS (GIBCO/BRL), pH 7.5. From day 3 onward, the culture medium was supplemented with 50 μM vitamin C (Sigma) and 10 mM β-glycerophosphate (Sigma). At days 14 and 21 of culture cells were fixed in 70% ethanol and stained for alkaline phosphatase (ALP) and alizarin red, respectively. For ALP staining, cells were incubated in Tris·HCL (pH 9.5) containing 50 mM MgCl2, 0.6 mg/ml bromo-chloro-indoryl phosphate (Sigma), and 150 μg/ml nitro blue tetrazolium (Sigma) for 20 min and washed with PBS. Alizarin red staining was performed, incubating the cells for 10 min in a saturated alizarin red S solution in distilled water (pH 4.2), after which the cells were washed with distilled water. Osteoblast colony forming potential and mineralisation potential were determined as previously described after respectively 14 and 21 days of culture [64]. Colonies were counted by eye, plates were scanned and colony surface area was determined by computer analysis (Bioquant software). Alizarin Red staining was quantified after extraction and measured at 405 nm on a plate reader.

Osteoclasts were cultured as previously described [64]. Shortly, cells were cultured for 6 days in the presence of 30 ng/ml recombinant M-CSF (R & D Systems) and 20 ng/ml recombinant murine RANKL-TEC (R & D Systems), and the media were refreshed at day 3. At the end of the human and murine cultures, cells were washed with PBS, fixed in PBS-buffered paraformaldehyde (4% vol/vol) or formalin (10% vol/vol), respectively, and stored at 4°C for tartrate-resistant acid phosphatase (TRACP) staining and immunocytochemistry. Bone resorption was analysed using the resorption pit assay. Osteoclasts were cultured on bovine cortical bone slices, after 6 days of culture the cells were lysed in water and the bone slices were sonicated in 10% (vol/vol) ammonia (Merck) for 10 min. After extensive washing, the cells were incubated in filtered potassium aluminum sulfate (Sigma) for 10 min and subsequently stained with filtered Coomassie brilliant blue (Phastgel Blue R; Amersham Pharmacia Biotech) for 5 s. Osteoclast number and resorption capacity were determined as previously described [64] and analysed using freely available Image J software (version 1.41; http://rsbweb.nih.gov/ij/).

Adipocytes were cultured on adipogenic (D-MEM (GIBCO, Paisley, UK) supplemented with P/S, amphotericin B (250 ng/ml,Sigma) and 15% heat-inactivated FCS (GIBCO)) medium. Adipogenesis was induced after a 3-week expansion phase by adding insulin (0.1μg/ml, Sigma), indomethacin (1mM, Sigma) and dexamethasone ($1*10^{-7}$M, Sigma) for two weeks.Adipocyte cultures were fixated O/N with 10% formaline, washed with 60% IPOH and stained with Oil-Red O solution (60-40 dilution of Oil-Red O stock solution (Clin-Tech limited) in H_2O) after which the total amount of adipocytes per well was determined.

PTH treatment
Twenty TTD females were weighed at the age of 45 weeks and randomly divided into the following two groups (n=10 per group): subcutaneous injection with human parathyroid hormone(1-34) (Bachem, Germany) (40 μg/kg body weight) in a weekly alternating regimen (PTH); or subcutaneous injection with phosphate buffered saline in a weekly alternating regimen (VEH). Animals were weighed at the start of every injection week. At 65 weeks of age animals were sacrificed and femurs were prepared for μCT scanning.

Chapter 4

Statistics

Micro-CT parameters, histomorphometric data, femur length, ultimate load, bone resorption and mineralization data and parameters of cell culture analyses were compared between the age groups (significance compared to 13 or 26 weeks of age) of both genotypes separately using one-way ANOVAs with Tukey post-hoc test (Graph Pad InStat version 3.05: Graph Pad Software, San Diego California, USA, www.graphpad.com). In addition, the micro-CT parameters, histomorphometric data, femur length, ultimate load, bone resorption data, and parameters of cell culture analyses were compared between genotypes for all age groups separately using two-tailed unpaired t-tests.

Results

To study the bone phenotype in normal and premature aging female TTD mice, we performed a systematic cohort study including 8 mice per age group per genotype. A previous study, performed on a hybrid C57BL/6J 129ola genetic background, showed that TTD mice live shorter than wild type mice [23]. In the present study, we were able to analyse 13, 26, 39, 52, 65 and 78 weeks-old wild type and TTD mice in a homogeneous C57Bl/6 genetic background. For wild type control mice we could in addition analyse 91 and 104 weeks old mice.

Bone geometry

First, 3D thickness distribution was analyzed using micro-computed tomography (μCT). In tibiae from wild type mice, a gradual progressive decline in 3D thickness distribution was observed with age (Figure 1A). In TTD mice this process was accelerated with a severe decrease in 3D thickness distribution after 39 weeks of age (Figure 1B). Already at 52 weeks of age, 3D thickness distribution in TTD tibiae reached a level that in wild type mice was only reached at 91 weeks of age (Figure 1C). Thus age-related decrease in bone mass occurred earlier in TTD mice than in wild type mice.

To study this difference in onset of decrease in bone mass in more detail, we analysed specific μCT parameters. In wild type mice, cortical bone volume gradually decreased with age, only reaching significance at 104 weeks of age at which time a 12% decrease in bone volume compared to 26-week-old wild type bones was observed (Figure 1D). At 26 and 39 weeks of age, tibiae of TTD mice had a bone volume similar to that of wild type mice (Figure 1D). However, in the period thereafter, bone volume rapidly decreased to 31% (78-week-old TTD mice dropping to 69% of the bone volume of 26-week-old TTD mice), which was significantly lower than the 9% decline in age-matched wild type mice at 78 weeks of age (Figure 1D). Already at 52 weeks of age TTD mice reached a cortical bone volume comparable to that of 104-week-old wild type mice (Figure 1D). In line with cortical bone volume, wild type tibiae maintained their cortical thickness up to 78 weeks of age and showed a decrease thereafter while TTD tibiae already displayed a rapid drop in cortical thickness after 39 weeks of age resulting in a significantly thinner cortex in TTD mice (Figure 1E). Next, we analyzed the bone perimeter. As depicted in Figure 1F, tibiae from young mice had a similar perimeter (at 26-weeks: 5,80 mm in wild type and 5,96 mm in TTD mice), again indicating normal bone development in TTD mice. From 52 weeks onwards, wild type tibiae showed a progressive increase in perimeter reaching 6,33 mm at 78 weeks (9% increase) and 6,78 mm at 104 weeks (17% increase). In contrast, TTD mice failed to

show an increase in perimeter (5,88 mm at 78 weeks). In 78 week-old wild type mice the perimeter is significantly higher compared to TTD mice (Figure 1F). Thus, TTD mice lack the age-related increase in perimeter as seen in wild type tibiae (Figure 1F).

Chapter 4
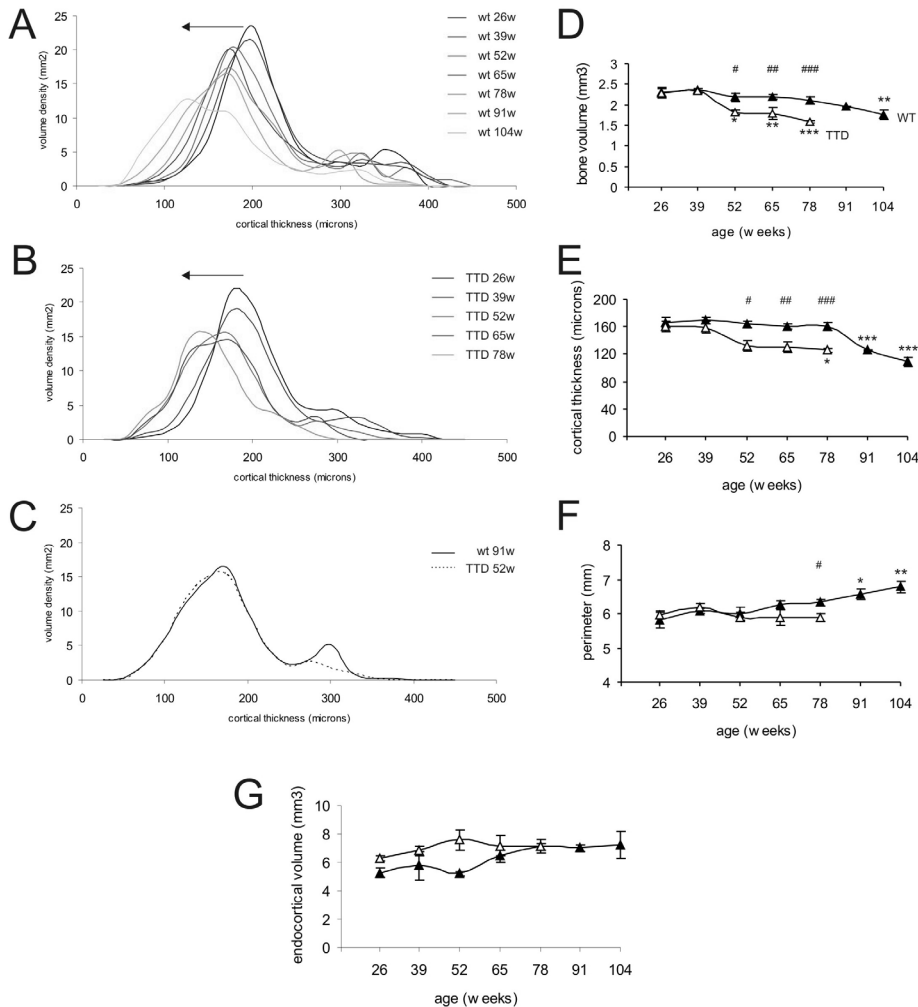
Figure 1: Thickness distribution and cortical bone parameters in wild type and TTD mice. Cortical thickness distribution in aging wild type (A) and TTD mice (B) with the arrow indicating the direction of change with aging. Comparison of thickness distribution in 52-week-old TTD mice (dotted line) compared to 91-week-old wild type mice (solid line) (C). Bone parameters in aging wild type mice (solid triangles) and TTD mice (open triangles): cortical bone volume (D), cortical thickness (E), perimeter (F) and endocortical volume (G). TTD mice compared to wild type animals: # $p<0.05$, ## $p<0.01$, ### $p<0.001$; TTD mice and wild type animals compared to their 26 week time point: * $p<0.05$, ** $p<0.01$, *** $p<0.001$; error bars represent SEM.

The endocortical volume was larger in TTD than in wild type mice in the early phase of life but later in life endocortical volume in wild type mice increased and becomes equal to that of TTD mice (Figure 1G). The temporal dynamics in endocortical volume in wild type mice, showing an increase after 52 weeks, match that observed for perimeter, showing an increase from 52 weeks of age onwards. However, periosteal apposition could no longer match the endocortical bone loss in wild type mice after 78 weeks of age leading to a decrease in cortical thickness (Figure 1E).

Next we analyzed trabeculae in the metaphyseal area. Aging wild type mice showed a gradual decrease in both BV/TV and trabecular number (Figure 2A and B) while trabecular thickness showed a mild increase with aging (Figure 2C). Overall no significant differences between wild type and TTD mice were observed. In contrast to wild type mice, the
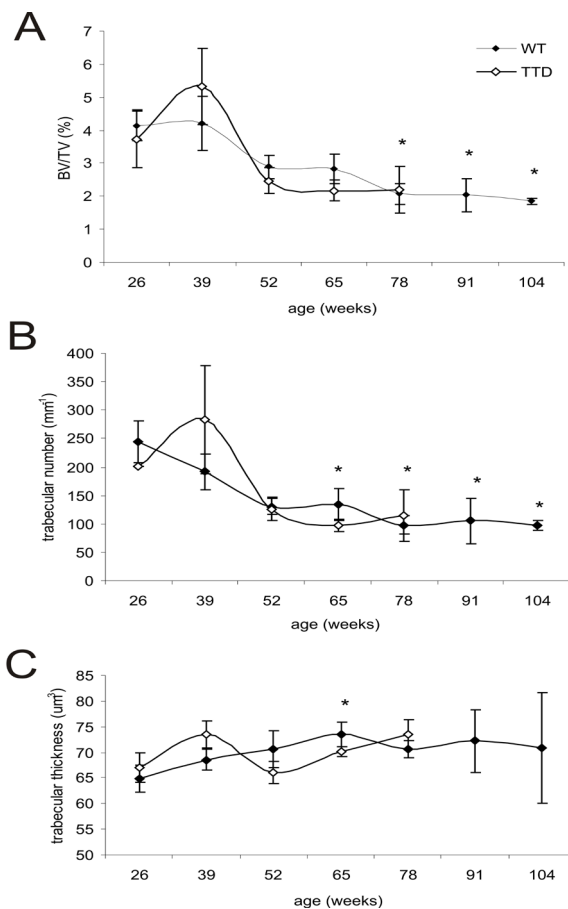
Figure 2: *Trabecular bone parameters in wild type and TTD mice.* Bone parameters measured in 100 crossections in the metaphysis of aging wild type mice (solid triangles) and TTD mice (open triangles): trabecular bone volume fraction (BV/TV; A), trabecular number (B) and trabecular thickness (C). Wild type animals compared to their 26 week time point: *p<0.05; error bars represent SEM.

trabecular bone in TTD mice showed a remarkable dynamic pattern around 39 weeks of age as exemplified by a transient non-significant increase in BV/TV, trabecular number and trabecular thickness (Figure 2A-C).

Histomorphometric analysis
In order to analyze the lack of periosteal expansion in TTD mice in more detail, we examined endosteal and periosteal bone apposition by double labeling studies. In wild type mice both periosteal and endosteal bone formation were present throughout life (Figure 3A). In contrast, in TTD mice endosteal apposition was present whereas periosteal apposition was virtually absent in older TTD mice (Figure 3A).

Quantitative analyses revealed no significant difference in endosteal bone formation between 13-week old wild type and TTD mice (Figure 3B). At 39 weeks of age, endosteal bone formation was significantly decreased in TTD mice compared to wild type mice, but after 39 weeks of age endosteal bone formation decreased in wild type mice as well (Figure 3B).

At 78 weeks of age, wild type and TTD mice showed a 20-25% decrease in endosteal bone formation when compared to 13-week-old animals. At 13 weeks of age, periosteal apposition showed no significant difference between wild type and TTD mice (Figure 3C). However, after 13 weeks of age, TTD mice showed a dramatic and significant decrease in periosteal apposition compared to wild type mice (Figure 3C). Only at 78 weeks of age, when periosteal apposition in wild type mice decreased as well, there was no significant difference compared to TTD mice anymore (Figure 3C). At that time, however, TTD mice exhibited a 60% decrease in periosteal apposition compared to a 25% decrease in wild type mice when compared to 13-week-old animals.

Osteocytes in cortical sections of tibiae of wild type and TTD mice were measured to assess whether a reduced number of osteocytes in TTD mice could play a role in impaired periosteal apposition. However, no significant difference in the number of osteocytes was found between wild type and TTD mice or in aging animals (data not shown). In addition, we analyzed the number of osteoblasts, osteoclasts and osteoid volume. The number of osteoblasts did not show a significant difference between wild type and TTD tibiae at the analyzed ages (Figure 3D). However, regression analyses showed a significant (p<0.01) lower number of osteoblasts in TTD mice over life. No significant difference in the number of osteoclasts was observed between wild type and TTD mice or in aging animals (Figure 3E).

Osteoid volume seemed to decrease with age in both wild type and TTD tibiae, but at none of the ages osteoid volume was significantly different between wild type and TTD mice (Figure 3F). Osteoid surface showed similar results (data not shown). These osteoid data exclude that the differences observed by μCT are due to a mineralization defect. This is further supported by Quantitative Backscatter Scanning Electron Microscopy showing no significant differences in degree of mineralization (Figure 3G).

Mechanical testing of bone strength
The overall picture that emerges is that compared to wild type mice, aging TTD mice show an accelerated decrease in bone mass, which initiated between weeks 39 and 52, and that

Chapter 4

TTD mice lack the age-related increase in perimeter. To analyze the consequence of these geometric changes, we calculated the polar moment of inertia, which is a measure of the geometrical distribution and a proxy for mechanical stiffness and strength per transversal cross-section.
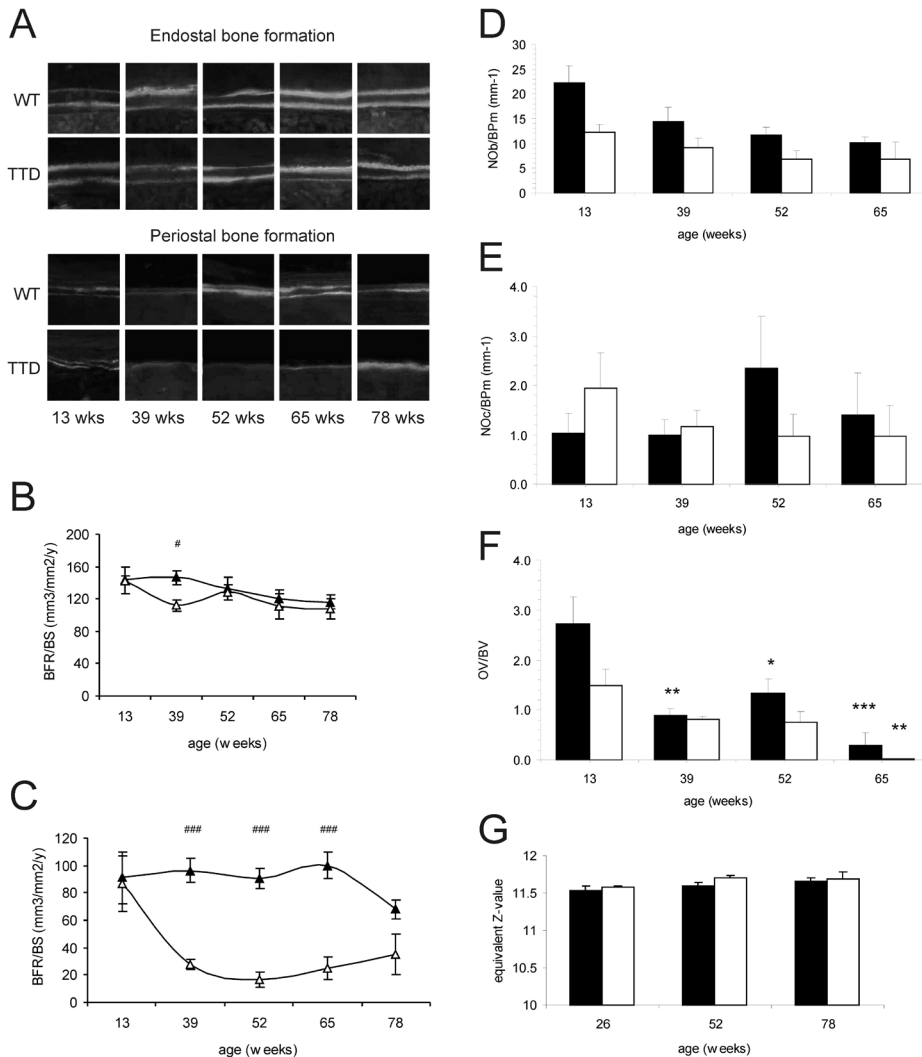
Figure 3: *Histomorphometric analysis and Backscatter Scanning Electron Microscopy of wild type and TTD mice.* Calcein double labeling of endosteal and periosteal bone formation in wild type and TTD mice (A). Quantified endosteal apposition (B), quantified periosteal apposition (C), number of osteoblasts (D), number of osteoclasts (E) and osteoid volume (F) and mineralization status (G) in wild type (solid symbols) and TTD (open symbols) mice. TTD mice compared to wild type mice: # $p<0.05$, ### $p<0.001$; TTD mice compared to their 13 week time point: * $p<0.05$, ** $p<0.01$, *** $p<0.001$; error bars represent SEM.

This demonstrated that tibiae from wild type mice maintained polar moment of inertia at a constant level throughout life, even at 91 and 104 weeks of age when bone volume and cortical thickness were reduced (Figure 4A). In contrast, TTD tibiae failed to maintain the polar moment of inertia and even showed a progressive decrease throughout life starting at 39 weeks of age (Figure 4A), i.e. 78-week old TTD mice showed a 65% decrease in moment of inertia compared to 39-week old TTD mice whereas the moment of inertia in 78-week old wild type mice showed a 106% increase compared to 39-week old wild type mice.
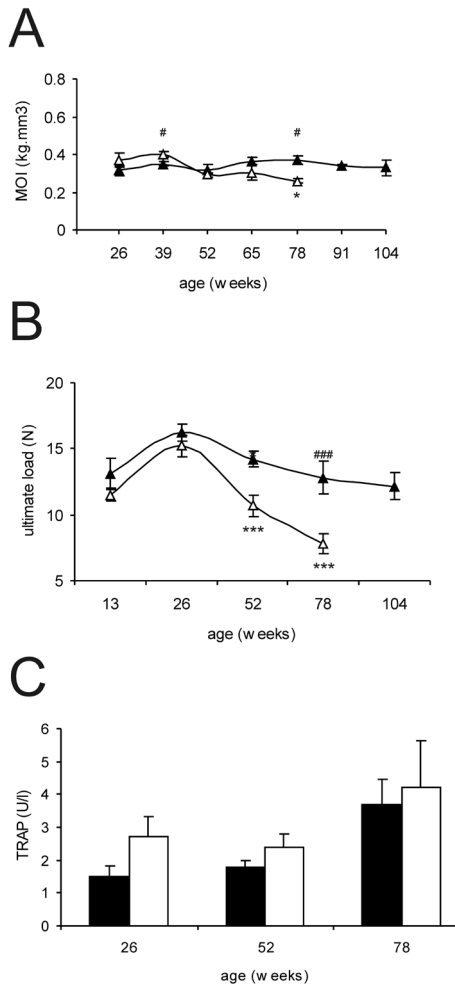
Figure 4: *Mechanical testing and TRAP assay in wild type and TTD mice.* Polar moment of inertia in tibiae (A), ultimate load applied on femurs (B), serum TRAP levels (C), of wild type (solid symbols) and TTD (open symbols) mice. TTD mice compared to wild type animals: # $p<0.05$, ### $p<0.001$; TTD and wild type mice compared to their 26 week time point: * $p<0.05$, *** $p<0.001$; error bars represent SEM.

Using a three-point bending assay, we tested whether the differences in polar moment of inertia and lack of periosteal apposition in TTD mice resulted in a difference in bone strength. Femurs from wild type and TTD mice showed a comparable and increasing ultimate fracture load up to 26 weeks of age (Figure 4B). After 26 weeks there was a progressive decrease in ultimate fracture load in both genotypes but this was clearly more prominent and significant in TTD mice showing a 50% decline compared to a 25% decline in wild type mice (Figure 4B). Femurs of TTD mice fractured at a lower ultimate load than femurs of wild type mice, which reached significance in 52 and 78 weeks old animals.

Bone resorption
In wild type and TTD mice the levels of tartrate resistant acid phosphatase (TRAP) were measured to assess whether differences in bone resorption could explain the observed morphometric differences. As expected, bone resorption seemed to increase with aging in both wild type and TTD mice (Figure 4C). In addition, TTD seemed to have higher levels of TRAP. However, no significant differences were observed between genotypes or with age.

Bone marrow cell cultures
To assess whether the differences in bone phenotype in TTD mice are due to an impaired osteoblast and/or osteoclast differentiation, we performed bone marrow cultures and assessed the capacity to form osteoblasts and adipocytes from mesenchymal stem cells as well as osteoclasts from hematopoietic stem cells for wild type and TTD mice of various ages. The number of TRAP-positive osteoclasts was similar in 13-weeks-old wild type and TTD cultures (Figure 5A).

In the following period wild type but not TTD mice showed a significant decline in the number of osteoclasts resulting in a significant higher number of osteoclasts at 26 weeks of age in TTD mice. At later ages the number of osteoclasts was similar in wild type and TTD mice (Figure 5A). The amount of resorption by mature osteoclasts was not significantly different between wild type and TTD (Figure 5B). At 13 weeks of age, the number of bone nodules was similar for wild type and TTD mice (Figure 5C). However, the number of bone nodules in TTD mice showed a rapid decline resulting in significantly lower numbers of bone nodules at 26 and 39 weeks of age compared to wild type mice (Figure 5C). Subsequently, the number of bone nodules in wild type mice also declined resulting in similar numbers as in 45-week old TTD mice (Figure 5C). There was no significant difference in bone nodule size between wild type and TTD mice at any age (Figure 5D). Both wild type and TTD nodules mineralized but no significant differences between the genotypes could be detected at any age (data not shown). Similarly, both wild type and TTD mice were able to form adipocytes but no significant differences between the genotypes could be detected at any age (Figure 5E).

PTH treatment
Albeit with an accelerated decrease in bone nodule formation the bone marrow cultures of TTD mice retained their capacity to generate osteoblasts and form bone. To investigate whether this bone forming capacity is still present and can be stimulated in vivo as well, we analyzed the effect of intermittent PTH treatment on bone structure in TTD mice. PTH treatment was started at 45 weeks of age, i.e. after the accelerated bone loss has started. Cortical bone volume showed an increase after 20 weeks intermittent PTH treatment as

can be seen from the right-shift in the 3D-thickness distribution (Figure 6C). PTH treatment significantly increased trabecular bone volume fraction, trabecular thickness as well as cortical thickness suggesting that osteoblasts in TTD mice can still be stimulated to increase bone formation (Figure 6A, B and D).
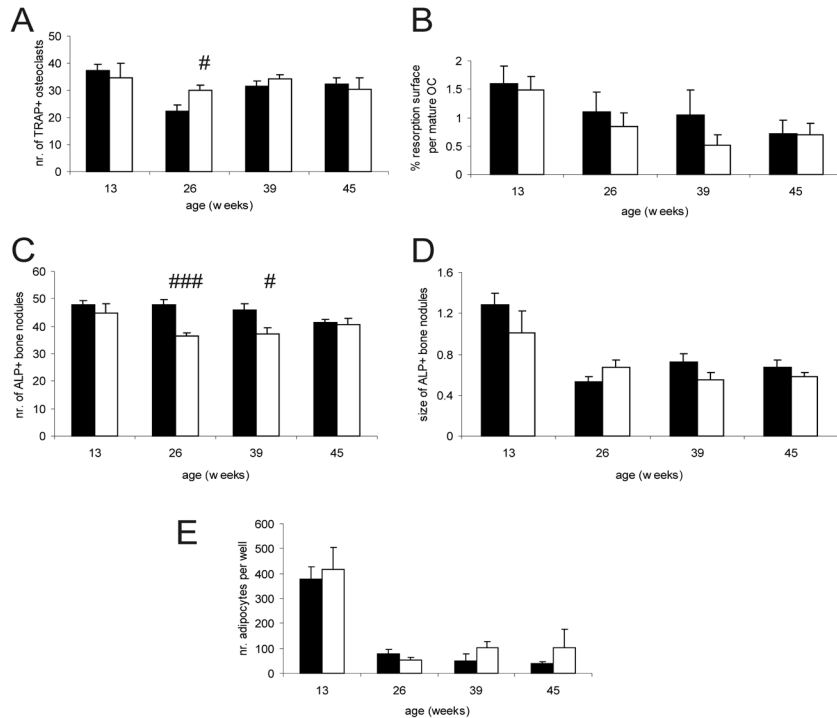
Figure 5: Stem cell cultures of wild type and TTD mice. Analyses of osteoclast, osteoblast and adipocyte differentiation capacity in bone marrow cell cultures in wild type (solid bars) and TTD mice (open bars). Number of TRAP-positive osteoclasts (A), resorption surface per mature osteoclast (B), number of alkaline phosphatase-positive bone nodules (C), size of alkaline phosphatase-positive bone nodules (D) and number of adipocytes (E). TTD mice compared to wild type animals: # $p<0.05$, ### $p<0.001$; error bars represent SEM.

Discussion

TTD mice display features of premature aging in many organs and tissues [23,25], but the progeroid symptoms do not affect all tissues to the same extent. In fact, paradoxically, a detailed, systematic large cohort analysis revealed that some organs and tissues even exhibit features resembling caloric restriction and delayed aging. For instance, the occurrence of cataract in the eyes in TTD mice was found to be significantly less compared to the isogenic wild type control mice kept under the same conditions [25]. This extends the notion that all human progeroid syndromes are segmental [37], i.e. that multiple organs suffer from

rapid aging, yet others seem relatively unaffected and as shown by TTD mice may even age slower than wild type controls. Microarray expression analysis of various accelerated aging mice revealed a strong parallel with expression profiles of normal aging [38,39]. To examine at the level of physiology, whether TTD mice are indeed a *bona fide* model for aging and to rule out that it is a developmental disorder, we examined in great detail the effect of aging on bone parameters of female wild type mice as well as progeroid TTD mice. The systematic analysis uncovered the consequence of a defect in DNA repair and basal transcription on the velocity of age-related skeletal changes and assessed to which extent the skeletal abnormalities reflect normal bone aging.
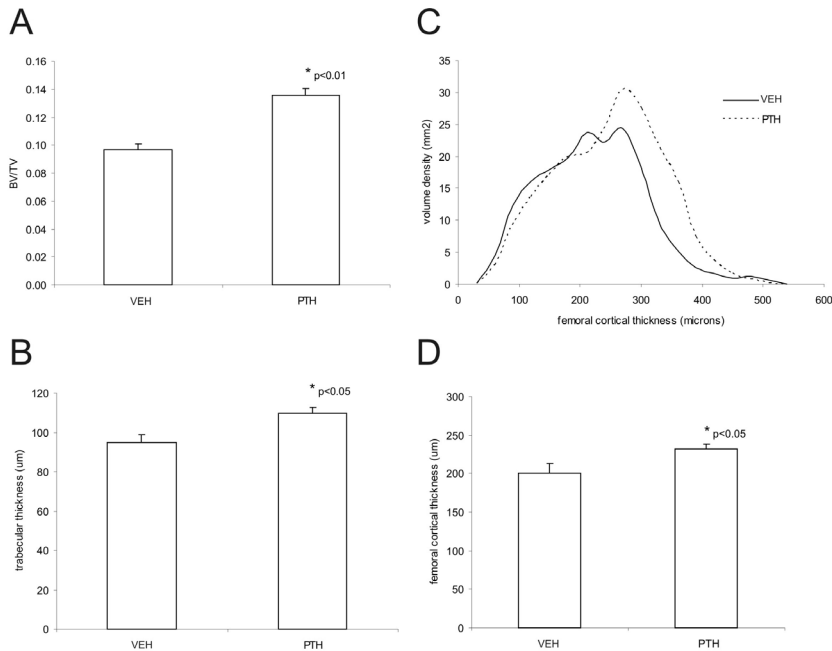
Figure 6: *PTH treatment in TTD mice.* Trabecular bone volume fraction (BV/TV; A), trabecular thickness (B), cortical thickness distribution (C) and cortical thickness (D) in femora from PTH treated (PTH) and control (VEH) TTD mice. * $p < 0.05$, ** $p < 0.01$; error bars represent SEM.

Normal skeletal development but accelerated skeletal aging in progeroid TTD mice
It should be emphasized that by all parameters measured bone develops normally in TTD female mice, i.e. bone volume, cortical thickness and perimeter are similar in wild type and TTD mice up to 39 weeks of age. In addition, similar numbers of osteoblasts and osteoclasts in bone marrow cultures as well as periosteal apposition are present up to at least 13-weeks of age. This observation excludes a developmental defect as explanation for the TTD phenotype and is in line with other studies on TTD mice [25]. After 39 weeks of age profound accelerated decrease in bone volume is observed in TTD mice. The decrease in bone volume and cortical thickness in TTD mice is almost 40 weeks ahead of that in wild type mice. This accelerated form of natural bone aging strongly underlines the premature

aging phenotype of TTD mice. Notably, the decrease in bone volume is paralleled by an accelerated decrease in bone strength in TTD mice after 26 weeks of age; i.e. an ultimate fracture load as observed in 52-week-old TTD mice was only noticed in 104-week-old wild type mice (Figure 4B). An important mechanism underlying the accelerated decrease in bone strength is that in TTD mice the larger endocortical volume is not compensated by an increase in age-related periosteal apposition and perimeter as seen in wild type mice. The accelerated decrease in bone strength can not be explained by a change in mineralization grade of the matrix as assessed by quantitative Backscatter Scanning Electron Microscopy analyses or increased bone resorption as assessed by measurement of serum TRAP.

Lack of periosteal apposition as a cause of decreased bone strength in TTD mice
The lack of effective periosteal apposition in TTD mice is intriguing as it is a localized phenomenon. Despite the important role of periosteal apposition in establishing structural strength during growth and in maintaining strength during aging, little is known about the mechanism and control of periosteal apposition [40]. Currently, it is tempting to speculate that, with aging, increased bending stress on the outer surface of bone (due to endosteal bone loss and subsequent cortical thinning) leads to the stimulation of periosteal bone apposition [41,42,43]. The force of mechanical bending and torsion varies linearly with the distance from the neutral axis and therefore bending stress is larger on the periosteal side of the bone [44]. Mechanical loading could thus influence periosteal apposition and a change in mechanical loading could consequently affect this process. In wild type mice we see the natural link between thinning of the cortex, increase in endocortical volume, the presence of periosteal apposition and increase in perimeter. In TTD mice this increase in perimeter is absent. As TTD mice, in contrast to wild type mice do not accumulate fat with aging, the difference in weight [25] might contribute to the difference in periosteal apposition. However, we could not detect an obvious correlation between body weight and perimeter (unpublished observations). Moreover, in mice a relationship between body weight and femur, vertebral and phalangeal bone parameters has not been found [45]. TTD mice may provide an excellent tool to study periosteal apposition and to unravel the underlying mechanisms.

DNA repair defect and bone marrow stem cells in TTD mice
With regard to the accelerated decrease in bone formation and bone mass, the deficiency of DNA damage repair is very likely to have a causative effect. DNA lesions e.g. induced by free radicals, which are a byproduct of normal metabolism, are incompletely repaired by DNA-repair deficient TTD mice [23]. The increased damage load will lead to dysfunctional senescent cells or will cause apoptosis [46]. Indeed, TTD mice appear to exhibit a decreased spontaneous tumor formation rate likely at least in part by an increased rate of apoptosis [25,47], which protects from cancer but at the same time likely accelerates aging. An increased rate of apoptosis can therefore be expected to cause accelerated depletion of stem cells or early progenitor cells leading to a disturbed osteoblasts and adipocyte differentiation from mesenchymal stem cells and osteoclasts derived from the hematopoietic stem cell lineage. A decrease in mesenchymal stem cell number or disturbed differentiation is suggested by the fact that TTD mice lack abdominal fat mass [48]. As the structural differences in bone became apparent after 39 weeks we analyzed bone marrow mesenchymal and hematopoietic stem cell differentiation in the period around this age starting at 13 weeks of age. Osteogenic analyses of the bone marrow

cultures demonstrated an accelerated decrease in bone nodule formation implicating an accelerated reduction in the number of mesenchymal stem cells that can differentiate into osteoblasts that precedes the decrease in bone mass. The absence of differences in size of the bone nodules shows that the proliferative capacity of the stem cells present is not changed in TTD mice.

Histomorphometric analyses showed that the number of osteoblasts *in vivo* was lower in tibia of TTD mice throughout life. These data suggest that DNA damage levels in TTD mice reach a critical threshold in (mesenchymal) stem cells between 13 and 26 weeks, which translates into reduced numbers of differentiated osteoblasts and a bone phenotype. Although we only studied bone marrow cultures up to 45 weeks, bone nodule formation in wild type mice seems to decrease starting at 45 weeks of age, which is in line with the observed significant decrease in the number of osteoblasts in wild type tibiae at 52 weeks of age. It was shown previously that old mice had significantly fewer stem cells with osteogenic potential than young animals [49,50]. In humans, the number of stem cells with osteogenic potential was shown to decrease already at young age [51,52,53].

Only at 26 weeks of age a drop in the number of osteoclasts observed in wild type mice leads to a significant difference in *in vitro* osteoclast formation between wild type and TTD mice while no significant differences in resorption capacity were observed. The decreased osteoblast differentiation at 26 weeks of age may explain the decrease in bone volume and structure as first observed after 39 weeks. Obviously, definite proof that the observed accelerated decrease in mesenchymal stem cells in TTD mice is due to accumulation of DNA damage as a consequence of deficient DNA repair is lacking and with current technology very difficult to obtain. However, the most plausible scenario is that loss of DNA repair indeed leads to accumulation of otherwise repaired DNA lesions, which triggers cell death and cellular senescence. In the case of bone metabolism this results in an accelerated decrease in mesenchymal stem cells, suppression of growth and differentiation, deranged bone metabolism and inevitably premature loss of bone strength.

Although there is an accelerated decrease in bone nodule formation, the current data show that TTD bone marrow mesenchymal stem cells retain bone forming capacity. This is further substantiated by the *in vivo* intermittent PTH treatment studies. Intermittent PTH administration to TTD mice demonstrated an increase in cortical thickness implicating that the stem cells/osteoblasts can still be stimulated to form bone. Considering the above mentioned relationship between DNA repair and apoptosis, it is interesting to note that PTH has been reported to inhibit osteoblast apoptosis [54,55]. The PTH effect on cortical thickness in TTD mice appears to be the result of increased endosteal bone formation and not periosteal apposition, as perimeter was not significantly changed. Interestingly, a recent study showed differences in mechanism by which intermittent PTH treatment increases bone formation at the endosteal and at the periosteal surface [56]. The increase in endocortical osteoblasts after intermittent PTH treatment is predominantly due to attenuated osteoblast apoptosis [56].

In periosteal bone where the rate of osteoblast apoptosis is low, PTH does not increase the number of osteoblasts by attenuating apoptosis, but by exerting pro-differentiating and/ or pro-survival effects on post-mitotic pre-osteoblasts [56]. These data are suggestive for different age-related mechanisms at the endosteal and periosteal level and in line with

our hypothesis that increased apoptosis of osteoprogenitors contributes to the decreased periosteal apposition in TTD mice. The adipocyte cultures support the fact that the intrinsic differentiation capacity of mesenchymal stem cells is not affected. *In vivo* TTD mice lack fat accumulation, but *in vitro* normal adipocyte differentiation is observed. Overall these observations point to an altered systemic environment in TTD mice. Currently, it should be concluded that the observed accelerated skeletal aging observed in TTD mice is the result from a combination of an accelerated decline in the number of osteogenic stem cells together with altered systemic influences.

In conclusion, we demonstrate that the increased and accelerated decrease in bone mass in DNA repair-deficient TTD mice is a premature aging feature, which implies that the other aging-like features in TTD mice and patients may also represent *bona fide* premature aging symptoms and which in a broader context substantiates the importance of DNA repair in healthy aging. The TTD mouse mutant constitutes a valid model for bone aging and the absence of periosteal apposition provides for identification of new targets for maintaining bone strength with aging.

Chapter 4

Chapter 4

References

1. Wakeling EL, Cruwys M, Suri M, Brady AF, Aylett SE, et al. (2004) Central osteosclerosis with trichothiodystrophy. Pediatr Radiol 34: 541-546.
2. Toelle SP, Valsangiacomo E, Boltshauser E (2001) Trichothiodystrophy with severe cardiac and neurological involvement in two sisters. Eur J Pediatr 160: 728-731.
3. Kousseff BG, Esterly NB (1988) Trichothiodystrophy, IBIDS syndrome or Tay syndrome? Birth Defects Orig Artic Ser 24: 169-181.
4. Przedborski S, Ferster A, Goldman S, Wolter R, Song M, et al. (1990) Trichothiodystrophy, mental retardation, short stature, ataxia, and gonadal dysfunction in three Moroccan siblings. Am J Med Genet 35: 566-573.
5. Civitelli R, McAlister WH, Teitelbaum SL, Whyte MP (1989) Central osteosclerosis with ectodermal dysplasia: clinical, laboratory, radiologic, and histopathologic characterization with review of the literature. J Bone Miner Res 4: 863-875.
6. Chapman S (1988) The trichothiodystrophy syndrome of Pollitt. Pediatr Radiol 18: 154-156.
7. Price VH, Odom RB, Ward WH, Jones FT (1980) Trichothiodystrophy: sulfur-deficient brittle hair as a marker for a neuroectodermal symptom complex. Arch Dermatol 116: 1375-1384.
8. McCuaig C, Marcoux D, Rasmussen JE, Werner MM, Gentner NE (1993) Trichothiodystrophy associated with photosensitivity, gonadal failure, and striking osteosclerosis. J Am Acad Dermatol 28: 820-826.
9. Itin PH, Sarasin A, Pittelkow MR (2001) Trichothiodystrophy: update on the sulfur-deficient brittle hair syndromes. J Am Acad Dermatol 44: 891-920; quiz 921-894.
10. Giglia-Mari G, Coin F, Ranish JA, Hoogstraten D, Theil A, et al. (2004) A new, tenth subunit of TFIIH is responsible for the DNA repair syndrome trichothiodystrophy group A. Nat Genet 36: 714-719.
11. Chalut C, Moncollin V, Egly JM (1994) Transcription by RNA polymerase II: a process linked to DNA repair. Bioessays 16: 651-655.
12. Seroz T, Hwang JR, Moncollin V, Egly JM (1995) TFIIH: a link between transcription, DNA repair and cell cycle regulation. Curr Opin Genet Dev 5: 217-221.
13. Hoeijmakers JH, Egly JM, Vermeulen W (1996) TFIIH: a key component in multiple DNA transactions. Curr Opin Genet Dev 6: 26-33.
14. Svejstrup JQ, Vichi P, Egly JM (1996) The multiple roles of transcription/repair factor TFIIH. Trends Biochem Sci 21: 346-350.
15. Hwang JR, Moncollin V, Vermeulen W, Seroz T, van Vuuren H, et al. (1996) A 3' --> 5' XPB helicase defect in repair/transcription factor TFIIH of xeroderma pigmentosum group B affects both DNA repair and transcription. J Biol Chem 271: 15898-15904.
16. Hashimoto S, Egly JM (2009) Trichothiodystrophy view from the molecular basis of DNA repair/transcription factor TFIIH. Hum Mol Genet 18: R224-230.
17. Gillet LC, Scharer OD (2006) Molecular mechanisms of mammalian global genome nucleotide excision repair. Chem Rev 106: 253-276.
18. Sugasawa K (2010) Regulation of damage recognition in mammalian global genomic nucleotide excision repair. Mutat Res 685: 29-37.
19. Hoeijmakers JH (2001) Genome maintenance mechanisms for preventing cancer. Nature 411: 366-374.
20. Hanawalt PC (2002) Subpathways of nucleotide excision repair and their regulation. Oncogene 21: 8949-8956.
21. Hoeijmakers JH (2009) DNA damage, aging, and cancer. N Engl J Med 361: 1475-1485.
22. de Boer J, de Wit J, van Steeg H, Berg RJ, Morreau H, et al. (1998) A mouse model for the basal transcription/DNA repair syndrome trichothiodystrophy. Mol Cell 1: 981-990.
23. de Boer J, Andressoo JO, de Wit J, Huijmans J, Beems RB, et al. (2002) Premature aging in mice deficient in DNA repair and transcription. Science 296: 1276-1279.
24. Leupold D (1979) [Ichthyosis congenita, cataract, mental retardation, ataxia, osteosclerosis and immunologic deficiency--a particular syndrome?]. Monatsschr Kinderheilkd 127: 307-308.
25. Wijnhoven SW, Beems RB, Roodbergen M, van den Berg J, Lohman PH, et al. (2005) Accelerated aging pathology in ad libitum fed Xpd(TTD) mice is accompanied by features suggestive of caloric restriction. DNA Repair (Amst).
26. Manolagas SC (2010) From Estrogen-Centric to Aging and Oxidative Stress: A Revised Perspective of the

Pathogenesis of Osteoporosis. Endocr Rev.

27. Ambrogini E, Almeida M, Martin-Millan M, Paik JH, Depinho RA, et al. (2010) FoxO-mediated defense against oxidative stress in osteoblasts is indispensable for skeletal homeostasis in mice. Cell Metab 11: 136-146.

28. Rached MT, Kode A, Xu L, Yoshikawa Y, Paik JH, et al. (2010) FoxO1 is a positive regulator of bone formation by favoring protein synthesis and resistance to oxidative stress in osteoblasts. Cell Metab 11: 147-160.

29. Chan GK, Duque G (2002) Age-related bone loss: old bone, new facts. Gerontology 48: 62-71.

30. Harada S, Rodan GA (2003) Control of osteoblast function and regulation of bone mass. Nature 423: 349-355.

31. Riggs BL, Khosla S, Melton LJ, 3rd (2002) Sex steroids and the construction and conservation of the adult skeleton. Endocr Rev 23: 279-302.

32. Seeman E (2002) Pathogenesis of bone fragility in women and men. Lancet 359: 1841-1850.

33. Kawaguchi H, Manabe N, Miyaura C, Chikuda H, Nakamura K, et al. (1999) Independent impairment of osteoblast and osteoclast differentiation in klotho mouse exhibiting low-turnover osteopenia. J Clin Invest 104: 229-237.

34. Seeman E (2001) During aging, men lose less bone than women because they gain more periosteal bone, not because they resorb less endosteal bone. Calcif Tissue Int 69: 205-208.

35. Seeman E (2003) Invited Review: Pathogenesis of osteoporosis. J Appl Physiol 95: 2142-2151.

36. Russo CR, Lauretani F, Seeman E, Bartali B, Bandinelli S, et al. (2006) Structural adaptations to bone loss in aging men and women. Bone 38: 112-118.

37. Martin GM (2005) Genetic modulation of senescent phenotypes in Homo sapiens. Cell 120: 523-532.

38. van der Pluijm I, Garinis GA, Brandt RM, Gorgels TG, Wijnhoven SW, et al. (2007) Impaired genome maintenance suppresses the growth hormone--insulin-like growth factor 1 axis in mice with Cockayne syndrome. PLoS Biol 5: e2.

39. Niedernhofer LJ, Garinis GA, Raams A, Lalai AS, Robinson AR, et al. (2006) A new progeroid syndrome reveals that genotoxic stress suppresses the somatotroph axis. Nature 444: 1038-1043.

40. Seeman E (2003) Periosteal bone formation--a neglected determinant of bone strength. N Engl J Med 349: 320-323.

41. Akhter MP, Cullen DM, Recker RR (2002) Bone adaptation response to sham and bending stimuli in mice. J Clin Densitom 5: 207-216.

42. Beck TJ, Stone KL, Oreskovic TL, Hochberg MC, Nevitt MC, et al. (2001) Effects of current and discontinued estrogen replacement therapy on hip structural geometry: the study of osteoporotic fractures. J Bone Miner Res 16: 2103-2110.

43. Lazenby RA (1990) Continuing periosteal apposition. II: The significance of peak bone mass, strain equilibrium, and age-related activity differentials for mechanical compensation in human tubular bones. Am J Phys Anthropol 82: 473-484.

44. Currey JD (1999) What determines the bending strength of compact bone? J Exp Biol 202: 2495-2503.

45. Beamer WG, Donahue LR, Rosen CJ, Baylink DJ (1996) Genetic variability in adult bone density among inbred strains of mice. Bone 18: 397-403.

46. Campisi J (2005) Senescent cells, tumor suppression, and organismal aging: good citizens, bad neighbors. Cell 120: 513-522.

47. de Boer J, Hoeijmakers JH (1999) Cancer from the outside, aging from the inside: mouse models to study the consequences of defective nucleotide excision repair. Biochimie 81: 127-137.

48. Compe E, Drane P, Laurent C, Diderich K, Braun C, et al. (2005) Dysregulation of the peroxisome proliferator-activated receptor target genes by XPD mutations. Mol Cell Biol 25: 6065-6076.

49. Bergman RJ, Gazit D, Kahn AJ, Gruber H, McDougall S, et al. (1996) Age-related changes in osteogenic stem cells in mice. J Bone Miner Res 11: 568-577.

50. Moerman EJ, Teng K, Lipschitz DA, Lecka-Czernik B (2004) Aging activates adipogenic and suppresses osteogenic programs in mesenchymal marrow stroma/stem cells: the role of PPAR-gamma2 transcription factor and TGF-beta/BMP signaling pathways. Aging Cell 3: 379-389.

51. D'Ippolito G, Schiller PC, Ricordi C, Roos BA, Howard GA (1999) Age-related osteogenic potential of mesenchymal stromal stem cells from human vertebral bone marrow. J Bone Miner Res 14: 1115-1122.

52. Nishida S, Endo N, Yamagiwa H, Tanizawa T, Takahashi HE (1999) Number of osteoprogenitor cells in human bone marrow markedly decreases after skeletal maturation. J Bone Miner Metab 17: 171-177.

53. Zhou S, Greenberger JS, Epperly MW, Goff JP, Adler C, et al. (2008) Age-related intrinsic changes in human bone-marrow-derived mesenchymal stem cells and their differentiation to osteoblasts. Aging Cell 7: 335-343.

54. Jilka RL, Weinstein RS, Bellido T, Roberson P, Parfitt AM, et al. (1999) Increased bone formation by prevention of osteoblast apoptosis with parathyroid hormone. J Clin Invest 104: 439-446.

55. Sowa H, Kaji H, Iu MF, Tsukamoto T, Sugimoto T, et al. (2003) Parathyroid hormone-Smad3 axis exerts anti-apoptotic action and augments anabolic action of transforming growth factor beta in osteoblasts. J Biol Chem 278: 52240-52252.

56. Jilka RL, O'Brien CA, Ali AA, Roberson PK, Weinstein RS, et al. (2009) Intermittent PTH stimulates periosteal bone formation by actions on post-mitotic preosteoblasts. Bone 44: 275-286.

57. Waarsing JH, Day JS, Weinans H (2004) An improved segmentation method for in vivo microCT imaging. J Bone Miner Res 19: 1640-1650.

58. Glatt V, Canalis E, Stadmeyer L, Bouxsein ML (2007) Age-related changes in trabecular architecture differ in female and male C57BL/6J mice. J Bone Miner Res 22: 1197-1207.

59. Hildebrand T, Laib A, Muller R, Dequeker J, Ruegsegger P (1999) Direct three-dimensional morphometric analysis of human cancellous bone: microstructural data from spine, femur, iliac crest, and calcaneus. J Bone Miner Res 14: 1167-1174.

60. Amling M, Priemel M, Holzmann T, Chapin K, Rueger JM, et al. (1999) Rescue of the skeletal phenotype of vitamin D receptor-ablated mice in the setting of normal mineral ion homeostasis: formal histomorphometric and biomechanical analyses. Endocrinology 140: 4982-4987.

61. Parfitt AM, Drezner MK, Glorieux FH, Kanis JA, Malluche H, et al. (1987) Bone histomorphometry: standardization of nomenclature, symbols, and units. Report of the ASBMR Histomorphometry Nomenclature Committee. J Bone Miner Res 2: 595-610.

62. Broderick E, Infanger S, Turner TM, Sumner DR (2005) Depressed bone mineralization following high dose TGF-beta1 application in an orthopedic implant model. Calcif Tissue Int 76: 379-384.

63. Roschger P, Fratzl P, Eschberger J, Klaushofer K (1998) Validation of quantitative backscattered electron imaging for the measurement of mineral density distribution in human bone biopsies. Bone 23: 319-326.

64. van der Eerden BC, Hoenderop JG, de Vries TJ, Schoenmaker T, Buurman CJ, et al. (2005) The epithelial Ca2+ channel TRPV5 is essential for proper osteoclastic bone resorption. Proc Natl Acad Sci U S A 102: 17507-17512.

CHAPTER 5

Age-related skeletal dynamics and decrease in bone strength in DNA repair deficient male trichothiodystrophy mice

Claudia Nicolaije[1,†], Karin E.M. Diderich[2,†], S.M. Botter[2], Matthias Priemel[3], Jan H. Waarsing[4], Judd S. Day[4], Renata M.C. Brandt[2], Arndt F. Schilling[3], Harrie Weinans[4], Bram C. Van der Eerden[1], Gijsbertus T.J. van der Horst[2], Jan H.J. Hoeijmakers[2] and Johannes P.T.M. van Leeuwen*[1]

Dept. of Internal Medicine, Erasmus MC, The Netherlands
[2] MGC Dept. of Cell Biology & Genetics, Center for Biomedical Genetics, Erasmus MC, The Netherlands
[3] Dept. of Trauma, Hand, and Reconstructive Surgery, Hamburg University School of Medicine, 20246 Hamburg, Germany
[4] Dept. of Orthopedics, Erasmus MC, 3000 DR Rotterdam, The Netherlands
[†] Both authors contributed equally to the manuscript.

Abstract

Accumulation of DNA damage caused by oxidative stress is thought to be one of the main contributors of human tissue aging. Trichothiodystrophy (TTD) mice have a mutation in the Ercc2 DNA repair gene, resulting in accumulation of DNA damage and several features of segmental accelerated aging. We used male TTD mice to study the impact of DNA repair on bone metabolism with age. Analysis of bone parameters, measured by micro-computed tomography, displayed an earlier decrease in trabecular and cortical bone as well as a loss of periosteal apposition and a reduction in bone strength in TTD mice with age compared to wild type mice. Ex vivo analysis of bone marrow differentiation potential showed an accelerated reduction in the number of osteogenic and osteoprogenitor cells with unaltered differentiation capacity. Adipocyte differentiation was normal. Early in life osteoclast number tended to be increased while at 78 weeks it was significantly lower in TTD mice. Our findings reveal the importance of genome stability and proper DNA repair for skeletal homeostasis with age and support the idea that accumulation of damage interferes with normal skeletal maintenance, causing reduction in the number of osteoblast precursors that are required for normal bone remodeling leading to a loss of bone structure and strength.

Chapter 5

Introduction

Osteoporosis, caused by a natural loss of estrogens, has been the main focus of the bone field for many years. However, recently a growing body of evidence supports a more general, age-related form of bone loss, which occurs independent of changes in sex steroid hormone levels and starts at an early age [1]. Epidemiological studies pin-point the onset of this age-related bone loss right after obtaining peek bone mass in humans [2,3]. Additionally, early onset and gradual bone loss has also been found in several mouse strains independent of a sudden loss of estrogens starting 2-3 months after birth [4,5]. This age-related bone loss is characterised by a slower, more gradual decline in bone mass than in case of post menopausal bone loss [6].

Oxidative stress has been postulated as one of the contributing mechanisms behind age-related bone loss [1]. Oxidative stress is induced by reactive oxygen species (ROS) formed as by-products of mitochondrial aerobic metabolism and fatty acid oxidation [7]. ROS at basal levels play an important role in a broad spectrum of signalling pathways [8]. An increase in ROS production in response to external stimuli can induce oxidative stress which causes DNA and protein damage that can lead to apoptosis [9]. All cells have a battery of defence mechanisms to prevent ROS-induced damage. Anti-oxidant enzymes scavenge ROS and reduce them to an inactive state. Additionally, ROS activate proteins, including forkhead box protein O (FOXO) transcription factors that regulate anti-oxidant enzyme expression and activate DNA repair pathways [10,11]. Besides ROS, cellular metabolism also produces various other reactive chemical species, with a tendency to damage DNA such as alkylating agents and reactive nitrogen species. Recent studies showed the importance of FOXO-mediated oxidative stress defence for osteoblast function and skeletal homeostasis [12,13]. Cells contain several DNA repair pathways. The global genome nucleotide excision repair (GG-NER) pathway removes helix-distorting damage anywhere in the genome, thus mainly preventing mutagenesis and consequently carcinogenesis. Transcription coupled repair (TCR) eliminates lesions in the transcribed strand of active genes when transcription is arrested by DNA damage, to allow rapid resumption of the vital transcription process. This repair system mainly promotes cell survival and prevents DNA damage induced cell death and senescence [14,15]. Both repair processes share a number of components, including the 10-subunit transcription factor II H (TFIIH) complex [16]. TFIIH opens up the DNA helix using the helicases xeroderma pigmentosum complementation group B (XPB) and D (XPD) after damage detection in global genome as well as transcription-coupled repair [17]. This allows damage verification and excision by dual incision of the damaged strand at some distance from the lesion, followed by gap-filling DNA synthesis and final ligation to the pre-existing strand [18].

Mutations in the NER pathway helicase XPD, cause -among several other inherited syndromes- a disease called Trichothiodystrophy (TTD) which is a rare, autosomal recessive DNA repair disorder presenting a wide range of characteristic features like photosensitivity, brittle hair and nails, impaired intelligence, short stature, infertility and a severely reduced lifespan. Additionally, skeletal abnormalities have been described [19]. An XPD mouse model was generated, using murine homologue Ercc2, which precisely mimics a causative point mutation in the essential Xpd gene of a TTD patient, causing a single amino acid substitution ($R^{722}W$) in the ERCC2 (XPD) helicase. Although mice were significantly lighter and smaller, radiographs of 2- to 4- month old TTD mice did not show any skeletal abnormalities, but those of 14 month old mice displayed kyphosis and a reduction in

radiodensity of the long bones, both hallmarks of human aging [20]. In addition, TTD mice in a C57BL/6J background, have strikingly similar symptoms and show several premature aging-like features [21].

We used the TTD mouse model, which lacks one of the basic defense mechanisms against DNA damage and undergoes accelerated aging, to study the impact of DNA-repair in maintaining bone metabolism with aging. Previous studies using TTD mice have shown that early TTD development progresses normally when compared to wild type mice. Clear changes between the two groups start to develop after 26 weeks of age when TTD mice start to lag behind in gaining body weight and develop their characteristic features [22]. Early bone development was not affected and no changes in bone length were measured in male or female bones at any of the time points studied (data not shown). In this study we investigated bone architecture, gene expression and mesenchymal and hematopoietic stem cell differentiation potential.

Material and Methods

Ethics Statement
As required by Dutch law, formal permission to generate and use genetically modified animals was obtained from the responsible local and national authorities. All animal studies were approved by the Dutch equivalent of the Institutional Animal Care and Use Committees, Erasmus MC Dier Ethische Commissie.

Mice and bones
All mice had a C57BL/6J background and all mice within one cohort were kept under equal conditions. For micro-computed tomography (μCT) analysis 8 wild type and TTD mice were sacrificed at various ages (13 – 104 weeks). Because of their reduced lifespan [22] TTD mice within the μCT cohort were not available for the last time point of wild type mice (104 weeks) and therefore were only analyzed till 78 weeks. Mice were killed by cervical dislocation. Femurs and tibiae were isolated and were either snap frozen in liquid nitrogen and stored at -80 °C or fixed in Burkhardt, which was replaced by 70% ethanol after 3 days. For bone marrow isolation 10 wild type and TTD mice were sacrificed after which bones were isolated and used for bone marrow isolation or fixed in 10% formalin for further testing.

Micro-computed tomography
Fixed tibiae from wild type and TTD mice (n = 4-6) were scanned by μCT from proximal end to mid-diaphysis using the SkyScan 1072 microtomograph (SkyScan, Antwerp, Belgium) with a voxel size of 8.82 μm. Bone parameters were quantified using the following software packages, Nrecon, CT-analyze and Dataviewer and MatLab (The Mathworks. Natick, MA,USA) (http://www.skyscan.be/products/downloads.htm) . For all mice, a metaphyseal (100 sections) and a diaphyseal (50 sections) area were selected for analysis starting respectively 30 or 400 sections below our offset landmark within the epiphyseal growth plate. We determined the following parameters; trabecular bone volume fraction (BV/TV), metaphyseal endocortical volume (metaphyseal Ec.V.), trabecular number (Tb.N), trabecular thickness (Tb.Th.), cortical thickness (Ct.Th.), cortical volume, (Ct.V) diaphyseal endocortical volume (diaphyseal Ec.V)., polar moment of inertia (MOI) and perimeter (Pm.) [46]. In addition, 3D thickness distribution was determined, using a larger standardized area

located 3.7-6.9 mm from the proximal end of the bones [47].For additional analysis proximal tibiae from male wild type and TTD mice at 13 weeks of age were scanned in the Skyscan 1076 in vivo X-ray microtomograph (Skyscan, Kontich, Belgium) as previously described [48]. Two regions were analyzed using the CTAnalyser software package (Skyscan): cortical thickness (Ct.Th.) and cortical porosity were determined in 20 cross sections of the mid-diaphysis of the tibia, and bone volume fraction (BV/TV), trabecular thickness (Tb.Th.) and cortical thickness (Ct.Th.) were measured in 50 cross sections of the proximal metaphysis, starting directly underneath the growth plate."

Histomorphometric analysis
To assess dynamic histomorphometric indices, mice received intraperitoneal injections with calcein (10 µg/g body weight) 10 and 3 days prior to sacrifice. Tibiae and sections were processed and stained as described previously [49]. Parameters of static and dynamic histomorphometry were quantified on not decalcified proximal tibia sections. For each animal, the bone formation rate was determined by fluorochrome (calcein) measurements using two non-consecutive 12µm-sections per animal. Additional histomorphometric analysis was performed on 13 and 78 week old wild type and TTD bones as previously described [50].

Mechanical testing
Defrosted femurs were disposed of residual soft tissue and tested in a three-point bending assay using a Lloyd LRX mechanical test frame, constructed with 3 mm hemi-cylindrical supports with a 9 mm total span. The femurs were aligned such that the neutral axis was parallel to the sagittal plane. The lesser trochanter was used as a reference point and aligned with one of the two supports. All samples were preconditioned for 5 cycles to 2 N at a rate of 0.01 mm/s before testing to failure at a rate of 0.02 mm/s. We measured ultimate load (N), energy (Nmm) and stiffness (N/mm).

Backscatter Scanning Electron Microscopy
Processing and quantitative backscatter scanning electron microscopic analyses were done as described previously [51]. From each image the histogram of equivalent Z-values was calculated, its mean value representing the mean mineralization of the bone tissue [24].

Bone marrow isolation, cell culture and cell culture staining
Bone marrow was collected immediately after the bones were obtained by spinning down the bone marrow into an Eppendorf tube at 5000rpm for 2 min. Erythrocytes were lysed using erylysis buffer (1.55M NH_4Cl, 0.1M $KHCO_3$, 1mM EDTA (10x)) and cells were washed and seeded at 1.000.000 cells/well (12 wells) for osteoblasts, 100.000 cells/well (96 wells) for osteoclasts and 750.000 cells/well, for adipocytes (24 wells). Osteogenic and osteoclastogenic cultures were performed as previously described [52]. Adipocytes were cultured on adipogenic (D-MEM (GIBCO, Paisley, UK) supplemented with P/S, amphotericin B (250 ng/ml, Sigma, Zwijndrecht, NL) and 15% heat-inactivated FCS (GIBCO) medium. Adipogenesis was induced after a 3-week expansion phase by adding insulin (0.1 µg/ml, Sigma), indomethacin (1 mM, Sigma) and dexamethasone ($1*10^{-7}$M, Sigma) for two weeks. Osteoblast colony forming potential and mineralization potential were determined as previously described after respectively 14 and 21 days of culture [52]. Colonies were counted by eye, next plates were scanned and colony surface area was determined by computer

analysis (Bioquant software, Nashville, TN, USA). Alizarin Red staining was extracted and quantified by absorptiometry at 405 nm on a plate reader (Victor^2 1420 multilabel counter, Wallac, Perkin Elmer, Waltham, MA, USA). Osteoclast number and resorption capacity were determined as previously described [30] and analyzed using freely available Image J software (version 1.41;http://rsbweb.nih.gov/ij/). Adipocyte cultures were fixated O/N with 10% formalin, washed with 60% IPOH and stained with Oil-Red O solution (60-40 dilution of Oil-Red O stock solution (Clin-Tech limited, Guiltford, UK) in H$_2$O) after which the total amount of adipocytes per well was determined.

RNA isolation and qPCR analysis

After removing tibiae from the mice, we removed the bone marrow and immediately homogenized the tissue into Trizol using a Tissuelyser (Qiagen, Venlo, NL). RNA was isolated and purified using a Qiagen RNeasy kit (Qiagen). Total RNA amount was determined using a spectrophotometer (ND1000, Nanodrop, Thermo Scientific, Wilmington, DE, USA). For cDNA synthesis 1 µg of total RNA was reverse transcribed using a cDNA synthesis kit according to the manufacturer's protocol (MBI Fermentas, Thermo Scientific, Wilmington, DE, USA). qPCR analysis was performed using a ABI 7500 Fats Real-Time PCR detection system (Applied Biosystems, Carlsbad, CA, USA). Reactions were performed in 25 µl volumes using a qPCR core kit (for assays using a probe) or a qPCR kit for SYBR green I (for assays using SYBR Green) (Eurogentec, Maastricht, NL). Primer and probe sets were designed using Primer Express software (version 2.0, Applied Biosystems).

Statistics

We performed 2-way ANOVA statistical analysis on all datasets to determine any interactions between age and phenotypes, as well as additional unpaired t-tests with two-tailed P-values to determine significant difference at each time point (Graph Pad Software, San Diego, CA, USA, www.graphpad.com

Results

Bone architecture

In order to analyze bone dynamics in wild type and TTD mice throughout life we analyzed trabecular bone parameters in the metaphysis by µCT analysis. The trabecular bone volume fraction (BV/TV) gradually but significantly decreased over time in wild type mice, dropping 75% between 13 and 104 weeks of age. Albeit that at 13 weeks the BV/TV in TTD mice was already half of that in wild type mice, BV/TV decreased as well further throughout life, losing about 50% between 26 and 78 weeks of age (Fig.1A). At all time points measured, BV/TV was significantly lower between wild type and TTD mice, with the largest difference observed at the first point measured at 26 weeks of age. No significant interaction between genotype and age was observed.

The endocortical volume (Ec.V.), also known as the total volume contained by the endosteal surface of the cortical bone, was significantly lower in 13 weeks old TTD mice compared to wild type mice of the same age. Ec.V. decreased between 13 and 26 weeks in both wild type and TTD mice after which it stabilized in wild type mice. Ec.V. increased again In TTD
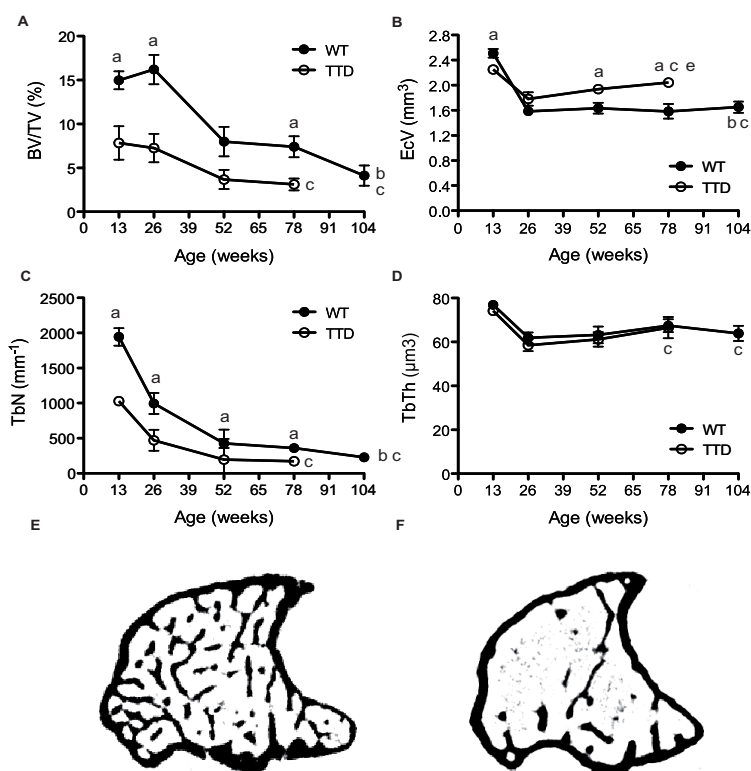
Figure 1: *Age-related trabecular bone loss in male TTD mice.* Trabecular bone parameters (A-D) were studied in aging wild type (solid) and TTD (open) tibial metaphyses. (A) Trabecular bone volume fraction (BV/TV), (B) Endocortical volume (Ec.V.), (C) Trabecular number (Tb.N.), (D) Trabecular thickness (Tb.Th.). 100 cross-sections were measured in the metaphysis of TTD and wild type mice. Representative cross-sections of 26 week old, male, wild type (E) and TTD mice (F) depict the loss of trabecular bone, the decrease in trabecular number and increase in endocortical volume. Statistics: a= student t-test; p<0.05 wild type vs. TTD, b-d = 2 way ANOVA; p<0.05. b= significant difference between wild type and TTD with aging, c= signifcant difference with aging within a genotype, d= a significant interaction between age and genotype. Error bars represent SEM.

mice, ending up significantly higher at 52 and 78 weeks of age compared to wild type mice (Fig.1B). For Ec.V. there was a significant interaction between genotype and age, which means that age is a determinant of the difference between wild type and TTD mice. Trabecular number (Tb.N.) which decreased in wild types throughout life, is significantly lower in TTD mice, with the biggest difference observed at 13 weeks when TTD mice have about half the number of trabecules found in wild type mice of the same age (Fig.1C). Trabecular thickness (Tb.Th.) however, was the same for both genotypes and did not change throughout life (Fig.1D). In summary, TTD mice (Fig.1F) displayed a reduction in trabecular bone compared to age-matched wild type mice (Fig.1E) as shown in the sample cross-sections in Figure 1E and F. In addition, both wild type and TTD exhibited age-related decline. Cortical thickness (Ct.Th.) significantly decreased throughout life in wild type mice,

losing approximately 20% between 13 and 104 weeks. The same gradual and significant decline was observed in TTD mice, which had thinner cortices compared to wild type mice at all time points measured, significantly so at 26 and 78 weeks (Fig.2A).

Figure 2: *Age-related cortical bone loss in male TTD mice.* Cortical bone parameters (A-D) were
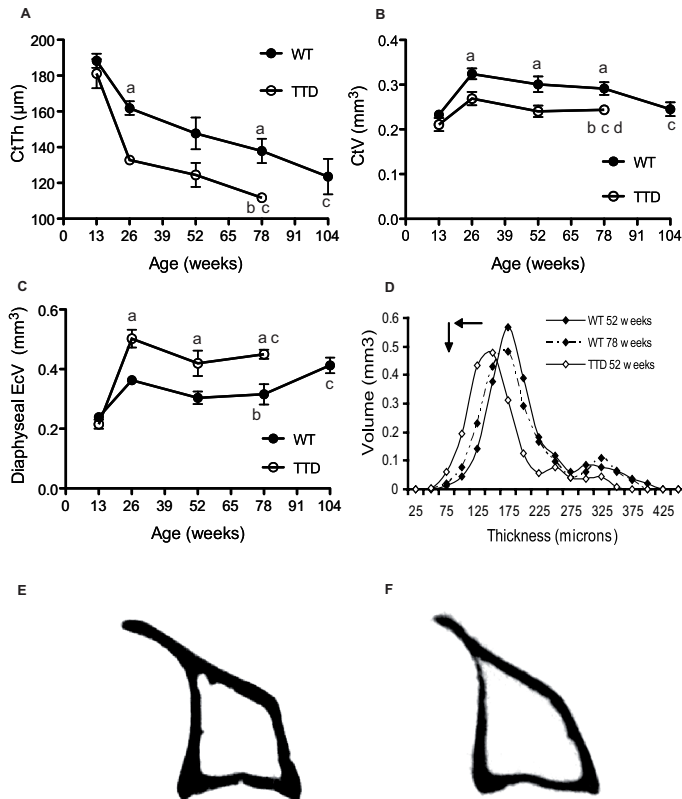
studied in aging wild type (solid) and TTD (open) tibial diaphyses.(A) Cortical thickness (Ct. Th.), (B) cortical volume (Ct.V.), (C) endocortical volume (Ec.V.), (D) 3D thickness distribution. Figures E and F depict the significant decrease in cortical thickness when comparing 26 week old wild type (E) and TTD (F) mice. Statistics: a= student t-test; p<0.05 wild type vs. TTD, b-d = 2 way ANOVA; p<0.05. b= significant difference between wild type and TTD with aging, c= signifcant difference with aging within a genotype, d= a significant interaction between age and genotype. Error bars represent SEM.

Cortical volume (Ct.V.) increased between 13 and 26 weeks after which it remained initially relatively stable in wild type mice, but rapidly and significantly dropped between 78 and 104 weeks of age reaching a level that is already obtained in TTD mice at 52 weeks. In TTD mice, Ct.V. also increased in the first time period, but less than in wild type mice, after which it stabilized throughout life but was significantly lower at all time points compared to wild type mice of the same age (Fig.2B). Statistical analysis showed a significant interaction between age and genotype, which translated into a significant decrease in Ct.V. over time

in TTD mice compared to wild type mice. Endocorital volume (Ec.V) followed a similar pattern in time as Ct.V (Fig.2C). After the initial increase TTD mice have a relatively stable but significantly increased endocortical volume compared to wild type mice throughout their entire life. Ec.V. is stable up to 78 weeks of age in wild type mice after which it rapidly and significantly increases, reaching TTD levels (Fig.2C). Analysis of the 3D thickness distribution within the diaphysis demonstrated a shift towards thinner bone fragments as well as a drop in the number of fragments when comparing young and old wild type as well as TTD mice. This is depicted for wild type mice in Figure 2D. Importantly, an accelerated age-related shift towards thinner fragments was observed in TTD mice when compared to wild type mice (Fig.2D). In general, at the age of 6 months, TTD mice (Fig.2F) already have much thinner cortices and less cortical bone compared to age-matched wild type mice (Fig.2E).

Data of histomorphometric analyses on 13 and 78 week old wild type and TTD tibiae are shown in Table 1. None of the eleven studied histomorphometric parameters were significantly different at 13 weeks (Table 1). In contrast in 78 week old mice, several parameters were significantly lower in TTD mice, including Tb.N, Tb.Th. and BV/TV, supporting the μCT findings, while trabecular spacing (Tb.Sp) was significantly higher in TTD mice. For most parameters a significant interaction between age and the TTD genotype was shown (Table 1).

Bone strength
Structural changes in bone architecture, like differences in cortices and alterations in matrix deposition can lead to changes in bone strength. To address this, we performed 3-point bending tests on wild type and TTD femurs. We measured three parameters; energy to failure, ultimate load and stiffness[23]. The amount of energy needed to break the bone – energy to failure – is with aging significantly lower in TTD that in wild type, but there was no significant interaction between genotype and age (Fig. 3A)

Wild type bones showed a gradual decrease in ulitmate force, reflecting general integrity of the bone structure, dropping from 18 N to 15.5 N over a period of 65 weeks (Fig. 3B). Ultimate force was similar in wild type and TTD mices at 13 weeks of age, consistent with the idea that initial bone development in TTD is not significantly affected. At 26 weeks, however, a drop to about 12.5 N was observed, which is in line with the differences found with other parameters at this age between TTD and wild type males. Bone stiffness was significantly decreased from 13 weeks onwards, with the exception of 26 week old bones (Fig. 3C). Quantitative backscatter scanning electron microscopic analysis of wild type and TTD femurs displayed no significant differences in mineralization of the cortex between genotypes or with aging (Fig.3D). Two μCT parameters related to bone strength, moment of inertia (MOI) and perimeter (Pm.), did not show significant differences between wild type and TTD mice throughout life and followed similar patterns (Fig.3E and Fig.3F). MOI decreases gradually during life in both wild type and TTD mice as expected, since older bones usually become more fragile. Although the difference is not significant, TTD mice have consistently lower MOI values compared to wild type mice up to 78 weeks. In wild type mice in which an additional time point of 2 years was available, we observed a significant increase in perimeter after 78 weeks.

	WT 13w (average ± SD)	TTD 13w (average ± SD)	p-value	WT 78w (average ± SD)	TTD 78w (average ± SD)	p-value	Interaction (p - value)
BV/TV (%)	4.06 ± 0.45	5.66 ± 0.84	0.19	7.47 ± 2.34	0.33 ± 0.10	0.05 *	0.003*
OV/BV (%)	1.02 ± 0.34	1.43 ± 0.68	0.65	0.43 ± 0.26	0.00 ± 0.00	0.07	0.311
OS/BS (%)	10.11 ± 1.62	20.35 ± 6.27	0.21	6.54 ± 3.51	0.00 ± 0.00	0.10	0.034*
ObS/BS (%)	10.48 ± 1.53	19.69 ± 5.56	0.20	6.19 ± 3.20	0.17 ± 0.15	0.05 *	0.022*
OcS/BS (%)	1.97 ± 0.26	2.74 ± 0.80	0.44	1.19 ± 0.23	0.00 ± 0.00	0.27	0.102
Tb.Th. (µm)	17.68 ± 1.14	22.11 ± 1.33	0.06	25.20 ± 3.71	10.94 ± 2.61	0.05 *	0.002*
O.Th. (µm)	0.77 ± 0.06	0.79 ± 0.19	0.93	0.62 ± 0.19	0.00 ± 0.00	0.07	0.032*
NOb/BPm (mm-1)	9.86 ± 1.32	18.10 ± 5.08	0.21	6.70 ± 2.78	2.84 ± 2.54	0.18	0.052
NOc/BPm (mm-1)	1.03 ± 0.14	1.5 ± 0.45	0.40	0.71 ± 0.14	0.00 ± 0.00	0.43	0.096
Tb.Sp. (mm)	431.84 ± 42.48	392.56 ± 46.68	0.60	441.28 ± 126.56	4202 ± 989.98	0.03 *	0.001*
Tb.N. (1/mm)	2.29 ± 0.2	2.52 ± 0.28	0.57	2.68 ± 0.57	0.27 ± 0.04	0.02 *	0.002*

Table 1: *Histomorphometric analyses.* Histomorphometric parameters were measured in 13 and 78 week old wild type and TTD tibiae (N=5). T-tests were performed at each time point, p-values are depicted in the table in the columns "p-value". Interaction between the age and phenotype of the mice was determined by performing 2-way ANOVA's, p-values are depicted in the table in the column "Interaction". * = significant difference between wild type and TTD bones, p<0.05.

Periosteal apposition

An increase in bone perimeter at an older age is a distinctive feature of periosteal apposition, which generally takes place in aging bones in order to maintain bone strength by depositing new bone on the outside (periosteal) of the cortex in order to compensate for the intrinsic bone loss on the inside (endosteal). To address this further we measured periosteal bone formation rates using calcein labeling in wild type and TTD mice (Fig.4A and Fig.4B). Periosteal apposition was significantly reduced in old but not in young TTD mice (Fig.4C). Endosteal bone formation was stable and unaffected throughout life (Fig.4D).

Serum osteocalcin measurements demonstrated that at 52 weeks but not yet at 13 weeks of age TTD mice a have significant lower level of this bone formation parameter (Figure 4E). A characteristic phenotype of TTD mice is that they lack development of adipose tissue with aging [20]. This is reflected by the significant difference we measured in the adipocyte-derived cytokine leptin (Figure 4F). Irrespective of this strong difference the TTD were able to control their serum glucose level and maintain similar levels as the wild type mice (Figure 4G).

Gene expression

 In order to gain more insight into the effects of a mutated Ercc2 (Xpd) gene on transcription in general and bone formation and remodeling specifically, we isolated RNA from tibiae and measured the expression levels of a number of osteoblast and osteoclast specific genes. Osteocalcin (*Bglap*) and collagen (*Col1A1*) were expressed at similar levels in wild type and TTD tibiae, both at 13 and 52 weeks. However, from 13 to 52 weeks of age, expression levels significantly decreased (Figs.5A and B). Two well known osteoclast markers tartrate-resistant acid phosphatase (TRAP/ACP5) and cathepsin K (CTSK) were expressed at equal levels in wild type and TTD tibiae at both ages analyzed (Figs 5C and D). Similar as for the osteoblast markers, both Trap and Ctsk expression significantly decreased from 13 to 52 weeks of age. Recently, the importance of the FOXO-mediated oxidative stress defence

for osteoblast function and skeletal homeostasis has started to become clear [12,13]. We studied the expression patterns of three Foxo genes as well as those of the three superoxide scavengers, Sod1, Sod2 and Sod3. Foxo1 was significantly lower at 13 weeks in TTD mice, whereas Foxo3 and Foxo4 were expressed at similar levels as in wild type tibiae. In 52 week old tibiae however, Foxo3 and Foxo4 expression was significantly decreased in TTD mice whereas *Foxo1* expression was similar in both genotypes (Fig.5C). Both Foxo1 and *Foxo4*, but not Foxo3, levels dropped when comparing 13 weeks old mice to 52 weeks old mice (Figs.5C-E).

Figure 3: *Decreased bone strength in TTD mice.* Bone strength, mineralization, perimeter, MOI and bone formation rates in long bones of aging wild type (solid bars or symbols) and TTD
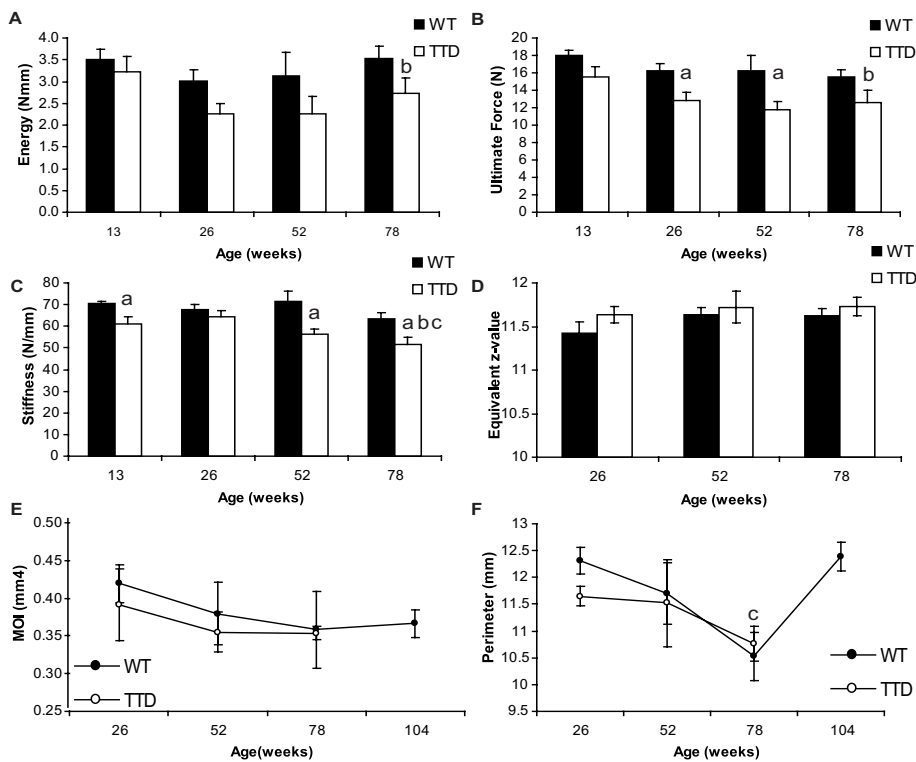
males (open bars or symbols). (A) Energy to failure (B) Ultimate load (C) Bone stiffness, (D) bone mineralization, (C) MOI and (D) perimeter (Pm.). Statistics: a= student t-test; p<0.05 wild type vs. TTD, b-d = 2 way ANOVA; p<0.05. b= significant difference between wild type and TTD with aging, c= signifcant difference with aging within a genotype, d= a significant interaction between age and genotype. Error bars represent SEM.

All 3 Sod genes were expressed at similar levels in wild type and TTD mice throughout life. Sod3 expression decreased from 13 to 52 weeks of age, whereas Sod1 and Sod2 expression remained at the same level in older mice (Fig.5D). Next we analyzed the expression of pro- and anti-apoptotic genes in wild type and TTD mice at various ages. No significant difference in expression was observed at 13 and 52 weeks indicating that the

observed skeletal phenotype in TTD mice is independent of apoptosis. At 104 weeks of age no consistent expression was observed supporting increased or decreased apoptosis. Pro-apoptotic genes were either higher (*Casp7* and *Casp9*) or lower (*Casp3* and *Casp6*) expressed in TTD tibiae (Figure S1).

Figure 4: *Periosteal apposition, bone formation and hormone levels.* TTD mice lack periosteal
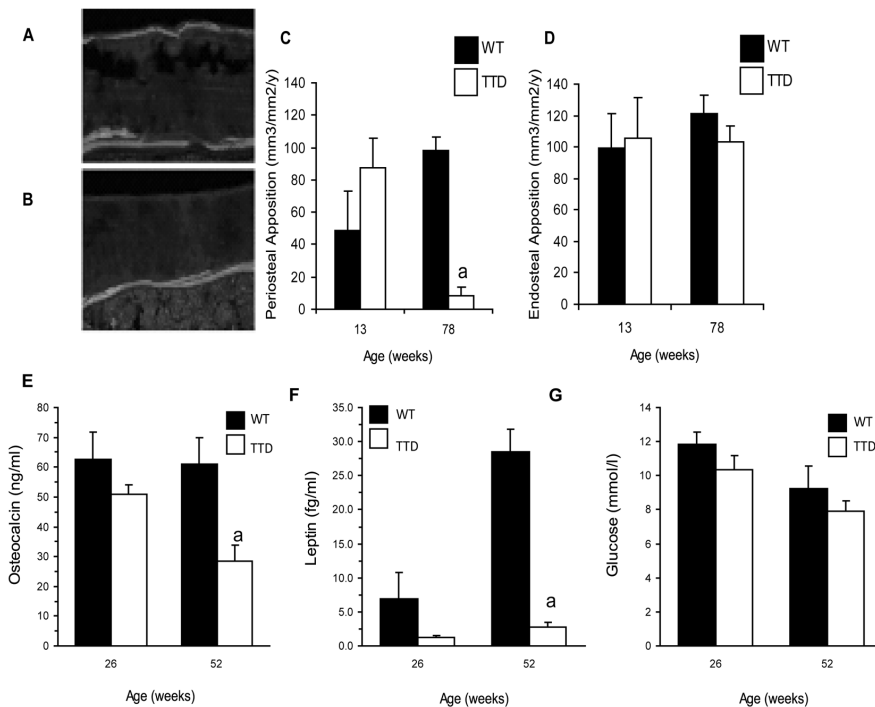
apposition at 78 weeks whereas endosteal apposition is not affected. Calcein labelling at sites of periosteal apposition in 78-week-old (A) wild type and (B) TTD mice. Quantitative analyses of (C) periosteal and (D) endosteal apposition at 13 and 78 weeks. Serum measurements of bone formation markers and hormones; (E) osteocalcin, (F) leptin, (G) glucose at 26 and 52 weeks. Statistics: student t-test a = $p < 0.05$ wild type vs. TTD. Error bars represent SEM.

Bone marrow differentiation potential

Besides a decrease in bone strength and a lack of periosteal apposition, older TTD mice also have a lack of body fat [21,22,24]. This could possibly be due to impairment in the number and/or differentiation capacity of mesenchymal stem cell (MSC), the common precursor of osteoblasts and adipocytes. In order to study this we isolated bone marrow containing MSCs and osteogenic and adipogenic progenitors from 26, 42 and 78 week old wild type and TTD mice and analyzed differentiation into osteoblasts and adipocytes in ex vivo cultures. In addition, we examined the osteoclastogenesis in these bone marrow samples.

The number of alkaline phosphatase (ALP) positive colonies formed in TTD mice showed a significant age-dependent decrease and was at 42 and 78 weeks significantly lower than in wild type mice (Fig.6A). No significant changes in colony size were measured with aging in wild type and TTD cells, and no significant differences between wild type and TTD cultures were observed indicating that at least in vitro proliferative potential was unaffected by aging and the TTD repair defect (Fig.6B). Both wild type and TTD colonies mineralized to the same extent implicating unaffected mineralization in TTD mice (data not shown). In contrast to the number of osteoblast colonies, we did not observe a significant decrease in adipocyte differentiation potential as assessed by the number of lipid-vesicle-forming adipocytes in in vitro cultures (Fig.6C).

Osteoclastogenesis analyses showed that the total number of TRAP+ (ACP5+) osteoclasts found in these in vitro cultures was stable throughout life in wild type mice up to the age of 78 weeks but significantly decreased in TTD mice (Fig.6D). When focusing on multinucleated osteoclasts (>2 nuclei), no significant differences were observed between wild type and TTD mice although TTD cultures showed a significant trend towards a decline in multinucleated osteoclasts with aging (Fig.6E). Additionally, osteoclasts were cultured on bone slices to analyze osteoclast resorption. Only mature osteoclasts are capable of resorbing bone, so we calculated the average size of a pit formed by a multinucleated osteoclast (Fig.6F). For both wild type and TTD mice we observed a trend towards a decrease in resorption with aging, both of which did not reach significance (Fig.6F). No significant differences were observed between wild type and TTD mice although at both 26 and 42 weeks, the resorbed area seemed about twice the size in TTD mice while at 78 weeks it was smaller (Fig.6F).

Discussion

The presented data reveal the significance of proper DNA repair and limiting DNA damage for bone metabolism and maintaining bone strength with aging. The TTD mice with impaired DNA repair display loss of bone structure and strength. Mice deficient in DNA repair are partially unprotected against DNA damage induced by ROS and other types of endogenous agents as has been shown in previous studies [25] and thereby the current study supports the concept of DNA damage-induced skeletal aging [1].

Our findings in aging wild type mice are in line with those presented in other studies that investigated male mice [4,5]. Age-related bone loss in humans has been stipulated to be mostly restricted to cortical bone [6]. We do, however, see a clear decrease in trabecular bone volume (BV/TV) and trabecular number along side the decrease in cortical thickness and cortical volume that was expected. This suggests that not only cortical but also trabecular bone is subjected to age-related bone loss. These data correspond with those found in other studies [5]. Analyses of the 13 weeks old mice demonstrated a temporal difference in skeletal changes with age between trabecular and cortical bone. μCT analyses demonstrated already significant differences at trabecular bone sites between wild type and TTD mice while at cortical bone sites no differences were found. On basis of the trabecular data we cannot exclude that in male TTD mice the observed bone phenotype is partially the result of a developmental disturbance. Nevertheless, viewing our current histomorphometric analyses and the cortical data of 13 weeks old mice, we propose that the skeletal phenotype in male TTD mice is predominantly an age-related phenomenon

Chapter 5

instead of a developmental disorder.

We postulate that up to a certain age, somewhere between 13 and 26 weeks, the still functional DNA repair mechanisms in the TTD mice are able to limit accumulation of DNA damage. This limits cellular malfunctioning and premature cell death, and prevents skeletal alterations. However, this fails with progressing age, leading to premature skeletal aging. In addition, the fact that clear changes between TTD and wilt type only start to develop after 26 weeks of age is inherent to the fact that there is an important temporal component in the process from altered bone cell function to altered bone turnover and eventual overt skeletal structural changes.
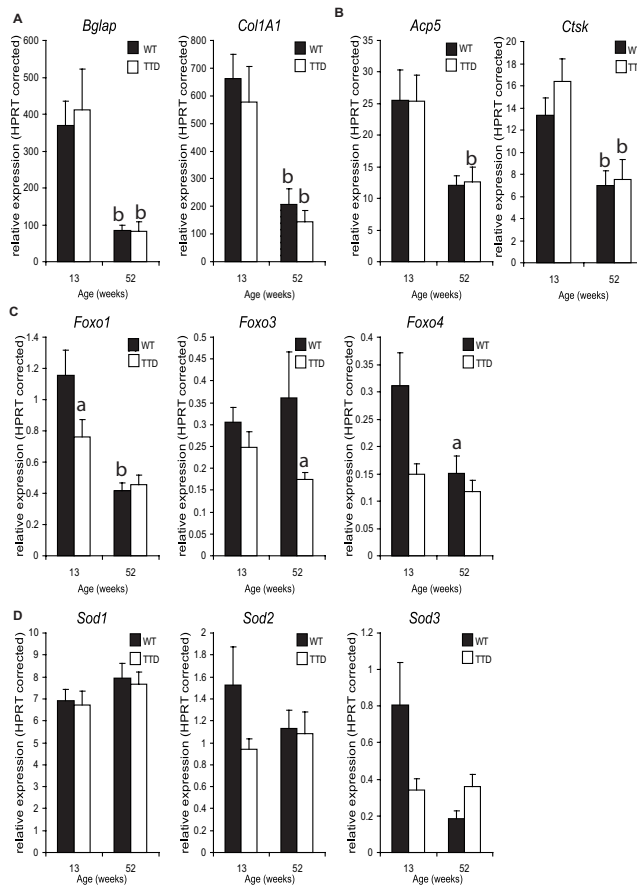
Figure 5: *Regulation of gene expression levels in tibiae.* Expression levels measured in RNA extracted from tibiae of 13 and 52 week old wild type and TTD mice; (A) osteoblast marker genes *Bglap* and *Col1A1*. (B) Osteoclast marker genes *Acp5* and *Ctsk*, (C) stress regulated genes *Foxo1, Foxo3* and *Foxo4*, (D) antioxidant enzyme scavengers *Sod1, Sod2* and *Sod3*. Statistics: student t-test a = $p < 0.05$ wild type vs. TTD, b = $p < 0.05$ time point x vs. time point 13 weeks within one genotype.

The large difference in trabecular bone volume and cortical thickness in 26 weeks old male TTD mice may partially explain the reduction in bone strength that is already apparent at that age in TTD mice compared to wild type mice as we do not detect any significant changes in bone perimeter. In addition, decreased stiffness has previously been correlated with a loss in ultimate strength and an increased fracture risk [26]. In view of these data, we would also expect a decrease in MOI in these young mice, which appears not to be the case in our μCT analysis. However, MOI in these analyses is only a computational proxy for bone strength and does not take into account bone composition, making three point bending tests the more reliable measure. An interesting observation with respect to maintaining bone strength with aging is the profound lack of periosteal apposition in TTD mice. Bone is added to the outside of the cortex in order to compensate loss at the endocortical side and to maintain bone strength as long as possible [27,28]. Disturbances in periosteal apposition and lack to compensate endocortical bone loss will lead to decreased bone strength and increased fracture risk. Involvement of estradiol, with opposite roles for estrogen receptors α and ß, testosterone and mechanical loading in the control of periosteal apposition have been reported [3]. However, the precise mechanisms underlying these age-related changes in bone and periosteal apposition are still poorly understood. Even though the current data do not yet provide a mechanism behind the lack of periosteal apposition, TTD mice might prove an excellent model to further unravel this important skeletal process with aging.

We did not observe an effect on endosteal apposition, whereas periosteal apposition id severely reduced. This might be explained by the segmental nature of the TTD phenotype, which has been previously observed. Where several organs and tissues in TTD mice are exposed to extremely accelerated aging, others are not affected at all [21,22,29]. These segmental effects might be due to differences between cell types, differences in timing and differences in intracellular metabolic stress levels. In the case of periosteal and endosteal apposition, timing might be the most important factor. Endosteal apposition is an important process early on in life, when redundant DNA repair mechanisms may still be able to limit the DNA damage. However, with aging periosteal osteoblast activity is the most important process to compensate for the age-related increased endosteal bone loss. This allows greater impact of DNA damage on periosteal than on endosteal apposition with aging.

The observed reduction in bone volume and perimeter throughout life in wild type and TTD mice will lead to a loss of bone strength. Up to 78 weeks of age there is a small decrease in perimeter which is in line with previous reports on cross-sectional area up to 20 months of age in male wild type mice [4]. Apparently, an increase in perimeter is not important to maintain bone strength up to this point in life. However, after 78 weeks wild type mice demonstrate the known age-related increase in perimeter due to periosteal apposition. Unfortunately, perimeter data on TTD mice over 78 weeks of age could not be obtained. Nonetheless, as TTD mice show a strong decrease in periosteal apposition at 78 weeks, it is unlikely that they would have shown an increase in perimeter as seen in wild type mice. This implicates that with progressing age and improper DNA repair a further and stronger decrease in bone strength will occur. The observed age-related difference in serum osteocalcin is supportive for a decreased periosteal bone formation.

Chapter 5
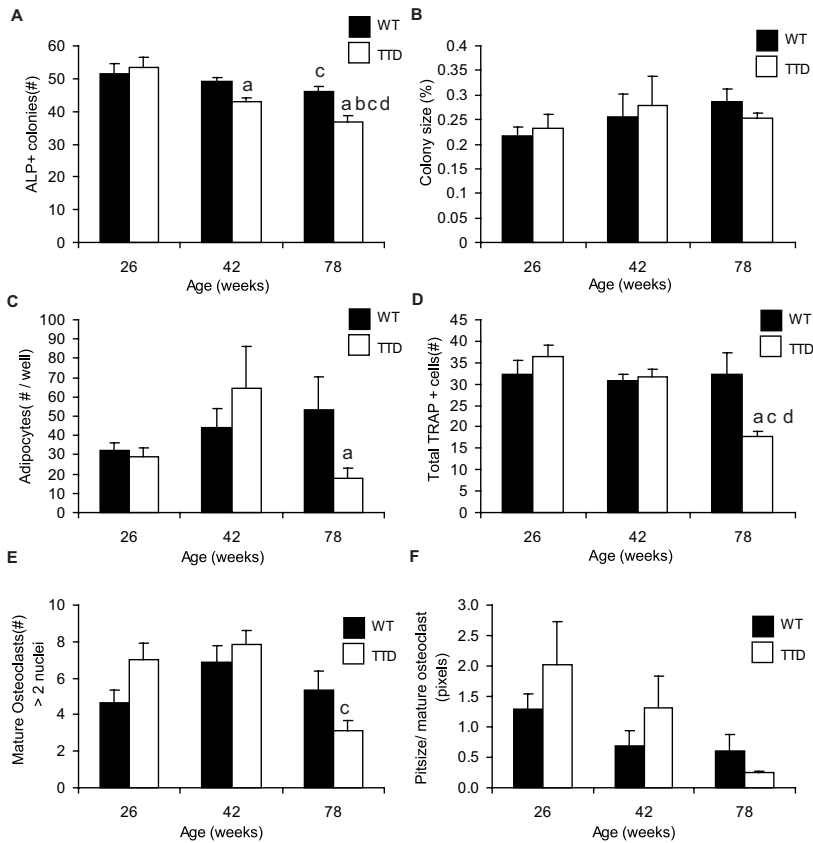
Figure 6: *Mesenchymal and hematopoietic stem cell differentiation.* Mesenchymal and hematopoietic stem cell differentiation in aging wild type (solid bars) and TTD males (open bars). (A) Average number of ALP+ colonies in ex vivo bone marrow cultures after 14 days of culture. (B) Average colony size at day 14 of culture. (C) The average number of adipocytes per well. (D) Average number of TRAP+ positive cells per picture. (E) Average number of mature osteoclasts per picture. (F) Average percentage resorption surface per osteoclast pit per mature osteoclast. Statistics: a= student t-test; p<0.05 wild type vs. TTD, b-d = 2 way ANOVA; p<0.05. b= significant difference between wild type and TTD with aging, c= signifcant difference with aging within a genotype, d= a significant interaction between age and genotype. Error bars represent SEM.

Since TTD mice carry a specific defect in TCR combined with a partial GG-NER deficiency they are predicted to suffer more from the consequences of cellular DNA damage notably an increase in senescent or apoptotic cells. Indeed it has previously been observed that TTD mice even have a decreased spontaneous tumor formation rate. However, overprotection from cancer likely caused by enhanced death of cells with DNA damage may at the same time trigger accelerated aging [15,22,30,31]. In order to get a first tentative look at how TTD cells might be affected by accumulating damage, we studied the mRNA expression of a number of oxidative stress related genes. FOXO proteins play an important role in the cell's defense against oxidative stress and accumulating damage. In addition, FOXO1 can control

bone mass. Osteoblast lineage specific deletion of Foxo1 leads to a decrease in osteoblast number, bone formation rate and bone volume [13]. Interestingly we already observed a significant decrease in Foxo1 expression in 13 weeks old TTD mice. This indicates that already at this young age, one of the fundamental mechanisms that protect the cells against stress is decreased and potentially contributing to decrease in bone structure in TTD mice.

Further support for a role of the FOXO proteins is provided by the reduced expression of *Foxo3* and *Foxo4* at 52 weeks in TTD mice. Our analysis current analyses didn't reveal a major difference in the expression of three *Sod* genes. To address these antioxidant mechanisms, additional detailed analyses at protein and functional level are needed but these were beyond the scope of our current study. The analysis of apoptosis genes in whole tibae suggest that the skeletal phenotype observed in TTD mice is independent of apoptosis. Up to 52 weeks no significant differences between wild type and TTD mice were observed while at 104 weeks pro-apoptotic genes were both down- and up-regulated in TTD mice. As these analyses are based on expression in whole tibae differences in apoptotic gene expression in specific subsets of cells (e.g. osteoblasts, osteoclasts, bone marrow cells including hematopoietic en mesenchymal stem cells) might have been missed and will be part of future studies to unravel the role of apoptosis. An increase in damage and apoptosis can lead to a decrease in the number of stem and progenitor cells and or change their differentiation potential. Bone marrow harbors both mesenchymal and hematopoietic stem cells and their differentiation is tightly regulated in order to maintain a balance between the number of osteoblasts and osteoclasts [32,33,34]. Furthermore, the balance between osteoblast and adipocyte formation within the mesenchymal lineage is known to be regulated and can be tipped either way by disrupting one of the differentiation pathways [35]. The age-related decrease in wild type osteoblast colony formation potential we describe is in line with previous data [36].

Our current ex vivo TTD bone marrow cultures, as well as the histomorphometric data, showed a reduction in the capacity to form bone nodules and a trend towards reduced osteoclast activity with age. Taking into account that systemic factors might even increase the effect of this significant reduction in osteoblasts and osteoclasts, this could cause a reduction in bone turnover capacity and thereby a reduced capacity to maintain healthy bone. It is tempting to conclude that this is part of the mechanism underlying the observed early onset of skeletal aging and decrease in bone strength, although the observed effects are too small to be the only contributing factor. In addition, earlier in life, at 26 and 42 weeks of age, the number of multinucleated osteoclasts and resorbed area are higher in TTD mice than in wild type mice, which may also contribute to the increase in bone loss and increased endocortical volume earlier in life. This effect on osteoclasts is supported by preliminary FACS analysis of wild type and TTD bone marrow (data not shown) showing a shift in HSC differentiation towards the myeloid lineages in TTD mice.

Overall, these effects on osteogenic and osteoblast precursors and on osteoclastogenesis in TTD mice may contribute to accelerated bone aging and loss of bone strength in case of compromised DNA repair and accumulation of DNA damage. Although the effects on osteoblast and osteoclast formation are relatively mild, they are present for a prolonged time, which might expand and accumulate their final impact on bone formation.

Chapter 5

Additionally in vivo systemic processes are most likely involved in causing the observed changes in bone formation. Hormone levels, cytokines and growth factors may change with age [37] and previous studies on TTD and other DNA repair deficient mice show that they play an important role in causing the accelerated aging phenotype observed in these mice. For example the growth hormone/insulin-like growth factor cascade is impaired in other murine DNA repair deficient mouse models (Csb/Xpa and Xpf/Ercc1 mice) and a significant downregulation of the IGF axis was measured in TTD livers, indicating that this might well be the case in TTD mice as well [25,38,39]. Downregulation of this axis will skew the cells towards survival instead of differentiation pathways. Another study using TTD mice has shown a disturbed PPAR target gene regulation, which can have wide ranging systemic effects. This might well explain the discrepancy between the results from our *ex vivo* adipocyte cultures and our *in vivo* observations on adipocyte tissue formation. PPAR target genes play an important role in regulating adipocyte differentiation and a disrepancy in their regulation might very well be the cause of the characteristic lack of fat deposition in the TTD mice[30]. The lack of adipose tissue in TTD mice disturbs their energy metabolism and has a profound effect on the leptin levels that are found in TTD serum. Leptin levels, which regulate appetite and subsequently food intake, are not significantly different in young wild type and TTD mice. At 52 weeks however, there is a profound and significant difference between wild type and TTD mice. Several studies have shown that leptin directly affects bone formation, reducing trabecular bone while stimulating cortical bone formation [40,41]. Logically, a lack in leptin would cause a loss of cortical bone, which fits our observations and might be one of the underlying factors for the observed decrease in cortical bone and loss of periosteal apposition. However, this would not fit our current observations on trabecular bone implicating that, once again, additional factors are involved.

In conclusion, accumulation of DNA damage induces skeletal aging in DNA repair deficient male TTD mice. This effect does not seem be sex specific. Recent observations in female mice by our group also show accelerated skeletal aging and loss of bone strength [42]. Considering the effect of ROS in DNA damage and aging [1,43,44,45]our study supports the importance of proper anti-oxidant defence mechanisms and optimal DNA repair for skeletal maintenance and maintaining bone.

Acknowledgements

Chapter 5

References

1. Manolagas SC (2010) From estrogen-centric to aging and oxidative stress: a revised perspective of the pathogenesis of osteoporosis. Endocr Rev 31: 266-300.
2. Looker AC, Wahner HW, Dunn WL, Calvo MS, Harris TB, et al. (1998) Updated data on proximal femur bone mineral levels of US adults. Osteoporos Int 8: 468-489.
3. Riggs BL, Khosla S, Melton LJ, 3rd (2002) Sex steroids and the construction and conservation of the adult skeleton. Endocr Rev 23: 279-302.
4. Glatt V, Canalis E, Stadmeyer L, Bouxsein ML (2007) Age-related changes in trabecular architecture differ in female and male C57BL/6J mice. J Bone Miner Res 22: 1197-1207.
5. Halloran BP, Ferguson VL, Simske SJ, Burghardt A, Venton LL, et al. (2002) Changes in bone structure and mass with advancing age in the male C57BL/6J mouse. J Bone Miner Res 17: 1044-1050.
6. Nordin BEC (1993) Metabolic Bone and Stone Disease; Nordin BEC, editor: Churchill Livingstone. 500 p.
7. Balaban RS, Nemoto S, Finkel T (2005) Mitochondria, oxidants, and aging. Cell 120: 483-495.
8. Janssen-Heininger YM, Mossman BT, Heintz NH, Forman HJ, Kalyanaraman B, et al. (2008) Redox-based regulation of signal transduction: principles, pitfalls, and promises. Free Radic Biol Med 45: 1-17.
9. Giorgio M, Migliaccio E, Orsini F, Paolucci D, Moroni M, et al. (2005) Electron transfer between cytochrome c and p66Shc generates reactive oxygen species that trigger mitochondrial apoptosis. Cell 122: 221-233.
10. Salih DA, Brunet A (2008) FoxO transcription factors in the maintenance of cellular homeostasis during aging. Curr Opin Cell Biol 20: 126-136.
11. van der Horst A, Burgering BM (2007) Stressing the role of FoxO proteins in lifespan and disease. Nat Rev Mol Cell Biol 8: 440-450.
12. Ambrogini E, Almeida M, Martin-Millan M, Paik JH, Depinho RA, et al. (2010) FoxO-mediated defense against oxidative stress in osteoblasts is indispensable for skeletal homeostasis in mice. Cell Metab 11: 136-146.
13. Rached MT, Kode A, Xu L, Yoshikawa Y, Paik JH, et al. (2010) FoxO1 is a positive regulator of bone formation by favoring protein synthesis and resistance to oxidative stress in osteoblasts. Cell Metab 11: 147-160.
14. Hanawalt PC (2002) Subpathways of nucleotide excision repair and their regulation. Oncogene 21: 8949-8956.
15. Hoeijmakers JH (2009) DNA damage, aging, and cancer. N Engl J Med 361: 1475-1485.
16. Giglia-Mari G, Coin F, Ranish JA, Hoogstraten D, Theil A, et al. (2004) A new, tenth subunit of TFIIH is responsible for the DNA repair syndrome trichothiodystrophy group A. Nat Genet 36: 714-719.
17. Bootsma D, Hoeijmakers JH (1993) DNA repair. Engagement with transcription. Nature 363: 114-115.
18. Ogi T, Limsirichaikul S, Overmeer RM, Volker M, Takenaka K, et al. (2010) Three DNA polymerases, recruited by different mechanisms, carry out NER repair synthesis in human cells. Mol Cell 37: 714-727.
19. Itin PH, Sarasin A, Pittelkow MR (2001) Trichothiodystrophy: update on the sulfur-deficient brittle hair syndromes. J Am Acad Dermatol 44: 891-920; quiz 921-894.
20. de Boer J, de Wit J, van Steeg H, Berg RJ, Morreau H, et al. (1998) A mouse model for the basal transcription/DNA repair syndrome trichothiodystrophy. Mol Cell 1: 981-990.
21. de Boer J, Andressoo JO, de Wit J, Huijmans J, Beems RB, et al. (2002) Premature aging in mice deficient in DNA repair and transcription. Science 296: 1276-1279.
22. Wijnhoven SW, Beems RB, Roodbergen M, van den Berg J, Lohman PH, et al. (2005) Accelerated aging pathology in ad libitum fed Xpd(TTD) mice is accompanied by features suggestive of caloric restriction. DNA Repair (Amst) 4: 1314-1324.
23. Turner CH (2006) Bone strength: current concepts. Ann N Y Acad Sci 1068: 429-446.
24. Roschger P, Fratzl P, Eschberger J, Klaushofer K (1998) Validation of quantitative backscattered electron imaging for the measurement of mineral density distribution in human bone biopsies. Bone 23: 319-326.
25. van der Pluijm I, Garinis GA, Brandt RM, Gorgels TG, Wijnhoven SW, et al. (2007) Impaired genome maintenance suppresses the growth hormone--insulin-like growth factor 1 axis in mice with Cockayne syndrome. PLoS Biol 5: e2.
26. Hoshaw SJ, Cody DD, Saad AM, Fyhrie DP (1997) Decrease in canine proximal femoral ultimate strength and stiffness due to fatigue damage. J Biomech 30: 323-329.

Chapter 5

27. Russo CR, Lauretani F, Seeman E, Bartali B, Bandinelli S, et al. (2006) Structural adaptations to bone loss in aging men and women. Bone 38: 112-118.

28. Seeman E (2003) Invited Review: Pathogenesis of osteoporosis. J Appl Physiol 95: 2142-2151.

29. Botter SM, Zar M, van Osch GJ, van Steeg H, Dolle ME, et al. (2011) Analysis of osteoarthritis in a mouse model of progeroid human DNA repair syndrome trichothiodystrophy. Age (Dordr) 33: 247-260.

30. Compe E, Drane P, Laurent C, Diderich K, Braun C, et al. (2005) Dysregulation of the peroxisome proliferator-activated receptor target genes by XPD mutations. Mol Cell Biol 25: 6065-6076.

31. de Boer J, Hoeijmakers JH (1999) Cancer from the outside, aging from the inside: mouse models to study the consequences of defective nucleotide excision repair. Biochimie 81: 127-137.

32. Horowitz MC, Xi Y, Wilson K, Kacena MA (2001) Control of osteoclastogenesis and bone resorption by members of the TNF family of receptors and ligands. Cytokine Growth Factor Rev 12: 9-18.

33. Metcalf D (2007) Concise review: hematopoietic stem cells and tissue stem cells: current concepts and unanswered questions. Stem Cells 25: 2390-2395.

34. Satija NK, Gurudutta GU, Sharma S, Afrin F, Gupta P, et al. (2007) Mesenchymal stem cells: molecular targets for tissue engineering. Stem Cells Dev 16: 7-23.

35. Atmani H, Chappard D, Basle MF (2003) Proliferation and differentiation of osteoblasts and adipocytes in rat bone marrow stromal cell cultures: effects of dexamethasone and calcitriol. J Cell Biochem 89: 364-372.

36. Bergman RJ, Gazit D, Kahn AJ, Gruber H, McDougall S, et al. (1996) Age-related changes in osteogenic stem cells in mice. J Bone Miner Res 11: 568-577.

37. Lamberts SW, van den Beld AW, van der Lely AJ (1997) The endocrinology of aging. Science 278: 419-424.

38. Niedernhofer LJ, Garinis GA, Raams A, Lalai AS, Robinson AR, et al. (2006) A new progeroid syndrome reveals that genotoxic stress suppresses the somatotroph axis. Nature 444: 1038-1043.

39. Park JY, Cho MO, Leonard S, Calder B, Mian IS, et al. (2008) Homeostatic imbalance between apoptosis and cell renewal in the liver of premature aging Xpd mice. PLoS One 3: e2346.

40. Ducy P, Amling M, Takeda S, Priemel M, Schilling AF, et al. (2000) Leptin inhibits bone formation through a hypothalamic relay: a central control of bone mass. Cell 100: 197-207.

41. Hamrick MW, Ferrari SL (2008) Leptin and the sympathetic connection of fat to bone. Osteoporos Int 19: 905-912.

42. Diderich KE, Nicolaije C, Priemel M, Waarsing JH, Day JS, et al. (2011) Bone fragility and decline in stem cells in prematurely aging DNA repair deficient trichothiodystrophy mice. Age (Dordr).

43. Calabrese V, Cornelius C, Mancuso C, Lentile R, Stella AM, et al. (2010) Redox homeostasis and cellular stress response in aging and neurodegeneration. Methods Mol Biol 610: 285-308.

44. Russell SJ, Kahn CR (2007) Endocrine regulation of ageing. Nat Rev Mol Cell Biol 8: 681-691.

45. Wauquier F, Leotoing L, Coxam V, Guicheux J, Wittrant Y (2009) Oxidative stress in bone remodelling and disease. Trends Mol Med 15: 468-477.

46. Bouxsein ML, Boyd SK, Christiansen BA, Guldberg RE, Jepsen KJ, et al. (2010) Guidelines for assessment of bone microstructure in rodents using micro-computed tomography. J Bone Miner Res 25: 1468-1486.

47. Hildebrand T, Laib A, Muller R, Dequeker J, Ruegsegger P (1999) Direct three-dimensional morphometric analysis of human cancellous bone: microstructural data from spine, femur, iliac crest, and calcaneus. J Bone Miner Res 14: 1167-1174.

48. Botter SM, van Osch GJ, Clockaerts S, Waarsing JH, Weinans H, et al. (2011) Osteoarthritis induction leads to early and temporal subchondral plate porosity in the tibial plateau of mice: An in vivo micro CT study. Arthritis Rheum.

49. Amling M, Priemel M, Holzmann T, Chapin K, Rueger JM, et al. (1999) Rescue of the skeletal phenotype of vitamin D receptor-ablated mice in the setting of normal mineral ion homeostasis: formal histomorphometric and biomechanical analyses. Endocrinology 140: 4982-4987.

50. Priemel M, von Domarus C, Klatte TO, Kessler S, Schlie J, et al. (2010) Bone mineralization defects and vitamin D deficiency: histomorphometric analysis of iliac crest bone biopsies and circulating 25-hydroxyvitamin D in 675 patients. J Bone Miner Res 25: 305-312.

51. Broderick E, Infanger S, Turner TM, Sumner DR (2005) Depressed bone mineralization following high dose TGF-beta1 application in an orthopedic implant model. Calcif Tissue Int 76: 379-384.

52. van der Eerden BC, Hoenderop JG, de Vries TJ, Schoenmaker T, Buurman CJ, et al. (2005) The epithelial Ca2+ channel TRPV5 is essential for proper osteoclastic bone resorption. Proc Natl Acad Sci U S A 102: 17507-17512.

CHAPTER 6

Concluding remarks and

future perspectives

Aging is a complex and multi-faceted process, driven by numerous players that differ from organ to organ. This is clearly depicted by many human progeroid syndromes that display segmental accelerated aging, with a number of organs that age very rapidly while other organs are seemingly unaffected [1]. In this thesis we have focused on several factors that might influence skeletal aging and may underlie age-related skeletal diseases like osteoporosis.

The effects of low oxygen tension on osteoblast differentiation and mineralisation

Part of the research in this thesis focuses on the more basal effects of oxygen and oxidative stress on osteoblast differentiation and bone matrix formation and mineralization. To date, the most enduring theory of aging stipulates that oxidative stress related damage is the major determinant of aging and lifespan. It is also the cause of several age-associated diseases including osteoporosis [2,3,4]. Aging seems to be accompanied by an increase in ROS, which cause oxidative stress related damage followed by senescence or cell death [5]. Formation of ROS is an inescapable consequence of life in an oxygen-rich environment and occurs primarily in the mitochondria during aerobic metabolism which is fueled by nutrients such as glucose and is responsible for the formation of ATP [4,6]. Osteoblasts are metabolically active cells that have to produce great amounts of matrix components while forming bone. Osteoblast differentiation consists of several highly energy-demanding phases including matrix production, maturation, and mineralization, which are coordinated by a switch from glycolysis to respiration that involves increased mitochondrial biogenesis [7,8]. By being metabolically active they produce a high amount of ROS and might be more susceptible to oxidative damage induced aging than cells that are metabolically less active.

One of the regulatory factors that can affect cell metabolism and ROS production is oxygen tension. In MSCs, low oxygen tension plays a role in maintaining stemness, inhibiting differentiation and mineralization [9]. Low oxygen tension is also involved in the regulation of cell metabolism, by limiting the available mitochondrial oxidants, necessary to induce metabolic pathways [10]. Importantly, almost all *in vitro* data on osteoblast proliferation, differentiation and aging, are obtained from standard culture experiments using 20% oxygen. Physiological oxygen tension never reaches these levels, especially in the bone marrow where oxygen tension can be even as low as 1% [11,12,13]. Knowledge on how low oxygen tension affects osteoblast proliferation and differentiation, and the effect of induced oxidative stress on these processes is therefore of great importance, in order to understand the impact of oxidative stress on osteoblasts and bone metabolism. In addition these experiments will provide us with important information that can be applied to related fields of research, including fracture healing and stem cell mediated medicine and repair. During a severe bone fracture, oxygen levels often drop to extremely low levels due to ruptured blood vessels at the fracture site [14,15]. This suggests that at least the initial repair stages, including the recruitment of pre-osteoblasts to the fracture site and their differentiation into matrix producing osteoblasts, take place under extremely low oxygen conditions until blood flow to the fracture site is adequately restored. In addition, novel tissue engineering approaches are often based on the transplantation of MSC loaded scaffolds into a fracture site [16]. These MSCs would undergo a change in oxygen tension upon transplantation, which could affect their further behavior. A better understanding of MSC and osteoblasts behavior under low oxygen conditions will be necessary to understand

the exact mechanisms that are studied in these processes and can be beneficial to the future application of tissue engineering approaches in patients.

Effects of low oxygen tension on cell metabolism, ROS production and induction of apoptosis

As mentioned above, low oxygen tension cultures mimic the physiologic environment of MSCs and osteoblasts more accurately than commonly used culture conditions. For the studies reported in this thesis we cultured cells under 2% oxygen tension. We observed a decrease in osteoblast differentiation, matrix formation and mineralization in low oxygen tension cultures. This was in accordance with previous studies on the effects of low oxygen tension [9,17]. As regulators of matrix formation and mineralization, differentiation state, apoptosis rates and matrix composition and modification were studied (chapter 2). Cells cultured under low oxygen tension displayed a reduction in free radical content, including a decrease in super oxide radical levels (chapter 2, Figure 2B). Super oxide radicals are formed during cell energy metabolism, which is the main intracellular source for radicals [6]. These findings as well as a reduction in cell proliferation rates, suggest a downregulation of cell metabolism due to low oxygen tension levels. Lower radical levels turned out to be beneficial for cell survival, significantly reducing apoptosis rates in osteoblast cultures. However, this is accompanied by a decline in differentiation potential and a decrease in the cell's anti-oxidant defense mechanisms. This leaves the cells in a pre-differentiation state and more vulnerable to induced oxidative stress (chapter 2, Figure 4B).

These are interesting findings because they show that low oxygen tension can be beneficial and detrimental at the same time. In tissue engineering for example, it might be beneficial to transplant MSCs cultured under low oxygen tension. Due to their oxidative priming these MSCs may have a better differentiation potential since they maintained their stemness and have lower apoptosis rates due to their lowered metabolism and radical levels. On the other hand the cells would also be primed to be more vulnerable to external oxidative stress cues that could trigger massive amounts of apoptosis. This puts forward the significance of finding the right balance between oxidative priming and cellular oxidative stress protection in order to facilitate maximal differentiation potential as well as cell survival.

A specific factor that was affected by low oxygen tension is collagen expression and production. While collagen expression levels were upregulated, total collagen levels in the matrix were reduced. More interestingly we measured significant changes in the expression levels of a number of proteins that regulate collagen modifications in the matrix (chapter 2, Figure 5D). MMPs are the major enzymes involved in matrix remodeling and collagen break down and they can influence a large number of signaling processes. While degrading matrix, MMPs can release bioactive breakdown products and disrupt matrix adherence [18,19,20,21]. It is tempting to speculate that MMP activity limits ECM turnover. This is important for the maturation and subsequent mineralization of ECM. A reduction in MMP expression may therefore contribute to the inhibition of bone formation and mineralization. This is supported by data from several MMP knock out models [22,23,24,25]. Additionally, mutations in the human MMP2 gene that disrupt MMP2 substrate binding and catalytic activity have been linked to multicentric osteolysis with arthritis (MOA), an osteolytic bone disease [26]. All these data indicate that a decrease in MMP expression can

Chapter 6

have a negative influence on matrix formation and mineralization as observed in the 2% oxygen condition. MMP activity is regulated by TIMPs. These proteins have been reported to inhibit MMPS by binding their catalytic domain [27] but can also activate MMPs [28,29] and possess growth-promoting activity [30]. Interestingly, TIMP-3 may contribute to the observed increase in apoptosis in the high (20%) oxygen condition as its expression is significantly higher in this condition (chapter 2, Figure 5D) and TIMP-3 has been shown to induce apoptosis of osteoblasts [31].

Our findings indicate that the matrix formed under low oxygen tension has a different composition than the matrix formed under high oxygen tension. More in depth studies into collagen production and secretion, collagen modification and matrix content and composition as well as its impact on cell function are needed to yield a detailed view on how low oxygen tension modifies matrix composition and eventual mineralization. Future experiments should include a comparison of the protein content of both matrices as well as a more detailed overview of MMP and TIMP activity under both oxygen conditions. It will be important to study differences in cell-matrix communication between the two oxygen conditions. Elegant work by Discher et al and others has shown the significance of extracellular matrix composition and rigidity for cell function [32,33]. It will be interesting to assess if the matrix formed under low oxygen conditions has different effects on osteoblast differentiation than a matrix formed under high oxygen conditions, especially since differentiation status turned out to be the most important factor affecting matrix formation and mineralization.

Effects of low oxygen tension on gene expression during different stages of osteoblast differentiation

We assessed that the expression levels of several genes (collagens, antioxidant enzymes and MMPs) differed between 20% oxygen cultures and 2% oxygen cultures. These findings only gave a limited view of the impact of oxygen on gene expression. Therefore we designed experiments to get a more complete and unbiased view of the impact of oxygen on gene expression during osteoblast differentiation. Gene expression profiling studies were performed against the backdrop of osteoblast differentiation and 2 % or 20% oxygen (chapter 3). We performed a large and intricate gene expression profile analysis on a wide variety of high and low oxygen combinations during osteoblast culture, but focused on the conditions described in chapter 2 for this thesis.

First, cells were cultured continuously under either 2% (low) or 20% (high) oxygen for the three week differentiation and mineralization process. The differentiation processes can be divided into three phases; the differentiations phase, the pre-mineralization phase and the matrix maturation and mineralization phase (Chapter 3, figure 1). RNA was collected at the end of each of these three characterized differentiation phases. Unbiased heatmap analyses (chapter 3, Supplemental figure 1) identified specific probe subsets based on regulation during the three osteoblast differentiation phases. GO-annotation analyses of the probes that were regulated in all phases of differentiation (chapter 3, subset 2; figure 5C) or predominantly regulated in the first 2 phases (chapter 3, subset 3; Figure 5D) revealed that 2% oxygen significantly impacted on the cell's energy metabolism, in particular on the carbohydrate metabolism. Most interestingly in this respect is that osteoblast differentiation consists of several highly energy-demanding phases including

matrix production, maturation, and mineralization, which are coordinated by a switch from glycolysis to respiration that involves increased mitochondrial biogenesis [7,8]. This is consistent with the results discussed above and supported by another study that demonstrates a role for PPARγ in osteoblast differentiation and mineralization in which oxygen radicals and antioxidant levels play an eminent role [34].

Another specific subset consists of probes increased in expression during phase 2 and 3 of differentiation (chapter 3, subset 1). GO-annotation analyses of these genes revealed different biological processes, cellular components and molecular functions than those directly related to energy metabolism. Interestingly, and supportive for a role in osteoblast differentiation and bone formation, were the GO-terms collagen, ECM and growth factor binding. Numerous collagen genes are expressed to a higher extent in cells cultured continuously on low oxygen tension, including *COL1A1*, the main component of bone matrix. This is in contrast with findings in chondrocytes, which showed a down regulation of collagen type I expression and could indicate osteoblast-specific regulation of collagen expression during low oxygen tension[35]. In addition, important hydroxylases including *PLOD1, PLOD2* and *P4HA2,* essential for collagen fibril formation, are higher expressed. This corresponds with previous findings in vascular smooth muscle cells and is most likely a direct response to HIF1α induction, caused by the drop in oxygen tension [36].

As shown in chapter 2, low oxygen tension in the first differentiation phase had a large impact on osteoblast differentiation and the final rate of matrix mineralization. To determine if low oxygen tension in this first phase had an effect on gene expression in the second phase, cells cultured under 2 % or 20% oxygen in the first phase followed by 2% in the second phase were studied. This comparative analysis showed that the number of probes regulated in phase 2 is higher for cells that previously received 20% oxygen in phase 1 (chapter 3, Figure 4A and 4B). The regulation of an additional number of genes might lead to the regulation of additional biological processes when compared to the processes regulated in cells continuously cultured on 2% oxygen. However, 81 % of the 263 regulated probes in the 2%-2% condition overlapped with those regulated in the 20%-2% condition and were linked to largely the same biological processes and cellular components including the cell metabolism-related biological processes and ECM-related cellular components mentioned above. Functional annotation of the 100 specific probes of the 20%-2% condition and the 49 specific probes of 2%-2% condition didn't identify any significant biological process or cellular components. However, amongst the 100 specific probes for the 20%-2% condition, where both *VEGFA* and *VEGFB*, strengthening the link we've observed between hypoxia and angiogenesis which is at least in part regulated by osteoblasts expressing these important regulators of angiogenesis [37]. The list of 49 probes specifically regulated in the 2%-2% condition contained several important genes related to bone metabolism. Among these were collagens and collagen-related proteins as well as PPARγ which we have recently shown to regulate osteoblast differentiation [34]. Moreover the presence of these bone-related genes in the group of 2%-2% specific regulated genes, stresses that 2% oxygen in the first phase is essential to observe these effects and are in line with the observation in Chapter 2. These gene profiles thereby hold interesting clues for the early stage effects of low oxygen on osteoblast differentiation and bone formation.

In conclusion, the osteoblast cell culture data and the unbiased gene expression profiling

Chapter 6

analyses indicate that the inhibition of osteoblast differentiation and mineralization is due to two main processes. First, changes in genes and processes that affect the energy metabolism such as glycolysis and hexose metabolic processes, substantiating the significance of these processes for the energy demanding osteoblast differentiation and bone formation. Second, differentiation and mineralization are affected by changes in the expression levels of the genes encoding ECM proteins. These analyses thereby identify processes and genes that can be targeted and controlled for optimal osteoblast differentiation and bone formation in situations with a change in oxygen tension such as fracture repair and regenerative medicine.

Effects of deficient DNA repair on skeletal aging in mice

Besides results obtained in in vitro cell culture experiment, the link between skeletal aging and an increase in ROS-induced damage was studied in vivo for this thesis. We studied female and male cohorts of TTD mice, which have previously shown features of premature aging, and carried out a detailed comparison of the effects of defective DNA repair on skeletal aging in comparison to aging wild type mice (chapter 4 and 5) [38,39]. To assess a possible underlying developmental defect, mice as young as 13 weeks old were included in our experiments. Data analysis showed that at such young age most bone parameters did not differ between wild type and TTD mice which is in line with results found in previous studies [39].

The first obvious and detrimental signs of accelerated aging can be observed after 26 weeks in male TTD mice. They display a significant decrease in trabecular and cortical bone volume accompanied by a significant decrease in bone strength around the same point in time (chapter 5, Figures 1-3). Female TTD mice display a similar decrease in cortical bone and bone strength but with a later onset, which lies after week 39 (chapter 4, Figure 1 and 3). At 52 weeks the decline in cortical bone volume of both male and female mice precedes a similar rate of decline in wild type mice by approximately 50 weeks. There are several factors that may underlie the observed difference in the onset of the bone phenotype in male and female mice. This might include a difference in circulating hormone levels but also the fact that male mice reach a higher peak bone volume than female mice [40]. In order to attain their higher peak bone volume, male mice will have to produce more bone matrix in the same amount of time, increasing the metabolic activity of their osteoblasts. This might lead to an increase in oxidative stress induced DNA damage in male osteoblasts that could significantly accelerate the aging process in male osteoblasts when compared to female osteoblasts.

Two processes underlying the decrease in bone volume and bone strength are the observed the change in mesenchymal stem cell (MSC) numbers and differentiation potential and the lack of periosteal apposition.

MSC proliferation and differentiation potential and the importance of systemic signaling factors

Mesenchymal stem cells give rise to a number of cell lineages, including osteoblasts, chondrocytes and adipocytes. Like all other cells, stem cells are affected by aging, resulting in a loss of their self-renewal capacity and the number of active MSCs. This is reflected

in a loss of differentiation and proliferation potential, an increasing number of senescent MSCs, and a loss of *in vivo* bone formation [41,42,43]. For example, the balance in MSC differentiation shifts in favor of adipocyte differentiation at the expense of osteoblast differentiation with aging. This results in reduced bone formation and an increased risk for osteogenic disorders like osteoporosis in humans and animals [44]. MSC aging can be affected by intrinsic (intracellular) and extrinsic (extracellular, circulating) factors. The effect of intrinsic accumulation of intracellular DNA damage was studied as part of this thesis, whereas the effects of extrinsic factor like circulating hormones and growth factors are shown in studies that used serum from aging rats to induce Wnt-signaling mediated MSC senescence [45].

Data from wild type and TTD bone marrow cultures support the decline in proliferation potential (chapter 4 and 5). Bone nodule formation decreased with time in both wild type and TTD mice. Although bone nodule formation decreased faster in TTD mice, their bone forming capacity remained intact. In addition, *in vitro* adipogenesis was not affected. Interestingly, *in vivo* TTD mice show both a lack of fat and a loss of bone while aging, which nicely illustrates the importance of extrinsic factors in regulating MSC proliferation and differentiation. The severe lack of body fat could be due to a loss of MSC differentiation potential or skewing of the adipocyte-osteoblast differentiation balance. A more likely cause however, is a lack of the correct extrinsic signaling cues. Additionally, *in vivo* intermittent PTH treatment had a positive effect on the long bones of female TTD mice (chapter 4, figure 6D). We observed a significant increase in cortical thickness which demonstrates that bone formation is functional and MSC differentiation can be stimulated in TTD mice. As mentioned before, PTH is an inhibitor of osteoblast apoptosis. It is therefore tempting to speculate that PTH can delay osteoblast apoptosis caused by defective DNA repair, thereby stimulating additional bone formation in TTD mice [46].

These results also suggest that systemic factors - or the lack thereof - must play an important role in causing the TTD bone phenotype. Further investigations are needed to determine their exact influence on the observed accelerated skeletal aging. It is well documented that a number of hormone levels decline with age and negatively affect bone formation as a result. During menopause estrogen levels drop, which results in an accelerated phase of bone loss in females [47]. In addition, aging also affects the GH/IGF1 axis, lowering the amount of circulating GH and IGF1. This leads to an increase in adipose tissue and an accompanying loss of bone [48]. Recently published data show that leptin deficiency leads to a decrease in cortical and trabecular bone and that these effects are at least partially age dependent [49]. Leptin is produced by adipocytes and regulates body weight and fat mass by affecting appetite and energy expenditure [50]. The lack of adipose tissue in TTD mice most likely caused the drop in leptin levels observed in male TTD mice (chapter 5, Figure 4G). This drop in leptin levels could have a negative effect on bone formation. A number of studies using other DNA repair deficient mouse models show that they exhibit a systemic downregulation of important regulatory axes, including the GH-IGF1 axis [51]. Additionally, preliminary data from female TTD mice show a drop in estradiol levels, which might also negatively affect bone formation, mimicking menopause. Further investigations are needed to determine the exact effects of systemic factors on bone formation and resorption in TTD mice.

Chapter 6

It will also be important to study bone marrow composition in more detail, with specific focus on age-related changes in the hematopoietic stem cell lineages and osteoclast formation. FACS analysis of hematopoietic stem cell lineages in a very limited number of young and old wild type and TTD mice displayed a shift in precursor populations in older TTD mice. This could point towards an increase in osteoclast formation thereby having additional effects on the balance between bone formation and degradation in TTD mice. It will be interesting to assess if transplantation of wild type bone marrow can at least partially rescue the observed accelerated skeletal aging in TTD mice. Preliminary results on the effects of bone marrow transplantation showed a positive effect on mesenchymal stem cell numbers and differentiation potential. A larger, more controlled study with a longer follow up and data on bone architecture would be required to come to an appropriate conclusion on the rescue effects of bone marrow transplantation.

An interesting and intriguing observation is that despite of their accelerated aging, TTD mice ultimately maintained a low but stable cortical and trabecular bone volume for an extended period of time. These levels coincide with the levels of bone volume that are reached in wild type mice at a very old age. This indicates that with aging mice are apparently able to maintain a minimum level of bone volume, needed to remain mobile and alive. Whether this holds for other vertebrates remains to be assessed. Despite maintenance of a bare minimum of bone volume to be at least mobile, bone strength is severely compromised. This is in line with observations in other vertebrates, for example humans. In humans this is accompanied by an increased fracture risk, which at older age is linked to increased mortality.

Periosteal apposition

Periosteal apposition, or radial bone growth, is an essential mechanism to maintain bone strength at a later age when endosteal bone formation rates decline and endosteal resorption continues at a regular rate. The lack of periosteal apposition and ongoing endosteal resorption in older male and female TTD mice is a major contributor to the observed decrease in bone strength. Since periosteal apposition is regulated by sex steroids it is tempting to speculate about their role in the observed lack of periosteal apposition [52,53]. As mentioned above, preliminary results show a decrease in estradiol levels in female TTD mice. Using TTD mice as a model system, detailed research into changes in hormone levels and their effects on radial bone growth could provide us with more decisive insights into the mechanisms underlying the regulation of periosteal apposition.

Many questions concerning the effects of defective DNA repair on skeletal aging still remain. In direct relation to our hypothesis it will be of great value to truly visualize and compare the amount of DNA damage as well as the rate of apoptosis in wild type and TTD MSCs. However this is still hampered by some technical limitations. For example, isolating a pure MSC population is currently impossible due to a lack of MSC specific markers. There are however techniques that utilize marker specificity and adherence properties to isolate MSC-like cell populations. Such a pool of MSC-like cells could be used to gather more information, especially concerning apoptosis rates. Also, direct measurement of DNA damage in cells, including MSCs, is currently not possible. A method that could measure spontaneous or induced DNA damage rates in MSCs, would provide us with direct proof that defective DNA repair does indeed lead to an increase in DNA damage, which might

increase throughout the live of a mouse.

Bone formation is an energy-demanding process that requires a high cell metabolism in order to produce all necessary bone matrix components and eventual mineralization. Changes in metabolism can affect ROS production and will have an effect on the amount of damage that will be caused. This suggests that TTD osteoblasts might be more susceptible to accelerated aging than other tissues, which is supported by the observed segmental aging of tissues in TTD mice [38]. As discussed in chapter 2, low oxygen tension lowers cell metabolism and ROS levels, which leads to a reduction in prospective DNA damage and a decrease in osteoblast apoptosis. In relation to this work, it might be interesting to investigate the effects of low oxygen tension on the data gathered from *in vitro* TTD MSC cultures. Low oxygen tension may positively affect bone nodule formation by TTD MSCs, although low oxygen tension inhibits matrix formation and mineralization [54]. These type of experiments are needed to take the current observations further and to tie together the potential mechanisms, the involvement of oxygen, ROS and energy metabolism put forward by our current studies.

In conclusion, we hypothesize that defective DNA repair leads to the accumulation of DNA damage in MSCs. Once this DNA damage reaches critical conditions, cells will undergo apoptosis or cellular senescence. This will lead to a reduction of the available osteoblast precursor pool and a subsequent decline in bone formation. Our findings support this theory and strongly indicate that the remaining precursors are capable of osteoblast differentiation and bone formation *in vitro* (MSC cultures) and *in vivo* (increased cortical thickness after PTH treatment (chapter 4, Figure 6D) when the correct differentiation cues are available. Finally, these findings indicate that there is an interplay between intrinsic (accumulating intracellular damage) and extrinsic (absence of circulating hormones or growth factors) factors that cause the observed phenotype of accelerated skeletal aging.

Final remarks

In conclusion, we have gathered valuable new information on the effects of oxygen tension, oxidative stress and defective DNA repair on osteoblast differentiation, bone formation and skeletal aging. The low oxygen tension studies demonstrated that variation in oxygen tension strongly affects gene expression in differentiating osteoblasts in a differentiation stage dependent manner. The pre-mineralization stage is most sensitive to changes in oxygen tension. Cell culture experiments and unbiased gene expression analysis showed that inhibition of osteoblast differentiation and mineralization by low oxygen tension is achieved by regulating two processes in the osteoblasts. First, a change in oxygen tension leads to a change in the osteoblast energy metabolism by changing the expression levels of genes and the biological processes they are involved in, e.g. glycolysis and the hexose metabolism. These findings underline the significance of these processes for the energy demanding osteoblast differentiation and bone formation. Secondly, low oxygen tension affects the expression levels of extracellular matrix proteins and matrix modification proteins. The analysis identified genes and processes that target and control optimal osteoblast differentiation and bone formation in situations of changing oxygen tension. These provide new insights and leads for research in the fields of fracture repair and regenerative medicine, both of which have to deal with changing oxygen environments.

Chapter 6

Deficient DNA repair leads to an increased and accelerated decrease in bone mass in TTD mice. This is a feature of premature aging and implies that the other aging-like features observed in TTD mice and patients may also represent *bona fide* premature aging symptoms. In a broader context this substantiates the importance of DNA repair in healthy aging. The obtained results support furthermore that TTD mice can be used as a valid model for bone aging. Especially the absence of periosteal apposition provides an excellent starting point for the identification of new targets that are of importance to maintain bone strength while aging. In addition, TTD mice can provide valuable *in vivo* information on the influence of a number of systemic factors on osteoblast differentiation and bone formation.

Chapter 6

References

1. Martin GM (2005) Genetic engineering of mice to test the oxidative damage theory of aging. Ann N Y Acad Sci 1055: 26-34.
2. Balaban RS, Nemoto S, Finkel T (2005) Mitochondria, oxidants, and aging. Cell 120: 483-495.
3. Finkel T, Holbrook NJ (2000) Oxidants, oxidative stress and the biology of ageing. Nature 408: 239-247.
4. Giorgio M, Trinei M, Migliaccio E, Pelicci PG (2007) Hydrogen peroxide: a metabolic by-product or a common mediator of ageing signals? Nat Rev Mol Cell Biol 8: 722-728.
5. Almeida M, Han L, Martin-Millan M, Plotkin LI, Stewart SA, et al. (2007) Skeletal involution by age-associated oxidative stress and its acceleration by loss of sex steroids. J Biol Chem 282: 27285-27297.
6. Turrens JF (1997) Superoxide production by the mitochondrial respiratory chain. Biosci Rep 17: 3-8.
7. Chen CT, Shih YR, Kuo TK, Lee OK, Wei YH (2008) Coordinated changes of mitochondrial biogenesis and antioxidant enzymes during osteogenic differentiation of human mesenchymal stem cells. Stem Cells 26: 960-968.
8. Komarova SV, Ataullakhanov FI, Globus RK (2000) Bioenergetics and mitochondrial transmembrane potential during differentiation of cultured osteoblasts. Am J Physiol Cell Physiol 279: C1220-1229.
9. D'Ippolito G, Diabira S, Howard GA, Roos BA, Schiller PC (2006) Low oxygen tension inhibits osteogenic differentiation and enhances stemness of human MIAMI cells. Bone 39: 513-522.
10. Nemoto S, Takeda K, Yu ZX, Ferrans VJ, Finkel T (2000) Role for mitochondrial oxidants as regulators of cellular metabolism. Mol Cell Biol 20: 7311-7318.
11. Chow DC, Wenning LA, Miller WM, Papoutsakis ET (2001) Modeling pO(2) distributions in the bone marrow hematopoietic compartment. II. Modified Kroghian models. Biophys J 81: 685-696.
12. Chow DC, Wenning LA, Miller WM, Papoutsakis ET (2001) Modeling pO(2) distributions in the bone marrow hematopoietic compartment. I. Krogh's model. Biophys J 81: 675-684.
13. Harrison JS, Rameshwar P, Chang V, Bandari P (2002) Oxygen saturation in the bone marrow of healthy volunteers. Blood 99: 394.
14. Brighton CT, Krebs AG (1972) Oxygen tension of healing fractures in the rabbit. J Bone Joint Surg Am 54: 323-332.
15. Lu C, Rollins M, Hou H, Swartz HM, Hopf H, et al. (2008) Tibial fracture decreases oxygen levels at the site of injury. Iowa Orthop J 28: 14-21.
16. Yoon SJ, Park KS, Kim MS, Rhee JM, Khang G, et al. (2007) Repair of diaphyseal bone defects with calcitriol-loaded PLGA scaffolds and marrow stromal cells. Tissue Eng 13: 1125-1133.
17. Salim A, Nacamuli RP, Morgan EF, Giaccia AJ, Longaker MT (2004) Transient changes in oxygen tension inhibit osteogenic differentiation and Runx2 expression in osteoblasts. J Biol Chem 279: 40007-40016.
18. Giannelli G, Falk-Marzillier J, Schiraldi O, Stetler-Stevenson WG, Quaranta V (1997) Induction of cell migration by matrix metalloprotease-2 cleavage of laminin-5. Science 277: 225-228.
19. Petitclerc E, Stromblad S, von Schalscha TL, Mitjans F, Piulats J, et al. (1999) Integrin alpha(v)beta3 promotes M21 melanoma growth in human skin by regulating tumor cell survival. Cancer Res 59: 2724-2730.
20. Alexander CM, Selvarajan S, Mudgett J, Werb Z (2001) Stromelysin-1 regulates adipogenesis during mammary gland involution. J Cell Biol 152: 693-703.
21. Lochter A, Galosy S, Muschler J, Freedman N, Werb Z, et al. (1997) Matrix metalloproteinase stromelysin-1 triggers a cascade of molecular alterations that leads to stable epithelial-to-mesenchymal conversion and a premalignant phenotype in mammary epithelial cells. J Cell Biol 139: 1861-1872.
22. Holmbeck K, Bianco P, Caterina J, Yamada S, Kromer M, et al. (1999) MT1-MMP-deficient mice develop dwarfism, osteopenia, arthritis, and connective tissue disease due to inadequate collagen turnover. Cell 99: 81-92.
23. Mosig RA, Dowling O, DiFeo A, Ramirez MC, Parker IC, et al. (2007) Loss of MMP-2 disrupts skeletal and craniofacial development and results in decreased bone mineralization, joint erosion and defects in osteoblast and osteoclast growth. Hum Mol Genet 16: 1113-1123.
24. Stickens D, Behonick DJ, Ortega N, Heyer B, Hartenstein B, et al. (2004) Altered endochondral bone development in matrix metalloproteinase 13-deficient mice. Development 131: 5883-5895.

Chapter 6

25. Zhou Z, Apte SS, Soininen R, Cao R, Baaklini GY, et al. (2000) Impaired endochondral ossification and angiogenesis in mice deficient in membrane-type matrix metalloproteinase I. Proc Natl Acad Sci U S A 97: 4052-4057.

26. Martignetti JA, Aqeel AA, Sewairi WA, Boumah CE, Kambouris M, et al. (2001) Mutation of the matrix metalloproteinase 2 gene (MMP2) causes a multicentric osteolysis and arthritis syndrome. Nat Genet 28: 261-265.

27. Willenbrock F, Murphy G (1994) Structure-function relationships in the tissue inhibitors of metalloproteinases. Am J Respir Crit Care Med 150: S165-170.

28. Butler GS, Butler MJ, Atkinson SJ, Will H, Tamura T, et al. (1998) The TIMP2 membrane type 1 metalloproteinase "receptor" regulates the concentration and efficient activation of progelatinase A. A kinetic study. J Biol Chem 273: 871-880.

29. Strongin AY, Collier I, Bannikov G, Marmer BL, Grant GA, et al. (1995) Mechanism of cell surface activation of 72-kDa type IV collagenase. Isolation of the activated form of the membrane metalloprotease. J Biol Chem 270: 5331-5338.

30. Gomez DE, Alonso DF, Yoshiji H, Thorgeirsson UP (1997) Tissue inhibitors of metalloproteinases: structure, regulation and biological functions. Eur J Cell Biol 74: 111-122.

31. Yuan LQ, Liu YS, Luo XH, Guo LJ, Xie H, et al. (2008) Recombinant tissue metalloproteinase inhibitor-3 protein induces apoptosis of murine osteoblast MC3T3-E1. Amino Acids 35: 123-127.

32. Discher DE, Janmey P, Wang YL (2005) Tissue cells feel and respond to the stiffness of their substrate. Science 310: 1139-1143.

33. Discher DE, Mooney DJ, Zandstra PW (2009) Growth factors, matrices, and forces combine and control stem cells. Science 324: 1673-1677.

34. Bruedigam C, Eijken M, Koedam M, van de Peppel J, Drabek K, et al. (2010) A new concept underlying stem cell lineage skewing that explains the detrimental effects of thiazolidinediones on bone. Stem Cells 28: 916-927.

35. Wernike E, Li Z, Alini M, Grad S (2008) Effect of reduced oxygen tension and long-term mechanical stimulation on chondrocyte-polymer constructs. Cell Tissue Res 331: 473-483.

36. Hofbauer KH, Gess B, Lohaus C, Meyer HE, Katschinski D, et al. (2003) Oxygen tension regulates the expression of a group of procollagen hydroxylases. Eur J Biochem 270: 4515-4522.

37. Wang Y, Wan C, Gilbert SR, Clemens TL (2007) Oxygen sensing and osteogenesis. Ann N Y Acad Sci 1117: 1-11.

38. de Boer J, Andressoo JO, de Wit J, Huijmans J, Beems RB, et al. (2002) Premature aging in mice deficient in DNA repair and transcription. Science 296: 1276-1279.

39. Wijnhoven SW, Beems RB, Roodbergen M, van den Berg J, Lohman PH, et al. (2005) Accelerated aging pathology in ad libitum fed Xpd(TTD) mice is accompanied by features suggestive of caloric restriction. DNA Repair (Amst) 4: 1314-1324.

40. Glatt V, Canalis E, Stadmeyer L, Bouxsein ML (2007) Age-related changes in trabecular architecture differ in female and male C57BL/6J mice. J Bone Miner Res 22: 1197-1207.

41. Banfi A, Muraglia A, Dozin B, Mastrogiacomo M, Cancedda R, et al. (2000) Proliferation kinetics and differentiation potential of ex vivo expanded human bone marrow stromal cells: Implications for their use in cell therapy. Exp Hematol 28: 707-715.

42. Digirolamo CM, Stokes D, Colter D, Phinney DG, Class R, et al. (1999) Propagation and senescence of human marrow stromal cells in culture: a simple colony-forming assay identifies samples with the greatest potential to propagate and differentiate. Br J Haematol 107: 275-281.

43. Stenderup K, Justesen J, Clausen C, Kassem M (2003) Aging is associated with decreased maximal life span and accelerated senescence of bone marrow stromal cells. Bone 33: 919-926.

44. Stolzing A, Scutt A (2006) Age-related impairment of mesenchymal progenitor cell function. Aging Cell 5: 213-224.

45. Zhang DY, Wang HJ, Tan YZ (2011) Wnt/beta-catenin signaling induces the aging of mesenchymal stem cells through the DNA damage response and the p53/p21 pathway. PLoS One 6: e21397.

46. Jilka RL, Weinstein RS, Bellido T, Roberson P, Parfitt AM, et al. (1999) Increased bone formation by prevention of osteoblast apoptosis with parathyroid hormone. J Clin Invest 104: 439-446.

47. Riggs BL (2002) Endocrine causes of age-related bone loss and osteoporosis. Novartis Found Symp 242: 247-259; discussion 260-244.

48. Perrini S, Laviola L, Carreira MC, Cignarelli A, Natalicchio A, et al. (2010) The GH/IGF1 axis and signaling pathways in the muscle and bone: mechanisms underlying age-related skeletal muscle wasting

and osteoporosis. J Endocrinol 205: 201-210.

49. van der Velde M, van der Eerden BC, Sun Y, Almering JM, van der Lely AJ, et al. (2012) An Age-Dependent Interaction with Leptin Unmasks Ghrelin's Bone-Protective Effects. Endocrinology 153: 3593-3602.

50. Leininger GM (2009) Location, location, location: the CNS sites of leptin action dictate its regulation of homeostatic and hedonic pathways. Int J Obes (Lond) 33 Suppl 2: S14-17.

51. van der Pluijm I, Garinis GA, Brandt RM, Gorgels TG, Wijnhoven SW, et al. (2007) Impaired genome maintenance suppresses the growth hormone–insulin-like growth factor 1 axis in mice with Cockayne syndrome. PLoS Biol 5: e2.

52. Riggs BL, Khosla S, Melton LJ, 3rd (2002) Sex steroids and the construction and conservation of the adult skeleton. Endocr Rev 23: 279-302.

53. Turner RT, Colvard DS, Spelsberg TC (1990) Estrogen inhibition of periosteal bone formation in rat long bones: down-regulation of gene expression for bone matrix proteins. Endocrinology 127: 1346-1351.

54. Fehrer C, Brunauer R, Laschober G, Unterluggauer H, Reitinger S, et al. (2007) Reduced oxygen tension attenuates differentiation capacity of human mesenchymal stem cells and prolongs their lifespan. Aging Cell 6: 745-757.

Chapter 6

CHAPTER 7

SUMMARY/SAMENVATTING

ABBREVIATION INDEX

SUPPLEMENTARY DATA
ACKNOWLEDGEMENTS

PhD PORTOFOLIO

CURRICULUM VITAE

PUBLICATIONS

Chapter 7

Summary

With an ever increasing average age of the world population, age related disorders become more frequent and take up an increasing part of the health care related costs. One of these age-related disorders is osteoporosis, which manifests as a decrease in bone mineral density and an increase in fracture risk, which in the long run lead to an increase in morbidity.

The free radical theory of aging states that organisms and their tissues because cells accumulate free radical induced damage to their DNA and proteins over time. Taking this theory as a starting point, we set out to study a number of parameters that could possibly affect the amount of damage that accumulates in bone cells and influence the rate of skeletal aging.

In **chapter 2** the effects of low oxygen tension on bone formation and matrix mineralization were studied. Low oxygen tension cultures (i.e. 2% oxygen) mimic the physiologic state of the cells in the body more accurately than the more commonly used 20% oxygen cultures. In our SV-HFO pre-osteoblast cell line, low oxygen tension inhibits osteoblast differentiation and mineralization, but also lowers the amount of ROS present in the cells, protecting the osteoblasts against oxidative damage and significantly reducing osteoblast apoptosis. In addition, the defense mechanisms that protect the cells against oxidative stress are downregulated, leaving them more susceptible to unexpected oxidative stress. Last, but not least, low oxygen tension has an effect on the expression of a number of matrix modification proteins. This suggests that the matrix produced under low oxygen tension might have a different composition than the mineralizing matrix found in cells cultured under 20% oxygen.

Since the expression levels of many of the genes studied in **chapter 2** were affected by a switch in oxygen tension, global gene expression profiling studies were performed as described in **chapter 3**, comparing cells cultured under 20% oxygen with those cultured on 2% oxygen. The changes in gene expression in each of the three predetermined differentiation stages were studied to determine which of the phases is most susceptible to 2% oxygen. The highest number of differentially regulated probes was found in phase 2, the pre-mineralization phase. Further analysis into the processes and functions behind the differentially regulated probes indicated that low oxygen tension affects osteoblast differentiation and matrix mineralization in two ways. First, they affect cell metabolism, lowering the metabolic state of the osteoblasts which drives them towards staying in an undifferentiated state. Secondly low oxygen tension changes the expression levels of genes involved in collagen matrix production and modification. Collagen expression and modification are severely affected by changes in oxygen tension. This fits with the results obtained in **chapter 2**.

In **chapters 4 and 5**, we moved away from cell lines and studied *in vivo* bone formation in DNA repair defective TTD mice. TTD is a rare autosomal recessive nucleotide excision repair disorder, caused by a mutation in XPD, a component of the basal transcription factor TFIIH, which is a major component of the nucleotide excision repair pathway. TTD mice, carrying a patient based mutation, resemble many of the features observed in the human TTD syndrome, including a range of skeletal abnormalities. The results, obtained

in female (**chapter 4**) and male (**chapter 5**) mice, display an accelerated skeletal aging, due to defective DNA repair. Both male and female mice undergo accelerated bone loss, affecting both cortical and trabecular bone. This loss in bone volume goes accompanied by a decrease in bone strength and a lack of periosteal apposition. When comparing wild type and TTD *in vitro* bone marrow cultures, we observed an age-related decrease in bone nodule formation, which was accelerated in TTD mice. Adipocyte differentiation was not affected *in vitro*. This is remarkable, since TTD mice display a severe lack of body fat. In conclusion, these data suggest that defective DNA repair leads to an increase in oxidative damage that leads to a decrease in the number of mesenchymal stem cells and a subsequent decrease in bone formation. In addition, the absence of the necessary systemic factors to drive osteoblast and adipocyte differentiation also contributes to the observed TTD phenotype.

In conclusion, oxygen tension plays an important role in regulating osteoblast cell metabolism, the production of ROS and protection against oxidative damage. While low oxygen tension inhibits osteoblast differentiation and mineralization, it also more accurately mimics physiologic circumstance in our bodies. Results might be of interest to the fields of fracture healing and MSC based tissue repair in which cells are exposed to very low concentrations of oxygen and still have to form bone. Defective DNA repair leads to accelerated skeletal aging in both male and female TTD mice. An accumulation of damage leads to a decrease in bone volume and strength as a result of a reduction in the number of MSCs present in the bone marrow of DNA repair deficient mice. TTD mice displayed a number of skeletal abnormalities, including a severe lack of periosteal apposition, which makes them an excellent tool to study the regulatory mechanisms that underlie bone formation and skeletal aging. Finally, the results obtained with the TTD mouse model underline the importance of optimal DNA repair for healthy aging and the maintenance of bone strength.

Chapter 7

Samenvatting

De afgelopen decennia is de gemiddelde leeftijd van de wereldbevolking gestaag gestegen. Een van de gevolgen van een steeds ouder wordende populatie is een groei in het aantal mensen dat leidt aan een verouderingssyndroom en de steeds groter wordende financiële last die dat met zich mee brengt. Eén van deze syndromen is osteoporose, in de volksmond beter bekend als botontkalking. Osteoporose wordt gekenmerkt door een verlaging van de mineraaldichtheid van het bot en een verhoogd risico op botbreuken, in het bijzonder in de heup, pols en wervelkolom.

De vrije radicalen theorie stelt dat veroudering wordt veroorzaakt doordat de cellen in ons lichaam gedurende het leven schade aan eiwitten en DNA ophopen. Deze schade wordt veroorzaakt door vrije radicalen die worden geproduceerd door de cellen zelf. Een groot deel van deze schade wordt meteen gerepareerd, maar gedurende het leven verzamelt een cel toch de nodige beschadigde eiwitten en DNA moleculen waardoor de cellen uiteindelijk gedwongen worden om dood te gaan. Dit kan dan op latere leeftijd leiden tot orgaanfalen en de dood van een organisme. Met deze theorie als uitgangspunt is in dit proefschrift onderzoek gedaan naar een aantal factoren dat de hoeveelheid schade in botcellen kan beperken en zodoende botveroudering zou kunnen vertragen.

In **hoofdstuk 2** zijn de effecten van lage zuurstofspanning op botvorming en matrixmineralisatie bestudeerd. Normaal gesproken is de zuurstofspanning voor celkweken 20%. Een lage zuurstofspanning (in dit geval 2% zuurstof)benadert de fysiologische condities waarin botcellen zich in ons lichaam bevinden echter veel beter. In SV-HFO pre-osteoblasten leidt een lage zuurstofspanning tot een vertraagde osteoblast differentiatie en matrixmineralisatie, een verlaging van het aantal te detecteren vrije radicalen en een vermindering in osteoblast apoptose. Verder wordt er een vermindering in de bescherming tegen vrije radicalen waargenomen, waardoor de cellen uiteindelijk vatbaarder zijn voor schade veroorzaakt door onverwachte externe stimuli. Als laatste zijn er een aantal veranderingen waargenomen in de expressiepatronen van een aantal genen die matrixmodificatie eiwitten coderen. Dit suggereert dat de opbouw van de botmatrix die in lage zuurstofkweken wordt geproduceerd anders is dan die van de botmatrix die bij 20% zuurstof wordt geproduceerd.

Naar aanleiding van de waargenomen veranderingen in genexpressie in **hoofdstuk 2**, is er verder onderzoek gedaan naar het effect van lage zuurstof op de genexpressie van osteoblasten met behulp van micro-array expressie analyse. De resultaten van deze analyse, waarin lage en hoge zuurstofkweken met elkaar vergeleken worden, staan beschreven in **hoofdstuk 3**. Een van de doelstellingen was om te bepalen welke van de drie bekende differentiatiestadia het meest vatbaar is voor veranderingen veroorzaakt door een daling in zuurstofspanning. Het grootste aantal differentieel gereguleerde probes werd gevonden in het tweede differentiatiestadium, de pre-mineralisatie fase. Verdere analyse van de data leverde een aantal belangrijke biologische processen en functies op die beïnvloed worden door de verlaging van de zuurstofspanning. Aan de hand van deze analyses werd geconcludeerd dat een lage zuurstofspanning osteoblastdifferentiatie op twee manieren beïnvloed. Om te beginnen verlaagd een lage zuurstofspanning het celmetabolisme waardoor de cellen hun pre-differentiatiestatus behouden. Vervolgens

beïnvloedt lage zuurstofspanning de productie van een aantal matrixcomponenten, waaronder een groot aantal collagenen en de productie van eiwitten die collagenen in de matrix kunnen modificeren. Zowel collageenproductie als collageenmodificatie wordt dan ook sterk beïnvloed door een lage zuurstofspanning. Dit komt overeen met de resultaten met betrekking tot matrixcompositie beschreven in **hoofdstuk 2**.

In **hoofdstuk 4 en 5** word vervolgens overgegaan van het bestuderen van cellijnen op het bestuderen van *in vivo* botvorming in muizen met een defect DNA-reparatiemechanisme, zogenaamde TTD muizen. TTD is een zeldzaam autosomaal recessief syndroom, veroorzaakt door een mutatie in XPD, een component van het basale TFIIH transcriptiefactorcomplex dat een belangrijke rol speelt in DNA reparatie. De TTD muizen dragen een bestaande mutatie in hun XPD gen - gekopieerd uit een patiënt - en vertonen een groot aantal aan het syndroom gerelateerde kenmerken waaronder een aantal botafwijkingen. De resultaten, die zijn behaald in vrouwelijke (**hoofdstuk 4**) en mannelijke (**hoofdstuk 5**) muizen, tonen aan dat er sprake is van een versnelde botveroudering als gevolg van het defecte DNA-reparatiemechanisme. Er is een versnelde afname in trabeculair en corticaal bot in TTD mannetjes en vrouwtjes en dit gaat gepaard met een verlies in botsterkte en een complete afwezigheid van periostale appositie. Vergelijking van mesenchymale stamcelkweken uit het beenmerg van TTD en controle muizen toont aan dat er een leeftijdsafhankelijke afname in botkolonieformatie optreedt, die versnelt plaatsvindt in het beenmerg van TTD muizen. *In vitro* vetcel productie is opmerkelijker wijs niet aangedaan, ondanks het feit dat TTD muizen *in vivo* bijna geen vetcellen produceren. Deze data suggereren dat een defectief DNA-reparatiemechanisme leidt tot een toename in oxidatieve schade, die op zijn beurt weer leidt tot een afname in het aantal mesenchymale stamcellen en de hoeveelheid bot die uiteindelijk geproduceerd kan worden. Verder lijkt er ook nog een rol weggelegd voor een aantal, in TTD muizen ontbrekende, circulerende factoren die normaalgesproken het differentiatieproces reguleren.

Uit de resultaten, besproken in dit proefschrift, valt te concluderen dat zuurstofspanning een belangrijke rol speelt in de regulatie van het celmetabolisme, de productie van vrije radicalen en de bescherming tegen oxidatieve schade. De onder lage zuurstofspanning verkregen resultaten geven een beter inzicht in de processen die zich afspelen in ons lichaam tijdens botvorming. Aangezien de zuurstofspanning bij een botbreuk bijvoorbeeld erg laag is, kunnen deze resultaten ook makkelijk toegepast worden in andere onderzoeksgebieden. Verder wordt er aangetoond dat een defectief DNA-reparatiemechanisme kan leiden tot een versnelde botveroudering. Ophoping van oxidatieve schade leidt tot een afname in het botvolume en de botsterkte van TTD muizen als gevolg van een afname in het aantal mesenchymale stamcellen in het beenmerg dat botcellen kan vormen. TTD muizen lijken verder een zeer geschikt onderzoeksmiddel om de regulatie van botvorming en botresorptie gedurende het leven te bestuderen.

Chapter 7

List of abbreviations

$1,25(OH)_2D_3$	1,25-dihydroxyvitamin D_3
6-4PP	Pyrimidine-(6,4)-pyrimidine adducts
8-oxodG	8-oxo-2′-deoxyguanosine
ADP	Adenosine diphosphate
ALP	Alkaline phosphatase
ATP	Adenosine triphosphate
BCL2	B-cell lymphoma 2
BER	Base excision repair
BGLAP	Osteocalcin
BMD	Bone mineral density
BMU	Bone multicellular unit
C57Bl/6	C57 black 6
CAT	Catalase
COL1A1	Collagen 1α1
CPD	Cyclobutane pyrimidine dimers
CX43	Connexin 43
DMP1	Dentin matrix acidic phosphoprotein 1
DNA	Deoxy ribonucleic acid
ECM	Extracellular matrix
ER	Estrogen receptor
ERCC1	DNA excision repair protein ERCC-1
FGF23	Fibroblast growth factor 23
FoxO	Forkhead box protein O
GGR	Global genome repair
GH	Growth hormone
GHRH	Growth hormone releasing hormone
GPX	Glutathione peroxidase
H_2O	Water
H_2O_2	Hydrogen peroxide
hHR23B	UV excision repair protein RAD23 homolog B
HIF1α	Hypoxia inducible factor 1α
HSC	Hematopoietic stem cells
IGF	Insuline-like growth factor
JNK	c-Jun terminal kinase
MAPK	Mitogen activated protein kinase
MEPE	Matrix extracellular phosphoglycoprotein
MMP2	Matrix metalloproteinase 2
MSC	Mesenchymal stem cell
NCP	Non -collagenous protein
NER	Nucleotide Excision Repair

OPG	Osteoprotegerin
PTH	Parathyroid hormone
RANK	Receptor activator of nuclear Factor κ B
RANKL	Receptor activator of nuclear factor kappa-B ligand
RNA	Ribonucleic acid
ROS	Reactive oxygen species
RUNX2	Runt-related transcription factor 2
SOD	Superoxide dismutase
SOST	Sclerostin
SPP1	Bone sialoprotein
TCR	Transcription coupled repair
TFIIH	Transcription factor II H complex
TTD	Trichothiodystrophy
TTDN1	TTD non-photosensitive 1 protein
UV	Ultraviolet
VEGF	Vascular endothelial growth factor
VHL	Von Hippel-Lindau tumor suppressor
XPA	Xeroderma pigmentosum complementation group A
XPB	Xeroderma pigmentosum complementation group B
XPC	Xeroderma pigmentosum complementation group C
XPD	Xeroderma pigmentosum complementation group D
XPG	Xeroderma pigmentosum complementation group G

Chapter 7

Supplementary Data

CHAPTER 1

phase 1
phase 2
phase 3

Column 1	Column 2	Column 3	Column 4
DKFZP451A211	ERRFI1	LPP	GYS1
EDN1	PGK1	C5ORF13	WSB1
NPIP	BCAR3	GAPDH	TMEM45A
CORIN	COBLL1	LIMS2	BNIP3L
FSCN1	ENO2	DLGAP4	AK3L1
ACTG2	FLJ14213	COL11A1	LOC731007
OXTR	P4HA2	WSB1	PLOD2
ADAM19	PAM	HS.560343	HK2
ITGA5	ALDOC	MUC1	HS.296031
MYADM	SLC2A1	HS.388347	INSIG2
GOLGA8B	IRS2	SYDE1	C3ORF58
COL8A1	GPI	YEATS2	NDRG1
ING2	HS.36053	CRYAB	VLDLR
RPESP	ALDOA	EFHD1	TMEM45A
C13ORF15	TAGLN	FAT	BHLHB2
LOC387882	ADARB1	CYTH3	PFKL
THBS1	RFNG	THBS2	PGAM1
COL4A1	TMEM178	SLC6A10P	NFIL3
KIAA0363	IGFBP3	NUAK1	ERO1L
COL1A1	NGF	PLOD1	STC1
COL4A2	FGF11	MUC1	PFKP
LEPR	RASSF7	PPP1R13L	LOC732165
PXDN	SELO	RUNX3	TBC1D9B
C1ORF198	FAM162A	DPYSL4	TGFBI
COL5A1	HS.10862	NTF3	INHBB
AHNAK	LBH	ACTA2	C10ORF10
TUBB2B	ALDOA	SLC16A3	TIGA1
ACTA1	HS.5724	PKD2	CLEC3B
SF3A2	PGM1	SPOCK1	ZNF581
COL1A2	PPFIA4	FSTL3	H19
PPP1R14A	ADARB1	HSPB2	PCTK3
FSTL1	MAPK7	NOG	TCEA3
HNRPDL	PBX3	NPAS1	HS.34447
COL1A2	PFKFB3	JAM2	PLEKHG3
TGFB1I1	AFAP1L1	NUAK1	NOPE
CYB5R3	IGFBP3	RNASE4	TSC22D3
GADD45B	LEP	RAB11FIP1	TSC22D3
PTPRF	MEX3B	DLK2	C7ORF10
RAB11FIP5	CA9	GREM1	DDIT4
TGFB1I1	P4HA2	HCFC1R1	CA12
BNIP3	LOX	ANKRD37	PPP1R3C
AK3L1	CHES1	C1ORF51	GBE1
AK3L1	HK2	ANG	LOC401152
PFKFB4	RORA	ID2	WFDC3
LOC644774	LIMCH1	FAM119B	WFDC3
SLC2A3	P4HA1	ID2	NPPB
DENND2A	PGK1	WSB1	SPRY1
TBC1D9B	PLOD2	C5ORF46	SNORD13
LDHA	CRISPLD2	PRKCQ	KLF2
STC2	COL7A1	ZNF395	RHOB
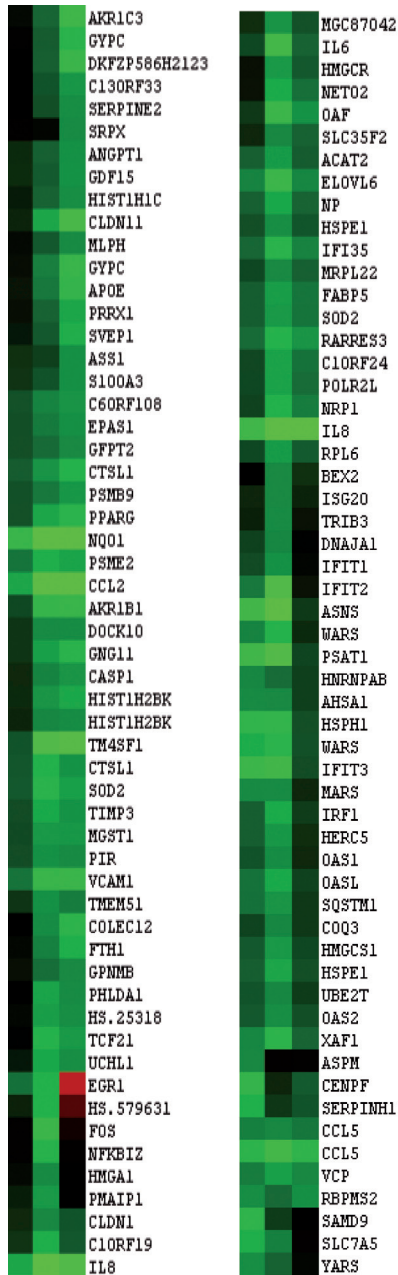
Supplemental Figure 1: *Heatmap of differentially expressed probes from cells continuously cultured under 20% or 2% oxygen.* Depicted are differentially expressed probes of the following comparisons; phase 1 (conditions 7 and 8), phase 2 (comparisons 4 and 6) and phase 3 (conditions 1 and 3). Higher expressed genes in 2% oxygen are depicted in red, lower expressed genes in 2% are depicted in green. Inclusion criteria: logFC >2 and q < 0,01.

Chapter 7

Subset 2	Subset 3	Subset 4
BNIP3	DLK2	DNAJA1
AK3L1	GREM1	IFIT1
AK3L1	HCFC1R1	IFIT2
PFKFB4	ANKRD37	ASNS
LOC644774	C1ORF51	WARS
SLC2A3	ANG	PSAT1
DENND2A	ID2	HNRNPAB
TBC1D9B	FAM119B	AHSA1
LDHA	ID2	HSPH1
STC2	WSB1	WARS
ERRFI1	C5ORF46	IFIT3
PGK1	PRKCQ	MARS
BCAR3	ZNF395	IRF1
COBLL1	GYS1	HERC5
ENO2	WSB1	OAS1
FLJ14213	TMEM45A	OASL
P4HA2	BNIP3L	SQSTM1
PAM	AK3L1	COQ3
ALDOC	LOC731007	HMGCS1
SLC2A1	PLOD2	HSPE1
IRS2	HK2	UBE2T
GPI	HS.296031	OAS2
HS.36053	INSIG2	XAF1
ALDOA	C3ORF58	
TAGLN	NDRG1	
ADARB1	VLDLR	
RFNG	TMEM45A	
TMEM178	BHLHB2	
IGFBP3	PFKL	
NGF	PGAM1	
FGF11	NFIL3	
RASSF7	ERO1L	
SELO	STC1	
FAM162A	PFKP	
HS.10862	LOC732165	
LBH	TBC1D9B	
ALDOA	TGFBI	
HS.5724	INHBB	
PGM1	C10ORF10	
PPFIA4	TIGA1	
ADARB1	CLEC3B	
MAPK7	ZNF581	
PBX3	H19	
PFKFB3	PCTK3	
AFAP1L1	TCEA3	
IGFBP3	HS.34447	
LEP	PLEKHG3	
MEX3B	NOPE	
CA9	TSC22D3	
P4HA2	TSC22D3	
LOX	C7ORF10	
CHES1	DDIT4	
HK2	CA12	
RORA	PPP1R3C	
LIMCH1	GBE1	
P4HA1	LOC401152	
PGK1	WFDC3	
PLOD2	WFDC3	
	NPPB	
	SPRY1	
	SNORD13	

Supplemental Figure 2: *Specific subsets of differentially expressed probes from cells continuously cultured under 20% or 2% oxygen.* Subset 2-3: higher expressed probes, Subset 4: lower expressed probes. For a more detailed description see legend Figure 4.

Phase 1	Phase 2	Phase 3	Overlap	Phase 1 only	Phase 2 only	Phase 3 only
ILMN_1653292	ILMN_1651254	ILMN_1653292	ILMN_1653292	ILMN_1661599	ILMN_1651254	ILMN_1656628
ILMN_1654809	ILMN_1652246	ILMN_1654809	ILMN_1654809	ILMN_1703617	ILMN_1652246	ILMN_1668629
ILMN_1658494	ILMN_1652287	ILMN_1656628	ILMN_1659027	ILMN_1720373	ILMN_1652287	ILMN_1672650
ILMN_1659027	ILMN_1653292	ILMN_1658289	ILMN_1663866	ILMN_1751028	ILMN_1653432	ILMN_1689088
ILMN_1661386	ILMN_1653432	ILMN_1659027	ILMN_1666733	ILMN_1763011	ILMN_1654639	ILMN_1691731
ILMN_1661599	ILMN_1654809	ILMN_1660733	ILMN_1667791	ILMN_1763382	ILMN_1656413	ILMN_1697363
ILMN_1663866	ILMN_1654639	ILMN_1661386	ILMN_1676629	ILMN_1766010	ILMN_1657111	ILMN_1704753
ILMN_1664516	ILMN_1656413	ILMN_1663866	ILMN_1679797	ILMN_1789909	ILMN_1657683	ILMN_1727633
ILMN_1665510	ILMN_1657111	ILMN_1665510	ILMN_1682176	ILMN_1799819	ILMN_1657871	ILMN_1743078
ILMN_1666503	ILMN_1657683	ILMN_1666733	ILMN_1685714	ILMN_1815184	ILMN_1658247	ILMN_1752510
ILMN_1666733	ILMN_1657871	ILMN_1667791	ILMN_1693334	ILMN_2329014	ILMN_1658926	ILMN_1775327
ILMN_1667791	ILMN_1658247	ILMN_1668629	ILMN_1695880	ILMN_2335718	ILMN_1660111	ILMN_1776788
ILMN_1668861	ILMN_1658289	ILMN_1672650	ILMN_1701789		ILMN_1662358	ILMN_1777220
ILMN_1676629	ILMN_1658494	ILMN_1674063	ILMN_1718866		ILMN_1663575	ILMN_1784871
ILMN_1679797	ILMN_1658926	ILMN_1676629	ILMN_1718961		ILMN_1664802	ILMN_1819854
ILMN_1682176	ILMN_1659027	ILMN_1679797	ILMN_1720048		ILMN_1665887	ILMN_2195621
ILMN_1685714	ILMN_1660111	ILMN_1680738	ILMN_1720282		ILMN_1666757	ILMN_2400935
ILMN_1691884	ILMN_1662358	ILMN_1680874	ILMN_1723486		ILMN_1667966	ILMN_2410924
ILMN_1692938	ILMN_1663575	ILMN_1682176	ILMN_1724658		ILMN_1668345	
ILMN_1693334	ILMN_1663866	ILMN_1685714	ILMN_1725139		ILMN_1669390	
ILMN_1695880	ILMN_1664516	ILMN_1689088	ILMN_1726928		ILMN_1669523	
ILMN_1701789	ILMN_1664802	ILMN_1691731	ILMN_1736700		ILMN_1669572	
ILMN_1703617	ILMN_1665887	ILMN_1693334	ILMN_1742618		ILMN_1670037	
ILMN_1707312	ILMN_1666503	ILMN_1695880	ILMN_1744963		ILMN_1671046	
ILMN_1712888	ILMN_1666733	ILMN_1697363	ILMN_1746085		ILMN_1671703	
ILMN_1713037	ILMN_1666757	ILMN_1697491	ILMN_1755749		ILMN_1672350	
ILMN_1718866	ILMN_1667791	ILMN_1701731	ILMN_1755974		ILMN_1674985	
ILMN_1718961	ILMN_1667966	ILMN_1701789	ILMN_1756417		ILMN_1675947	
ILMN_1720048	ILMN_1668345	ILMN_1702301	ILMN_1757877		ILMN_1676728	
ILMN_1720282	ILMN_1668861	ILMN_1704753	ILMN_1758164		ILMN_1676899	
ILMN_1720373	ILMN_1669390	ILMN_1706505	ILMN_1760727		ILMN_1678842	
ILMN_1720998	ILMN_1669523	ILMN_1712998	ILMN_1761260		ILMN_1679093	
ILMN_1723486	ILMN_1669572	ILMN_1713037	ILMN_1764090		ILMN_1679478	
ILMN_1724658	ILMN_1670037	ILMN_1718866	ILMN_1765796		ILMN_1681703	
ILMN_1725139	ILMN_1671046	ILMN_1718961	ILMN_1770922		ILMN_1683792	
ILMN_1726928	ILMN_1671703	ILMN_1720048	ILMN_1772876		ILMN_1684114	
ILMN_1727271	ILMN_1672350	ILMN_1720282	ILMN_1775708		ILMN_1684391	
ILMN_1733421	ILMN_1674063	ILMN_1723486	ILMN_1777499		ILMN_1685763	
ILMN_1736670	ILMN_1674985	ILMN_1724658	ILMN_1779258		ILMN_1687978	
ILMN_1736700	ILMN_1675947	ILMN_1725139	ILMN_1779448		ILMN_1689318	
ILMN_1742618	ILMN_1676629	ILMN_1726928	ILMN_1789507		ILMN_1691097	
ILMN_1744963	ILMN_1676728	ILMN_1727633	ILMN_1789702		ILMN_1691364	
ILMN_1746013	ILMN_1676899	ILMN_1729216	ILMN_1793990		ILMN_1691376	
ILMN_1746085	ILMN_1678842	ILMN_1736700	ILMN_1798249		ILMN_1692219	
ILMN_1747759	ILMN_1679093	ILMN_1739428	ILMN_1800659		ILMN_1692865	
ILMN_1751028	ILMN_1679478	ILMN_1741148	ILMN_1803647		ILMN_1694075	
ILMN_1755749	ILMN_1679797	ILMN_1742618	ILMN_1809931		ILMN_1694140	
ILMN_1755974	ILMN_1680738	ILMN_1743078	ILMN_1827736		ILMN_1698419	
ILMN_1756417	ILMN_1680874	ILMN_1744963	ILMN_1843198		ILMN_1699574	
ILMN_1757877	ILMN_1682176	ILMN_1745374	ILMN_2083469		ILMN_1699651	
ILMN_1758164	ILMN_1683792	ILMN_1746085	ILMN_2098126		ILMN_1699856	
ILMN_1760727	ILMN_1684114	ILMN_1749892	ILMN_2106902		ILMN_1699980	
ILMN_1761260	ILMN_1684391	ILMN_1752510	ILMN_2148527		ILMN_1701308	
ILMN_1763011	ILMN_1685714	ILMN_1755749	ILMN_2148913		ILMN_1701461	
ILMN_1763382	ILMN_1685763	ILMN_1755974	ILMN_2184373		ILMN_1701613	
ILMN_1764090	ILMN_1687978	ILMN_1756417	ILMN_2186061		ILMN_1701875	
ILMN_1765796	ILMN_1689318	ILMN_1757387	ILMN_2207504		ILMN_1702837	
ILMN_1766010	ILMN_1691097	ILMN_1757877	ILMN_2216852		ILMN_1703650	
ILMN_1767556	ILMN_1691364	ILMN_1758164	ILMN_2306903		ILMN_1703791	
ILMN_1768534	ILMN_1691376	ILMN_1760727	ILMN_2313001		ILMN_1707695	
ILMN_1770922	ILMN_1691884	ILMN_1761260	ILMN_2338038		ILMN_1708375	
ILMN_1772876	ILMN_1692219	ILMN_1764090	ILMN_2396875		ILMN_1709623	
ILMN_1775708	ILMN_1692865	ILMN_1765796			ILMN_1710937	
ILMN_1776602	ILMN_1692938	ILMN_1767556			ILMN_1711289	
ILMN_1777499	ILMN_1693334	ILMN_1769787			ILMN_1714587	
ILMN_1779258	ILMN_1694075	ILMN_1770338			ILMN_1715748	
ILMN_1779448	ILMN_1694140	ILMN_1770922			ILMN_1717490	
ILMN_1784110	ILMN_1695880	ILMN_1772876			ILMN_1718182	
ILMN_1789507	ILMN_1697491	ILMN_1775327			ILMN_1718977	
ILMN_1789702	ILMN_1698419	ILMN_1775708			ILMN_1719695	
ILMN_1789909	ILMN_1699574	ILMN_1776602			ILMN_1719938	
ILMN_1793543	ILMN_1699651	ILMN_1776788			ILMN_1723048	
ILMN_1793990	ILMN_1699856	ILMN_1777220			ILMN_1723846	
ILMN_1796417	ILMN_1699980	ILMN_1777499			ILMN_1723912	
ILMN_1797372	ILMN_1701308	ILMN_1779258			ILMN_1724686	
ILMN_1798249	ILMN_1701461	ILMN_1779448			ILMN_1724994	
ILMN_1799139	ILMN_1701613	ILMN_1784871			ILMN_1726327	
ILMN_1799819	ILMN_1701731	ILMN_1786612			ILMN_1726981	
ILMN_1800659	ILMN_1701789	ILMN_1789507			ILMN_1727184	
ILMN_1803647	ILMN_1701875	ILMN_1789702			ILMN_1728570	
ILMN_1805737		ILMN_1792356			ILMN_1729749	
		ILMN_1793990				

ILMN_1807106	ILMN_1702301	ILMN_1795778		ILMN_1730670	
ILMN_1808238	ILMN_1702837	ILMN_1798249		ILMN_1733110	
ILMN_1809931	ILMN_1703650	ILMN_1799139		ILMN_1734486	
ILMN_1814305	ILMN_1703791	ILMN_1800659		ILMN_1734833	
ILMN_1815184	ILMN_1706505	ILMN_1803647		ILMN_1736720	
ILMN_1827736	ILMN_1707312	ILMN_1807106		ILMN_1740415	
ILMN_1839019	ILMN_1707695	ILMN_1808238		ILMN_1740604	
ILMN_1843198	ILMN_1708375	ILMN_1809931		ILMN_1742534	
ILMN_1892403	ILMN_1709623	ILMN_1812995		ILMN_1745242	
ILMN_2051684	ILMN_1710937	ILMN_1819854		ILMN_1745397	
ILMN_2083469	ILMN_1711289	ILMN_1827736		ILMN_1747067	
ILMN_2086095	ILMN_1712888	ILMN_1843198		ILMN_1748124	
ILMN_2098126	ILMN_1712998	ILMN_1892403		ILMN_1751161	
ILMN_2106902	ILMN_1714567	ILMN_2083469		ILMN_1752333	
ILMN_2148527	ILMN_1715748	ILMN_2098126		ILMN_1752968	
ILMN_2148913	ILMN_1717490	ILMN_2106902		ILMN_1754220	
ILMN_2156172	ILMN_1718182	ILMN_2111187		ILMN_1754795	
ILMN_2164373	ILMN_1718666	ILMN_2148527		ILMN_1756992	
ILMN_2186061	ILMN_1718961	ILMN_2148913		ILMN_1760493	
ILMN_2207504	ILMN_1718977	ILMN_2173451		ILMN_1760849	
ILMN_2216852	ILMN_1719695	ILMN_2184373		ILMN_1761247	
ILMN_2308903	ILMN_1719938	ILMN_2186061		ILMN_1761968	
ILMN_2313901	ILMN_1720048	ILMN_2195821		ILMN_1762899	
ILMN_2315979	ILMN_1720282	ILMN_2207504		ILMN_1763260	
ILMN_2329914	ILMN_1720998	ILMN_2216852		ILMN_1763638	
ILMN_2335718	ILMN_1723048	ILMN_2307903		ILMN_1764320	
ILMN_2338038	ILMN_1723486	ILMN_2308903		ILMN_1766595	
ILMN_2361862	ILMN_1723846	ILMN_2313901		ILMN_1773352	
ILMN_2390227	ILMN_1723912	ILMN_2322498		ILMN_1780671	
ILMN_2396875	ILMN_1724658	ILMN_2338038		ILMN_1781373	
	ILMN_1724666	ILMN_2374036		ILMN_1787461	
	ILMN_1724994	ILMN_2376403		ILMN_1788462	
	ILMN_1725139	ILMN_2396875		ILMN_1788547	
	ILMN_1726327	ILMN_2400935		ILMN_1789338	
	ILMN_1726928	ILMN_2410924		ILMN_1789492	
	ILMN_1726981			ILMN_1789627	
	ILMN_1727184			ILMN_1789733	
	ILMN_1727271			ILMN_1790669	
	ILMN_1728570			ILMN_1790741	
	ILMN_1729216			ILMN_1792679	
	ILMN_1729749			ILMN_1795325	
	ILMN_1730670			ILMN_1796339	
	ILMN_1733110			ILMN_1796712	
	ILMN_1733421			ILMN_1796762	
	ILMN_1734486			ILMN_1797001	
	ILMN_1734833			ILMN_1797342	
	ILMN_1736670			ILMN_1797728	
	ILMN_1736700			ILMN_1798081	
	ILMN_1736720			ILMN_1798975	
	ILMN_1739428			ILMN_1802252	
	ILMN_1740415			ILMN_1802380	
	ILMN_1740604			ILMN_1802603	
	ILMN_1741148			ILMN_1804929	
	ILMN_1742534			ILMN_1808707	
	ILMN_1742618			ILMN_1809364	
	ILMN_1744063			ILMN_1810100	
	ILMN_1745242			ILMN_1813314	
	ILMN_1745374			ILMN_1837428	
	ILMN_1745397			ILMN_1844692	
	ILMN_1746013			ILMN_1846922	
	ILMN_1746085			ILMN_1861909	
	ILMN_1747067			ILMN_1898518	
	ILMN_1747759			ILMN_1900156	
	ILMN_1748124			ILMN_2061435	
	ILMN_1749692			ILMN_2079786	
	ILMN_1751161			ILMN_2082209	
	ILMN_1752333			ILMN_2084059	
	ILMN_1752968			ILMN_2099301	
	ILMN_1754220			ILMN_2103547	
	ILMN_1754795			ILMN_2104295	
	ILMN_1755749			ILMN_2130838	
	ILMN_1755974			ILMN_2139396	
	ILMN_1756417			ILMN_2139761	
	ILMN_1756992			ILMN_2146761	
	ILMN_1757387			ILMN_2172174	
	ILMN_1757877			ILMN_2181692	

ILMN_1758164			ILMN_2195482	
ILMN_1760493			ILMN_2196097	
ILMN_1760727			ILMN_2198376	
ILMN_1760849			ILMN_2201678	
ILMN_1761247			ILMN_2211065	
ILMN_1761260			ILMN_2216637	
ILMN_1761968			ILMN_2231928	
ILMN_1762809			ILMN_2234956	
ILMN_1763260			ILMN_2239754	
ILMN_1763638			ILMN_2248970	
ILMN_1764090			ILMN_2294762	
ILMN_1764320			ILMN_2304512	
ILMN_1765796			ILMN_2305407	
ILMN_1767556			ILMN_2308649	
ILMN_1768534			ILMN_2311537	
ILMN_1768595			ILMN_2318011	
ILMN_1769787			ILMN_2318568	
ILMN_1770338			ILMN_2319326	
ILMN_1770922			ILMN_2336781	
ILMN_1772876			ILMN_2337655	
ILMN_1773352			ILMN_2340052	
ILMN_1775708			ILMN_2355168	
ILMN_1776602			ILMN_2363658	
ILMN_1777499			ILMN_2364022	
ILMN_1779258			ILMN_2371911	
ILMN_1779448			ILMN_2375870	
ILMN_1780871			ILMN_2376108	
ILMN_1781373			ILMN_2380163	
ILMN_1784110			ILMN_2381697	
ILMN_1786612			ILMN_2383305	
ILMN_1787461			ILMN_2387553	
ILMN_1788462			ILMN_2389876	
ILMN_1788547			ILMN_2390974	
ILMN_1789338			ILMN_2402392	
ILMN_1789492			ILMN_2404135	
ILMN_1789507			ILMN_2406572	
ILMN_1789627			ILMN_2410826	
ILMN_1789702			ILMN_2415748	
ILMN_1789733				
ILMN_1790689				
ILMN_1790741				
ILMN_1792356				
ILMN_1792879				
ILMN_1793543				
ILMN_1793990				
ILMN_1795325				
ILMN_1795778				
ILMN_1796339				
ILMN_1796417				
ILMN_1796712				
ILMN_1796762				
ILMN_1797001				
ILMN_1797342				
ILMN_1797372				
ILMN_1797728				
ILMN_1798081				
ILMN_1798249				
ILMN_1798975				
ILMN_1800859				
ILMN_1802252				
ILMN_1802380				
ILMN_1802803				
ILMN_1803647				
ILMN_1804929				
ILMN_1805737				
ILMN_1808707				
ILMN_1809364				
ILMN_1809931				
ILMN_1810100				
ILMN_1812995				
ILMN_1813314				
ILMN_1814305				
ILMN_1827738				
ILMN_1837428				
ILMN_1839019				
ILMN_1843198				

Chapter 7

	ILMN_1844692				
	ILMN_1846922				
	ILMN_1881909				
	ILMN_1898518				
	ILMN_1909156				
	ILMN_2051684				
	ILMN_2061435				
	ILMN_2079786				
	ILMN_2082209				
	ILMN_2083469				
	ILMN_2084059				
	ILMN_2086095				
	ILMN_2098126				
	ILMN_2099301				
	ILMN_2103547				
	ILMN_2104295				
	ILMN_2106002				
	ILMN_2111187				
	ILMN_2130638				
	ILMN_2139396				
	ILMN_2139761				
	ILMN_2146761				
	ILMN_2148527				
	ILMN_2148913				
	ILMN_2156172				
	ILMN_2172174				
	ILMN_2173451				
	ILMN_2181692				
	ILMN_2184373				
	ILMN_2186061				
	ILMN_2195482				
	ILMN_2196097				
	ILMN_2196376				
	ILMN_2201676				
	ILMN_2207504				
	ILMN_2211065				
	ILMN_2216637				
	ILMN_2216852				
	ILMN_2231928				
	ILMN_2234956				
	ILMN_2239754				
	ILMN_2248970				
	ILMN_2294762				
	ILMN_2304512				
	ILMN_2305407				
	ILMN_2307903				
	ILMN_2308649				
	ILMN_2308903				
	ILMN_2311537				
	ILMN_2313901				
	ILMN_2315079				
	ILMN_2318011				
	ILMN_2318568				
	ILMN_2319326				
	ILMN_2322498				
	ILMN_2336781				
	ILMN_2337655				
	ILMN_2338038				
	ILMN_2340052				
	ILMN_2355168				
	ILMN_2361602				
	ILMN_2363658				
	ILMN_2364022				
	ILMN_2371911				
	ILMN_2374036				
	ILMN_2375870				
	ILMN_2376108				
	ILMN_2376403				
	ILMN_2380163				
	ILMN_2381697				
	ILMN_2383305				
	ILMN_2387553				
	ILMN_2389876				
	ILMN_2390227				
	ILMN_2390974				
	ILMN_2396875				

ILMN_2402392					
ILMN_2404135					
ILMN_2408572					
ILMN_2410826					
ILMN_2415748					

Supplemental Table 1: *Illumina IDs of probes found to be differentially regulated after a switch from high to low oxygen in phase 1,2 or 3*. Data were used for analysis in Figure 4B and 7. Lane 1-3; complete sets of regulated probes for phase 1, phase 2 and phase 3. Lane 4; overlapping probes, found to be regulated in all three phases. Lane 5-7; phase specific probes found to be specific for respectively phase 1, phase 2 and phase 3.

CHAPTER 5
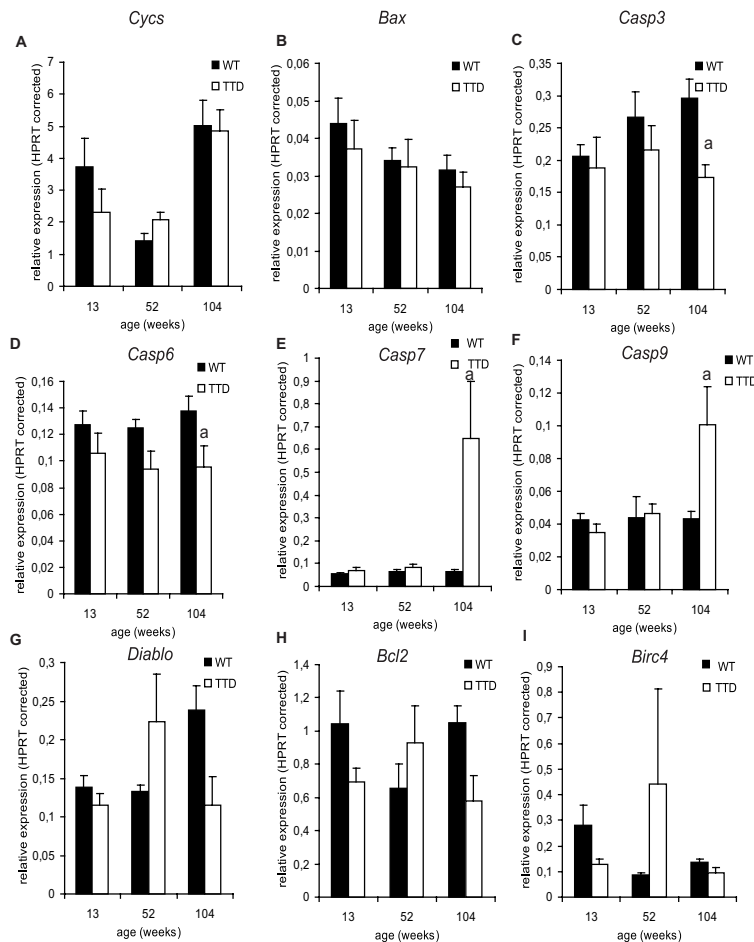
Figure S1: *Expression of apoptosis related genes in wild type and TTD tibiae at various ages.* Expression levels of anti- and pro-apoptotic genes were measured in RNA extracted from tibiae of 13, 52 and 104 week old wild type and TTD mice; (A-G) pro-apoptotic genes; Cycs, Bax, Casp3, Casp6, Casp7, Casp9 and Diablo (H-I) Anti-apoptotic genes; Bcl2 and Birc4. Statistics: student ttest a = $p < 0.05$ wild type vs. TTD.

Chapter 7

Dankwoord

Ik dacht altijd dat dit dankwoord lang voor de rest van dit boekje af zou zijn, zo ergens tegen de tijd dat ik mijn papers af had, maar nog geen zin had om aan mijn introductie te beginnen. Maar soms lopen de dingen anders dan gedacht en zoals wel vaker begin ik gewoon graag aan het begin en eindig ik met het einde.

Ondanks het feit dat het schrijven van een proefschrift uiteindelijk iets is dat je zelf moet doen, is het ontstaan van een proefschrift het werk van vele handen. Zonder velen van jullie had dit eindresultaat er nooit gelegen en aan mij dus de eer om jullie van harte te bedanken.

Ik wil graag beginnen met het bedanken van Hans van Leeuwen, die niet alleen één van mijn promotoren is, maar mij ook van het begin tot het einde begeleid heeft bij dit onderzoek. Beste Hans, ik herinner mij nog goed dat jij tijdens mijn sollicitatiegesprek informeerde of ik ook af en toe eigenwijs kon zijn. Ik antwoordde toen heel diplomatiek dat ik alleen eigenwijs ben als dat nodig is. Ik hoop dat ik mij aan mijn eigen woorden heb gehouden. Bedankt voor alle advies, inzichten en commentaar, maar vooral ook voor je eeuwige optimisme tegenover mijn altijd aanwezige vorm van resultaten pessimisme en het feit dat ik altijd kon en mocht zeggen wat ik ergens van vond.

Ook Jan Hoeijmakers en Bert van der Horst van de afdeling Genetica wil ik graag bedanken voor de goede begeleiding, het advies met betrekking tot de TTD muizen en de snelle commentaren op dit boekje.

Viola en Joep, bedankt dat jullie mijn paranimfen wilden zijn. Nu dat dit boekje af is beloof ik er echt nooit meer over te klagen. Ook jullie moeten straks even op het linkje klikken (zie beneden). Lieve Viola, heel erg bedankt voor de leuke tijd die wij samen hebben gehad in en buiten Rotterdam. Zonder jouw waren de afgelopen vijf jaar niet half zo leuk geweest. En het hielp het afgelopen jaar heel erg mee dat jij een paar weken op mij voorliep en dus alles maar meteen voor twee mensen uitzocht. Er staat straks een fles wijn met onze naam klaar om te toosten op proefschriftvrije jaren. Joep, ondanks het feit dat ik ooit, heel lang geleden, als eerste aan ons ambitieuze PhD avontuur begon, ben ik nou toch nog als laatste klaar. Crikey! Gelukkig hebben we na 13 jaar gedeeld wetenschappelijk leed nog steeds geen Nature paper op onze naam staan. Wat zou er anders wel niet van ons terecht komen. Bedankt voor je altijd effectieve, stress reducerende Amsterdamse perspectief op de zaak, het heerlijke Belgische bier en natuurlijk Kate en Oskar. Jullie gaan gemist worden maar gelukkig heb ze in Australië ook gewoon Skype.

Karin, mijn onderzoek borduurde voort op jouw werk en uiteindelijk hebben we er samen twee papers van weten te maken. Bedankt voor de prettige samenwerking en je snelle reacties wanneer ik data, commentaar of figuren nodig had.

Al mijn collega's op het 'botten' lab; Bram, Marco, Viola, Rodrigo, Martijn, Sander, Yvonne, Nadia, Claudia, Marjolein, Marijke, Bianca, Ksenia, Ruben, Jeroen en al onze studenten, bedankt voor alle gezelligheid en hulp op het lab.

Al mijn andere collega's bij Inwendige Geneeskunde op de vijde verdieping, bedankt

voor jullie vragen en inzichten tijdens de werkbesprekingen, de hulp bij verschillende experimenten en de gezelligheid en goede raad tussen de bedrijven door.

Al mijn collega's bij Genetica, DNAge en het RIVM; Irene, Ingrid, Lieke en Susan, bedankt voor jullie hulp met het opzetten van de TTD beenmergstudies en het delen van jullie muizen. Irfan en Janto, bedankt voor alle hulp tijdens de vele donderdagmiddagen waarop we als een geoliede machine tissues hebben lopen verzamelen.

Bram en Rodrigo, het was mij een waar genoegen om een kantoor met jullie te delen. We waren het in ieder geval meestal wel eens over de temperatuur in ons hokje, dus dat was weer meegenomen. Bram, bedankt voor het delen van al je kennis en kunde ondanks het feit dat ik officieel niet jouw AIO was. Zonder jou was er van heel veel dingen die nu in dit boekje staan niets terecht gekomen en had ik het moeten doen zonder heel veel goede raad. Rodrigo, ik bedank je gewoon in het Nederlands voor alle gezellige ritjes Utrecht CS -Rotterdam CS (soms kort, soms heel erg lang), voor al die keren dat jij mijn vouwfiets de trap op en af hebt gedragen en voor alle weggekletste uren op kantoor. Obrigado.

Jeroen, bedankt voor alle hulp met de arrays, de analyses en het daarbij behorende hoofdstuk en voor de Utrechtse lab roddels, stoere poezenfoto's en de beste schouwburgtips.

Marco, de lijst is lang en als ik alles opschrijf moet ik nog een katern extra kopen, maar in ieder geval bedankt voor alle gezelligheid binnen en buiten het lab. Naar Rotterdam verhuizen was niet half zo leuk geweest als ik niet gewoon jouw oude appartement had kunnen krijgen. Ik denk niet dat ik ooit de HAS had gevonden zonder jou, laat staan dat ik een fervent kapsalon liefhebber zou zijn geworden. En mochten we nog een keer samen op een gipsvlucht terecht komen, dan zal ik ervoor zorgen dat je in ieder geval een broodje krijgt voordat je door de regen naar huis mag fietsen.

Bianca en Marijke, bedankt voor alle ondersteuning, de invalbeurten als ik weer eens op reis was en onze nooit overtroffen ladies nights. Ik zal jullie nooit meer meenemen naar de Notenkraker van het Scapino en nog vele pogingen doen om van de heren te winnen tijdens het pokeren om onze eer hoog te houden.

Annelies, heel erg bedankt voor alle handtekeningen die je het afgelopen jaar voor mij hebt verzameld. Zonder jou zou alles twee keer zo langzaam zijn gegaan.

Lieve Miriam, Marlieke en Dineke, bedankt dat jullie al 13 jaar mijn beste vriendinnetjes zijn en dus verplicht naar mijn geklaag moeten luisteren. Het is dan eindelijk af! Bedankt voor jullie last minute contributies aan dit boekje, waardoor er toch nog iets van jullie in zit. Ik ging een geweldig passend lied voor jullie citeren maar ik denk niet dat Mir in één zin genoemd wil worden met het oeuvre van Guus Meeuwis. Jullie moeten dan ook thuis maar even achter de computer kruipen, de volgende link in typen en het geluid lekker hard aan zetten: http://www.youtube.com/watch?v=6sYW5TPYN5M. Moniek, Jilles en Ton jullie horen hier natuurlijk ook thuis. Bedankt voor de gezellige middagen/avonden vol met spelletjes en het lekkere eten. Mijn surprise wordt dit jaar helaas met enige zekerheid gewoon weer een ingepakte doos, ik stel voor dat jullie daar allemaal maar weer mee leren leven.

Erwin, proefschrift coach extraordinair….bedankt voor alle aanmoedigingen en de proefschrift ontwijkende BBQs in het Vroesepark. Dat het maar gauw weer BBQ weer mag worden nu ik weer alle tijd heb om te komen.

Het grootste deel van dit proefschrift is geschreven terwijl ik al weer hard aan het werk was bij Evers + Manders. Ik wil dan ook al mijn 'nieuwe collega's' bedanken voor al hun interesse, de achterliggende statistiek voor stelling 11 en een luisterend oor wanneer ik weer eens moest klagen over het één of ander. Jullie weten waarschijnlijk ondertussen allemaal meer over promoveren dan je lief is. Marco, heel erg bedankt voor al je werk aan de omslag, ik had het zelf nooit zo mooi voor elkaar gekregen. Annelies, bedankt voor de Nederlandse spelcheck, nu maar afwachten of we niets over het hoofd hebben gezien. Johan en Paul, bedankt voor al jullie steun, ook bij het tot stand brengen van dit boekje. Ik kwam binnen als bijna gepromoveerd, maar dat bijna liet nog even op zich wachten. Nu is het alleen nog maar wachten op die nieuwe visitekaartjes!

Papa en mama, Carla en Alexandra, bedankt voor alle weekendjes in Limburg die ervoor zorgden dat ik weer fris en uitgerust aan een nieuwe week vol met proefschriftperikelen kon beginnen. Ondanks het feit dat ik er niet zo vaak ben, is toch een significant deel van dit proefschrift gewoon geschreven achter papa's bureau. Of dat ligt aan de frisse Limburgse buitenlucht of het feit dat mama erg goed is in het uitbannen van proefschrift ontwijkend gedrag zullen we maar in het midden houden. Ik beloof in ieder geval dat ik in 2013 de computer gewoon in Amersfoort zal laten als ik kom logeren.

Curriculum Vitae

Claudia Nicolaije was born on September 18th, 1981 in Heerlen. From 1993 to 1999 she attended Scholengemeenschap Sophianum in Gulpen to obtain her VWO degree. After graduation she moved to Utrecht to study Biomedical Sciences at Utrecht University, completing internships at the Hubrecht Institute and Yale University. In 2004 she obtained her Master of Science degree in Biomedical Sciences with a specialization in Developmental Biology and Biomedical Genetics (DBBG). In 2005 she applied for a joined PhD position at the laboratories of Prof. dr. Hans van Leeuwen (department of Internal Medicine) and Prof. dr. Jan Hoeijmakers (department of Genetics) at the Erasmus University Medical Centre in Rotterdam. From 2006 to 2010, she worked on the studies presented in this thesis; 'Bone formation and skeletal aging – effects of oxygen and DNA repair'. Since October 2010 she is employed as a consultant at Evers + Manders Subsidieadviseurs in Hoevelaken.

Claudia Nicolaije werd geboren op 18 september 1981 in Heerlen. Van 1993 tot 1999 doorliep zij het VWO aan de Scholengemeenschap Sophianum in Gulpen. Na het behalen van haar VWO diploma verhuisde zij naar Utrecht om Medische Biologie te studeren aan de Universiteit Utrecht. Zij liep stage aan het Hubrecht Instituut in Utrecht en aan Yale University in de Verenigde Staten. In 2004 behaalde zij haar Master of Science diploma in de Biomedische Wetenschappen met een specialisatie in ontwikkelingsbiologie en biomedische genetica (DBBG). In 2006 begon zij met haar promotieonderzoek onder de leiding van Prof. Dr. Hans van Leeuwen (afdeling Inwendige Geneeskunde) en Prof. Dr. Jan Hoeijmakers (afdeling Genetica) aan het Erasmus Medisch Centrum van de Erasmus Universiteit in Rotterdam. Dit onderzoek werd afgesloten in 2010 en leidde tot de in dit proefschrift beschreven resultaten. Sinds oktober 2010 is zij werkzaam als adviseur bij Evers + Manders Subsidieadviseurs te Hoevelaken.

Chapter 7

PhD portofolio

Name:	Claudia Nicolaije
Erasmus MC Departments:	Internal Medicine/ Genetics
Graduate School:	Molmed/MGC
PhD Period:	January 2006 – June 2010
Promotor:	Prof. dr. J.P.T.M. van Leeuwen / Prof. J.H.J. Hoeijmakers

PhD training activities

General Courses

Annual Molecular Medicine Course (MolMed)	2006
Biomedical Research techniques V (Molmed)	2006
Literature Course (MGC/ Dept. of Cell Biology/Genetics)	2007
Biomedical English Writing and Communication (MolMed)	2008
Basic Introduction Course on SPSS (MolMed)	2009

Specific courses

SNP Course IV (MolMed/NIHES)	2006
Neuro-Immuno-Endocrinology (MolMed)	2006
Cell and Developmental Biology Course (MGC/ Dept. of Cell Biology/Genetics)	2007
Summer Course on Aging (Erasmus Summer Programme)	2007
International PhD training course on Bone Metabolism (ECTS)	2008

Awards

1st prize in the poster awards of the Science Days of Internal Medicine	2007

Presentations at (inter)national conferences

Science Days Internal Medicine (poster presentation)	2007/2008/2009/2010
11th Molecular Medicine Day (oral presentation)	2007
European Symposium on Calcified Tissues (poster presentation)	2007/2008/2009
Annual Meeting of the Dutch Society for Calcium and Bone	

Metabolism, (oral presentation), Zeist	2007/2008/2009
Science Days Internal Medicine (oral presentation)	2008
Molecular Medicine Day (poster presentation), Rotterdam	2008/2009/2010

Attended Conferences

European Symposium on Calcified Tissues, Copenhagen, Denmark	2007
European Symposium on Calcified Tissues, Barcelona, Spain	2008
European Symposium on Calcified Tissues, Vienna, Austria	2009
Annual Meeting of the Dutch Society for Calcium and Bone Metabolism	2006-2009
Molecular Medicine Day	2006-2010
Science Days Internal Medicine	2007-2010

Erasmus MC - Internal Medicine Seminars

Endocrinology Lectures	monthly
Internal Medicine Departmental Seminar	weekly
Bone and Calcium Research Literature Discussion	monthly
Bone and Calcium Research Work Discussion	weekly
Bone and Calcium Research Lab meeting	weekly

Lecturing

Erasmus Summer Program – course on aging and disease -lecture on accelerated aging in DNA repair deficient mice.	2007
Vaardigheids Onderwijs 2nd year medical students; Hypothalamus –hypophysis-thyroid axis	2007/2008/2009

Chapter 7

List of Publications

C. Nicolaije, M. Koedam, J.P.T.M. van Leeuwen; Decreased oxygen tension lowers reactive oxygen species and apoptosis and inhibits osteoblast matrix mineralization through changes in early osteoblast differentiation; *Journal of Cellular Physiology, 2012 Apr;227(4).*

C. Nicolaije, J. van de Peppel, J.P.T.M. van Leeuwen; Oxygen-induced transcriptional dynamics in human osteoblasts are most prominent at the onset of mineralization; *Submitted*

K.E.M. Diderich, **C. Nicolaije**, M. Priemel, J.H. Waarsing, J.S. Day, R.M.C. Brandt, A.F. Schilling, S.M. Botter, H. Weinans, G.T.J. van der Horst, J.H.J. Hoeijmakers, J.P.T.M. van Leeuwen; Bone fragility and decline in stem cells in prematurely aging DNA repair deficient trichothiodystrophy mice**;** *Age. 2012 Aug;34(4): 845-61*

C. Nicolaije, K.E.M. Diderich, S.M. Botter, M. Priemel, J.H. Waarsing, J.S. Day, R.M.C. Brandt, A.F. Schilling, H. Weinans, B.C. van der Eerden, G.T.J. van der Horst, J.H.J. Hoeijmakers, J.P.T.M. van Leeuwen; Age-related skeletal dynamics and decrease in bone strength in DNA repair deficient male trichothiodystrophy mice; *PloS One – 2012;7(4)*

Chapter 7